EXPERIMENTAL AND THEORETICAL STUDIES OF ELECTRONICALLY EXCITED ATOMS

by

Constantine Fotakis, B.Sc.

A Thesis presented for the degree of Doctor of Philosophy in the Faculty of Science at the University of Edinburgh.

1977

ACKNOWLEDGEMENTS

Thanks first and foremost are due to Dr. R.J. Donovan, who in a manner appropriate to the subject of this work energetically transferred his knowledge and enthusiasm (in a truly near resonant fashion!) during the whole study. I would like also to thank Drs. M.F. Golde, H.M. Gillespie and K.P. Lawley for many enlightening discussions.

I would like also to thank my colleagues Dr. R.H. Strain and Messrs. J. McElroy, A. Leitch, D. Fernie and A. Kvaran for the conducive atmosphere that they provided during the course of this study. Their sense of humour was a great stimulus even during the less inspired hours. I also thank Dr. R.H. Strain and Mr. J. McElroy for the use of some of their computer programmes. Furthermore, I would like to thank Ms. M.J. Soutar for typing this thesis and Ms. C. Codrington for proofreading and both of them for their achievement in reading the manuscript. Thanks also go to Messrs. J. Broom and A. McKenzie (Glassblowers), D. Shaw (Electronic Workshop), J. Ashfield and P. Daly (Mechanical Workshop) and H. McKenzie for their continual assistance.

Finally, I would like to thank the Royal Society and the University of Edinburgh for making this thesis possible through their financial support.

CONTENTS

page

ABSTRACT

This work is concerned primarily with the study of the various mechanisms which lead to the relaxation of excited atoms by small molecules. Spin-orbit relaxation of $I(5^2P_{\frac{1}{2}})$ atoms by the molecules CH_3I, CD_3I, GeH_3I, SiH_3I, H_2O, D_2O, HCl, DCl, HBr, DBr, HI and DI has been studied experimentally, at room temperature, using time resolved atomic absorption spectrophotometry. For some of these molecules (CH_3I, CD_3I, HCl, HBr) the temperature dependence of the decay efficiency was studied over the range 200-450 K.

Large isotope effects have been observed for the removal of $I(5^2P_{\frac{1}{2}})$ by the isotopic pairs CH_3I-CD_3I and H_2O-D_2O. A practical application of the large isotope effect for the former pair has been demonstrated in the iodine photodissociation laser, for which CD_3I exhibits a superior performance in terms of laser output. The large isotope effect along with the data obtained for the temperature coefficients for CH_3I and CD_3I are rationalised in terms of a mechanism based on long range dipole-quadrupole interactions leading to an efficient quenching of $I(5^2P_{\frac{1}{2}})$ via near resonant electronic-to-vibrational + rotational energy transfer. In contrast to these proposals the removal of $I(5^2P_{\frac{1}{2}})$ by SiH_3I and GeH_3I has been shown to occur by reactive pathways.

The results obtained for the relaxation of $I(5^2P_{\frac{1}{2}})$ by the hydrogen and deuterium halides are compared with other recent data involving $Br(4^2P_{\frac{1}{2}})$ and the hydrogen halides. It is concluded that deactivation of both $I(5^2P_{\frac{1}{2}})$ and $Br(4^2P_{\frac{1}{2}})$ by the most efficient molecule, HF and also to some extent of $I(5^2P_{\frac{1}{2}})$ by HBr, may proceed via near resonant energy transfer channels due to multipolar interactions. A "curve crossing" mechanism at long range, which may lead either to quenching or reaction, is proposed to account for the kinetic behaviour observed for the rest of the hydrogen and deuterium halides.

Theoretical data, obtained using a model based on long range multipolar interactions, for the quenching of $I(5^2P_{\frac{1}{2}})$ and $Br(4^2P_{\frac{1}{2}})$ by the hydrogen halides, H_2 and HD reveal that near resonant energy transfer processes can play an important role in the quenching of these excited states. Further calculations are presented for the quenching of $Te(5^3P_{0,1})$, $Bi(6^2D_{3/2,\ 5/2})$, $Sb(5^2D_{3/2,\ 5/2})$, $Sn(5^3P_2)$, $Pb(6^3P_2)$ and $Tb(6^2P_{3/2})$ by H_2, HD and D_2 which show that long range near resonant energy transfer is important in a wide range of systems and allows a better understanding of the kinetic data for these excited atomic states.

A) GENERAL REMARKS

It has long been recognised that the chemical behavior of atoms in excited states may differ substantially from that of their ground state. Such differences are due to the change in the electronic structure of the atom following excitation of the ground state. Thus, when the electronic configuration, or the spin-orbit state arising from the same electronic configuration, is changed, the features of the interaction potential associated with the reacting species will be altered. This may lead to marked differences in the topology of the potential surfaces which correlate with the excited and ground atomic states, and thus to differences in the dynamics of the reactions which occur on these surfaces.

Physical quenching provides an additional removal pathway for excited states. If an excited atom can be removed efficiently by physical quenching, the relative importance of reactive pathways may be reduced. In such cases the excess electronic energy of the atom appears in the various degrees of freedom of the colliding species.

There are numerous examples which illustrate the above remarks. Here, we consider the marked differences in the chemistry of the low lying states of atomic oxygen. The first excited state of the oxygen atom, $O(2^1D_2)$, shows an increased chemical activity in comparison to that of the ground state atom.[1,2] In sharp contrast the second excited state, $O(2^1S_o)$ is seen to be collisionally metastable,[1] despite its larger electronic energy content. Thus the reaction of $O(2^1D_2)$ with H_2 is very fast, having a rate constant $k = 2.7 \times 10^{-10}$ cm^3 molecule^{-1}s^{-1}, in contrast to the corresponding reaction with $O(2^3P_J)$ atoms, which proceeds efficiently only at high temperatures. The removal of $O(2^1S_o)$ by H_2 is about five orders of magnitude slower[4] than for $O(2^1D_2)$. Comparison of the quenching efficiencies of $O(2^1D_2)$ and $O(2^1S_o)$ in the presence of noble

gases is also striking in this respect, the $^1D_2$ state being relaxed by more than four orders of magnitude faster.[1]

This work is concerned primarily with the study of the removal efficiency of excited atoms in the presence of small molecules. Attention has been focused on the determination of the conditions which may lead to efficient relaxation, with particular emphasis placed on the study of electronic energy transfer processes of the type:

$$A^* + Q\ (v'' = o,\ J'' = k) \rightarrow A + Q\ (v' = n,\ J' = l) + \Delta E \qquad (1.1)$$

where A^* and A represent an atom in its excited and ground state respectively and Q is a quenching molecule in vibrational level v and rotational state J.

Studies of elementary processes like 1.1, which can determine the kinetic behavior of excited atoms in bulk, have received considerable attention recently.[2,5] This may be understood, in view of the current interest in practical applications of the findings of molecular dynamics in isotope separation,[6] selective synthetic pathways[7] and developing chemical laser systems.[8]

In this section, some of the theoretical considerations and experimental methods often used in the kinetic investigation of excited atoms will be described briefly.

B) SOME THEORETICAL CONSIDERATIONS

There are four main categories of processes which may result in the removal of excited atomic states, namely:

1) Energy transfer[9] (Resonant, Non-resonant)

2) Reaction[2] (Abstraction, Addition, Dissociative Excitation)

3) Radiation[8,10] (Collisional, Spontaneous, Stimulated)

4) Ionisation[10,11] (Collisional, Dissociative, Associative, Penning)

The low energies of the excited states, which are of concern in the present work, preclude the interference of processes belonging to the last category. Furthermore, the relatively high optical metastability of these states imposed by the experimental requirements (cf.Chapter 2), eliminates the importance of radiative processes. Thus the relative efficiency of reactive and quenching pathways in removing excited atoms is of primary importance in this study.

The main factors usually considered in discussing the kinetic behavior exhibited by excited atoms are:

i) The spin conservation rule

ii) The adiabatic correlations and non-adiabatic processes

iii) The energetic requirements, which will be examined in section C.

The concept of a conserved quantity is embodied in these items. The theoretical basis of conservation laws is provided by the commutation relationship of an effective Hamiltonian describing a system and involving this conserved quantity, with the elements of some symmetry group associated with the permutations of the spatial electronic indices. If such a commutation relationship exists, then the irreducible representations of the group are conserved, i.e. are good quantum numbers.[12] A crucial point therefore, when discussing the dynamics governing the interactions of two colliding species on the basis of conservation rules, is the assumption of a reasonably effective Hamiltonian for each specific system at various ranges of atom-molecule separations.

1) The spin conservation rule:

The Breit-Pauli Hamiltonian given by 1.2 is usually applied[12] in describing atoms or molecules.

$$H = H_o + \Lambda \qquad (1.2)$$

where Λ contains all terms dependent on spin, like the spin-orbit coupling, and H_o is spin independent.

The systems for which spin is conserved are those described well by H_o. For atoms of low atomic number and molecules composed of such atoms, Λ is negligible in comparison to H_o and therefore spin is a good quantum number.[13] As a consequence the Wigner and Witmer spin conservation rule[14] may be applied in discussing the molecular dynamics of their reactions. According to this rule, processes requiring a change of the total spin angular momentum should be expected to proceed with very small cross sections. However, for systems involving heavier atoms the spin interaction operator must be included in the expression of the effective Hamiltonian, as in 1.2. In such cases the commutational relationship of H with the symmetry group of the permutations of the spatial electronic indices is invalid and spin is not a good quantum number.

Despite the above considerations, when the dependence of the form of the effective Hamiltonian upon the separation of the colliding species is taken into account, even for systems comprised of atoms with small atomic numbers, inclusion of spin dependent terms in H at certain atom-molecule distances provides a better understanding of the molecular dynamics. The electrostatic interactions between the reactants, for example, can be comparable to the atomic or molecular fine structure splitting at large or intermediate separations[15] and therefore a spin dependent Hamiltonian is more suitable in describing processes due to interactions of the corresponding range. Most interesting however, are spin-forbidden processes, which occur with an unexpectedly high efficiency at relatively short separations. A typical example is provided by the quenching of $O(2^1D_2)$ by $N_2(^1\Sigma_g^+)$:

$$O(2^1D_2) + N_2\,(^1\Sigma_g^+) \rightarrow O(2^3P_J) + N_2(^1\Sigma_g^+) \qquad (1.3)$$

The high efficiency[16] of 1.3, ($k = 6.9 \times 10^{-11}$ cm^{3}molecule^{-1}s^{-1}), has been explained in terms of transitions from the singlet potential surfaces correlating with the reactants to the triplet surfaces emanating from the products, in a region where these surfaces approach each other closely. In the original calculations of Fisher and Bauer[17] and Delos,[18] the

interaction region was crossed twice, i.e. in the approach and the recession of the species, leading to a theoretical rate constant more than one order of magnitude smaller than that experimentally obtained. This is indicative of the small probability of such singlet-triplet curve crossing processes. However, as Tully pointed out[19] in a later work, the violation of spin conservation should be associated with crossings of the intersection region more than twice during a collision and thus favoured by the formation of a long lived intermediate complex. By applying a statistical model for the decay of the complex, he determined a quenching rate, which was in good agreement with the experimental results.[20] Furthermore, he predicted that electronic to vibrational ($E \rightarrow V$) energy transfer should take place efficiently in 1.3, which accords well with experimental observations.[20,127] A comparison of the theoretical and experimental distributions of the vibrational excitation in N_2 is expected to clarify these aspects further.

2) The adiabatic correlations and non-adiabatic processes:

The fundamental assumption enabling one to introduce the concept of a potential energy hypersurface into the discussion of molecular processes is the adiabatic principle. The basis of this principle is the Born-Oppenheimer approximation, according to which the energy of the various electronic states in a molecular system is determined parametrically by each fixed internuclear separation. The adiabatic principle then states[12] that the transition probability between two electronic states differing in energy by ΔE, under the influence of some time dependent perturbation acting effectively over a time τ, is small if the Massey criterion expressed by 1.4 is satisfied.

$$\frac{\Delta E \tau}{h} \gg 1 \qquad (1.4)$$

At internuclear separations for which 1.4 is not valid transitions between different potential hypersurfaces may occur and the corresponding processes are referred to as non-adiabatic.

Knowledge of the topological features of the potential hypersurfaces associated with a chemical process is of primary importance in understanding its dynamics. Strictly speaking, these features should be determined fully quantum-mechanically, but this is extremely difficult for polyatomic systems and has been achieved only in very few cases.[21,22] A qualitative approximate picture of this topology may however, be obtained in a convenient way by using the orbital correlation diagrams, as has been described by Shuler[23] and extensively applied by Donovan and Husain.[1] The primary step in applying the latter method is the classification of the adiabatic wavefunctions according to their transformation properties under the different symmetry operations of an effective Hamiltonian for fixed geometries of the reactants and the products. As explained in the previous section, the choice of the effective Hamiltonian depends on the relative magnitude of the various interactions at each internuclear separation, and specifies whether the irreducible representations of the symmetry group assumed for the least symmetrical configuration of the interacting species are conserved or not.

Non-adiabatic transitions, i.e. non-conservation of the irreducible representation during the course of a chemical or physical process are usually associated with an effective Hamiltonian which includes either spin dependent terms, as for example spin-orbit interactions, or rovibronic interactions in the region in which the potential surfaces approach closely, i.e. where ΔE becomes very small and 1.4 does not hold.

Teller's "non-crossing rule" for diatomic systems[24] is usually applied in constructing correlation diagrams involving three or more atoms. According to this rule, curves of the same symmetry species will strongly repel each other. However, it should be pointed out that there is some controversy regarding the rigorous application of this rule in polyatomic systems. In a series of papers Naqvi and Byers Brown[25]

criticised the conditions leading to the "non-crossing rule", originally given by Teller, and by following a different approach they concluded that this rule can be rigorously applied to potential surfaces of polyatomic systems as well. These derivations, supported strongly by Hoytink[26] who attempted to point out the error in Teller's treatment, were severely criticised in a recent work of Longuet-Higgins.[27] Furthermore, the latter author established a general topological condition, which is in accord with the original suggestions of Herzberg and Longuet-Higgins,[28] for a loose applicability of the "non-crossing rule" in polyatomics. Thus, the more the number of independent internuclear coordinates, the smaller the probability that potential hypersurfaces characterised by the same symmetry species will give rise to "avoided crossing".

Usually, fast exothermic reactions of ground or excited state atoms are associated with the existence of a direct adiabatic correlation from reactants to products. Thus, the efficient insertion of $C(2^3P_J)$ atoms in the H_2 bond may be well understood on the basis of the appropriate correlation diagram.[1] High energy barriers corresponding to high activation energies can also be explained in terms of correlation diagrams, in the absence of a direct adiabatic correlation between reactants and products. These usually result from "avoided crossings" of hypersurfaces emanating from the reactants and the products and correlating with highly excited states of the interacting species. The recent considerations of diabatic correlations reported by Wiesenfeld[29] extended the applicability of correlation diagrams, by providing a satisfactory explanation for the observed efficiencies of processes involving molecules like N_2O or CO_2. Thus, several cases which were, in the past, considered incompatible with the expectations of adiabatic correlations, are now well understood, supporting the utility of correlation diagrams as a simple qualitative method for predicting the efficiency of a reactive

or quenching process in the majority of cases.

Finally, we consider the case in which the outcome of a reaction can be two sets of products formed on the same adiabatic potential hypersurface, as in 1.5

$$A + BC \rightarrow \begin{cases} AB + C & (1.5a) \\ AC + B & (1.5b) \end{cases}$$

In 1.5, molecular orbital (M.O.) considerations should be applied in predicting the final products. If these considerations do not impose any limitations for either 1.5a or 1.5b, the ratio of the products will be determined purely by statistical requirements. A typical example is provided by the reaction of $F(2^2P_{3/2})$ with HD, in which the formation of HF is slightly favoured[30] over that of DF. On the other hand, limitations in the formation of one of the products of 1.5 due to M.O. considerations can result in a non-statistical product formation, as it occurs in the reaction of $O(2^3P_J)$ with ICl or IBr in which IO is the main product,[31] although unanticipated on energetic grounds.

C) ENERGETIC CONSIDERATIONS

Progress in the experimental techniques employed in gas phase kinetics in recent years[32] has made possible the probing of elementary chemical processes at the microscopic level. This has allowed a detailed direct observation of the energetic requirements in many systems involving ground and excited state atoms. Summarising the basic trends, which characterise energy disposal and energy consumption, we distinguish two main categories of processes corresponding to: (1) reactive and (2) inelastic collisions.

(1). Reactive Collisions

Frequently, the energy released in an elementary exoergic reaction is characterised by a high degree of specificity. Conversely, the energy consumption exhibits high selectivity. The latter should be expected on the basis of the principle of microscopic reversibility. If, for

example, the "forward" reaction leads to products, which are excited internally, the "reverse" reaction proceeds more readily when energy is supplied in the internal degrees of freedom, than in relative translation. Polanyi and other workers,[33,34] exploited the implications of microscopic reversibility in investigating the specificity in energy release in several exothermic reactions of the general type $A + BC \rightarrow AB + C$, by employing mainly IR chemiluminescence techniques. An example of one of these reactions is that described by 1.6, which is of great importance as a pumping mechanism in the HF chemical laser.[35]

$$F(2^2P_{3/2}, \tfrac{1}{2}) + H_2 \rightarrow HF\ (v) + H(1^2S_{\frac{1}{2}}) \qquad (1.6)$$

Some 67% of the available exoergicity in 1.6 appears as rovibrational excitation in HF, resulting in a population of the v = 2 vibrational state about 18 times larger than that of the v = o state.

The effect of vibrational excitation in the reacting molecules on the rate of chemical reaction, as in the inverse of process 1.6, has been examined in several systems. Such studies raise novel questions concerning the interaction of molecules with reactive atoms, due to the possibility of competition between reactive and quenching pathways in deactivating the excited molecules. As a result of the observed trends, it can be stated that when vibrational excitation is used to overcome the endothermicity for reaction of the ground state species there is usually a dramatic increase in the reaction rate. This remark can be extended to the general case of reactions with an activation energy. The degree of the increase in the reaction rate is dependent on how parallel the reaction and vibrational coordinates are in the region of the energy barrier.[36] An example illustrating the above considerations is provided by the relaxation of HCl (v=1,2) by $Br(4^2P_{3/2})$ atoms, studied recently in laser induced fluorescence experiments.[37] HCl (v=2) is

relaxed by about one order of magnitude faster than HCl (v=1), the relaxation occuring by reaction, instead of vibrational to translational-rotational (V→T,R) energy transfer, as for HCl (v=1). Finally, one should mention an interesting result obtained by Smith,[38] in a very recent theoretical investigation involving quasiclassical trajectories and an accurate potential for the $H + H_2$ ($1 \leqslant v \leqslant 4$) and $D + D_2$ ($1 \leqslant v \leqslant 4$) systems: Although the rate of the reactive pathway was enhanced with vibrational excitation, the degree of selectivity was found to decrease as the vibrational energy was increasing. It should be noted here, that a low selectivity in energy consumption should also be expected in some reactions proceeding via the formation of long-lived intermediate complex.[39]

The effects of electronic excitation on reactivity are in many cases similar to those of vibrational excitation, i.e. an enhancement of the reaction rate is observed, especially when electronic excitation is in excess of the endothermicity for reaction. However, as it has been pointed out by using correlation diagrams, electronically excited species are not always more reactive than their ground states. Thus, the rate of reaction 1.6 for $F(2^2P_{\frac{1}{2}})$ is predicted to be about one order of magnitude smaller than for $F(2^2P_{3/2})$, in contrast to the efficient removal of $F(2^2P_{\frac{1}{2}})$ by quenching, which effectively dominates the decay process.[40,41]

2) Inelastic Collisions

As mentioned in section A, inelastic collisions, particularly of the type described by 1.1, are of primary concern in this work. In this section, a brief summary of the energetic conditions for efficient energy transfer will be given, with special emphasis placed on E → V energy transfer processes.

The possibility of competition between inelastic and reactive collisions

has already been pointed out. To further illustrate their relative importance, we recall Table 1.I, based on kinetic data obtained[42] in molecular beam experiments for processes 1.7 and 1.8,

$$Hg(6^3P_2^o) + ACl \rightarrow HgCl(B^2\Sigma^+) + A \qquad (1.7)$$
$$\hookrightarrow HgCl(X^2\Sigma^+) + h\nu$$

$$Hg(6^3P_2^o) + Q \rightarrow Hg(6^3P_1^o) + Q \qquad (1.8)$$
$$\hookrightarrow Hg(6^1S_o) + h\nu$$

where ACl denotes the chlorinated compound and Q = ACl or N_2.

It is noted that for the chlorinated molecules relative cross sections were measured and were normalised to the absolute cross section for N_2. Also included in Table 1.I are data for the C-Cl bond energies. It becomes clear that the efficiency of reaction decreases as the C-Cl bond strength increases, while for the quenching efficiency a reversed trend is observed. This is indicative of the increased interference of energy transfer processes as the reaction pathway becomes less favourable. This remark however, does not imply that a decrease in the reaction rate is necessarily followed by an increase in the quenching efficiency.

A discussion of the various mechanisms for energy transfer can facilitate the specification of the energetic requirements which lead to efficient quenching of an excited state. For processes of the type 1.1, we can distinguish three main categories of quenching mechanisms which can be further subdivided into groups according to the features of each specific model considered. These mechanisms include:

i) Non-adiabatic transitions between crossing potential hypersurfaces of either covalent or ionic nature. Exit and entrance channels can be coupled either directly or indirectly, as for example via an ionic hypersurface.

ii) The formation of a long-lived intermediate complex.

TABLE 1.I

Reactive (σ_R) and Quenching, (σ_Q) cross sections for the removal of $Hg(6^3P_2)$

Reactant	$\sigma_R \times 10^{16}$ (cm^2)	$\sigma_Q \times 10^{16}$ (cm^2)	D* (kJ $mole^{-1}$)
Cl_2	90 ± 25	0.13	238.9
CCl_4	34 ± 10	0.22	284.5
$CHCl_3$	8 ± 2	1.01	301.2
CH_3Cl	<0.5	6.3	334.7
N_2		19.2	941.4

* Dissociation energies for C-Cl and N-N bonds, based on data given in Ref. 63.

iii) Adiabatic transitions between parallel potential hypersurfaces.

Selected models often invoked in interpreting experimental data for energy transfer processes will be discussed within the context of the above mechanisms.

i) Electronically non-adiabatic collisions.

In contrast to reactive collisions, which frequently proceed more readily on a single adiabatic surface, non-adiabatic collisions tend to favour electronic energy transfer. Following Nikitin,[43] the operator $-ih\frac{\partial}{\partial t}$ in the time dependent Schrödinger equation, which describes the evolution of a system in time under the influence of some perturbation, can be expressed as in 1.9,

$$-ih\frac{\partial}{\partial t} = -ih\left(\dot{R}\frac{\partial}{\partial R} + \dot{\gamma}\frac{\partial}{\partial \gamma}\right) + \sum_i \omega_i J_i \qquad (1.9)$$

where R and γ are the radial and angular velocities describing the relative motion of the colliding particles, ω_i are instantaneous angular velocities of rotation about the principal axis of inertia and J_i is the operator corresponding to the projection of the orbital angular momentum along the same molecular axis (Coriolis interaction). In consequence, we can encounter two sources for electronically non-adiabatic transitions, originating from (a) the radial motion, which in the case of a polyatomic system, is related to the translational, vibrational and angular motions and (b) the rotational motion, which is associated with the orbital-rotational interaction and is usually of smaller importance than (a).

The Landau-Zener (Linear) model

The radial motion can cause coupling of states of the same symmetry, giving rise to a non-adiabatic transition in the case of an "avoided crossing", which is referred by Nikitin[9] as "pseudocrossing". This type of coupling was first treated for atomic collisions by Landau[44] and Zener[45] and by Stückelberg,[46] by applying first order perturbation

theory, approximating the potential surfaces by hyperbolas in the range of crossing and assuming a constant relative velocity in the vicinity of the crossing point R_o. The thermal cross section σ for such a non-adiabatic process is given by 1.10, although more involved formulations also exist;[43]

$$\sigma = \pi R_o^2 < P_o > \exp\left(-\frac{\Delta E_o}{kT}\right) \qquad (1.10)$$

where, k is the Boltzmann constant, ΔE_o is an energy barrier due to the repulsion of the colliding species at R_o and $<P_o>$ is the mean transition probability between the potential surfaces at R_o, calculated from P_o on the basis of the transition state method. In the case of a two atom system, the intersection point must be crossed twice and P_o, the net transition probability, is related to the probability for non-adiabatic transitions P_{12} through the expression 1.11,

$$P_o = 2 P_{12} (1 - P_{12}) \qquad (1.11)$$

where for pseudocrossing, P_{12} is given by the Landau-Zener formula:

$$P_{12} = \exp \frac{-2a^2}{h v |F_1 - F_2|} \qquad (1.12)$$

In 1.12, 2a represents the minimum separation of the intersecting surfaces, v is the relative velocity due to the radial motion and F_1, F_2 the slopes of the two surfaces at R_o.

Similar considerations can be applied for non-adiabatic transitions between potential surfaces of different symmetry, resulting in expression 1.13 for P_{12};

$$P_{12} = \frac{2\pi\omega^2 C_{12}^2}{h v |F_1 - F_2|} \qquad (1.13)$$

where ω is the angular velocity and C_{12} is a coupling matrix element between the surfaces 1 and 2, of the form:

$$C_{12} = < 2 \mid J_\omega \mid 1 > \qquad (1.14)$$

An illustration of the cases which 1.12 and 1.13 refer to is given in Figure 1.1.

It should be noted that for systems consisting of three or more atoms, the corresponding formulations are much more involved. The above expressions however, reveal some basic features of non-adiabatic transitions, which can be summarised as follows:

1) From 1.12, it is evident that P_{12} is small for a large splitting of the adiabatic surfaces. At low thermal energies relatively weak spin-orbit coupling can usually cause transition between potential surfaces of the same symmetry species. Potential surfaces having different species can be connected by the extremely weak Coriolis interaction, (cf. 1.13 and 1.14).

2) Due to the existence of $| F_1 - F_2 |$ in the denominator of 1.12, it is concluded that non-adiabatic transitions due to spin-orbit coupling are particularly favoured by strongly converging potential surfaces.

3) Introduction of the relative translational energy E in both 1.12 and 1.13 and then in 1.11 can show that P_o should be expected to increase slightly with increasing E. As shown by Nikitin,[9] evaluation of $< P_o >$ is likely to give rise to a similar trend for the energy dependence of the corresponding cross section for collision energies within the thermal range.* This conclusion can also be extended to triatomic systems, in which E→V energy transfer takes place via a non-adiabatic transitions between potential hypersurfaces of different symmetry species (cf. Nikitin's model).

4) Near-resonance between the entrance and exit channels, i.e.

*However, in some cases of transitions due to spin-orbit coupling a weak negative energy dependence may be observed for the cross section (cf. also footnote on page 20).

Figure 1.1

1) The Linear Model

a) Non-adiabatic transitions between surfaces of the same symmetry (eq. 1.12)*

b) Non-adiabatic transitions between surfaces of different symmetry (eq. 1.13)*

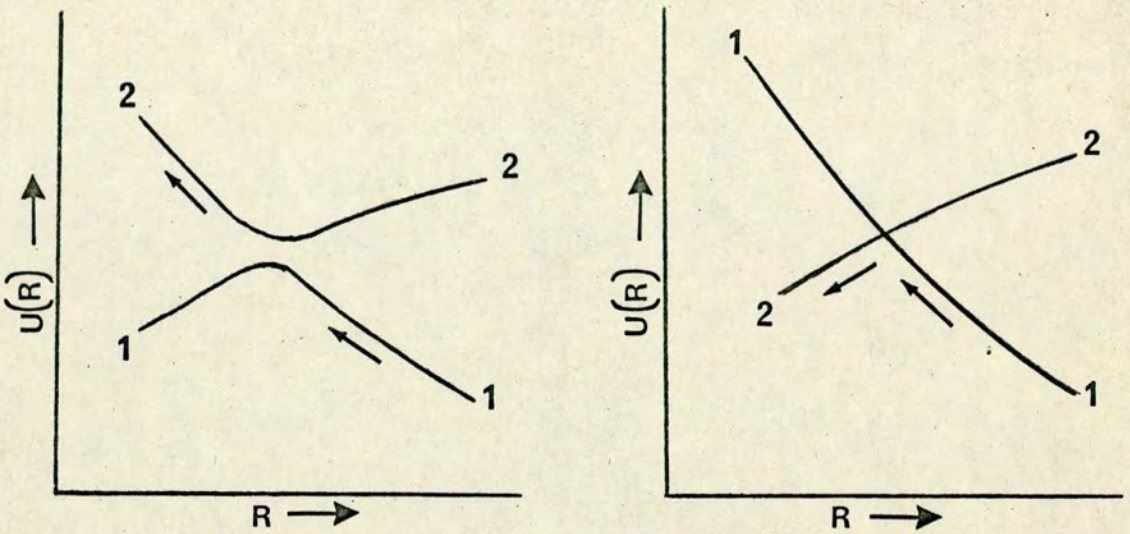

*The arrows indicate non-adiabatic paths, which can be followed by the system.

2) The BFG Model*

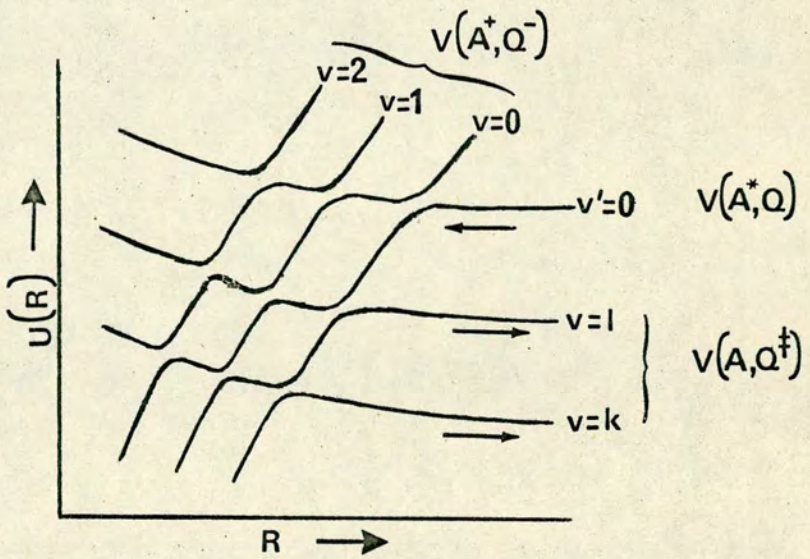

* The arrows indicate the entrance and exit channels.

minimization of ΔE in 1.1, does not seem to account for the efficiency of non-adiabatic processes in diatomic systems. However, for a triatomic system a weak dependence should be expected.[43] As can be shown, $\langle P_o \rangle$ and consequently σ are inversely proportional to ΔE.

Nikitin's model

From a very early stage it was observed that the efficiency of decay of excited atoms in the presence of noble gas atoms is usually several orders of magnitude smaller in comparison to quenching by diatomic or polyatomic species.[1] This has been attributed to the importance of E → V energy transfer processes in the latter systems. It would therefore be interesting to consider the effect of vibrational excitation in electronically non-adiabatic transitions.

Nikitin and co-workers[43,47,48] have developed a "curve-crossing" model which can account for V - T energy transfer processes via non-adiabatic transitions. Kinetic data obtained for non-reactive collisions of vibrationally excited hydrogen and deuterium halides by P state atoms, as for example the relaxation of HCl (v = 1) and DCl (v = 1) by $O(2^3P_J)$, accord well with the predictions of this model,[49] which can also be applied in E → V energy transfer processes.[48] The basic features of this model can be summarized as follows: First, in a system in which at least one of the colliding species is in a degenerate electronic state, i.e. in a state characterized by a non-zero orbital angular momentum, the degeneracy is removed due to the interaction between the species, as these approach each other.[50] This has as an effect the emergence of more than one potential hypersurface, with the splitting between them increasing with decreasing separation. Secondly, vibronic terms may be taken into account by assuming that the amplitude of molecular vibrations is much smaller than the range of the interaction potential. Vibronic hypersurfaces can then be obtained by displacing the adiabatic electronic

hypersurfaces by the values of the vibrational quantum hν. Divergence of the hypersurfaces associated with the same vibrational level and different electronic states can lead to efficient non-adiabatic transitions, leading to E → V energy transfer.

The calculation of $\langle P_o \rangle$ is usually frustrated by lack of good potential hypersurfaces. However, approximate expressions for $\langle P_o \rangle$ have been obtained for several systems[43,48] by assuming exponential forms for the interaction potentials. In most cases, the predictions of this model seem to be in accord with the experimental data. It is interesting to note that for exponential potentials the quenching cross section is expected,

a) to be inversely proportional to the energy mismatch ΔE (cf. 1.1).

b) to be proportional to the square of a vibrational matrix element, in which the vibrational wavefunctions of the molecule are coupled via exp(ax), where x is the vibrational amplitude and 1/a is the characteristic range of action of the potential. Multiquantum vibrational transitions are in general not favoured.

The Bauer-Fisher and Gilmore (BFG) model

This is a tractable model involving indirect non-adiabatic coupling and accounting for several E → V energy transfer processes. According to the BFG model,[51] the coupling between the covalent potential hypersurfaces $V(A^*,Q)$ and $V(A,Q^{\ddagger})$ associated with the reactants and products respectively, takes place via non-adiabatic transitions to an ionic hypersurface $V(A^+,Q^-)$ or $V(A^-,Q^+)$, as was originally outlined by Magee and Ri.[52] It therefore has a lot of similarities with the "harpoon" model of chemical reactions proposed by Polanyi[53] and Magee[54] to explain reactions between metal atoms and halogen molecules. Thus, it has been

used in interpreting kinetic data in systems in which one of the species has a low ionization potential (I.P. $\leq$ 5eV) and the other an appreciable electron afinity, as for example in $Na(3^2P_J) + N_2$. The basic features of the BFG model are shown schematically in Figure 1.1. The approach of the excited atom to the quenching molecule on a covalent hypersurface is followed by non-adiabatic transitions to ionic hypersurfaces, from which the system is relaxed non-adiabatically to hypersurfaces correlating with the ground state atom. This type of quenching can lead to efficient E $\rightarrow$ V energy transfer by incorporating the vibrational levels of the quencher in a similar manner as in Nikitin's model. In this way a grid of crossings can be obtained, as indicated in Figure 1.1, resulting in the population of various vibrational levels of the quencher.

The BFG model uses a modified Landau-Zener transition probability expression at each pseudocrossing point. Thus, this expression, which is similar to 1.12, includes in the numerator of the exponential, Franck-Condon factors,* characteristic of the overlap between the Q(n) and $Q^-(n')$ or $Q^+(n')$ vibrational states. Concluding, we note that according to the formulation of the B.F.G. model, near-resonance is of no importance and therefore a high degree of non-specificity in the populated vibrational states is observed. For example, in the $Na(3^2P_J) + N_2$ system, although the excited v' = o vibronic level falls between the v" = 7 and v" = 8 ground vibronic levels, the cross section of E $\rightarrow$ V energy transfer is largest for the v" = 3 final vibrational level of N_2.

Recently, the BFG model has been criticised by Gislason and Sachs[55] and especially by Barker,[56] who proposed several modifications, so that it will account for experimental data,[57,58] which became available in the period since the BFG theory appeared. Particularly interesting in this respect

* Franck-Condon factors result from the treatment of the long range "curve-crossing", between vibronic hypersurfaces.

is that the quenching cross section for $Na(3P_J) + N_2$ was found to exhibit a negative energy dependence,* in contrast to the BFG model expectations.[57] This discrepancy was attributed mainly to a breakdown of the classical trajectory assumption employed in the Landau-Zener formulation.[56]

To sum up this section, we emphasise that the energetic considerations of inelastic processes involving non-adiabatic transitions are not likely to be specified in a generalised concrete manner. They will largely depend upon the form of the interaction potentials in the crossing region and the type and strength of coupling, which will determine the energy (or temperature) at which $\langle P_o \rangle$ is maximised. However, we may summarize some general guidelines relating to the effect of kinetic energy on the transition probability. By increasing the translational energy, the most probable trend, within the thermal energetic range, is a small increase in the efficiency of inelastic collisions involving potential hypersurfaces of different symmetry. In contrast, coupling of surfaces of the same symmetry, via strong spin-orbit coupling, may lead in some cases, to a slight decrease of the inelastic cross sections with increasing energy. In several systems the quenching efficiency of processes like 1.1 may be also weakly dependent on the degree of near resonance.

* A negative relative energy dependence has also been reported for the quenching cross section of $Hg(6^3P_2)$ atoms in the presence of several molecules, including H_2, D_2, and N_2. The cross section was found to vary as $E^{-\frac{1}{2}}$ over the range 160-1600 cm^{-1}, where E is the relative energy. For H_2 and D_2 a maximum was observed at $\sim$80 cm^{-1}. A simplified expression given by Landau[12] is in accord with such an energy dependence of non-adiabatic processes due to spin-orbit coupling.

ii) Formation of long-lived intermediate complexes

By "long-lived intermediate complex" we mean the formation of a stable species with a lifetime longer than a typical vibrational period (10^{-13}s), during the course of a molecular collision. Such compound collisions can be very effective in the removal of excited atoms by inelastic pathways. The role of intermediate complexes in spin-forbidden processes has already been discussed in section B. Here we give one additional example which clearly illustrates the importance of stable intermediates in determining the outcome of a removal process. Removal of $S(3^1D_2)$ atoms by N_2O can occur via three channels:[59]

$$S(3^1D_2) + N_2O \rightarrow N_2 + SO(a\ ^1\Delta g) \qquad (1.15a)$$

$$\rightarrow NS + NO \qquad (1.15b)$$

$$\rightarrow S(3^3P_J) + N_2O \qquad (1.15c)$$

From these channels, 1.15c, i.e. quenching, has been shown to dominate the removal process, by accounting for ~80% of the total cross section. In sharp contrast, quenching of $O(2^1D_2)$ by N_2O is very inefficient,[60] reaction being the dominant pathway. These findings have been discussed in terms of the possible formation of a long-lived intermediate of the type SNNO in the case of $S(3^1D_2) + N_2O$. The corresponding intermediate for $O(2^1D_2) + N_2O$ is expected to have a smaller binding energy and therefore has a shorter lifetime. However, it should be emphasised that possible formation of a complex does not necessarily lead to efficient quenching.

The formation of a long-lived complex is associated with the existence of a potential "well" on the hypersurface determining the dynamics of the collision. It is therefore favourable for reactants with attractive potentials and a large number of degrees of freedom, which can stabilise the complex. For excited state atoms, attractive potentials should be anticipated especially in processes involving

reactants with either a sizeable electron affinity acting as electron acceptors or a small ionization potential acting as electron donors. In addition, bound intermediates, formed in orbiting collisions, can make large contributions to inelastic cross sections.

In the majority of cases the formation of a complex is associated with a total absence of specificity in the release of the available energy. Thus in an E → V energy transfer process, as in 1.1, the sharing of energy in the vibrational levels of the quenching molecule is expected to be determined mainly by statistical factors and the energy conservation law. Near resonant channels do not appear to play any role in quenching processes proceeding via the formation of a complex. However, in the case of orbiting collisions, a weak dependence of the quenching cross section on the energy mismatch, having the form $\sigma \propto \Delta E^{-2}$, is expected.[61]

The efficiency of inelastic processes proceeding via the formation of long-lived complexes usually exhibits a strong negative temperature dependence. Thus, the quenching of $I(5^2P_{\frac{1}{2}})$ atoms by I_2 has been explained in terms of this type of mechanism,[62] since it has an activation energy of -13.8 kJ $mole^{-1}$. A theoretical treatment of orbiting collisions has shown that a minimum should be expected[61] in the temperature function of the quenching efficiency. The temperature for this minimum efficiency is related to the depth of the potential "well". Thus, for attractive potentials deeper than 800 cm^{-1}, a slight increase is expected in the quenching efficiency of orbiting collisions for temperatures larger than 300 K.

iii) Electronically adiabatic transitions

Mechanisms belonging to this category tend to attribute the coupling between the entrance and exit channels to electrostatic potential energy terms rather than terms refering to the relative motion of the nuclei, as in the case of electronically non-adiabatic transitions. Although an accurate description of the collision dynamics would in general require consideration of both short and long range interactions, most of the models take into account only one type of interaction. In many cases this assumption is justified, since usually one of the possible interactions appears to contribute dominantly to the inelastic cross section. However this is not an inviolable rule. Furthermore, even for the same system, the relative importance of short, intermediate or long range forces may vary substantially with temperature and thus various models must be considered in carrying out calculations over different temperature ranges.

There are numerous theoretical treatments of V-T, V-V and in two atom systems E-E energy transfer in inelastic collisions. In contrast, E-V or E-R energy transfer processes, occuring via electronically adiabatic transitions have not as yet been studied extensively, despite the fact that their possible importance in the quenching of excited state atoms has been repeatedly suggested. Of particular interest in this respect are the large isotope effects observed in the removal of excited atoms by small isotopically substituted molecules. Recent data of such large isotope effects are included in Table 1.II. In most of these cases quenching had been the only available channel and in general, when reactive channels were available, the isotope effects were relatively small. As Table 1.II indicates, large isotope effects may come about in the event of substituting D for H atoms in hydrogen-containing quenching molecules. Such observations can provide a

TABLE 1.II

Some Recent Results of Isotope Effects

Type of process: $A^{*}+Q(v = n, J = k) \rightarrow A+Q^{*}(v = m, J = l)+\Delta E$

Transition	$\Delta E/cm^{-1}$	Q	σ/cm^{2}	Ratios	Comments	Ref.
$I(5^2P_{1/2})\rightarrow I(5^2P_{3/2})$	7603	H_2	7.4×10^{-19}	92	$\Delta v=2$(2 channels with $\Delta E<200$ cm^{-1} and $\Delta J=\pm2$; positive temperature dependence)	64
		D_2	8.0×10^{-21}	$\frac{1}{260}$	$\Delta v=2$(0 channels with $\Delta E<200$ cm^{-1} and $\Delta J=\pm2$; negative temperature dependence)	
		HD	2.1×10^{-18}		$\Delta v=2$(4 channels with $\Delta E<200$ cm^{-1} and $\Delta J=\pm2$).	
		CH_4	1.7×10^{-18}	46	$\Delta v=3$	65
		CD_4	3.7×10^{-20}		$\Delta v=4$	
$Te(5^3P_{1,0})\rightarrow Te(5^3P_2)$	4707	H_2	5.8×10^{-17}	840	$\Delta v=1$	66
		D_2	6.9×10^{-20}		$\Delta v=2$	
$Tl(6^2P_{3/2})\rightarrow Tl(6^2P_{1/2})$	7793	H_2	2.8×10^{-18}	7		67
		D_2	3.9×10^{-19}			
$Pb(6^3P_1)\rightarrow Pb(6^3P_0)$	7819	H_2	1.6×10^{-20}	3.5	$\Delta v=2$	68
		D_2	$<4.7\times10^{-21}$			

Table 1.II

contd.

Transition	$\Delta E/cm^{-1}$	Q	σ/cm^2	Ratios	Comments	Ref.
$Pb(6^3P_2) \rightarrow Pb(6^3P_1)$	2831	H_2	8.4×10^{-18}	1/8	$\Delta v=1$ not near resonant	69
		D_2	$\sim 6.8 \times 10^{-17}$		$\Delta v=1$ near resonant	
$Cs(6^2P_{3/2}) \rightarrow Cs(6^2P_{\frac{1}{2}})$	554	H_2	2.6×10^{-15}	1.6	E↔R, negative temperature dependence	
		D_2	1.6×10^{-15}		positive " "	
		HD	2.2×10^{-15}	0.7	positive " "	
		C_3H_8	8.0×10^{-15}		negative " "	
		C_3D_8	1.2×10^{-14}	0.7	negative " "	
		C_2H_6	5.8×10^{-15}		negative " "	
		C_2D_6	7.5×10^{-15}	0.8	negative " "	
		CH_4	1.4×10^{-15}		~600 K slightly negative temperature dependence	71
		CH_3D	1.6×10^{-15}		slightly negative temperature dependence	
		CH_2D_2	1.8×10^{-15}		slightly positive temperature dependence	
		CHD_3	2.0×10^{-15}		strongly positive temperature dependence	

Table 1.II

contd.

Transition	$\Delta E/cm^{-1}$	Q	σ/cm^2	Ratios	Comments	Ref.
		CD_4	2.2×10^{-15}		strongly positive temperature dependence	
$Ar(4^3P_1)\rightarrow Ar(3^1S_0)$	93747	H_2	5.2×10^{-16}	3.2	$\Delta v=3$ (E→E+V+R)	
		D_2	1.8×10^{-16}		$\Delta v=4$	
		HD	2.4×10^{-15}	0.07		
					$\Delta v=3$ (for one channel $\Delta E=4\ cm^{-1}$)	72
$Ar(4s\ ^1P_1)\rightarrow Ar(3^1S_0)$	95402	H_2	3.4×10^{-17}		$\Delta v=4$ (2 channels)	
		D_2	2.8×10^{-16}	0.16	$\Delta v=5$ (1 channel)	
		HD	1.9×10^{-15}	0.15	$\Delta v=6$ (8 channels)	
					$\Delta v=5$ (7 channels, for one of them $\Delta E = 8\ cm^{-1}$)	72
$O_2(^1\Sigma_g^+)\rightarrow O_2(^1\Delta_g)(\Delta v_{O_2}=0)$	5315	H_2	5.8×10^{-18}		$\Delta v=1$ $\Delta E = 844\ cm^{-1}$	
$O_2(^1\Sigma_g)\rightarrow O_2(^1\Delta_g)(\Delta v_{O_2}=1)$	3806	HD	2.2×10^{-17}	0.2	$\Delta v=1$ $\Delta E = 87\ cm^{-1}$	
		D_2	1.0×10^{-17}	2.2	$\Delta v=1$ $\Delta E = 612\ cm^{-1}$	73
$O_2(^1\Sigma_g)\rightarrow O_2(^1\Delta_g)$ or $O_2(^3\Sigma_u)$	5315	H_2	5.5×10^{-18}		Possibly four centre reactions :	
	13195	D_2	3.0×10^{-19}	18.3	$O_2(^1\Sigma_g)+H_2(D_2)\rightarrow 2OH(OD)$	

Table 1.II

contd.

Transition	$\Delta E/cm^{-1}$	Q	σ/cm^2	Ratios	Comments	Ref.
		HD	2.0×10^{-18}	0.15		
		H_2O	7.4×10^{-17}	1.4	± 50% error	
		D_2O	5.3×10^{-17}			
		C_2H_2	6.8×10^{-18}	0.8		
		C_2D_2	1.3×10^{-18}			
		C_2H_4	6.8×10^{-18}	3.1		
		C_2D_4	2.2×10^{-18}			
		C_3H_6	1.1×10^{-17}	3.1		
		C_3D_6	3.5×10^{-18}			74
$O_2(^1\Delta_g) \rightarrow O(^3\Sigma_g^-)$	7880	H_2O			2 μs lifetime in solution	*
		D_2O			20 μs " " "	

* D.R. Kearns and P.B. Merckel, J. Am. Chem. Soc., 68, 1603, (1972)

powerful means of examining the molecular dynamics of energy transfer, as one can perceive that the potential hypersurfaces are not altered by isotopic substitution within the Born-Oppenheimer approximation.

Explanation of the large isotope effects observed, simply in terms of the mass effect on the reduced partition function ratio of the isotopic molecules is inadequate. For example, the ratio of the cross section for quenching of $Te(5^3P_{o,1})$ atoms[66] by H_2 and D_2 is 840 and lies far away from any expected ratio due to the mass effect. The quenching of $I(5^2P_{\frac{1}{2}})$ by H_2, HD and D_2 is more revealing. As shown in Table 1.II, the cross section for HD does not lie between those for H_2 and D_2, as would be expected on the basis of mass effect. On the contrary, it is larger than both of them.[64] The temperature dependences of the relaxation rates of $I(5^2P_{\frac{1}{2}})$ in the presence of H_2 and D_2 have also been examined and show marked differences, exhibiting opposite signs.[62]

These findings have been primarily discussed in terms of long range interactions leading to near resonant E→V energy transfer. Other results for the quenching of excited species, as those for $O_2(^1\Sigma g^+)$ + H_2, HD and D_2, for which appreciable isotope effects have also been observed, have been explained in terms of both short and long range interactions inducing near resonant energy transfer.[73,75,76] The kinetic data for the quenching of $Ar(4^3P_1, {}^1P_1)$ by H_2, HD and D_2, which is accompanied by a highly specific excitation of the rovibrational levels of the $B^1\Sigma_u^+$ excited state of these molecules, have also been discussed along these lines,[72] by considering near resonant energy transfer due to dipole-dipole interactions. However, it is clear that further evidence is necessary to more firmly substantiate these proposals and one of the objectives of the present work is to contribute in this respect.

Short range interaction model

The short and long range interaction theories which have been applied in describing electronically adiabatic collisions are basically extensions of corresponding models for V-T and V-V energy transfer. The most popular theory attributing V-T or V-V energy transfer to short range interactions is the Schwartz, Slawsky and Herzfeld (SSH) theory.[77] In this approach only collinear collisions have been treated explicitly by assuming an exponential repulsive potential of the form

$$V(x,R) = C \exp(-a(R-x)) \qquad (1.16)$$

where C is a constant, R is the relative position vector of the colliding species and a and x are as previously defined (cf. page 18).

The original SSH theory has been criticised and improved by several authors.[78,79] Thus, in a modified version, a more sophisticated fitting to Lennard-Jones potentials derived from gas kinetic data has been considered in an attempt to account for long range effects.[78] However, since short range interactions dominate the experimental Lennard-Jones potentials, this is a poor approach if long range forces are important.

The following predictions can be made for the transition probability, P, evaluated originally on the basis of simple first order perturbation theory and in a latter version on the basis of the first order distorted-wave approximation, in which terms dependent on x and R can be separated:

(a) P is proportional to the square of translational and vibrational matrix elements, in which the translational wavefunctions are coupled by the exp(-aR) part of the potential and the vibrational wavefunctions by exp(-ax) respectively, for V-T energy transfer. For V-V energy transfer, only vibrational matrix elements appear in the expression of the transition probability. In general multiquantum vibrational transitions are expected to be extremely inefficient.

(b) A positive temperature dependence should be expected for the efficiency of energy transfer, over a wide range of temperatures.

(c) In general, transition probabilities calculated for near resonant processes are expected to be larger than those for non-resonant processes. As will be shown in the discussion of the long range interaction models, the range of energy mismatches, for which a process is characterised as near resonant, is mainly determined by the parameter a^{-1}, which defines the range of the interaction potential.

The SSH model has been extended to E-V energy transfer processes by Dickens, Linnet and Sovers.[80] These authors emphasized the importance of multiquantum vibrational transitions when these result in an effective minimization of ΔE (cf. process 1.1). The expression for the quenching cross section contains, apart from a vibrational matrix element as in the previous cases, an electronic matrix element, in which the two atomic states are coupled by an operator of the form $C'(1 + br_1)$, where C' is a constant, $b \sim 10^8$ cm^{-1}, and r_1 represents an electronic coordinate of the atom.

A version of this approach has been applied by Kear and Abrahamson,[73] in calculating quenching cross section of $O_2(^1\Sigma_g^+)$ by several molecules and very recently by Braithwaite et. al.,[76,81] who modified Kear and Abrahamson's calculations to include rotational transitions as well. In all cases, a positive temperature dependence was predicted for the quenching efficiency.

Long range interaction model

The basic feature of the long range parts of the intermolecular potenial is that they may give significant transition probabilities for near resonant energy transfer but are dramatically decreased as the energy mismatch increases. This was one of the main reasons for

attributing the large isotope effects observed for processes like 1.1 to long range interactions. A comparison of the sensitivity between the transition probabilities, due to the long or short range parts of the interaction potential as a function of the energy mismatch, can be obtained[82] by considering that P has an almost constant maximum value for a range of energy discrepancies determined by 1.17,

$$\Delta E \sim \frac{hvn}{a} \qquad (1.17)$$

where n determines the variation of the potential as a function of R ($V \propto R^{-n}$), v is a typical average velocity at room temperature, ($v \sim 10^5$ cm s^{-1}) and a^{-1} is the range of the potential. Assuming that $n = 6$ and $a^{-1} \sim 4 \times 10^{-8}$ cm for the long range part of the potential and that $n = 12$ and $a^{-1} \sim 5 \times 10^{-9}$ cm for the short range interactions, we deduce that near resonant conditions prevail up to $\Delta E \sim 80$ cm^{-1} in the case of long range interactions, vs. $\Delta E \sim 1200$ cm^{-1} for short range interactions.

Over the past decade it has been recognised that the large cross sections along with the T^{-1} dependence of the transition probability observed for many near resonant V-V energy transfer processes can be explained in terms of long range interactions . Mahan first suggested[83] the importance of dipole-dipole interactions, exhibiting an R^{-3} dependence, in vibrational energy transfer between CO molecules. Numerous modifications of this original formulation have appeared in the meantime. Experimental results supporting the validity of these proposals have been reviewed by Moore.[84]

From the various theoretical treatments the approach of Sharma and Brau is particularly noteworthy.[85,86] Sharma and Brau, by expanding the interaction potential in terms of multipole moments and employing the Born approximation[12] showed that higher multipolar interactions can make

significant contributions to the overall efficiency of V-V energy transfer. Their model, which also includes the effect of rotational motion was developed along the lines of Cross and Gordon's calculations[87] of dipole-dipole rotationally inelastic scattering and Gray and Van Kranedock's theory[88] of pressure broadening. More sophisticated numerical calculations have been carried out by Dillon and Stephenson,[89,90] who showed that multiquantum processes, both rotational and vibrational can play an important role in V-V energy transfer, if higher order approximations are included. The dependence of the transition probability on ΔE was found less drastic than that predicted on the basis of the first Born approximation. This has been also recognised by Sharma et.al., who, in a recent work,[91] emphasised the importance of higher order approximations for large ΔE.

Based on the outcome of the above treatments, the following general predictions can be made:

a) P and consequently the inelastic cross section is strongly dependent on the magnitude of ΔE and usually at first order approximation, this dependence takes the form: $P \propto \exp\left(\frac{-2\,\Delta E b}{h\nu}\right)$, where b is the impact parameter and v the mean relative velocity. Due to this dependence, a high specificity is expected for the excited vibrational levels populated.

b) P is proportional to the square of the rovibrational matrix elements for optical transitions. In consequence, for the same range of ΔE, the efficiency of a V-V process will be largely determined by the optical selection rules.

c) For inelastic collisons within the thermal range, P is expected to exhibit a negative temperature dependence.

Extension of the multipolar interaction models in systems in which electronic relaxation occurs has been applied by several authors. Thus, Melton and Klemperer[92] and Gordon and Chiu[93] developed a dipole-dipole

interaction theory to explain the efficient relaxation of $^{14}N^{16}O$ ($A\ ^2\Sigma^+$) by $^{14}N^{16}O$ ($X\ ^2\Pi$) and $^{15}N^{16}O$ ($X\ ^2\Pi$). Breckenridge et.al.[94] discussed the deactivation of $Zn(4^1P_1)$ by $NO(X^2\Pi)$ along these lines. The first attempt to extend the Sharma and Brau model for higher multipolar interactions to E↔V energy transfer processes was made by Ewing.[95] More recently, Braithwaite et.al.[75,76,81] used a more refined version of this model to explain the quenching of $O_2(^1\Sigma_g^+)$ by several molecules. Finally, a quadrupole-quadrupole theory, accounting for intramultiplet transitions in some heavy atoms, when they are quenched by hydrogen isotopes has been developed by French and Lawley.[96] It should be noted here that a serious questioning of some of these multipole-multipole formulations, especially those based upon the Born approximation, has appeared in several papers.[97-99]

D) SOME CONSIDERATIONS IN CALCULATING INELASTIC CROSS SECTIONS

Accurate theoretical treatments of energy transfer processes tend to be difficult even when the interactions of the colliding species are assumed to occur on a single adiabatic potential hypersurface. Furthermore, for processes involving electronic transitions, as in the case of E↔V energy transfer, couplings of two or more hypersurfaces must be considered, which leads to additional complications in calculating inelastic cross sections. As a result, attempts at a systematic theoretical treatment of inelastic electronic transitions have only recently appeared and mainly for atom-diatom collisions. The basic steps usually followed in such calculations can be outlined as follows:

i) First, a convenient and appropriate method of approximation* in treating the dynamics of the collision is selected. A discussion of the various theoretical techniques usually applied is beyond the scope of this introduction. A comprehensive review summarizing the recent

*A flow chart for using various criteria to arrive at a reasonable choice of a method has been formulated by Gordon.[114]

developments in theoretical methods has been given by Secrest.[133] Quantum mechanical and classical theories solve Schrödinger's and Hamilton's equations respectively, either analytically or numerically. Although a purely classical treatment is feasible for many systems, even when these consist of more than three atoms, it can be highly inaccurate in accounting for certain "quantum effects", such as quasi-bound states, selection rules and resonances. In contrast, quantum mechanical calculations always account correctly for all dynamical effects, but are not feasible in most cases. Thus, exact quantum mechanical studies have only appeared in the last three years, and mainly for collinear geometries and only recently extended in three dimensions. Particularly interesting in this respect, is the work of Zimmerman and George[100,103] who studied the E↦V energy transfer processes in $X(^2P_{\frac{1}{2}}) + H_2$ systems, where $X(^2P_{\frac{1}{2}})$ denotes an excited halogen atom. This work indicated the existence of strong resonance effects between the electronic and vibrational modes of the system, in accordance with the findings in a previous study by Top and Baer[104], for a reactive collinear system, and the latest work of Rebentrost and Lester[105] for the quenching of $F(2^2P_{\frac{1}{2}})$ by H_2. A detailed comparison of classical and quantum mechanical calculations for V↦V energy transfer has been carried out recently by Gordon[106] and Patengill.[107]

Due to the limitations of both quantal and classical approaches semiclassical approximations are the most widely used in describing inelastic collisions. A usual assumption in these approximations is the representation of the trajectory by a straight line, although lately, curved trajectories have been used as well.[108] The transition probability is calculated quantum mechanically, by using time dependent perturbation theory. Thus, despite the use of classical trajectory data as input, semiclassical theories can account for "quantum effects" without involving the difficulty of purely quantum mechanical calculations.[109] Gentry and

and Giese[110] have explored the validity of semiclassical approximations in inelastic collisions, by comparing the results obtained for several model systems with those from rigorous quantum mechanical calculations. The restrictions imposed by the use of classical trajectories have been discussed by Child.[117]

ii) The form of the Hamiltonian of a system depends on the coordinate system used. Although the calculated results must be similar when transformed from one coordinate system to another, the computational difficulties associated with each system may differ substantially. The most frequently used systems of coordinates are either space fixed (SF) or body fixed (BF). In the former all angular momenta are defined with respect to an SF arbitrary z-axis. In the latter, the z-axis lies along one of the characteristic vectors of the molecular systems, such as the R vector, defined by the distance between the centres of mass of the atom and the molecule. Calculations within the BF system usually lead directly to a good approximation but the results must always be transformed back to the SF frame.[111] Other coordinate systems, simplifying the computations significantly have appeared as well, but are not as yet in wide use.[112]

iii) As noted in the previous section, the form of the interaction potential giving rise to an energy transfer process will essentially determine both the temperature dependence of inelastic cross sections and the conditions for efficient energy transfer. In general, the Hamiltonian describing the collision of an atom with a rovibrator may be expressed[113] as in 1.18.

$$H = -\frac{h^2}{2\mu} \nabla^2 (R) + H_{int}(x) + V(x,R) \qquad (1.18)$$

where H_{int} is the Hamiltonian refering to the internal motion of the rovibrator, μ is the reduced mass of the system, x and R are as previously defined and V(x,R) is the interaction potential defined by

1.19 at infinite separations.

$$\lim_{R \to \infty} V(x,R) = 0 \qquad (1.19)$$

From 1.18 it becomes clear that the effect of $V(x,R)$ is to couple the relative motion described by the first term with the motion due to the internal degrees of freedom, described by the second term. Equivelantly, it can be stated that $V(x,R)$ causes a change in the internal state $\phi_i(x)$ of the system, where $\phi_i(x)$ represents a product of rotational-vibrational-electronic wavefunctions for the rovibrator and the electronic wavefunction of the atom at infinite separations.

As indicated in 1.18, there are two potential functions, which should be taken into account in a calculation. First, a potential must be assumed for the isolated rovibrator. Usually, harmonic oscillator potentials or anharmonic functions, as the Morse potential are employed. Secondly, an interaction potential $V(x,R)$ must be included. This can be achieved either by using a model potential, as for example the Lennard-Jones potentials, or the repulsive and attractive potentials discussed in the previous section,[77,85] or by applying numerical techniques in determining accurate ab initio potentials.[114] These analytically modelled potentials introduced in the last few years, do not contain any parameters and therefore the obtained quantum mechanical results are unambigious.

For the interaction of an atom with a diatomic molecule, a generalised form of $V(x,R)$ is given by 1.20.

$$V(x,R) = V_o(R) + \sum_n V_n(R)\, P_n(\cos\gamma) \qquad (1.20)$$

where $P_n(\cos\gamma)$ are Legendre functions and γ is the angle between R and the bond distance in the molecule.

Orientation dependent potentials of the type described by 1.20 are applied in calculations in which rotational transitions are important, although the spherically symmetric potentials $V_o(R)$ can be adequate for simple approximate calculations in some systems.

E) SOME EXPERIMENTAL METHODS

Throughout the last decade there have been numerous experimental studies on the removal of electronically excited atoms.[2] In the majority of these studies kinetic data have been obtained in the form of bulk rate constants and therefore provide only indirect evidence for the various mechanisms which determine the decay process at the microscopic molecular level. Unfortunately, direct observations of the product species, as for example the vibrationally excited molecules produced in process 1.1, are usually extremely difficult to make and reliable kinetic data in this respect are still scant. However, it should be noted that in the last three years the number of investigations, in which the internal states of the product molecules emerging in an elementary process are directly resolved, has considerably increased. This is mainly due to the recent developments in laser technology,[8,118,129] which have allowed for a more extensive utilization of laser sources either instead of a flash or as a monitoring beam. Thus, some of the experimental methods which have been employed in V-V or V-T energy transfer studies [119] have now been extended to yield data for the quenching of excited atoms. A typical example is provided by the work of Leone and Wodarczyk,[120] who investigated the E↔V energy transfer from $Br(4^2P_{\frac{1}{2}})$ to HCl and HBr. In their experiments, $Br(4^2P_{\frac{1}{2}})$ atoms were produced by photolysing Br_2 at 473 nm by means of a frequency-doubled Nd: YAG laser. The relaxation rates were measured by following the time-resolved fluorescence from both $Br(4^2P_{\frac{1}{2}})$ and HCl(v=1) or HBr(v=1).

Several reviews[2,121-124] deal in detail with the various experimental methods employed in kinetic studies of excited atomic states. However, we propose here to summarize the basic features of some of these techniques.

1) Kinetic spectroscopy.

This is one of the oldest techiques, originally developed by Porter and Norrish.[125] An intense pulse of light is used to produce the atomic transients of interest, and their subsequent kinetic behavior can be observed either by flash spectroscopy or time resolved atomic absorption spectrophotometry. In the first method, a spectroflash of short duration, giving essentially white light from 200 nm to the near I.R. wavelengths, is fired at different time intervals after the photolysis flash by means of a delay unit. A spectrograph is employed to record the absorption spectra of the intermediates photographically.

In time resolved atomic absorption spectrophotometry, instead of recording the whole range of wavelengths at a single time, the rate of reaction is monitored at a single wavelength over all times. Suitable monochromatic radiation, corresponding to the atomic resonance radiation, is passed through the reaction vessel which is usually adapted to a monochromator and is recorded photoelectrically. The atomic resonance radiation is produced by a microwave or r.f. discharge in an atomic vapour.

In general, it is not possible to use a kinetic spectroscopy arrangement with the combined photometric sensitivity and kinetic accuracy of absorption spectrophotometry. Thus, despite the fact that kinetic spectroscopy allows in principle the recording of a large part of the spectral range of transients and therefore can provide useful information when these transients are uncertain, the much simpler and more accurate absorption spectrophotometry is to be prefered. Typical atomic concentrations detected in most experiments employing the latter method are of the order 10^{12} atoms cm^{-3}. However, by using repetitive photolytic pulses and signal averaging this range of concentrations can be further decreased. It should be noted here that in many absorption experiments the absorbance is not a linear function of the concentration

and corrections should be made (cf. Chapter 2), which may introduce a source of inaccuracy.

2) Time-resolved atomic resonance fluorescence

Excited or ground state atoms are produced by employing flash photolysis as in atomic spectrophotometry. The species of interest are further excited by absorbing resonance radiation emitted from an atomic emission lamp, which is set at right angles to the flash lamp. Induced fluorescence following this excitation is detected photoelectrically, the axis of observation being perpendicular to the plane formed by the flash lamp and atomic lamp axis. The main drawback in applying this technique is associated with the possible fluorescence of both excited and ground states produced by the photolytic flash.[2] To avoid this, the atomic resonance radiation must be monochromated, without a drastic decrease of its intensity. The use of the intense, highly monochromatic radiation of tunable dye lasers as an exciting beam is ideal in this respect, allowing for observation of concentrations as low as 10^4 atoms cm^{-3} vs. typically 10^{10} atoms cm^{-1} when conventional atomic emission lamps are employed. To date, only the removal of $I(5^2P_{\frac{1}{2}})$ atoms in the presence of various molecules has been extensively studied[64,65,126] by this technique. In these studies, the problem of monochromating the input radiation is overcome by employing the atmospheric O_2 as a filter for all the wavelengths emitted from the atomic iodine lamp, with the exception of the 206.2 nm line.

In contrast to the experiments employing absorption techniques, the fluorescence intensity is essentially a linear function of the atomic concentration, and thus a source of possible errors present in absorption studies is non-existent here.

3) Chemical lasers

There are two ways in which chemical lasers can be used to study molecular dynamics. Firstly, the radiation emitted by a CW laser can be used as a monitoring beam to probe the concentrations of transients or products by time resolved resonance absorption or fluorescence. The experimental method employed by Lin and Shortridge,[127] in which the vibrational excitation in CO following E→V energy transfer from $O(2^1D_2)$, $Br(4^2P_{\frac{1}{2}})$ or $I(5^2P_{\frac{1}{2}})$ atoms was directly observed, falls within this category. Secondly, kinetic information can be extracted by observing the conditions of operation of the chemical laser itself. Thus, considering that many bimolecular processes can yield vibrational lasers based upon excited diatomic or triatomic products, the dependence of gain upon vibrational population inversion and temperature can be used to obtain information about the specificity of energy release from such chemical lasers, (cf. highest gain method, equal-gain temperature method and other methods developed by Pimentel and coworkers).[8] Furthermore, even the fact that laser action can be obtained from several bimolecular processes can be quite informative for the dominating mechanism. An example is provided by the recently developed NO, H_2O and HCl I.R. lasers in which population inversion was achieved by E→V energy transfer from $Br(4^2P_{\frac{1}{2}})$ atoms.[130-132] Finally, it should be noted that comparative studies of the performance of various photochemical lasers, as for example the $I(5^2P_{\frac{1}{2}})$ and $Br(4^2P_{\frac{1}{2}})$ lasers, when different parent molecules are used, can be useful in studying the dynamics of photodissociation and the subsequent removal processes.[8]

The use of chemical lasers in experimental investigation of molecular dynamics is limited by the necessary precondition for laser action, i.e. the existence of a population inversion, which can not be achieved in many systems of interest.

F) OBJECTIVES OF THE PRESENT WORK

As was mentioned in section A, the main objective of this work is to explore the conditions which may lead to efficient deactivation of low lying excited atomic states. In this respect, mechanisms which can give rise to large isotope effects, as those included in Table 1.II, have received particular attention. Essentially, such mechanisms can be of great importance in E→V energy transfer processes and therefore may have interesting practical implications.

The experimental data obtained in this work are primarily concerned with the determination of deactivation rates of $I(5^2P_{\frac{1}{2}})$ atoms by pairs of isotopically substituted molecules. Bulk rate constants were obtained by using time resolved atomic absorption spectrophotometry. In addition, rate data for spin-orbit relaxation of $I\ 5(^2P_{\frac{1}{2}})$ by some of the molecules studied here have been reported previously, by using mainly flash spectroscopy, which is less precise and in some cases has been proved unreliable.[2] As one of the aims of the present work is to make a detailed comparison between isotopically substituted species, these data have been redetermined in order to provide a self-consistent and reliable set of data. In order to establish more concrete information about the nature of the potential hypersurfaces involved in some of the studied systems, the temperature dependence of the rate constants was determined over wide temperature ranges. Furthermore, as indicated in Table 1.II, previous studies of large isotope effects involve mostly such molecules as H_2 and D_2, which can not be studied by the I.R. fluorescence techniques. The present work has therefore been extended to include I.R. active molecules in the hope of stimulating further I.R. fluorescence studies, which can provide direct evidence for the importance of E→V energy transfer in quenching processes.

The competition between reactive and quenching pathways in the

deactivation of $I(5^2P_{\frac{1}{2}})$ by various molecules and in particular by some iodides has also been examined, and the performance of these iodides in the iodine photodissociation laser has been explored in the light of the kinetic data obtained.

Finally, in order to further test the proposals, according to which near resonant energy transfer due to long range interaction can be of great importance for the removal of excited atoms and for the observed large isotope effects, theoretical calculations were carried out on the basis of a simplified multipolar interaction model.

Chapter 2

EXPERIMENTAL SECTION

A) Introduction

The general features of the experimental arrangements employed in this work have been discussed by several authors.[62,134,135] We shall, therefore, confine our discussion here to a brief consideration of the salient features of the systems used and the modifications made in this particular study. A brief description of the iodine photodissociation laser system will be included in Chapter 3.

In general, there are three main problems which arise in the experimental investigation of the deactivation of excited species by time resolved atomic absorption spectrophotometry. The first problem is connected with the time resolution of the method. The decay process of interest must be initiated in a time which is short in comparison with the overall decay time. If the scattered light effects and the time constant of the detection system are negligible, the time resolution is essentially determined by the duration of the electric discharge lamp and can be improved to a few microseconds. The advent of various pulsed laser systems in recent years, has transformed this limit notably by improving the resolution by a factor of 10^6. However, in most conventional systems, the "dead time" of the detection system exceeds the length of the flash. In such cases, the time resolution is determined either by the scattered light effects, (e.g. actual flash duration in the visible, and overloading of the photomultiplier), or by the time constant of the detection system.

The second problem is associated with the choice of an appropriate compound, which can be easily photolysed to yield the species of interest in high concentrations. In this respect the following properties are desirable: a) The relaxation of the studied intermediates should be highly inefficient in the presence of the "parent" compound. b) The compound should not absorb strongly the resonance radiation used to monitor the excited species. c) It is imperative that the molecular fragments

produced in the photolysis do not form undesirable byproducts, as for example polymers, which would eliminate a repetitive use of the reaction vessel.

The third problem is due to the fact that, under the conditions prevailing in most experiments, the attenuation of resonance radiation is not a linear function of the atomic concentration. For quantitative kinetic studies, the functional relationship between the atom concentration, c, and the intensity of resonance absorption must be known. In general, this relationship depends upon the line profiles of the source and of the absorber of resonance radiation and it is usually determined by employing a modified expression of the Beer-Lambert law,[2] viz:

$$\ln(I_o/I) = a(c.l)^{\gamma} \qquad (2.1)$$

where a is an arbitrary constant analogous the extinction coefficient but with units $(cl)^{-\gamma}$, I_o is the intensity of light transmitted in the absence of an absorbing atomic species, I the intensity in the presence of such species and γ is a coefficient which is determined experimentally. Recently, there has been some controversy regarding this approach. Clyne and Bemand[136] have criticized the above procedure and proposed a more involved formulation of the problem. This criticism indicates that as rate measurements become more precise, a more detailed determination of the relationship between light intensity and concentration of absorber ("curve of growth") will be necessary.

As in all investigations employing flash photolytic techniques, we can distinguish three main parts in the experimental arrangement used in the present work:

a) A flash lamp for producing a short photolytic flash, along with energy storage units, namely; capacitors, power supply and triggering unit.

b) A reaction vessel with a coaxial housing for the thermal bath in the temperature dependence experiments.

c) A system for detecting $I(5^2P_{\frac{1}{2}})$ atoms. This comprised of an iodine atomic lamp, powered by means of a microwave discharge, a photomultiplier for detecting the resonance radiation emitted by the iodine lamp and a data recording system.

For the purposes of the present work, two main experimental arrangements were employed. In the first, which was used in the early studies of isotope effects, the flash lamp was placed close to the reaction vessel with their axes parallel. For the temperature dependence experiments a coaxial flash lamp reaction vessel system was used.

Temperature dependence experiments: Considering that the temperature coefficients measured for the spin-orbit relaxation of $I(5^2P_{\frac{1}{2}})$ are generally small, an investigation of the decay rates of $I(5^2P_{\frac{1}{2}})$ at different temperatures requires a considerable degree of accuracy and reproducibility for the experimental conditions normally employed. In addition, the concentrations of $I(5^2P_{3/2})$ and $I(5^2P_{\frac{1}{2}})$ following the flash photolysis must be kept at low levels. High atomic concentrations can give rise to an appreciable interference of kinetic effects due to atomic recombination, and the kinetic behavior of such processes at different temperatures can significantly complicate the measurement of the $I(5^2P_{\frac{1}{2}})$ decay rates. The method used in the present work eliminates these experimental difficulties. The low concentrations of $I(5^2P_{\frac{1}{2}})$ atoms produced following the pulsed irradiation of the samples with low flash energies ensured the absence of any radical-radical effects and in particular the formation of I_2, which is a very efficient quencher[137] of $I(5^2P_{\frac{1}{2}})$ atoms.

B) ENERGY LEVELS OF IODINE ATOMS AND FORMATION OF $I(5^2P_{\frac{1}{2}})$

The ground state configuration of halogen atoms is $np^5\ ^2P_J$. In consequence, this state is split into two J sub-levels, $^2P_{3/2}$, and $^2P_{\frac{1}{2}}$

with the latter having a higher energy according to Hund's rules. Excited halogen atoms in the $np^5\ ^2P_{\frac{1}{2}}$ state are optically metastable, as the transition to the ground state is electric dipole forbidden and magnetic dipole and electric quadrupole allowed. The two 5^2P_J states of iodine atoms are separated[138] by 7603.15 cm^{-1}, and consequently, the Boltzmann population of this state at 300 K is very small, namely $7x10^{-17}$. The mean radiative lifetime of $I(5^2P_{\frac{1}{2}})$ has been theoretically determined[139] to be 0.13 s, corresponding to a transition rate of 7.7 s^{-1}. An experimental determination of the lifetime is difficult due to the high metastability of $I(5^2P_{\frac{1}{2}})$ atoms. Thus, the contribution of spontaneous emission, (i.e. the inverse of the radiative lifetime), as a rate coefficient, is very small in comparison with the overall decay rate. Therefore, measurements of the radiative lifetime on the basis of kinetic data are difficult to make. Despite these difficulties, Derwent and Thrush[140] have measured the total radiative transition rate of $I(5^2P_{\frac{1}{2}})$ to be 5.9 s^{-1} and Zuev et.al.[141] determined a value of 5.4 s^{-1}. The importance of these measurements is that they can be used to test the basis of the theoretical result for this quantity.

The hyperfine structure of the 5^2P_J state of atomic iodine has also been examined. In zero field the $^5/_2$ nuclear spin of I^{127} couples with the total angular momentum of the $5p^5$ electrons to give two hyperfine levels of the $^2P_{\frac{1}{2}}$ upper state and four hyperfine levels of the $^2P_{3/2}$ state. The zero magnetic field splitting of the former level,[142] is 0.662 cm^{-1} and the overall splitting of the latter[142] 0.237 cm^{-1}.

The optical transitions of iodine atoms that have been observed[1a] by absorption spectroscopy in the vacuum U.V.,along with a few absolute f values,[143] are included in Figure 2.1. These and other transitions have been well established in emission from discharges.[1]

In general, halogen atoms may be produced by photolyzing several

Figure 2.1: Some optical transitions (in nm) of atomic iodine

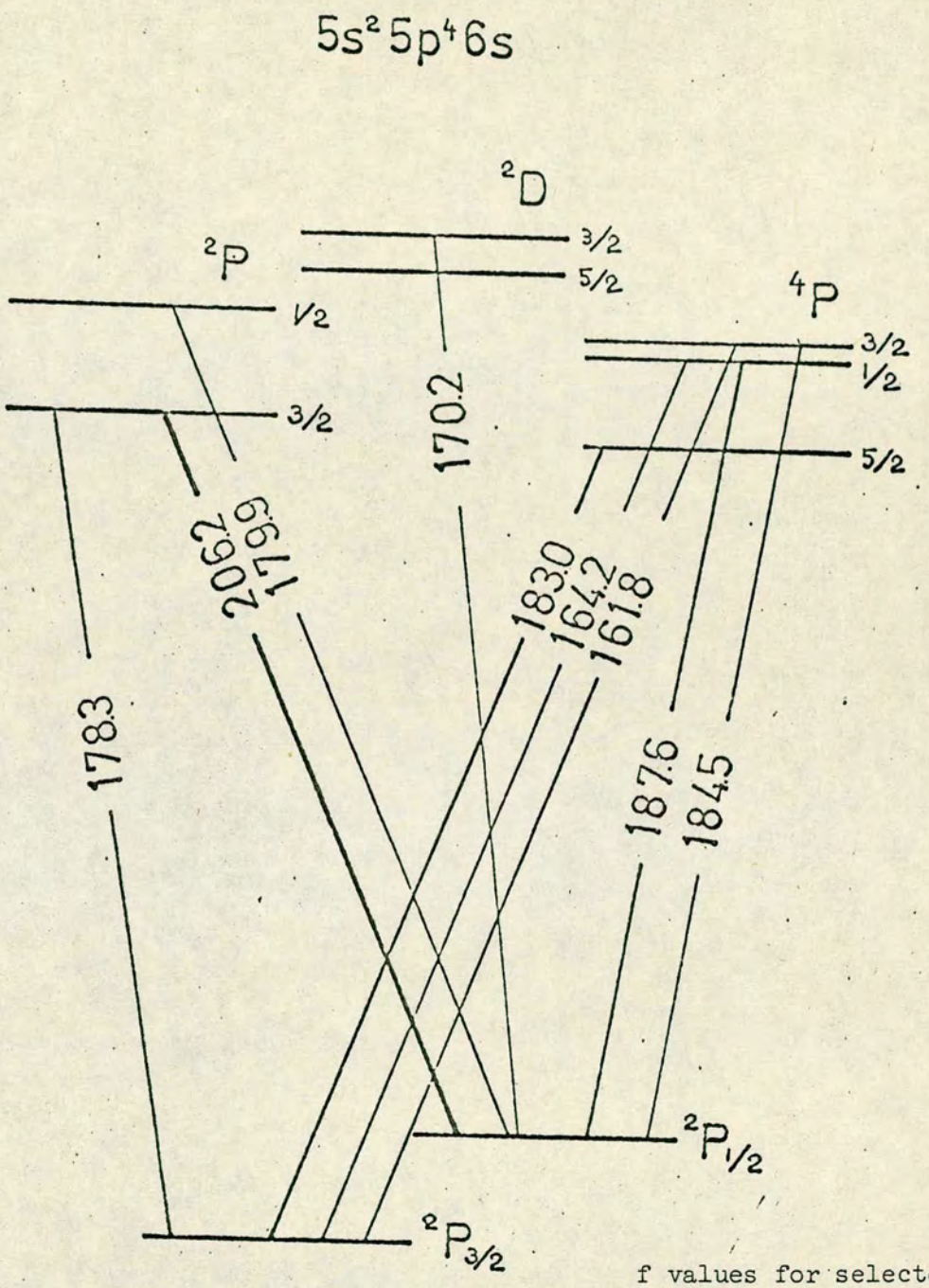

f values for selected transitions

λ/nm	f
161.8	5.3×10^{-2}
178.3	1.2×10^{-1}
179.9	1.0×10^{-1}
184.5	7.1×10^{-3}
206.2	3.8×10^{-3}

alkyl or fluoro-alkyl halides. The continuous nature of the electronic spectra of these compounds does not allow the prediction of the spin orbit states produced. Thus, these can be only determined by direct spectroscopic observation of the atomic state of interest. The photolysis products of various iodides have been extensively studied by stimulated emission experiments in the infra-red and time resolved absorption spectroscopy in the U.V.[1,144]. Some of the iodides which yield $I(5^2P_{\frac{1}{2}})$ following broad-band U.V. photolysis, along with the fractional yield of the excited atom[144,145] are given in Table 2.I.

In most of the experiments of this work, $n\text{-}C_3F_7I$, CF_3I and CD_3I were employed. As was demonstrated (cf. Chapter 3), the decay efficiency of $I(5^2P_{\frac{1}{2}})$ atoms in the presence of these compounds is minimal and adequate concentrations of $I(5^2P_{\frac{1}{2}})$ can be produced, ($c \sim 10^{12} - 10^{13}$ atoms cm^{-3}), following photolysis with wavelengths, $\lambda > 200$ nm, even when very small flash energies ($E \sim 10$ J) are employed, without using a reflector to condense light from the photolysis flash. In addition, as the U.V. absorption spectra indicate, these iodides do not strongly absorb the 206.2 nm line used to monitor the $I(5^2P_{\frac{1}{2}})$ atoms. In some of the experiments, in which the decay efficiency of other iodides (e.g. HI, CH_3I, GeH_3I) was investigated, these iodides were used as the source of $I(5^2P_{\frac{1}{2}})$ atoms.

Flash excitation system: There are three main requirements which characterize an ideal photolytic flash system: a) The light pulse must have a rectangular shape and short duration in comparison with the lifetime of the species of interest; b) the total energy must be easily adjusted to produce a flash of the desired intensity, and c) the wavelength distribution in the flash must correspond to the absorption bands of the substance irradiated. In practice these three aspects of the flash are all dependent on the type of gas discharge chosen as light source and upon the electrical circuit supplying this discharge.

TABLE 2.I

Iodides yielding $I(5^2P_{\frac{1}{2}})$ following broad band U.V. photolysis and fractional yields p^* of the excited atom.[144,145]

Iodide	p
CH_3I	0.92±0.02
C_2H_5I	0.69±0.05
$n\text{-}C_3H_7I$	0.67±0.04
$i\text{-}C_3H_7I$	<0.10
$n\text{-}C_4H_9I$	0.82±0.04
$t\text{-}C_4H_9I$	<0.10
CD_3I	0.99
CF_3I	0.91±0.03
C_2F_5I	>0.98
$n\text{-}C_3F_7I$	>0.99
$i\text{-}C_3F_7I$	0.90±0.02
HI	0.10±0.05

$$^*p = \frac{[I(5^2P_{\frac{1}{2}})]}{[I(5^2P_{\frac{1}{2}})] + [I(5^2P_{3/2})]}$$

Furthermore, we should note that requirements (a) and (b) can conflict with one another. As has been shown by Porter,[122] the flash duration increases with increasing energy.

For a fixed power level, the flash duration is determined primarily by the oscillatory behavior of the electrical circuit, which can be treated as an LCR network[122,146] and additionally by any "afterglow" arising from long lived excited states in the gas. In general, the average power dissipated in a flash is proportional to V^2/Z, where V is the charging voltage of the capacitor and Z the impedance of the flash lamp circuit. Thus a high V and low Z is required for high power levels. Low impedances can be achieved by minimizing the inductance of the circuit, i.e. choosing a capacitor of low inductance and high capacitance, using a switch and a flash lamp of low inductance, and keeping the connecting cables short. For a given capacitor, a low inductance also results in a reduction of the oscillation frequency of the circuit and in consequence, of the flash duration. The 10 μF capacitors employed in this experimental work were typically charged from 1 to 5 kV, which corresponds to electrical energies of 10-125 J. In the coaxial system in particular, very low flash energies had to be used to prevent overloading of the detection system. Low flash energies were generally prefered, whenever the absorption signal was strong and the signal to noise ratio large. This was one way of eliminating possible thermal effects and of maintaining relatively low atomic concentrations for a more reliable analysis of the kinetic data (cf. section E).*

Two types of flash lamp were used in the present work. The first was made up by using a quartz B14 double socket tubing, ($\lambda > 200$ nm) with electrodes of mild steel, as has been described by Little.[147] The other flash lamp was concentric to the reaction vessel and had brass electrodes. Both flash lamps were filled up with Kr at a pressure of

* Small flash energies enjoy also the advantage of reducing the effects of scattered light and minimising the photolysis of added reactants.

$\sim$400-533 Nm^{-2}. The continuum emission of Kr is appropriate for photolysing the iodides. Use of Xe, which also emits in the same spectral range, was avoided, since Xe tends to exhibit strong "afterglow" effects. Following the charging of the capacitor, using a commercial power supply (Hartley Measurements Limited) with a 300-0060 model control unit, the lamp was fired by means of a manual switch, comprised of a brass disc mounted on a teflon plunger across two copper electrodes. One of the electrodes was connected to the lamp and the other to earth as shown in Figure 2.2.

The flash duration, determined by the tail of the flash profile, is wavelength dependent. For the first type of flashlamp used the flash duration was $\sim$6 μs at about 300 nm and $\sim$72 μs in the visible. However, the time resolution, determined effectively by the time constant of the detection system was typically $\sim$100 - 130 μs in most experiments. In this context we note that the time resolution appeared to remain almost unaltered for a given detection system, over a wide range of discharge energies. Thus, for discharges of $\sim$10 and $\sim$160 J through the flashlamp of the coaxial system, the time resolution was 120 and 132 μs respectively.

C) REACTION VESSEL ARRANGEMENTS

The parallel quartz flashlamp (l = 24 cm, i.d. = 1.5 cm) and reaction vessel (l = 20.2 cm, i.d. = 2 cm) system was used for the isotope effects investigation. The efficiency of photolysis was highly dependent on the distance between the lamp and the vessel and the presence of a light reflector. Thus aluminium foil wrapped around the lamp and the vessel increased the extent of photolysis considerably. In some of the experiments however, and especially when high discharge voltages were employed the reflector resulted in a concomitant increase in the level of scattered light and was therefore removed.

Figure 2.2: Experimental arrangement used in time resolved atomic absorption spectrophotometry studies.

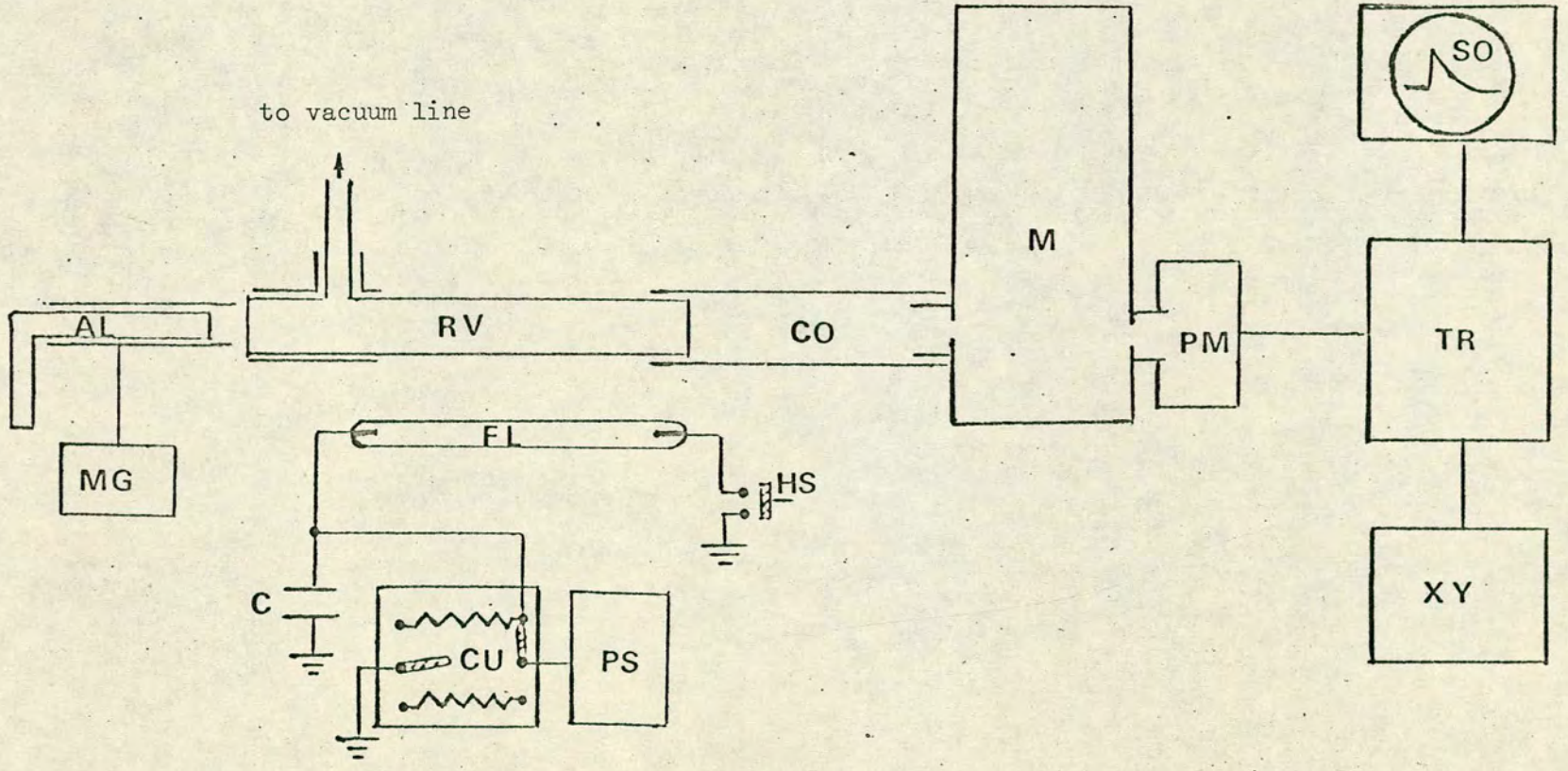

A simple "collimator", consisting of a tube lined with black paper, together with masking apertures at the ends of the reaction vessel, greatly reduced the level of scattered light. Thus in many experiments photolysis occurred only in an optimum length of the reaction vessel, which was determined by the requirement of a reasonable absorption signal and the simultaneous absence of any scattered light effects. It should be mentioned here that the simple low resolution monochromator (Hilger and Watts D 292, grating blazed at 320 nm) situated at one end of the reaction vessel had also as a main function the reduction of scattered light reaching the photomultiplier. Usually slitwidths of 200-250 μm were employed. An attempt to use an interference filter having a maximum transmission at 206 nm, instead of the monochromator proved unsuccessful due to second order transmission of wavelengths coinciding with those emitted from the iodine lamp in the range ∿320-450 nm.

The reaction vessel arrangement employed in the temperature dependence experiments consisted basically of three coaxial tubes. As shown in Figure 2.3, the inner tube was a quartz B14 double socket (l = 28 cm, i.d. = 1.4) and comprised the reaction vessel. The anulus formed by the outer section of the reaction vessel and the second coaxial tube, (pyrex, l = 15 cm, i.d. = 2.1 cm) was the flashlamp. The reaction vessel-flashlamp assembly was surrounded by the third concentric tube of purex, having an i.d. = 4.2 cm and a shorter length, l = 9 cm. This outer jacket served for the circulation of a heating or cooling gas. The second tube forming the lamp was attached to two brass electrodes by using epoxy resin. The inner jacket was made airtight at the electrodes by means of O-ring seals. Similarly, the two rings made out of teflon which kept the outer tube in position, were sealed by using O-rings. This type of arrangement was similar to that employed earlier by Smith and Zellner.[135]

Figure 2.3: Reaction vessel arrangement used in temperature dependence studies.

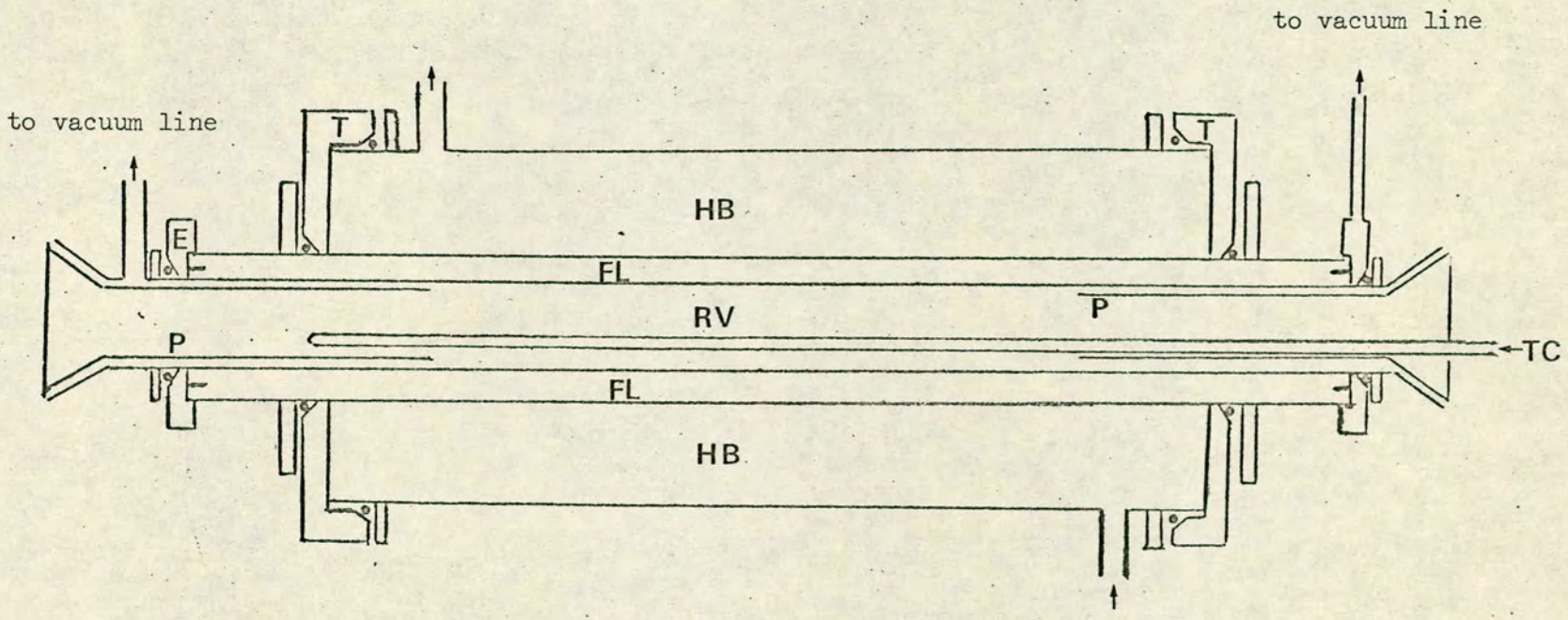

RV Reaction Vessel
FL Flash Lamp
HB Thermal Bath
E Brass Electrodes
P Pyrex Insert
T Teflon Rings
TC Thermocouple

In order to prevent condensation of water vapour on the spectrosil end windows of the reaction vessel at low temperatures, only the central part of the reaction vessel was used for temperature measurements, leaving extensions of 6.5 cm at both ends of the vessel at room temperature. Photolysis of the reagents in these sections was avoided by using pyrex tube extensions, which transmit light only above 300 nm, inside the reaction vessel. These internal extensions were even entering by 0.5 cm the part of the reaction vessel surrounded by the thermal bath, in an attempt to minimize temperature gradients across the part of the vessel where photolysis occured.

Low temperatures were obtained by passing a stream of cold nitrogen through the outer jacket. Nitrogen gas was cooled in narrow spiral tubing which, for measurements at different temperatures, was placed in different cooling baths, e.g. isopropanol-dry ice (195 K), n-pentane - solid (141 K), or liquid nitrogen (77 K). High temperatures were obtained by means of a heating tape wrapped around the outer tube. A flow of hot air passing through the outer jacket served in preheating the reaction vessel and in reducing temperature gradients. In most applications, the temperature range of ∿230-450 K was easily covered by regulating the voltage of the heating tape and the flow rates of nitrogen or air. Temperatures were measured by means of a stainless steel sheath Ni-Cr/Ni-Al (MISR) thermocouple, which was placed inside a capillary tube entering the reaction vessel through a small hole at one of the end windows and extending up to the other end. By changing the position of the thermocouple inside the capillary, it was possible to measure the temperature at different positions along the vessel. At the very low or very high temperatures employed, the temperature gradient along the photolyzed length of the reaction vessel varied from 2 to 14 K depending mainly on the nitrogen or air flows in each experiment. For intermediate temperatures the temperature variations were smaller. A limitation in the present investigation at low temperatures was imposed by the low vapour pressure of some iodides at such temperatures.

D) DETECTION OF $I(5^2P_{\frac{1}{2}})$ ATOMS

An ideal monitoring source in atomic absorption spectrophotometry would combine emission of a monitoring atomic line of high intensity with a large f value for the corresponding atomic transition. The decay of $I(5^2P_{\frac{1}{2}})$ atoms in the present work was monitored by using the 206.2 nm line, $I(5^2P_{\frac{1}{2}}) \rightarrow I(6s\ ^2P_{3/2})$ (cf. Figure 2.1). This line can be produced at a very high intensity and its attenuation does not require a vacuum U.V. arrangement. Its use is therefore advantageous in comparison with that of other transitions emanating from the $^2P_{\frac{1}{2}}$ state, despite the relatively small f value it involves.

The 206.2 nm line was produced by a microwave discharge through molecular iodine in a quartz tube terminating in a flat "spectrosil" window ($\lambda > 160$ nm). The discharge was run close to the window but never directly against it, preventing a decrease of its transparency. The construction of this type of sealed lamps has been described by Little.[147] In order to obtain stable signals, without 50 Hz mains ripple superimposed, the 2450 MHz microwave generators (EMS Microtron 200 Mark 2 and Mark 3) used, had extra DC smoothing and stabilization. Two types of microwave cavities were employed. One was a cylindrical cavity and the other was a standard Evenson cavity. Although the latter was found more efficient when tuned properly, the former maintained constant characteristics of operation over longer periods of time. The optimum conditions of operation using the Evenson cavity were obtained for incident powers* of ~30-40 W

The iodine lamp was placed at one end of the reaction vessel as shown in Figure 2.2. The intense light emission obtained resulted in sufficient levels of photocurrent at the photomultiplier, so that focussing of the emission onto the slit of the monochromator was not essential. The lamp was placed inside a piece of pyrex tubing, which fitted the microwave cavity and was extended close to the window of the reaction vessel. This

* The cylindrical cavity was usually run at incident powers of ~50-60 W.

tube, acting as a light pipe, helped to increase the intensity of light from the lamp detected by the photomultiplier. In addition it cut down ozone formation during the operation of the lamp.

The resonance absorption signals were detected by means of an EMI 9661 B photomultiplier tube with a Corning 9741 side window. The tube contained in a brass light tight can was mounted at the exit slit of the monochromator. This type of photomultiplier has nine grid dynodes and a caesium-antimony cathode with an S-5 spectral response. In this work two types of photomultiplier circuit were employed. The first type was of conventional design, in which the whole dynode chain was used and thus high gains could be obtained. However, for the purposes of the present work there was no need for a very high sensitivity. On the contrary, there are several reasons associated mainly with the level of shot noise and the limits to the anode current, for which a relatively low gain was required. The main points are:-
(a) the high intensity of the monitoring beam ensures a high photocathode current and consequently a good signal-to-noise ratio;[122] secondly, emission, instead of reducing the fundamental shot noise, can cause its enhancement due to statistical fluctuations of emission at the dynodes.
(b) maximisation of the photocathode current, which is necessary to optimize the signal-to-noise ratio, may lead to excessive anode currents. These can in turn result in a non-linear dependence between the anode current and the light intensity. Scattered flash light reaching the photomultiplier can produce similar effects. The maximum anode current for a linear response is essentially determined by fatigue caused by the anode dissipation, dynode heating and space charge effects, occuring particularly at the final dynodes.[148]

To avoid complication due to (a) and (b) the last three dynodes of the photomultiplier used were combined with the anode as has been originally described by Hunt and Thomas.[149] The sixth dynode of the tube employed

was flat,[148] which is considered as a favourable geometry for its use as an anode.[122] In this way, the gain of the photomultiplier was reduced, while maximum photocathode currents were retained.

When the tube was connected as in the latter circuit, it was typically run at 800-900 V (Fluka 408B power supply) and the output of the photomultiplier was developed across a 47 kΩ resistor. When the first circuit was used, the employed voltages were somewhat smaller (~700 V) (Farnell E2 power supply) and were limited by overloading effects in the detection system. Such effects could be eliminated by using an 1N914 silicon diode, forward biased and connected in parallel with the load resistor. The effect of this diode, having a conducting voltage of 0.6 V was to reduce the detected signals and noise. As an extensive comparison of decay rates in the presence and absence of the diode proved, the measured rates were not affected.

The majority of data was collected from single flash experiments by using a fast 8-bit, 1024 point ,analogue to digital converter with integral memory (Datalab DL905). They were then inspected on a visual display unit (Telequipment DM64 storage oscilloscope) before being recorded in analogue form on an XY plotter for subsequent analysis by means of a Ferranti Freescan digitizer (cf. Figure 2.2) Only a small part of the temperature dependence results was obtained by feeding the digital data from the transient recorder onto a tapepunch (cf. Chapter 3). In some early experiments the output of the photomultiplier was monitored directly on an oscilloscope and photographed for subsequent kinetic analysis.

E) GAS HANDLING AND REAGENTS

Reagents were handled using a vacuum line, evacuated by a two stage 2520B Edwards rotary pump and a mercury diffusion pump, and constructed with greaseless

taps (Young Scientific) capable of holding a vacuum of better than 10^{-4} Nm^{-2}. For experiments with deuterated molecules (DCl, D_2O, DBr, DI), the vacuum line was deuterated several times with D_2O over a period of two or three days. The extent of deuteration was checked by means of a Centronic AIG.50 analytical ionisation gauge, used in conjunction with a mass scan generator. In the majority of experiments, isothermal conditions were maintained by diluting mixtures of the iodide and deactivating gas by about one hundred fold of an inefficient quenchin gas, usually pure nitrogen, yielding a total pressure of ca. 2.7-3.9 kNm^{-2}. Gas mixtures were either made up in 500 cm^3 bulbs and allowed to mix for at least two hours before use, or in a magnetically driven stirrer, where they were mixed for at least thirty minutes. Care was taken to prevent photolysis of some reagents due to room light, by covering the bulbs with black cloths. Pressures were measured either by a mercury manometer or more accurately by a calibrated spiral gauge (~2% error). To obtain some of the low pressures required, sharing ratios were determined with less than 10% error.

A detailed list of the reagents used along with their purity is contained in Appendix I. The procedures used to purify particular reagents are included in the experimental sections of Chapters 3 and 4. Here we only note that when necessary purities were checked by using mass spectrometry and U.V. and I.R. spectroscopy.

F) DATA ANALYSIS

The deactivation of $I(5^2P_{\frac{1}{2}})$ involves only two states, namely the $^2P_{\frac{1}{2}}$ and $^2P_{3/2}$ states; the general formalism for the kinetic treatment of such systems has been given in several papers.[1a,62,134] Here we quote the master rate equation which is valid unless a large excess of the ground state atoms is present.

$$-\frac{dc}{dt} = (\sum_q k_q [Q] + b + A_{if} + B_{if})c \qquad (2.2)$$

where, c is the concentration of $I(5^2P_{\frac{1}{2}})$, $\sum_q k_q [Q]$ is the sum of first order rate coefficients for reactive removal or quenching of $I(5^2P_{\frac{1}{2}})$ in the presence of Q, b is the rate coefficient for diffusion, A_{if} and B_{if} are the Einstein coefficients for spontaneous and stimulated emission respectively. Under the conditions used in the present kinetic experiments contributions from the first term, or more concisely the first set of terms in 2.2, dominate the decay process. Thus, as has been already mentioned, the contribution of spontaneous emission as a rate coefficient is negligible and the threshold conditions for stimulated emission following the photolysis of the iodides used are substantially higher than those employed. The rate of diffusion, being inversely proportional to the pressure, may become important at very low total pressures and this has been observed in some cases (cf. Chapter 3).

Typical decay traces of $I(5^2P_{\frac{1}{2}})$ in the presence of various molecules are shown in Chapters 3 and 4. The experimentally measured absorptions (I/I_o), at different times after the flash, were related to the concentration c by means of the modified Beer-Lambert law, (cf. 2.1). Plots of $\ln\ln(I_o/I)$ against time were found to be sensibly linear under the conditions employed. The linearity of such plots in the presence of all added deactivating gases indicated that it is reasonable to analyse the kinetic decay of $I(5^2P_{\frac{1}{2}})$ atoms on the basis of the pseudo first-order rate approximation. Pseudo first-order plots were obtained from the digitised decays by means of a weighted

least squares computer program *, $\ln\ln(I_o/I)$ at each point being assigned a weight proportional to its displacement from the baseline. Results from the decay traces were generally omitted in the leading edge due to scattered light from the photolytic flash and at very low degrees of light absorption where the noise level gave rise to a large scatter in the values of $\ln\ln(I_o/I)$. Similarly, the computer program * used for analysing the data from the tapepunch was designed to omit these results.

The first order rate coefficients derived from the slopes of the pseudo first-order plots were then plotted against the partial pressure of the deactivating gas and the slopes of the latter plots, calculated by using a weighted least squares computer program , yielded γk, where k was the second order quenching rate constant for a given quenching gas, and γ was determined by following various empirical procedures.

Resonance absorption and the Beer-Lambert relationship

The relationship between the atom concentration c and the intensity of the absorbed radiation is basically determined by the relative coincidence between the profile of the line emitted from the lamp and the line profile of the absorbing atoms. The intensity distribution in the emission line is of primary importance in this respect. This distribution can be complicated by several effects associated with the discharge plasma in the microwave-powered lamp. In general, it is difficult to determine the exact nature of processes occuring in the lamp. It is possible however, to distinguish two major effects determining the profile of the emitted line namely: (a) Self-absorption

* I would like to thank Robin Strain, who prepared the computer programs for analysing the digitised data from the digitizer[150] and John McElroy who prepared the program for obtaining results from the tapepunch data.

and (b) line broadening.

(a) Self-absorption: Light emitted from a resonance lamp has a high probability of being reabsorbed before leaving the discharge lamp. As the atom concentration increases, the intensity of the emitted line initially increases linearly with atom concentration, but the rate of increase eventually falls off due to absorption by ground state atoms. Self-absorption strongly affects the intensity distribution on the emission line, resulting in a "dip" in the observed profile of emission.[151]

(b) Line broadening: Generally, the spectral profile observed from a discharge lamp is very much broadened. This is due to the fact that various processes occuring in the discharge plasma (e.g. energy transfer between colliding species and photolysis) may lead to translationally hot atoms and a broad emission profile.[152] Thus, the output of a microwave lamp has a rather ill defined line profile. For lamps operating at low pressures however, a Doppler profile, with a width determined by the temperature of the plasma, is a good approximation.[124]

The line profile of the absorbing atoms in the reaction vessel is effectively determined by the pressure (Doppler-broadening for pressures lower than about 1300 Nm^{-2}, Lorenz-broadening at higher pressures) and the temperature. As can be deduced by considering the overlap of the broad and reversed emission line with the line profile of the absorber, absorption at the line centre will be saturated at all but the lowest atomic concentrations. In consequence the Beer-Lambert relationship is valid only at low concentrations. This has been verified by Bemand and Clyne,[136] who deduced a non-empirical relationship, in which the absorption is correlated to the concentration c in terms of a power series of c for various emission and absorption line profiles. One of the main conclusions in this work was that the Beer-Lambert function with $\gamma=1$ (cf. 2.1) is always satisfactory at low absorption

intensities.

In the data analysis of the present work, the modified Beer-Lambert expression was employed. The γ coefficient can be determined by using empirical procedures, which involve extrapolation of the quantity $\ln\ln(I_o/I)$ to t = o, either for different lengths l or for different initial atomic concentrations. Figure 2.4 shows such a standard plot for the determination of γ, under the conditions used in the majority of experiments involving C_3F_7I as the parent molecule: $\ln\ln(I_o/I)_{t=o}$ is plotted against $\ln(P_{C_3F_7I})$, where $P_{C_3F_7I}$ is the partial pressure of the iodide in the reaction vessel, at a given total pressure of N_2 ($P \sim 2.7$ kNm^{-2}). This procedure constitutes a device for determining relative atomic concentrations, by applying the weak light absorption approximation, according to which $(c)_{t=o} \propto P_{C_3F_7I}$. As shown in Figure 2.4, this plot can be well represented by a straight line over a wide range of pressures of the iodide, and the slope of this line yields γ under these conditions. Using this procedure γ was determined to be 0.82 ± 0.03, and this value was used to determine the second order rate constants from γ k. In the errors given for the measured rate constants the error in γ has not been included.

It should be noted that this procedure is sensitive to variations of the experimental parameters, as for example the flash energy, which can lead to a large scatter. In an attempt to minimize the scatter, the points included in Figure 2.4 represented averages over three to four experiments.

Another empirical method of determining γ from a single decay trace, on the basis of relative absorptions, will be described in Chapter 3.

Figure 2.4: Empirical determination of γ coefficient

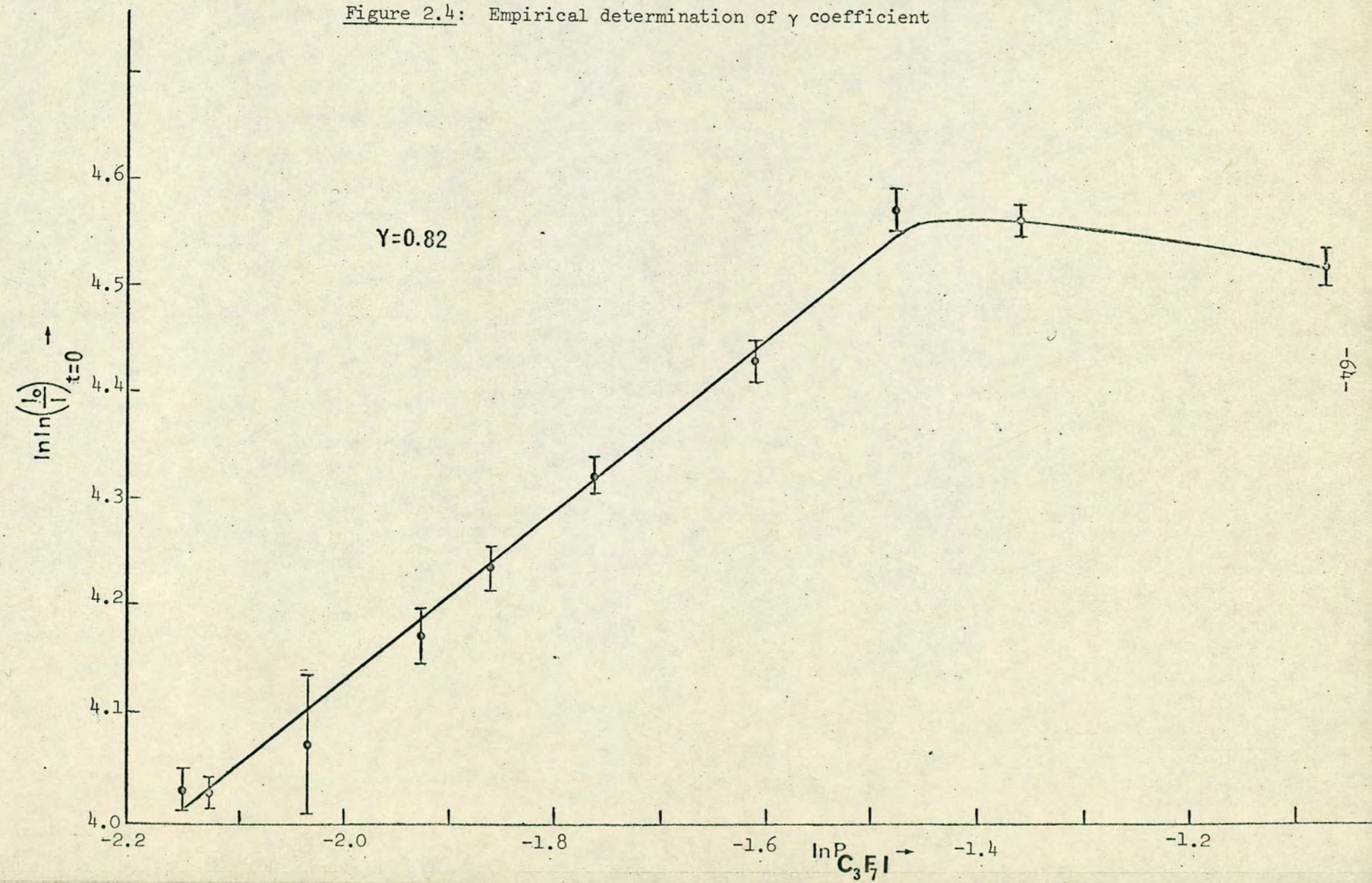

Chapter 3

RELAXATION OF $I(5^2P_{\frac{1}{2}})$ ATOMS BY CH_3I, CD_3I, GeH_3I and SiH_3I AND PHOTODISSOCIATION LASER ISOTOPE EFFECTS

A) INTRODUCTION

Considerable interest has been focused in recent years on the dynamics of the photolysis of iodides and the resulting chemical kinetics. Part of this interest stems from the fact that photolysis of iodides leads to population inversion between the atomic iodine $5^2P_{\frac{1}{2}}$ and $5^2P_{3/2}$ states and the corresponding transition can be applied for laser action at 1.315 μm. As it has been practically demonstrated for some iodides,[153,154] laser pulses of high energy and small duration can be generated following the photodissociation process. To date outputs of at least 8.5 GW have been obtained and the iodine photochemical laser is of interest in connection with laser produced plasma and nuclear fusion experiments.[155]

The fraction of $I(5^2P_{\frac{1}{2}})$ atoms produced by the photolysis of iodides and the rate of their removal are questions central to the operation of the iodine laser. The relative efficiency of removal of ground and excited state iodine atoms is also of great importance since it determines the population inversion, which is necessary for laser action. In addition, it is interesting from the theoretical point of view, since it is connected with the more general problem of branching ratios between inelastic and reactive pathways for the removal process.

Several experimental techniques have been used to study the yield and the kinetics of $I(5^2P_{\frac{1}{2}})$ atoms following the photolysis of iodides. Donovan et al.[1] have monitored the excited and ground state iodine atoms in the vacuum ultraviolet using kinetic spectroscopy. Comparing the initial absorptions of the two lines they concluded that population inversion was formed following the photolysis of CH_3I. They also correctly suggested that failure to observe laser action following the photolysis of i-C_3H_7I was

due to the low initial yield of electronically excited atoms, rather than their fast removal by the source gas. However, no accurate quantitative measurements were possible due to the interference of the atomic lines by molecular absorption bands. Riley and Wilson[156] used photofragment spectroscopy to measure the fraction of $I(5^2P_{\frac{1}{2}})$ produced when CH_3I is photolysed by 266.2 nm radiation from a quadrupled Nd laser. More recently, Donohue and Wiesenfeld[144,145] determined the fraction of $I(5^2P_{\frac{1}{2}})$ produced by broad-band flash photolysis of CH_3I and other alkyl and fluoro-iodides by using time resolved atomic absorption spectroscopy.

The decay of excited iodine atoms in the presence of CH_3I has been investigated by several authors. This decay may come about as the result of two exothermic processes.

$$I(5^2P_{\frac{1}{2}}) + CH_3I \xrightarrow{k_1} CH_3 + I_2 , \qquad \Delta H_o = -14.5 \text{ kJ mole}^{-1} \quad (3.1)$$

$$I(5^2P_{\frac{1}{2}}) + CH_3I \xrightarrow{k_2} CH_3I + I\,(5^2P_{3/2}), \qquad \Delta H_o = -90.9 \text{ kJ mole}^{-1} \quad (3.2)$$

Donovan et al.[157] in their kinetic spectroscopy work determined the total rate $k_1 + k_2$ for the $I(5^2P_{\frac{1}{2}})$ removal by CH_3I to be 1.7×10^{-12} cm^3 molecule^{-1} s^{-1}. They also suggested that the inelastic channel (3.2) was dominating the removal process. Their suggestion was based on the observation of the intense molecular $I_2(M \leftarrow X)$ system. No significant formation of molecular iodine could be detected simultaneously with the relaxation of the excited atomic state. Molecular I_2 bands appeared at late times, following slow termolecular recombination. Their suggestion was in good agreement with the results of the work of Aditya and Willard,[158] who estimated k_1 by considering the upper limit for the quantum yield for the photochemical exchange of I_2[131], photolysed in the I_2 (B - X) continuum, in the presence of CH_3I. The results of this work combined with data obtained by time resolved atomic absorption

spectrophotometry[134] yielded a maximum value for k_1, $k_1 \leq 3 \times 10^{-16}$ cm^3 $molecule^{-1}$ s^{-1}. However, Haaland and Meyer,[159] using time resolved mass spectroscopy obtained a value for k_1 of about two orders of magnitude larger, $k_1 = (1.0 \pm 0.6) \times 10^{-14}$ cm^3 $molecule^{-1}$ s^{-1} (over the temperature range 316-447 K). They also reported an upper limit for k_2, $k_2 \leq 4 \times 10^{-14}$ cm^3 $molecule^{-1}$ s^{-1}.

The purpose of the present work is to clarify the controversy regarding the relative efficiencies of the quenching (3.2) vs. reactive (3.1) channels, i.e. to obtain a more detailed understanding of the importance of electronic energy transfer or reactive processes leading to the removal of electronically excited atoms. To achieve that, we determined the overall removal rate constant for CH_3I and compared it to that determined for CD_3I over a wide range of temperatures. Furthermore, the corresponding overall rate constants for the decay of excited iodine atoms in the presence of SiH_3I and GeH_3I were studied. Comparison of the efficiency of these iodides to that of CH_3I may provide information for the relative importance of inelastic and reactive channels. The contribution of these channels is altered as the central atom of group IV of the periodic table is altered.

By using these iodides as source molecules in the photochemical iodine laser it was demonstrated how the various possibilities for removal of $I(5^2P_{\frac{1}{2}})$ atoms can affect the laser output.

B.) EXPERIMENTAL

1) Time resolved atomic absorption spectrophotometry

The rates of decay of excited iodine atoms in the presence of the various iodides was investigated using time resolved atomic absorption spectrophotometry. The experimental arrangements, which were employed,

have been described in detail in the experimental section (Chapter 2). For the determination of the decay rate constants at room temperature, the parallel flashlamp reaction cell system was initially employed. For the temperature dependence measurements of the rate constants for CH_3I and CD_3I and a more detailed investigation of the decay efficiency of GeH_3I, the coaxial flashlamp system was employed. Part of the results for CH_3I have been obtained by feeding the digital data from the transient recorder directly onto a tapepunch and calculating the pseudo first order rate coefficients by using appropriate computer programs. In this way, subjective errors in digitizing analogue traces by means of the Ferranti Freescan digitiser disappeared and the time of obtaining the decay rates was minimized.

The iodides were thoroughly degassed and fractionally distilled at least twice from an isopropanol-dry ice bath (195 K) to liquid nitrogen temperature (77 K) before use. In this way, it was ensured that no molecular iodine was present. This procedure was repeated several times for CD_3I, the least efficient of the examined iodides. Mixtures were prepared in blackened bulbs and the experiments with SiH_3I and GeH_3I were carried out in the dark to minimize their decomposition prior to photolysis. The flash energies employed in experiments with these iodides never exceeded 45 J.

2) Photochemical laser

Two different arrangements were employed in the present work.

(a) The first arrangement was of conventional design. A quartz flash lamp and photolysis cell both 1 m in length and 15 mm i.d. were placed parallel and optically coupled using aluminium foil. Microscope slides, set at the Brewster angle, served as windows. The mirror mounts,

constructed in the workshop, could give independent motion about two axes. The mirrors forming the optical cavity were gold coated, totally reflecting in the infrared yet partially transparent in the visible. Thus, it was made possible to align the laser by means of a He-Ne laser. In some of the experiments, one of the mirrors had been replaced by a totally reflecting (in the I.R.)mirror, having a small hole (0.5 mm) at its centre for coupling out a fraction of the radiation. One of the mirrors was concave having a radius of curvature 1.5 m and the other, (the coupling mirror when a coupling hole was used), was flat, (Fig. 3.1).

(b) The second arrangement consisted out of a quartz reaction vessel, having an active length of 15 cm and 21 mm i.d., with demountable sapphire windows set up at the Brewster angle to minimize the losses. This reaction cell was set parallel to two Kr-filled flashlamps in an aluminium reflector. The lamps were fired simultaneously in parallel, so that the substantial time varying magnetic fields associated with the two lamps cancel along the axis of the reaction vessel. Therefore, higher gains could be achieved since the Zeeman splitting of the zero field hyperfine sublevels of iodine atoms and the magnetic field induced mixing between these states was reduced. With these short lamps easy and reproducible firing could be obtained. A 10 μF rapid discharge capacitor was employed and the connecting cables were kept as short as possible to minimize the inductance of the charging circuit. The flash energies employed were typically 125 - 720 J. The flash duration was $\sim$ 80 μs in the visible for flash energies of 180 J.

Detection: Laser emission at 1.315 μm was detected by an In-Sb, room temperature detector (model Mullard ORP 10). Radiation was coupled to the detector either via the reflection at one of the Brewster windows or via the coupling hole of one of the mirrors, when a mirror with a hole was used. The output of the detector was displayed on a storage

Figure 3.1 Schematic representation of photochemical laser apparatus.

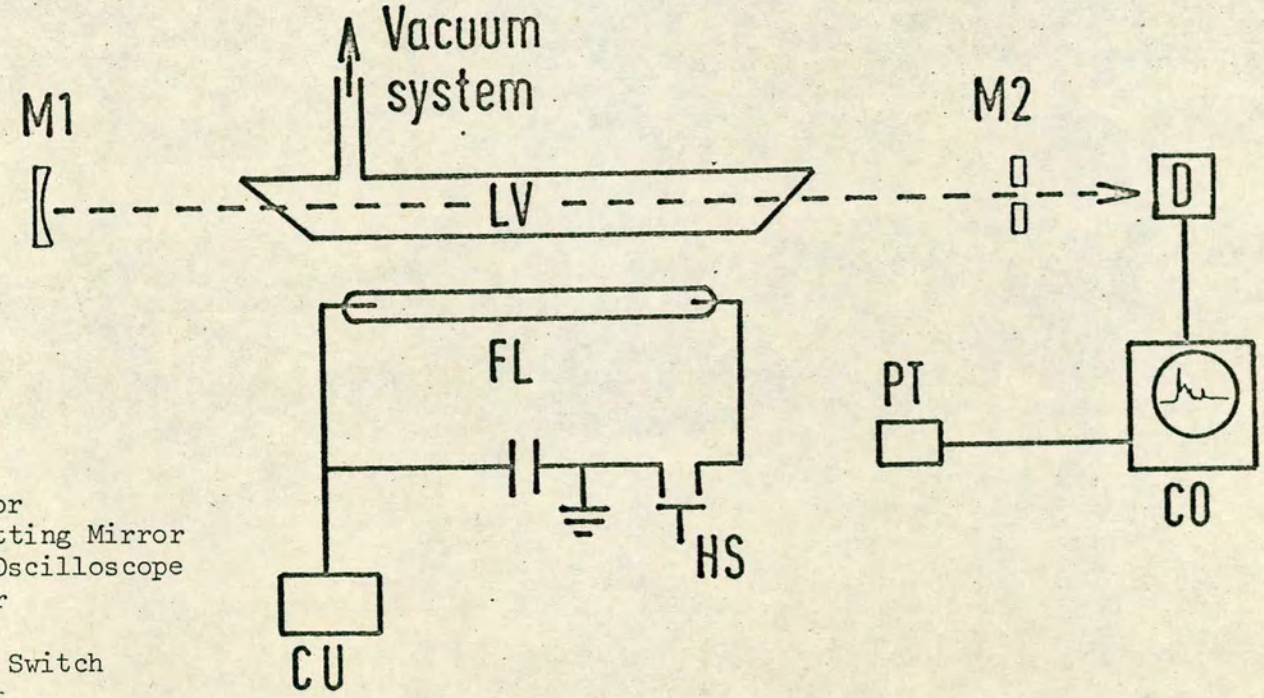

LV	Laser Vessel
D	Detector
M1	Concave Mirror
M2	Flat Transmitting Mirror
CO	Cathode Ray Oscilloscope
PT	Photo Trigger
FL	Flash Lamp
HS	High Voltage Switch
CU	Charging Unit

oscilloscope (Tektronix 549), having a bandwidth of 30 MHz.

C) RESULTS

1) Decay of $I(5^2P_{\frac{1}{2}})$ in the presence of CH_3I and CD_3I

Following the photolysis of an alkyl iodide in the reaction vessel, the processes which may occur are described by the following set of equations.

$$RI + h\nu\ (\lambda > 185\ nm) \rightarrow R. + I(5^2P_{3/2}\ \text{or}\ 5^2P_{\frac{1}{2}}) \qquad (3.3)$$

$$RI + I(5^2P_{\frac{1}{2}}) \rightarrow RI + I(5^2P_{3/2}) \quad \Delta H_o = -90.9\ kJ\ mole^{-1} \qquad (3.2)$$

$$RI + I(5^2P_{\frac{1}{2}}) \rightarrow R. + I_2 \quad \Delta H_o = -14.5\ kJ\ mole^{-1} \qquad (3.1)$$

$$I(5^2P_{\frac{1}{2}}) + \text{wall} \rightarrow I(5^2P_{3/2}) + \text{wall} \qquad (3.4)$$

$$I(5^2P_{\frac{1}{2}}) \rightarrow I(5^2P_{3/2}) + h\nu\ (1.315\ \mu m). \qquad (3.5)$$

$$R. + R. + M \rightarrow R_2 + M(\text{third body}) \qquad (3.6)$$

$$R. + I(5^2P_{\frac{1}{2}}) + M \rightarrow RI + M \qquad (3.7)$$

$$R. + I(5^2P_{\frac{1}{2}}) \rightarrow R. + I(5^2P_{3/2}) \qquad (3.8)$$

$$R. + I(5^2P_{3/2}) + M \rightarrow RI + M \qquad (3.9)$$

$$R. + RI \rightarrow R_2 + I(5^2P_{3/2}\ \text{or}\ 5^2P_{\frac{1}{2}}) \qquad (3.10)$$

The present work was primarily concerned with the determination of $k_1 + k_2$ when $R = CH_3$, CD_3. Physical quenching (3.2) and chemical reaction (3.1) are exothermic and both may occur on thermodynamic grounds. The experimental conditions employed were such as to allow for the use of pseudo first-order kinetic analysis of the data, as it has been described in Chapter 2. The low flash energies employed (typically $\sim$80 J in the parallel flashlamp reaction cell system and <45 J in the coaxial system)

at λ >200 nm ensured that [RI] >> [R.] (3.3). A rough calculation based on data given in previous work[157] on CH_3I, the branching ratio $\frac{[I(5^2P_{\frac{1}{2}})]}{[I(5^2P_{3/2})]}$ for CH_3I and the assumption that the percentage photolysis is proportional to the flash energy, indicated less than 0.6% photolysis for CH_3I under the conditions used.

The rate of the radical recombination (3.6) has been measured for CH_3 and has been found to be very fast, It occurs in every 5-10 collisions. This ensured the absence of any bimolecular effects due to the processes described by (3.7-3.10). First order kinetic behaviour of the de-excitation of $I(5^2P_{\frac{1}{2}})$ atoms was verified experimentally. The traces in Fig. 3.2 show typical exponential decays for CH_3I and CD_3I, for t > ~150 μs, which was the recovery time of the detection system after its distortion due to the flash. According to the data-analysis described in Chapter 2, pseudo first order rate coefficients were obtained from such decay traces by plotting $\ln\ln\frac{I_o}{I}$ against t. These rate coefficients were plotted vs. the partial pressure of the iodide and after a weighted least mean squares analysis, the slopes of the plots yielded the second order rate coefficients. The intercepts at $P_{RI} = 0$ represented the rates of decay of $I(5^2P_{\frac{1}{2}})$ due to spontaneous emission, diffusion and quenching by the diluent gas N_2 and existing impurities. Experiments with CD_3I were carried out initially by preparing mixtures of CD_3I and He or N_2. However, after CD_3I was found inefficient in removing $I(5^2P_{\frac{1}{2}})$ atoms, samples of pure CD_3I were used at pressures ~2.66 kNm^{-2}. We consider that the most accurate results were those obtained in the latter case, although the discrepancy was not important. The rate constant determined at 293 K from the few experiments, in which mixtures of CD_3I and N_2 were used was $k_{CD_3I} = (5.6 \pm 1.0) \times 10^{-15} cm^3$ $molecule^{-1}$ s^{-1} vs. $k_{CD_3I} = (4.6 \pm 0.8) \times 10^{-15} cm^3$ $molecule^{-1}s^{-1}$ obtained from samples of pure CD_3I.

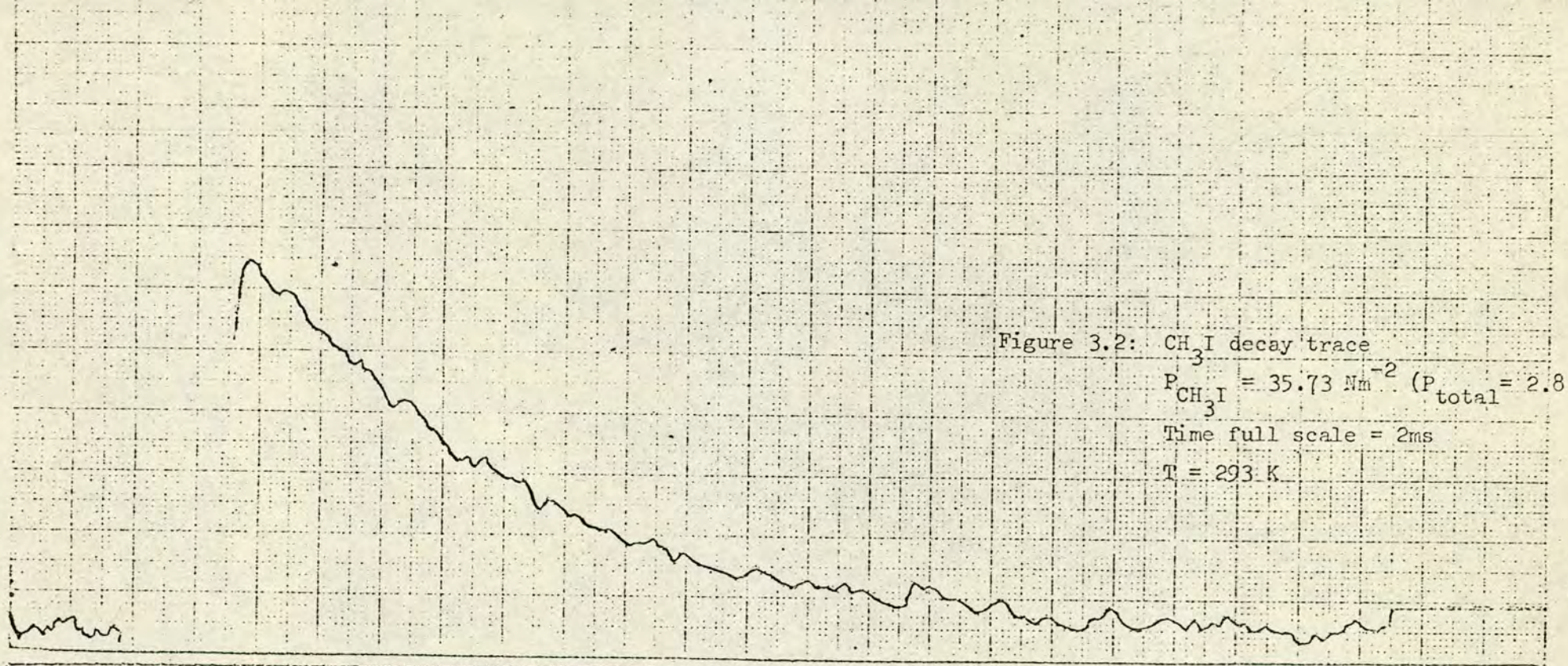

Figure 3.2: CH_3I decay trace
$P_{CH_3I} = 35.73\ Nm^{-2}$ ($P_{total} = 2.8\ kNm^{-2}$)
Time full scale = 2ms
T = 293 K

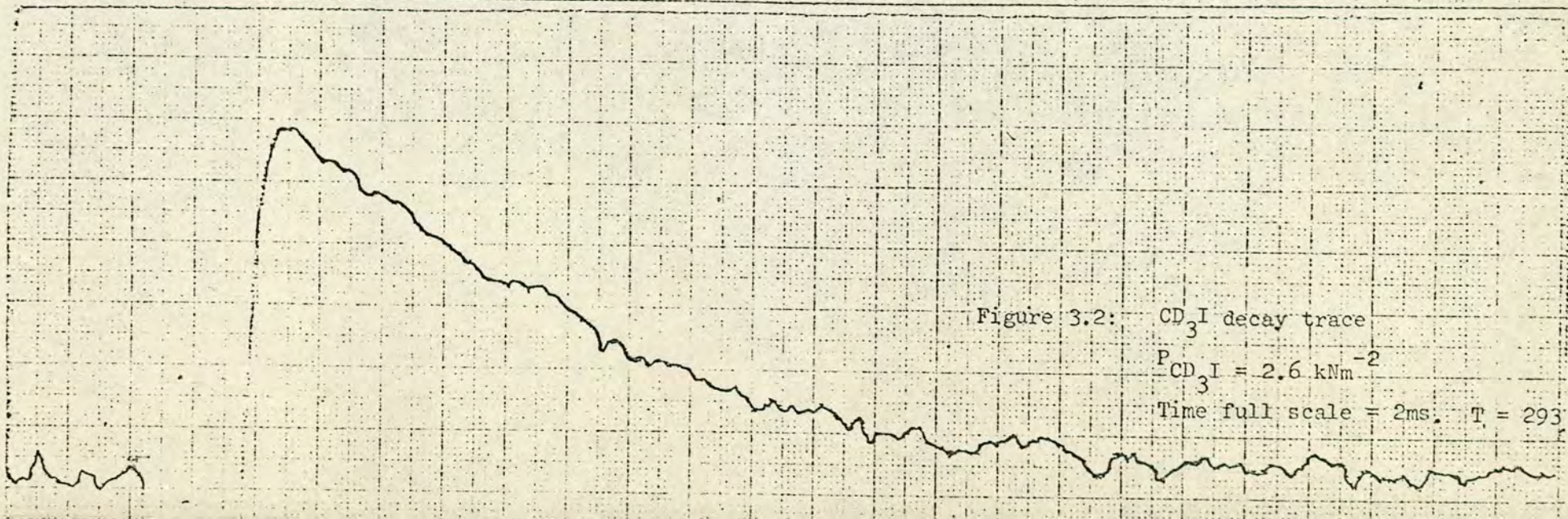

Figure 3.2: CD_3I decay trace
$P_{CD_3I} = 2.6\ kNm^{-2}$
Time full scale = 2ms. T = 293 K.

Kinetic data for the decay of excited iodine atoms in the presence of CH_3I, at different temperatures in the range 233 - 443 K are given in Table 3.I. Fig. 3.3 shows a plot of the determined rate constants as a function of temperature. A negative temperature dependence can be observed. By using the approximate relationship, $\sigma_T = \frac{k_T}{v_T}$, where σ_T is the average cross section at a temperature T, k_T and v_T the measured rate constant and the average relative velocity at the same temperature, ($v_T = (\frac{8KT}{\pi\mu})^{\frac{1}{2}}$, where μ is the reduced mass of the system), an even stronger negative temperature dependence is obtained for the cross section. This is shown in Table 3.II.

A test for secondary effects, (accumulation of molecular I_2, and pyrolysis of CH_3I), was carried out at each temperature by flashing the same mixture three to four times or different mixtures in time intervals between 2 and 10 min. In all cases the decay traces were found to coincide with the trace obtained following the first flash. These results indicated that a) no substantial amounts of molecular I_2 had been formed after four flashes of maximum energy 20 J and thus the measured decay rates were due entirely to CH_3I, and b) the pyrolysis of the iodide was insignificant even at the higher temperatures employed.

The empirical coefficient γ, which appears in the modified expression of the Beer-Lambert law and relates the measured intensity to the concentration (cf. Chapter 2), was determined at different temperatures by plotting the intercepts of the first order decay coefficients against $\ln [CH_3I]$. The assumption made was that $[CH_3I] \propto [I(5^2P_{\frac{1}{2}})]$ for the employed pressures of the iodide. The results are recorded in Table 3.III. Considering that the results obtained at room temperature represent averagings over a number of experimental data, (3 to 4 experiments), at each partial pressure of CH_3I and the relatively large error limits determined for γ for most of the other temperatures, we considered

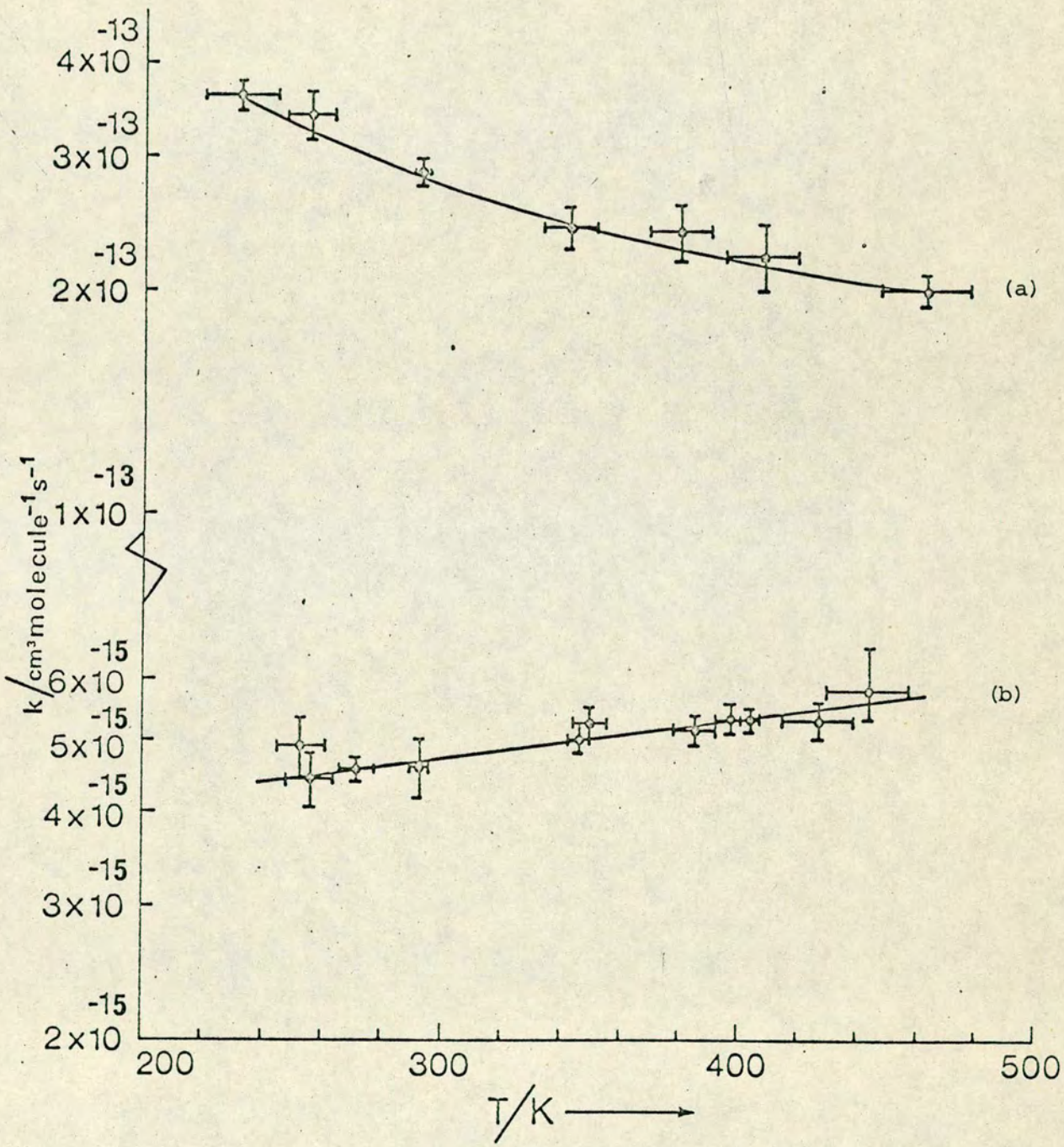

Figure 3.3: Rate constants k for the deactivation of $I(5^2P_{\frac{1}{2}})$ by CH_3I, (a), and CD_3I (b).

TABLE 3.I

Rate data for the removal of $I(5^2P_{\frac{1}{2}})$ by CH_3I (Total pressure=2.8 kNm^{-2})

Temperature (K)	Pressure CH_3I (Nm^{-2})	Rate (s^{-1})	$k \times 10^{13}$* (cm^3 $molecule^{-1}s^{-1}$)
233 ± 13	24.80	2876 ± 106	
	25.86	3028 ± 53	
	30.90	3601 ± 278	
	35.73	4062 ± 334	
	36.66	4138 ± 81	3.63 ± 0.18
256 ± 8	24.80	2580 ± 47	
	25.86	2696 ± 125	
	30.90	3280 ± 124	
	35.73	3547 ± 149	
	36.66	3660 ± 110	3.43 ± 0.50
293 ± 2	24.80	2013 ± 43	
	25.86	2102 ± 130	
	30.90	2440 ± 76	
	31.06	2452 ± 68	
	35.73	2729 ± 139	
	36.66	2820 ± 166	2.91 ± 0.15
343 ± 9	24.80	1530 ± 29	
	25.86	1572 ± 87	
	30.90	1789 ± 20	
	35.73	2045 ± 68	
	36.66	2133 ± 98	2.44 ± 0.30

Table 3.I contd.

Temperature (K)	Pressure CH_3I (Nm^{-2})	Rate (s^{-1})	k x 10^{13} (cm^3 $molecule^{-1}s^{-1}$)
381 ± 10	24.80	1512 ± 22	
	25.86	1612 ± 59	
	30.90	1833 ± 90	
	35.73	2033 ± 71	
	36.66	2006 ± 64	2.46 ± 0.38
408 ± 12	24.80	1316 ± 42	
	25.86	1408 ± 117	
	30.90	1553 ± 75	
	35.73	1683 ± 55	
	36.66	1809 ± 57	2.24 ± 0.58
443 ± 14	24.80	1127 ± 52	
	25.86	1135 ± 27	
	30.90	1317 ± 34	
	35.73	1456 ± 56	
	36.66	1465 ± 83	2.03 ± 0.36
293 ± 2	24.80	2064 ± 46**	
	25.86	2113 ± 47	
	30.90	2331 ± 53	
	35.73	2818 ± 85	2.76 ± 0.18

* Errors correspond to two standard deviations.
** Rates obtained from tapepunch.

TABLE 3.II

Deactivation of $I(^2P_{\frac{1}{2}})$ by CH_3I.
Average cross sections at different temperatures

T (K)	$\sigma \times 10^{18}$ (cm^2)
233	13.4 ± 0.8
256	12.1 ± 2.0
293	9.3 ± 0.4
343	7.4 ± 0.9
381	7.1 ± 1.1
408	6.3 ± 1.6
443	5.4 ± 0.6

TABLE 3.III

Deactivation of $I(5^2P_{\frac{1}{2}})$ by CH_3I. γ coefficient at different temperatures

T (K)	γ
233	0.95 ± 0.02
293	0.93 ± 0.03
381	1.08 ± 0.43
408	0.91 ± 0.18
443	0.72 ± 0.27

$\gamma = 0.93 \pm 0.03$ for the whole temperature range.

An Arrhenius plot for the deactivation of $I(5^2P_{\frac{1}{2}})$ atoms by CH_3I was constructed, based on the kinetic data given in Table 3.I. The slope of this plot was found by employing a least mean squares analysis and yielded a negative activation energy, $E_a = (-2.3 \pm 0.1)$ kJ mol^{-1}. The intercept obtained resulted in a frequency factor, $A = (1.13 \pm 0.06)\ 10^{-13}$ cm^3 $molecule^{-1}$ s^{-1}. Considering the small errors involved in E_a and A, it is reasonable to assume that the rate constant for the removal of $I(5^2P_{\frac{1}{2}})$ atoms by CH_3I can be described by the equation:

$$k_{CH_3I} = (1.13 \pm 0.06)\ \exp\left(\frac{2.3 \pm 0.1\ kJ\ mole^{-1}}{RT}\right) \times 10^{-13} cm^3\ molecule^{-1}\ s^{-1}$$

As it was mentioned above, the intercepts of the second order plots can provide information for the efficiency of removal of $I(5^2P_{\frac{1}{2}})$ atoms by the diluent gas N_2, impurities contained in it, diffusion and emission processes. The most important impurity for the purposes of this work was O_2, with a concentration of less than 10 p.p.m. Based on these data, an attempt was made to obtain information on the temperature dependence of the collisional deactivation of $I(5^2P_{\frac{1}{2}})$ by N_2 molecules. The estimations were rough, since they were based on the following assumptions:

a) The contribution of diffusion and spontaneous emission processes to the decay rate was neglected. The observed rate data however may in part be due to the temperature variation of the diffusional rate of $I(5^2P_{\frac{1}{2}})$ atoms in N_2, with efficient deactivation taking place on the walls of the reaction vessel.

b) The only important impurity was O_2. Its decay efficiency as a function of temperature has been measured by Deakin and Husain [62] but the results contain a high uncertainty. The quoted expression for the rate constant is:

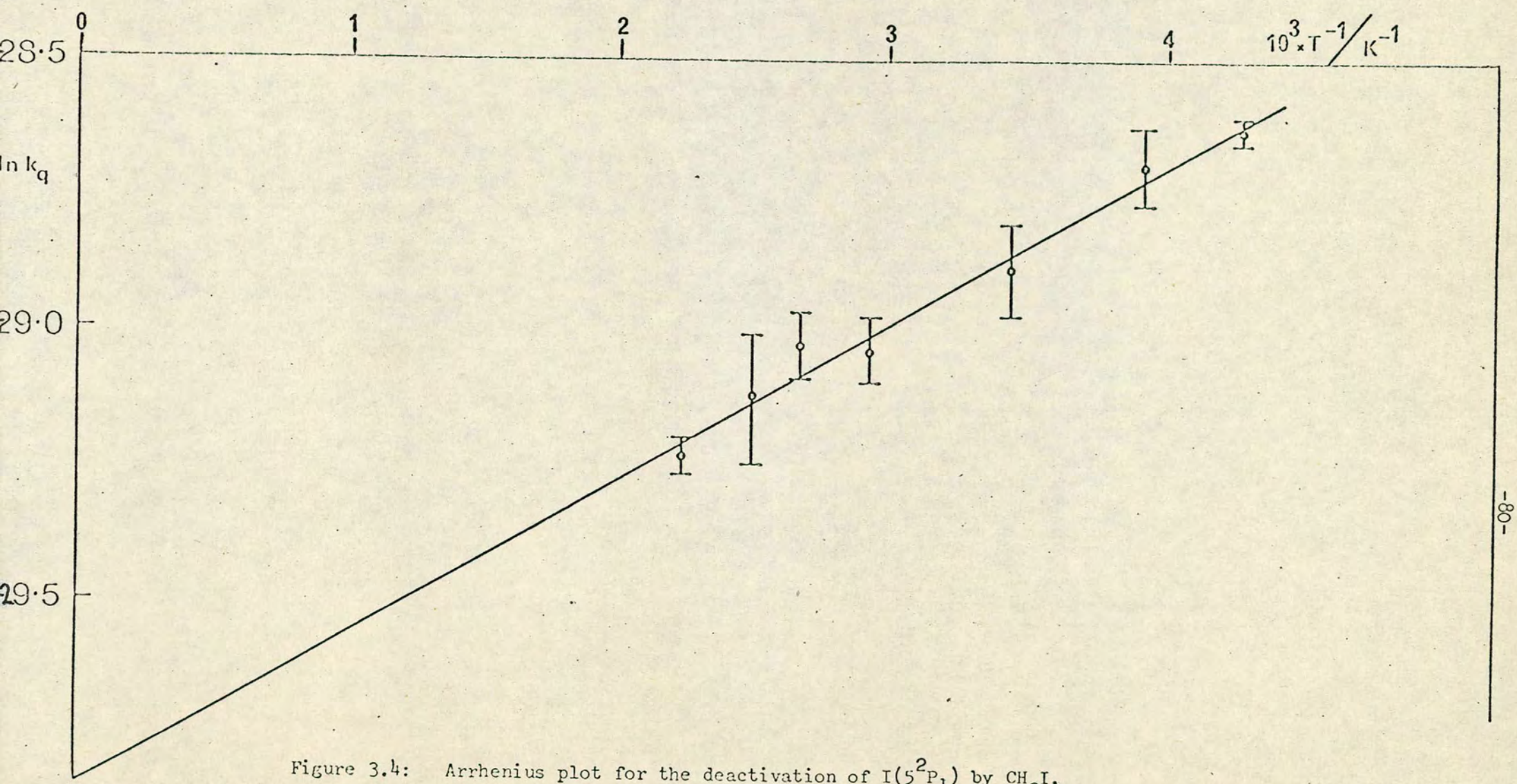

Figure 3.4: Arrhenius plot for the deactivation of $I(5^2P_{\frac{1}{2}})$ by CH_3I.

$$k_{O_2} = (3.55 \pm 1.21) \exp-\left(\frac{0.8 \pm 0.8 \text{ kJ mole}^{-1}}{RT}\right) \times 10^{-11} \text{ cm}^3 \text{ molecule}^{-1} \text{ s}^{-1}.$$

c) The concentration of O_2 molecules in the system was determined by the upper limit of O_2 impurity contained in the N_2 used, i.e. $[O_2]$ = 10 p.p.m. The removal of $I(5^2P_{\frac{1}{2}})$ by O_2 can be described by eq. 3.11

$$I(5^2P_{\frac{1}{2}}) + O_2(X\,^3\Sigma_g) \rightleftarrows I(5^3P_{3/2}) + O_2(a\,^1\Delta_g) \qquad (3.11)$$

The equilibrium constant at 300 K has been measured[140], $K = \frac{k_{-11}}{k_{11}} = 2.94$. As Husain et al. have shown[161], the rate with which equilibrium is reached, depending on the experimental conditions used, may facilitate corrections in the kinetic data. For the present estimation, only the effect of the forward reaction was considered and calculated rates for the $I(5^2P_{\frac{1}{2}})$ removal by $O_2(X^3\Sigma_g)$ were substracted from those determined by the intercepts at each temperature.

Based on data given in Table 3.IV, an Arrhenius plot resulted in a positive activation energy for N_2, $E_a \simeq 5.0$ kJ mol^{-1}; rate constant(293 K) $k_{N_2} \simeq 2.6 \times 10^{-16}$ cm^3 molecules s^{-1}. These values are in relatively close agreement with those existing in the literature[1,62], namely: $E_a = (6.3 \pm 0.4)$ kJ mole^{-1}, and $k_{N_2} = (6.5 \pm 3.0) \times 10^{-17}$, 2.0×10^{-16}, 1.5×10^{-16} cm^3 molecule^{-1} s^{-1}.

The first experiments with CD_3I were carried out in the parallel flashlamp reaction vessel system. However, most of the recorded results were obtained by using the coaxial system. Table 3.V contains the decay rates obtained for various pressures of CD_3I at room temperature. By plotting these results, a deviation from straight line behaviour was observed for pressures less than 0.8 kNm^{-2}. This is attributed to the increased importance of the diffusional quenching of $I(5^2P_{\frac{1}{2}})$ for pressures smaller than 0.8 kNm^{-2}. The second order rate constant determined from

TABLE 3.IV

Determination of the temperature dependence of the quenching of $I(5^2P_{\frac{1}{2}})$ by N_2

T (K)	10^3T^{-1} (K^{-1})	Rate (s^{-1})	$k_{O_2} \times 10^{11}$ (cm^3 molecule $^{-1}$ s^{-1})	$Rate_{O_2}$ (s^{-1})	$k_{N_2} \times 10^{16}$ (cm^3 molecule $^{-1}s^{-1}$)	ln k_{N_2}
233	4.283	305 ± 93	2.31	160	1.67	-36.33
256	3.906	369 ± 199	2.40	190	2.26	-36.03
293	3.413	359 ± 40	2.59	180	2.59	-35.9
343	2.911	328 ± 87	2.65	156	2.91	-35.77
381	2.625	449 ± 98	2.73	145	5.71	-35.10
408	2.481	410 ± 120	2.77	138	5.47	-35.14
443	2.257	347 ± 47	2.80	130	4.76	-35.28

TABLE 3.V

Deactivation of $I(5^2P_{\frac{1}{2}})$ by CD_3I at 293K

P (Nm^{-2})	Rate (s^{-1})
133.32	1062 ± 46
333.30	1261 ± 18
733.26	1334 ± 28
1133.22	1916 ± 118
1533.18	2230 ± 52
2039.80	2669 ± 46
2586.41	3116 ± 61
2666.40	3015 ± 90
2813.05	3529 ± 70
2879.71	3564 ± 101
3199.68	3716 ± 207
3532.98	4163 ± 49

$$k_{CD_3I} = (4.59 \pm 0.40) \times 10^{-15} cm^3 \text{ molecule}^{-1} s^{-1}$$

the gradient of this plot was found to be $k = (4.59 \pm 0.40) \times 10^{-15} cm^3$ $molecule^{-1}s^{-1}$ i.e. in excellent agreement with $k = (4.6 \pm 0.8) \times 10^{-15} cm^3$ $molecule^{-1}s^{-1}$, determined earlier in the parallel flashlamp reaction cell system.

The determination of the γ coefficient appearing in the modified Beer-Lambert law could not be based, for CD_3I, on the same method used for CH_3I. A plot of the intercepts $\ln\ln(\frac{I_o}{I})_{t=o}$ against the pressure of CD_3I, P_{CD_3I}, resulted in negative slopes for $P_{CD_3I} > 1.1$ kNm^{-2}. This is attributed to the optical thickness of CD_3I, which has as an effect the inhomogeneous photolysis of CD_3I, with the highest concentrations of excited iodine atoms occuring next to the walls of the reaction cell. Therefore, the assumption that $[I(5^2P_{\frac{1}{2}})] \propto P_{CD_3I}$, made in the determination of the γ coefficient for CH_3I, was not valid for the monitored concentrations of $I(5^2P_{\frac{1}{2}})$ atoms along the central axis of the reaction cell, when large pressures of CD_3I were used. In order to determine the γ coefficient for CD_3I, we compared the rates obtained for different parts of the decay traces, corresponding to different absorptions and assumed that for absorptions less than 5% the measured decay rate corresponds to $\gamma = 1$. Values for γ were obtained at three different temperatures covering the whole range of temperatures in which decay rates were determined and for a pressure $P_{CD_3I} = 2.59$ kNm^{-2}. The results are summarized in Table 3.VI. These data suggest that for absorptions less than ~25%, which were the maximum absorptions used in obtaining decay rates, γ is constant over temperature within the experimental errors and equal to 1. At room temperature, the same result was obtained for a wide range of pressures (2.04 - 3.53 kNm^{-2}).

More recent determination of k_{CD_3I} by employing time resolved fluorescence spectroscopy, where no correction to the Beer-Lambert law is required, were found to be in very close agreement with the results

TABLE 3.VI

Determination of γ coefficient for CD_3I

T (K)	Absorption (max) %	γ
255	7	1.00 ± 0.05
	31	0.98 ± 0.06
	51	0.96 ± 0.05
293	5	1.00 ± 0.05
	25	0.99 ± 0.07
	42	0.99 ± 0.06
444	7	1.00 ± 0.04
	25	0.99 ± 0.06
	46	0.81 ± 0.05

TABLE 3.VII

Deactivation of $I(5^2P_{\frac{1}{2}})$ by CD_3I at different temperatures

Total pressure: 2.59 kNm^{-2}

T (K)	R (s^{-1})	k x10 ^{15} * (cm^3 molecule $^{-1}s^{-1}$)
253 ± 8	3603 ± 107	4.86 ± 0.88
255 ± 8	3292 ± 249	4.48 ± 0.70
272 ± 6	3168 ± 57	4.60 ± 0.16
293 ± 2	(Table V)	4.59 ± 0.40
346 ± 5	2722 ± 77	5.03 ± 0.28
349 ± 6	2828 ± 114	5.27 ± 0.42
385 ± 7	2505 ± 44	5.15 ± 0.16
397 ± 10	2516 ± 88	5.33 ± 0.38
404 ± 11	2465 ± 41	5.32 ± 0.10
427 ± 12	2315 ± 128	5.28 ± 0.25
444 ± 14	2462 ± 228	5.83 ± 0.54

* Errors correspond to two standard deviations.

of this work.[126] This provided additional evidence that $\gamma = 1$.

Results for the temperature dependence of the rate constants for deactivation of $I(5^2P_{\frac{1}{2}})$ atoms by CD_3I are given in Table 3.VII. The measured rates at each temperature represent the average obtained from rates corresponding to 3 to 4 decay traces, for absorptions less than 25% and $P_{CD_3I} = 2.59\ kNm^{-2}$. The result obtained from a second order plot at room temperature is also given. An Arrhenius plot constructed on the basis of these results, gave a positive activation energy for CD_3I, $E_a = (0.9 \pm 0.1)\ kJ\ mole^{-1}$ and a frequency factor $A = (6.95 \pm 2.24) \times 10^{-15} cm^3$ molecule $^{-1}s^{-1}$. Therefore, for the range of temperatures covered in the present experiments, the rate constant can be represented by the equation:

$$k_{CD_3I} = (6.95 \pm 2.24) \exp - \left(\frac{0.9 \pm 0.1\ kJ\ mole^{-1}}{RT}\right) \times 10^{-15} cm^3 molecule^{-1}s^{-1}$$

It is worthwhile noticing that repetitive flashing of the same sample of CD_3I with flash energies of about 20 J did not have any apparent effect on the measured rates. Therefore, we can conclude that for the conditions we used the formation of I_2 molecules was insignificant, i.e. $I_2 \leq 3 \times 10^{12}$ molecules cm^{-3} or $P_{I_2} \leq 0.013\ Nm^{-2}$, which is the maximum concentration or pressure of molecular iodine ($k_{I_2} = 3.6 \times 10^{-11} cm^3$ molecule $^{-1}s^{-1}$),[137] so that the results will be affected at the first decimal point. As with CH_3I, no pyrolysis was observed at the high temperatures employed.

2) Decay of $I(5^2P_{\frac{1}{2}})$ atoms in the presence of SiH_3I

To our knowledge, the removal of excited iodine atoms in the presence of SiH_3I molecules has not been studied before. The recorded data have been obtained from a limited number of experiments, due to the easy decomposition of SiH_3I and subsequent formation of $(SiH_3)_n$ polymers following the photolytic flash. These products were deposited on the walls and the

windows of the reaction vessel, resulting in a substantial decrease of the detected signal and the already weak absorption. This necessitated cleaning of the reaction vessel after a limited number of experiments, (after about 20 flashes under the conditions used).

Experiments were carried out in the parallel flashlamp reaction vessel system and flash energies less than 45 J were employed. Although photolysis of SiH_3I resulted in the formation of excited iodine atoms, as the absorption profiles of the 206.2 nm line indicated, mixtures of SiH_3I + C_3F_7I and N_2 (C_3F_7I: N_2 = 1:148) were used in the present work. Photolysis of such mixtures resulted in higher yields of $I(5^2P_{\frac{1}{2}})$ and consequently larger absorption signals, without affecting the measured rates.

The γ coefficient of the Beer-Lambert law was determined by comparing the rates obtained from the decay traces for absorptions of less than 17% to those obtained for absorptions of less than 5%, for which it is assumed that $\gamma = 1$. This determination, although rough, gave a result in close agreement to that determined for pure C_3F_7I + N_2 mixtures (cf. Chapter 2) for a wide range of total pressures. For a total pressure of 2.7 kNm^{-2} $\gamma = 0.80 \pm 0.05$ and for total pressure 1.6 kNm^{-2} $\gamma = 0.81 \pm 0.07$.

The plot shown in Fig. 3.5 is based on decay rates obtained for SiH_3I pressures within the range of 36.26 - 116.92 Nm^{-2}. From the gradient of this plot and considering the γ coefficient the decay rate constant was found:

$$k_{SiH_3I} = (5.7 \pm 0.7) \times 10^{-14} cm^3 \text{ molecule}^{-1} s^{-1}.$$

A test for atom-radical effects following the photolysis was carried out by photolysing mixtures under the same conditions with flashes of different energies. For example, photolysis with flashes of 45 J and 180 J (P_{SiH_3I} = 48.53 Nm^{-2}) resulted in decay rates of 498 ± 38 s^{-1} and 518 ± 31 s^{-1} respectively. We can therefore conclude that atom-radical effects

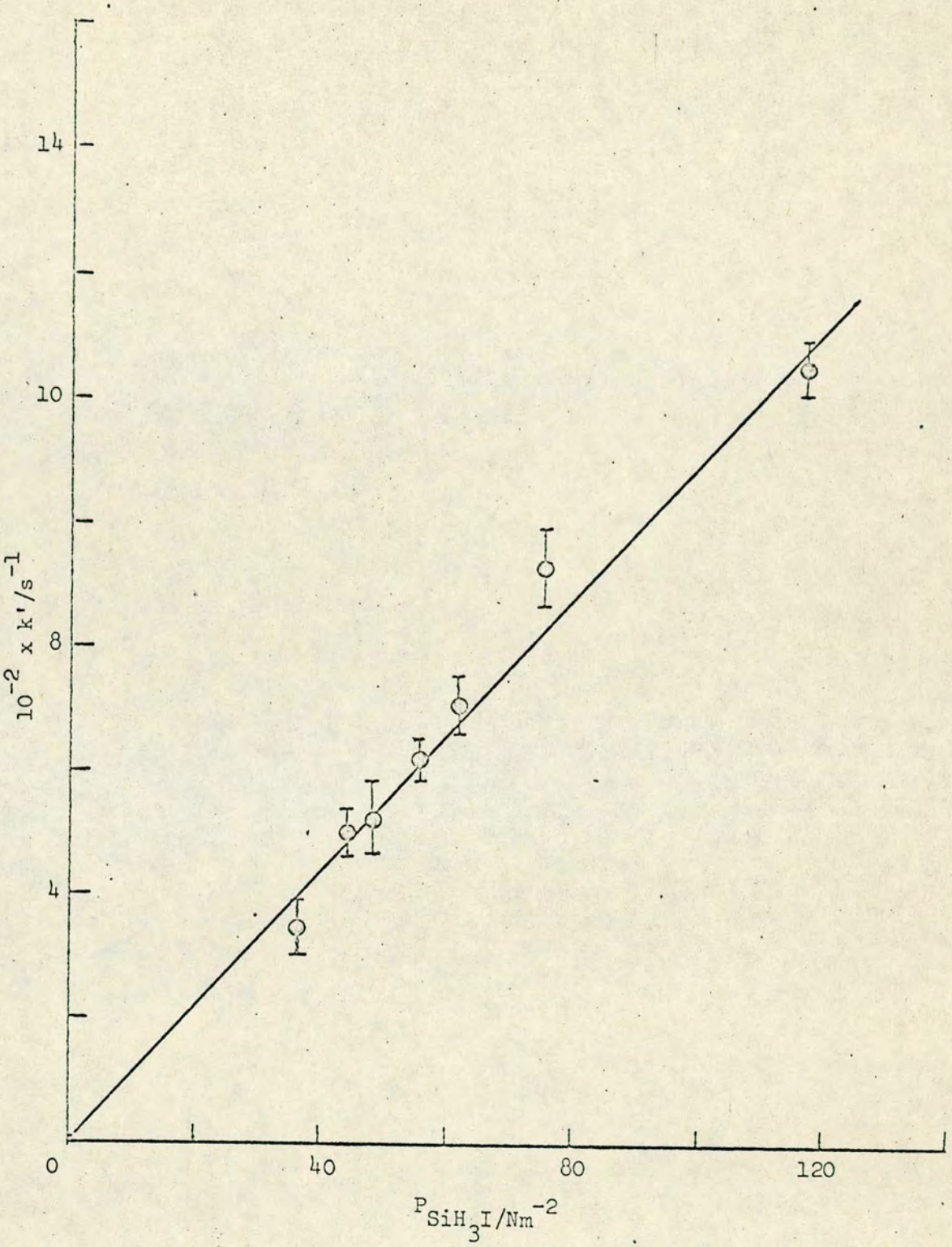

Fig. 3.5: Plot of first order rate coefficients k', (after substracting contributions due to the $C_3F_7I + N_2$ mixture), for the decay of $I(5^2P_{\frac{1}{2}})$ versus pressure of SiH_3I. Flash energy $\leq$ 45 J.

were not important.

3) Decay of $I(5^2P_{\frac{1}{2}})$ in the presence of GeH_3I

The removal of excited iodine atoms by GeH_3I was found to be very fast. A plot of decay rates, obtained after flashing mixtures of GeH_3I and N_2, against pressure of GeH_3I is shown in Fig. 3.6. The rate constant obtained from this plot was: $k_{GeH_3I} = (6.9 \pm 1.0) \times 10^{-12} cm^3$ $molecule^{-1}s^{-1}$. The total pressure used in all experiments was 2.8 kNm^{-2} and the flash energies employed were typically ∿45 J. It was proved, however, that the measured rates for identical mixtures remained constant for flash energies within the range 10 - 125 J. This was indicative of the absence of any radical-radical processes. Flashing the same mixture repetitively had no effect on the rate of removal of excited atoms, showing that there was no significant build up of products which have substantially different rate constants for removal of $I(5^2P_{\frac{1}{2}})$ atoms, such as I_2.

The γ coefficient of the Beer-Lambert law was taken to be equal to that determined for C_3F_7I - N_2 mixtures ($\gamma = 0.82 \pm 0.03$), since by comparing the decay rates for absorptions less than 17% and 5% in one of the decay traces, γ was found 0.84 ± 0.07.

Deposition of the products following GeH_3I photolysis lead, as in the case of SiH_3I, to a reduction in the detected signal and increased the scattered light. Therefore only a limited number of experiments was performed. Polymers can be formed more easily than for SiH_3I, substantial photolysis of gaseous GeH_3I taking place even by the room lights. Experiments therefore were carried out in the dark and no longer than two hours after the preparation of the mixtures.

When mixtures of C_3F_7I + N_2 and GeH_3I were used, the measured rates were smaller than that of GeH_3I + N_2 mixtures, having the same partial pressure of GeH_3I. This decrease is attributed to the removal of part

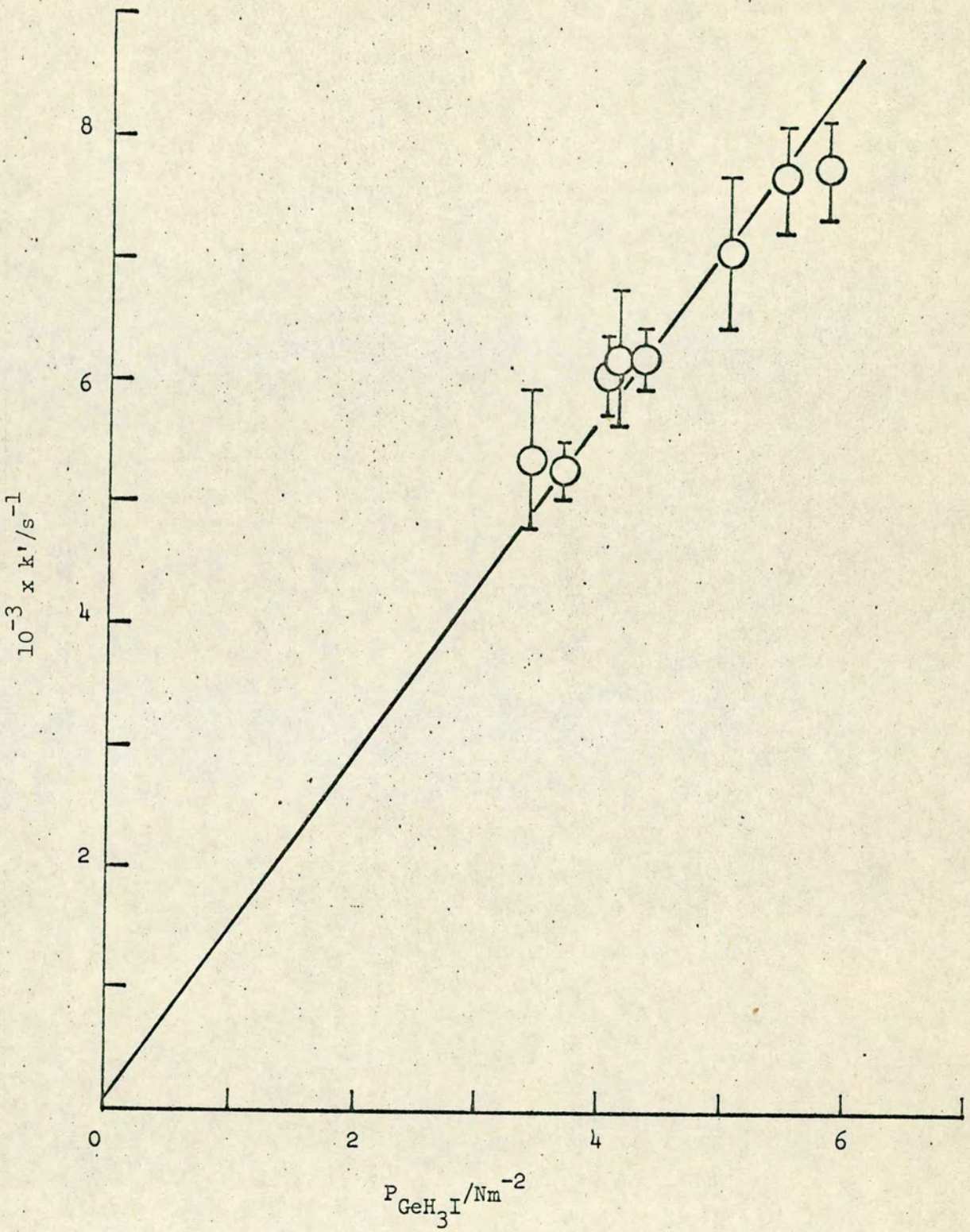

Fig. 3.6 Plot of first order rate coefficients k' for decay of $I(5^2P_{\frac{1}{2}})$ <u>versus</u> pressure of GeH_3I. P_{total} (with N_2) = 2.8 kN m^{-2}, flash energy = 45 J.

of the GeH_3I, which is a very efficient deactivator of $I(5^2P_{\frac{1}{2}})$ atoms. This can take place either due to an increase in the rate of polymerisation in the presence of C_3F_7I or due to possible reaction of GeH_3I with C_3F_7I. The latter seems more probable by analogy to the observed reaction of CF_3I with GeH_4[162]. This reaction proceeds in a sealed tube at 25°C and the initial products are CHF_3 and GeH_3I. GeH_3I reacts further with CF_3I forming copious amounts of yellow-orange solids, which have been attributed to GeH_2I_2, $GeHI_3$ and GeI_4 since no H_2 or HI was detected. To test this proposal, a mixture of 2.5 kNm^{-2} of C_3F_7I and 2.7 kNm^{-2} of GeH_3I was prepared in a small gas I.R. cell and the I.R. spectra were compared immediately and then 3 hours after the preparation. Both spectra contained the I.R. bands of the pure compounds and no other bands could be detected. Comparison of the relative intensities of the corresponding bands was not possible since the walls and the windows of the cell started covering immediately after the mixing with yellow-orange solids. A similar I.R. cell, containing 2.7 kNm^{-2} of pure GeH_3I, under the same conditions had not been covered up with any coloured solids even after 24 hours.

4) Photochemical laser investigation

The comparative performance of six iodides, (n - C_3F_7I, CF_3I, CH_3I, CD_3I, SiH_3I and GeH_3I), was examined in the photochemical laser system. Laser outputs were investigated over a wide range of conditions such as pressure of the iodide, flash energy, presence of buffer gas, enhanced or absent magnetic field due to the flashlamp discharge. Comparisons of the laser efficiency of the various iodides at low pressures were based on measurements of:

a) Threshold pressures at a fixed flash energy.

b) Threshold energies at a fixed pressure of the iodide.

c) The characteristics of laser output, as spike and time behaviour of the output envelope and the maximum number of flashes before laser action stopped.

At first, the iodides were photolysed in the laser cell without using any diluent gas. This could have as an effect the pyrolysis of the iodide and the formation of molecular I_2, (eq.3.6), at the higher flash energies used. In the present work, flash energies were typically 180 - 320 J and never exceeded 720 J. The results were very sensitive to the alignment, which could differ from day to day. The recorded results were obtained in experiments made on the same day and after special care was taken, so that the alignment of the laser cavity will not be distorted during the experiments. They therefore provide a reliable measure of the relative performance of the various iodides as active sources in the iodine laser.

i) Threshold pressures and threshold energies

The results given in Table 3.VIII are threshold pressures and flash energies obtained for fluoro/alkyl and alkyl iodides by using the conventional experimental arrangement. For a given flash energy (320 J), the threshold pressure was determined as the minimum pressure for which laser action occured, within ± 26.7 Nm^{-2}. The determination of the threshold energies for a given pressure of the iodide was less accurate due to the uncertainty in measuring flash energies.

ii) Thermal effects

The use of a buffer gas in the laser cell ensures a reduction of any temperature rise due to the flash. Thermal effects can cause pyrolysis of the iodides and the accumulation of molecular I_2, an efficient quencher

TABLE 3.VIII

Comparative laser performance of iodides

a) Threshold pressure (E=320 J)

Iodide	P threshold (Nm^{-2})	No. of spikes	T_i (μs)	T_f* (μs)
C_3F_7I	106.7	3	100	143
CF_3I	200.0	1	50	50
CD_3I	186.6	2	25	50
CH_3I	426.6	1	20	20

b) Threshold flash energy at different pressures

Iodide: C_3F_7I		CF_3I		CD_3I		CH_3I	
P (Nm^{-2})	E_{thresh} (J)	P (Nm^{-2})	E_{thresh} (J)	P (Nm^{-2})	E_{thresh} (J)	P (Nm^{-2})	E_{thresh} (J)
66.7	500	66.7	720	66.7	720	266.6	720
200.0	361	200.0	361	200.0	361	333.3	500
266.6	320	333.3	320	266.6	361	400.0	500
400.0	245	533.3	320	400.0	320	533.3	320
600.0	180	800.0	180	600.0	180	666.6	180
733.3	180	1066.6	180	800.0	180	933.2	320
1173.2	125	1333.2	125	1199.9	180	1173.2	No laser action

* T_i and T_f are the times at which the first and final spikes appear.

of excited iodine atoms, in the laser cell. Other products due to the thermal effects of the flash can be produced as well. For example, heating of a perfluoroalkyl iodide such as n-C_3F_7I can cause the liberation of free fluorine atoms.[163] This can cause a decrease in the population inversion via the following reaction:

$$C_3F_7I + F \rightarrow C_3F_8 + I(5^2P_{3/2}) \qquad (3.11)$$

In general, the larger the alkyl iodide molecule, the more stable it should be against pyrolytic break up as it possesses more internal degrees of freedom and a resultant greater heat capacity. It should be noted here, that long duration flashlamps as those used in the present investigation, produce more pyrolysis than fast flashlamps delivering comparable energies.[164]

An attempt was made to investigate the effect of the use of a buffer gas on the laser output. Mixtures of C_3F_7I and N_2, as well as CD_3I and N_2 were prepared and the threshold pressures were determined by decreasing the total pressure. The results are recorded in Table 3.IX. The purity of the nitrogen sample used was known from previous kinetic experiments.

iii) Qualitative observations on the envelope of laser emission

By using pressures well above the threshold limit for each iodide, the following observations could be made:

C_3F_7I: When C_3F_7I was used as the laser medium, the highest outputs were obtained, for a given set of conditions. For pressures $\sim$0.8 kNm^{-2} and flash energies $\sim$320 J a broad envelope was observed, made up from superposition of spikes of laser emission, lasting from 15 to 70 μs. The number of spikes was reduced as the number of flashes increased. Laser action from the same sample could be observed up to seven flashes. By increasing the flash energy to $\sim$720 J, laser action took place seven more

TABLE 3.IX

Effect of buffer gas on threshold pressure (E = 320 J)

	N_2/RI	P_{total} (Nm^{-2})	$P_{threshold\ RI}$ (Nm^{-2})
RI = C_3F_7I	0	106.7	106.7
	4	959.9	239.9
	8	2666.4	333.3
	12	7212.6	599.9
RI = CD_3I	0	186.6	186.6
	8	4679.5	586.6
	12	8799.1	733.3

times. The superiority of C_3F_7I as a laser source allowed its use in experiments for optimizing the quality of the alignment of the laser cavity.

CF_3I: In good agreement with previous work the laser output observed when CF_3I was used as laser medium was somewhat smaller than that of C_3F_7I. For CF_3I pressures of $\sim$0.8 kNm^{-2} the broad envelope emission lasted from 18 to 70 μs. The same sample could be flashed two or three times before laser action ceased. As the pressure of CF_3I was reduced, the duration of laser action was reduced until at the threshold pressure (0.2 kNm^{-2}) a single spike was observed at 50 μs (Table 3.VIII).

CH_3I: As it has been reported in previous work, CH_3I is an inefficient laser material in comparison to C_3F_7I and CF_3I. For the determined optimum conditions, (P = 800 ± 67 Nm^{-2}, E $\sim$180 J), a single spike was observed at $\sim$20 μs. Increase of the flash energy under the used pressure did not affect the output significantly. No laser action occured for pressures larger than 1.2 kNm^{-2}, even for a flash energy of $\sim$720 J. Flashing the same sample of CH_3I twice, never resulted in laser action.

CD_3I: To our knowledge, laser action from CD_3I has not been reported before. Laser outputs from CD_3I were surprisingly large in relation to those of CH_3I, even somewhat larger than those from CF_3I, under the conditions we used. The output envelope, obtained at a pressure of 0.8 kNm^{-2} and flash energies of 320 J, was lasting from 16 to 65 μs. By increasing the pressure of CD_3I at 1.5 kNm^{-2} the duration of the envelope was extended to 84 μs. Typical laser outputs for CH_3I and CD_3I are shown for comparison in Fig. 3.7. In contrast to CH_3I, the same sample could be flashed 3 to 4 times before laser action stopped.

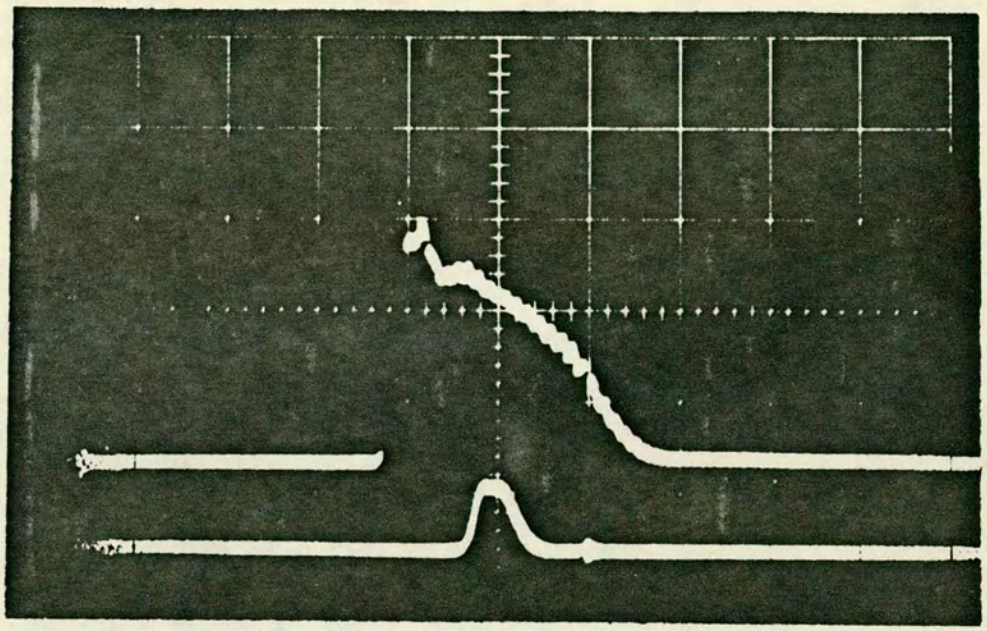

time ⟶

Figure 3.7: Laser emission at 1.315 μm; upper trace CD_3I; lower trace CH_3I. The conditions for both traces were identical; flash energy 125 J; pressure of iodide 450 Nm^{-2} (3.4 Torr); oscilloscope settings, 0.1 Volts per division (vertical) and 5 μs per division (horizontal).

iv) Effect of the magnetic field due to the flash on the laser output

The experimental arrangement employing the two parallel flashlamps was used in these experiments. The flashlamps connection was in series and it could be arranged so that the currents in the two lamps to be either parallel or antiparallel. The first type of connection resulted in cancellation of the time varying magnetic field associated with the two lamps. On the contrary, antiparallel flows of currents resulted in an enchancement of the magnetic field alongside the laser axis. The magnetic field produces Zeeman splitting of the zero field hyperfine sublevels. The detailed effect is quite complex since the relative gains of the hyperfine transitions and hence the overall time behaviour or the emission are changed, but the gross effect is that the gain is reduced by broadening of the atomic line. The output characteristics obtained for 0.8 kNm^{-2} of CD_3I (E = 320 J), were as follows:

a) Antiparallel flow of current during the discharge

The output envelope consists of 3 small spikes. The first 2 spikes appear 30 - 40 μs after the flash and the third spike appears after 58 μs. The same sample of CD_3I stopped lasing after 3 flashes.

b) Parallel flow of current during the discharge

A typical trace of the laser output consists of an envelope with 4 sets of spikes. The first set appears after 16 μs and the third set ends at ∿110 μs. The fourth spike occurs at about 150 μs, i.e. at a time in which the pumping flash has terminated. The appearance of this spike after the end of the flash was reproducible for a wide range of pressures of CD_3I and was observed only for parallel flow of current. The same sample of CD_3I could be flashed up to eight times, during which laser action decreased progressively.

v) Investigation of GeH_3I and SiH_3I as laser materials

The laser system with the two parallel flash lamps was employed in these experiments. At first, the alignment of the laser cavity was checked by optimizing the laser output by using CH_3I as the source of $I(5^2P_{\frac{1}{2}})$ atoms. Then, the optimum conditions for CH_3I laser operation were determined, ($P \sim 0.8$ kNm^{-2}, E = 180 - 320 J), and GeH_3I or SiH_3I were photolysed initially under the same conditions. However, no laser action could be observed for any of these molecules, even at the wide range of pressures and flash energies finally employed. The number of the possible experiments was limited by the easy decomposition of these two iodides, particularly at the higher flash energies employed.

D) DISCUSSION

1) Deactivation of $I(5^2P_{\frac{1}{2}})$ by CH_3I and CD_3I

The rate constants and the corresponding cross sections obtained for CH_3I and CD_3I in this and other kinetic studies of excited iodine atoms are summarised in Table 3.X. The result for CH_3I is in excellent agreement with that obtained in previous work,[134] which also used absorption spectrophotometry. The observed discrepancy with the result obtained by using plate photometry is attributed to the contribution of radical-radical effects, which are possibly present in the latter case due to the high atomic and radical concentrations used. Additional evidence for the validity of the measured rate constant for CH_3I has been recently provided by a successful simulation of the photochemical iodine laser output, employing CH_3I as the active medium.[165] The simulation resulted in possible values of $k_1 + k_2 \sim 2\text{-}3 \times 10^{-13} cm^3 molecule^{-1} s^{-1}$, which are in very good agreement with the value determined here. The decay rate constant for CD_3I has not been determined before. However, unpublished results obtained in very recent experiments by using fluorescence spectroscopy are found in very close agreement with the result given in Table 3.X.

Haaland and Meyer determined[159] the upper limit for the collisional deactivation of $I(5^2P_{\frac{1}{2}})$ by CH_3I to be: $k_2 \leq 4 \times 10^{-14} cm^3 molecule^{-1} s^{-1}$. The rate constant of the reactive pathway was found to be $k_1 = (1.0 \pm 0.7) \times 10^{-14} cm^3 molecule^{-1} s^{-1}$ and therefore $k_1 + k_2 \leq 5 \times 10^{-14} cm^3 molecule^{-1} s^{-1}$. This result diverges from that obtained in this and in other studies.[134] Furthermore, the value determined for k_1 conflicts with previous work and with the work of Aditya and Willard[158] when combined with the present and previous data,[166] yielding $k_1 \leq 3 \times 10^{-16} cm^3 molecule^{-1} s^{-1}$. However, the large isotope effect observed for the removal of $I(5^2P_{\frac{1}{2}})$ atoms by CH_3I and CD_3I,

TABLE 3.X

Rate constants (k) and cross sections (σ) (at 293 K) for removal of electronically excited iodine atoms by CH_3I, CD_3I, SiH_3I and GeH_3I.

Iodide	$(k_1 + k_2) \times 10^{13}$ $cm^3 molecule^{-1} s^{-1}$	$\sigma \times 10^{16}$ cm^2	
CH_3I	17		a
	2.8 ± 0.6		b
	0.5		c
	2.8 ± 0.2[e]	0.092 ± 0.007	This work
CD_3I	0.043 ± 0.04		d
	0.046 ± 0.04	0.0015 ± 0.0002	This work
SiH_3I	0.57 ± 0.07	0.019 ± 0.003	This work
GeH_3I	69 ± 10	2.5 ± 0.4	This work

[a]Reference 157 [b]Reference 134 [c]Reference 159 [d]Recent results obtained by H.M. Gillespie and R.J. Donovan 126. [e]The result obtained in early work from oscillograms and reported in reference 166 was $k = (2.6 \pm 0.6) \times 10^{-13} cm^3 molecule^{-1} s^{-1}$.

($\sigma_{CH_3I} : \sigma_{CD_3I} \simeq 61$), may clarify this controversy regarding the relative efficiencies for the quenching (3.2) and reactive (3.1) channels.

The rate constant for the reactive channel, k_1, is expected to be almost identical for the isotopomers CH_3I and CD_3I, as the potential surface and the C - I bond dissociation energies are essentially the same. Based on the obtained results we can therefore conclude that an upper limit for k_1 is determined by the largest possible value of the less efficient isotopomer CD_3I and consequently $k_1 \leqslant 5.0 \times 10^{-15} cm^3\ molecule^{-1} s^{-1}$. Although this is consistent with the lower bound given for k_1 by Haaland and Meyer, it requires that removal of $I(5^2P_{\frac{1}{2}})$ by CD_3I occurs almost exclusively via reaction. In addition, the ratio $k_2 : k_1 \geqslant 61$ determined for CH_3I, here compared to $k_2 : k_1 \leqslant 4$ found by these authors, suggests a substantial underestimation of k_2 in their work. This is possibly due to the experimental difficulties involved in the technique they used to monitor the rapid formation of I_2, (time resolved mass spectrometry). These difficulties have been discussed by Meyer.[167] It would be interesting therefore if the experiments employing time resolved mass spectrometry could be repeated using CD_3I.

Although the large isotope effect observed establishes beyond any doubt, that the inelastic channel, (3.2), dominates the decay of $I(5^2P_{\frac{1}{2}})$ by CH_3I, there still remains the question of the energy transfer mechanism, which leads to efficient quenching.

In general, we can distinguish three classes of mechanisms, which could explain this kind of process:

i) Mechanisms involving non-adiabatic transitions between the surfaces correlating with the ground and excited atomic states.

ii) Mechanisms involving the formation of a long-lived intermediate complex.

iii) Mechanisms involving near resonant energy transfer due to long range interactions.

We shall discuss the possible contributions of these mechanisms to the quenching cross section in the light of the two pieces of information obtained in the present work, the large isotope effect and the temperature coefficients for the deactivation of $I(5^2P_{\frac{1}{2}})$ by CH_3I and CD_3I.

For the iodine atoms and methyl iodide system a detailed discussion of mechanisms based on non-adiabatic collisions is extremely complicated, since the potential surfaces correlating with the ground and excited atomic states are multidimensional for which there is no concrete formulation of the transition probability. On the contrary, in the case of two dimensional surfaces, expressions in closed form for the transition probability can be obtained by various treatments including the Landau-Zener formulation . We shall therefore examine the possibilities arising from this kind of mechanism in greater detail when discussing the collisional deactivation of $I(5^2P_{\frac{1}{2}})$ by diatomic molecules, (cf. Chapter 4).

For an efficient, non-resonant, energy transfer process of the type

$$A^* + Q \rightarrow A + Q^{\ddagger} + \Delta E ,$$

(where A^* and A are the excited and ground state atom respectively and Q the quenching molecule denoted by $Q^{\ddagger}$ when vibrationally excited), the potential between A^* and Q is considered to be weakly attractive, while that between $Q^{\ddagger}$ and A is repulsive. Energy transfer is favoured if the curves cross in the vicinity of the separated species A^* and Q. The deactivation of $Hg(^3P_{1,0})$ to yield vibrationally excited CO and NO has been explained by Polanyi[168] in terms of this type of non-resonant process. However, considering that the potential surfaces for isotopically substituted molecules are almost identical, no large isotope effect should be expected on the basis of this mechanism.

Non-adiabatic transitions between vibronic surfaces, accompanied by changes in the vibrational and electronic states, have been introduced by

Nikitin.[43,47,48] Thus, the interaction of iodine atoms and CH_3I or CD_3I molecules can give rise to non degenerate electronic states, with the energy between them increasing as the species approach one another, (cf. Chapter 1). Curve crossing or pseudocrossing can then occur, leading to the deactivation of the excited atom and the simultaneous vibrational excitation of the molecule. This is a type of quasiresonant energy transfer as electronically non-adiabatic transitions are favoured most in regions where the energy gap between the separating electronic levels is equal to that of a molecular vibrational transition. The expression for the transition probability includes a vibrational matrix element, which does not favour multiquantum transitions.[43] Therefore, the decay efficiency of the two isotopomers is expected to be different, since the required vibrational excitation for quasiresonant energy transfer to occur is different for the two molecules, with a higher vibrational excitation taking place in the deuterated species. However, it seems rather improbable that an isotope effect due to this mechanism will be of the order of magnitude observed here, expecially if one takes into consideration the fact that the regions, in which non-adiabatic transitions are possible, considerably increase in the case of multidimensional surfaces. Furthermore, the negative activation energy observed for the deactivation of $I(5^2P_{\frac{1}{2}})$ by CH_3I is inconsistent with the predictions of a "curve-crossing" type of mechanism, indicating that some other mechanism dominates the quenching process for CH_3I. Conversely, the slightly positive temperature coefficient observed for CD_3I can be attributed to non-adiabatic transitions leading either to energy transfer or to the abstraction of an iodine atom.

The formation of a complex as an intermediate in the quenching process can account for the observed negative temperature dependence of the quenching efficiency of CH_3I. Complexes of the type CH_3IX, where X is a

halogen atom have been directly observed only in the case of X = F, in crossed molecular beam experiments involving beams of F_2 or F and CH_3I.[169,170] This collision complex was reported as stable by at least 83 - 125 kJ $mole^{-1}$ relative to CH_3I and F. In general, the existence of such complexes, based upon the well known polyvalency of iodine, should be expected, especially in view of a recent discussion of the stability of trihalogen systems with an iodine atom, i.e. the less electronegative atom, at the middle position of the molecule.[31]

Additional evidence for the possible formation of these types of intermediates is offered by the observation of charge-transfer spectra of transient complexes between acceptor iodine atoms produced by the flash photolysis of molecular iodine and a series of five alkyl iodide donors, including CH_3I.[171] However, the existence of these compounds does not necessarily imply that deactivation of $I(5^2P_{\frac{1}{2}})$ proceeds via complex formation. We should therefore compare the expectations arising from this kind of mechanism to kinetic experimental data.

A qualitative criterion for the importance of an intermediate complex formed in a collision process is the complexity of the colliding species. High complexity tends to favour complex formation since the collision energy can be well dissipated to many vibrational modes. Therefore, if the removal of $I(5^2P_{\frac{1}{2}})$ was based on such a mechanism there should be a tendency for the collision efficiency to increase slightly as the alkyl group becomes larger. Table 3.XI contains selected literature values for the decay rate constants of excited iodine atoms in the presence of various iodides. It is obvious that there is no correlation between the size of the alkyl group and the decay efficiency.

Another qualitative criterion for complex formation is that of the correlation between the removal efficiency of the iodides and their ionization potential, (I.P.). Complex formation is expected to be favoured by iodides

with small I.P., since these can act more easily as electron donors to iodine atoms. A linear correlation between the logarithms of the removal rate constants and the I.P. has been reported in many cases, in which an intermediate complex has been assumed, as in the deactivation of both $P(3^2D_J)$ and $P(3^2P_J)$ by polyatomic species[2] and $I(5^2P_{\frac{1}{2}})$ by olefins[1a] From the data given in Table 3.XI for various alkyl iodides, we can deduce that there is no correlation between the decay rate constants and the I.P. whatsoever.

Despite the fact that the above comparisons indicate that quenching of $I(5^2P_{\frac{1}{2}})$ by different iodides via the formation of a complex is unlikely to contribute anything of significance to the overall decay process, it is worthwhile to compare here the predictions of this mechanism with the observed isotope effect and temperature coefficients for CH_3I and CD_3I. A kinetic scheme involving an intermediate complex can be described as follows:

$$A^* + Q \underset{k_{-12}}{\overset{k_{12}}{\rightleftarrows}} AQ \qquad (3.12)$$

$$AQ \xrightarrow{k_{13}} A + Q^{\ddagger} \qquad (3.13)$$

A and A^* denotes the ground and excited atoms respectively and Q the quenching molecule. $Q^{\ddagger}$ refers to the vibrationally or translationally hot quencher.

In reaction 3.12, k_{12} and k_{-12} depend on the ionization potential (I.P) of Q, which is expected to be identical for the two isotopomers. (For CH_3I and CD_3I I.P. $\simeq$ 9.54 eV).[172] The existence of an isotope effect can then be realized only as a consequence of 3.13, i.e. as a result of a non-radiative transition, (NRT), to a repulsive state followed by the dissociation of the complex. Large isotope effects have been well established for the rates of NRT in polyatomic molecules. For example, the rate of NRT in D_2CO (4^1) is at least 500 times slower[173] than in H_2CO (4^1).

TABLE 3.XI

Selected rate constants for the deactivation of $I(5^2P_{\frac{1}{2}})$ by RI and ionization potentials (I.P.) of RI.

RI	k x 10^{13} (cm^3 $molecule^{-1}s^{-1}$)	I.P.[b] (eV)
CH_3I	2.8	9.54
C_2H_5I	1.9[a]	9.35
n-C_3H_7I	2.0[a]	9.26
i-C_3H_7I	2.0[a]	9.18
n-C_4H_9I	2.9[a]	9.23

a) Reference 2 b) References 171, 172a, 172.

TABLE 3.XII

Fundamental frequencies of iodides
ν (cm^{-1})

	ν_1	ν_2	ν_3	ν_4	ν_5	ν_6
CH_3I[a]	2953	1251	533	3060	1437	882
CD_3I[b]	2155	950	501	2300	1048	660
CF_3I[c]	1073	741	285	1185	540	267
SiH_3I[d]	2192	903	355	2206	941	592
GeH_3I[c]	2112	812	248	2121	853	559

a)Reference 174 b)Reference 175 c)Reference 176 d)Reference 177

Similarly, the lifetime of the triplet state of aromatic molecules increases in the deuterated species.[237] Large isotope effects have also been predicted[178] for the photodissociation of triatomics like HCN and DCN, although this theoretical treatment has been criticised in a more recent work.[179] The existence of these isotope effects has been interpreted mainly on the basis of differences in the Franck-Condon transition amplitudes for two isotopomers. It is therefore justified to assume that a large isotope effect can arise from 3.13.

By applying the steady state approximation for the complex AQ in the above set of equations, we end up with the following rate equation for the deactivation of A^*:

$$-\frac{d\,A^*}{dt} = \frac{k_{12}\,k_{13}}{k_{-12}+k_{13}}\,[A^*]\,[Q] \qquad (3.14)$$

We deduce then, that in the case of complex formation, the measured rate constant should be given by the expression involving k_{12}, k_{-12} and k_{13} as in 3.14. In order to compare the behaviour of such a system to the one observed in the deactivation of $I(5^2P_{\frac{1}{2}})$ by CH_3I and CD_3I we can distinguish three possibilities:

i) $k_{13} << k_{-12}$: This is the most probable case for both isotopomers, since formation of the complex presumably occurs in almost every collision by analogy to addition reactions of atoms to stable molecules.[180] Reaction 3.13 is the rate determining step and the quenching rate constant, k_Q, takes the form:

$$k_Q \simeq \frac{k_{12}\,k_{13}}{k_{-12}} \simeq K_e\,k_{13} \qquad (3.15)$$

where K_e is the equilibrium constant for 3.12. Considering that the intermediate complex has been already energized, k_{13} is expected to be temperature independent and the temperature dependence of k_Q will be solely determined by the variations of K_e with temperature, which should be the same for both isotopomers. This is in contrast with the experimental

data.

ii) and iii) $k_{13} \simeq k_{-12}$ or $k_{13} >> k_{-12}$: For both cases, k_Q is totally independent from k_{13}, since $k_Q = \frac{1}{2}k_{12}$ and $k_Q = k_{12}$ correspondingly. Therefore, if any of these relationships holds for both isotopomers, no large isotope effect is predicted and the present mechanism is not compatible with the experimental data. However, considering that k_{13} may differ substantially for the two isotopomers, condition (i) may still be satisfied for the less efficient isotope, while it falls within the limits covered by (ii) and (iii) for the other. In such a case a deactivation mechanism based upon complex formation is not contradictory to the existence of a large isotope effect. Furthermore, the possible temperature dependencies for k_{12} do not exclude the negative temperature dependence observed for CH_3I. The only drawback of this scheme is the Arrhenius preexponential factor observed for CH_3I, which is very small in comparison with those usually obtained in bimolecular recombination reactions.[180] As the above discussion indicates, although the formation of an intermediate complex is possible during the interaction of iodine atoms and CH_3I or CD_3I molecules, this can not play an important role in the deactivation of $I(5^2P_{\frac{1}{2}})$.

Electronic to vibrational energy transfer may be a very efficient process in systems where the amount of energy transfered into translation, i.e. the energy mismatch, is minimal. In the above discussion of non-adiabatic transitions the role quasiresonant transitions may play in the deactivation of $I(5^2P_{\frac{1}{2}})$ by CH_3I or CD_3I has already been emphasised. The importance of near resonant energy transfer has been directly demonstrated in several cases and has found a practical application in pumping new chemical laser systems (cf. Chapter 1).

Long range multipolar interactions may result in substantial inelastic cross sections, the magnitude of which is highly dependent on the energy mismatch

of the corresponding channel (cf. Chapter 5). This dependence decreases with the range of the multipolar interactions and for small energy discrepancies the longest range forces are expected to contribute most to the quenching cross section. For the system of iodine atoms and CH_3I or CD_3I molecules, the longest non-zero interaction is that involving coupling between quadrupole transitions in the iodine atoms and dipole transitions in the iodides (d-q coupling). The electronic energy transferred in translation and the internal degrees of freedom is equal to the spin-orbit coupling of the iodine atoms, $\Delta E\ (I(5^2P_{\frac{1}{2}}) - I(5^2P_{3/2}))$ = 7603 cm^{-1}, and from the vibrational frequencies given in Table 3.XII, we can estimate the number of vibrational quanta required to take up most of this energy. For CH_3I, near resonance, i.e. $\Delta E^* \leq 50\ cm^{-1}$, where ΔE denotes the energy mismatch, can be achieved by the excitation of three vibrational quanta. A relatively strong overtone band has been experimentally observed at $\sim$6800 cm^{-1} converging towards $\sim$7500 cm^{-1}. In contrast, for CD_3I at least four vibrational quanta should be excited so that the near resonant condition will be fulfilled. The vibrational matrix element for the latter is expected to be about one order of magnitude smaller than that for the overtone transition in CH_3I. Excitation of three vibrational quanta in CD_3I would result in energy discrepancies larger than 1400 cm^{-1}.

As explained in Chapter 5 , the cross section for this type of process is proportional to the square of the vibrational transition matrix element of the quenching molecule, and the order of the isotope effect observed

* This limiting value reflects the dramatic decrease of the cross section for larger energy mismatches, (cf. Chapter 5) in the case of d- q coupling.

reflects the differences in the CH_3I and CD_3I overtone matrix elements, for near resonant transitions. The extremely low efficiency of CF_3I in deactivating $I(5^2P_{\frac{1}{2}})$ may be discussed on a similar basis. For CF_3I, at least seven vibrational quanta should be excited to match up with the electronic energy of iodine atoms (Table 3.XII), involving extremely small matrix elements. Thus, even if we assume that the cross section given for CF_3I is entirely due to quenching, the ratios of the cross sections recorded below reflect the effect of near resonant processes on the quenching rate:

$$\frac{\sigma_{CH_3I}}{\sigma_{CD_3I}} = 61 \; ; \; \frac{\sigma_{CH_3I}}{\sigma_{CF_3I}} > 767$$

It is worthwhile to notice here some analogies existing between the removal of $I(5^2P_{\frac{1}{2}})$ by alkyl iodides and alkanes. For both sets of compounds, the quenching process seems to be effectively localised. For alkyl iodides with up to four carbon atoms the decay rate constant falls within the range 1.9 to 2.9 x 10^{-13} cm^3 $molecule^{-1}$ s^{-1} (Table 3.XI). Correspondingly, for the alkanes the rate constants lie within the range 1.0 to 2.7 x 10^{-13} cm^3 $molecule^{-1}$ s^{-1}. This should be expected in terms of a near resonant energy transfer mechanism, since energy matching in each of the two sets of the hydrogen containing compounds requires the same number of vibrational quanta, as a consideration of the vibrational frequencies reveals.[174] On the contrary, for the deuterated compounds a larger number of vibrational quanta should be involved and a large isotope effect is in general predicted and has been experimentally verified[65] for CH_4 and CD_4. Furthermore, the activation energy obtained for CH_3I has the same sign and magnitude with activation energies obtained for alkanes, as shown in Table 3.XIII. Alternatively, these small negative temperature coefficients can be attributed to a temperature variation of the preexponential factor as T^{-1}. This is in very good agreement with

the theoretical expectations of the long range multipolar interaction mechanism.

TABLE 3.XIII

Arrhenius parameters for the deactivation of $I(5^2P_{\frac{1}{2}})$ by CH_3I and alkanes

Gas	log A ($cm^3 molecule^{-1} s^{-1}$)	E_a ($kJ\ mole^{-1}$)
CH_3I[a]	-12.95 ± 0.05	-2.9 ± 0.1
CH_4[b]	-13.40 ± 0.17	-2.1 ± 0.8
C_2H_6[b]	-13.43 ± 0.11	-2.1 ± 0.4
C_3H_8[b]	-13.24 ± 0.14	-2.9 ± 0.4
$n\text{-}C_4H_{10}$[b]	-12.73 ± 0.11	-1.3 ± 0.4

a) This work b) Reference 62

However, there still remains the question of the possible removal mechanism for the less efficient molecule, CD_3I. The positive E_a obtained for CD_3I is incompatible with a mechanism based on near resonant energy transfer due to long range forces. Both the abstraction reaction and non-adiabatic transitions can account for the temperature behaviour observed, although contributions from long range forces, presumably involving higher order of coupling, are not entirely excluded (cf. Chapter 5)

To sum up, the large isotope effect observed for the deactivation of $I(5^2P_{\frac{1}{2}})$ by CH_3I and CD_3I proves that for the most efficient isotopomer CH_3I, the reactive pathway (3.1) is of much less importance than quenching (3.2). This isotope effect, when combined with temperature dependence data for the decay rates, can be explained in terms of near resonant energy transfer due to dipole-quadrupole coupling. The removal process by the less efficient isotopomer may involve contributions from various

decay mechanisms, including reaction.

2) Deactivation of $I(5^2P_{\frac{1}{2}})$ by N_2

As was explained in section C, the kinetic data obtained for N_2 should be considered as approximate. Apart from the reasons given there there is one additional reason which possibly introduces some unestimated error in the recorded data. The observed E_a for N_2 may in part be due to the temperature variation of the diffusional rate of $I(5^2P_{\frac{1}{2}})$ in N_2, with efficient deactivation taking place at the walls of the reaction vessel. To our knowledge, there are no available data for the diffusion of iodine atoms in N_2, so that corrections could be made.

Long range interactions do not seem to be important for the quenching process, especially considering the strongly positive temperature dependence of the quenching rate . On the contrary, the model proposed originally by Andreev and Nikitin,[181] in which relaxation occurs via potential energy surface crossings is in good agreement with the experimental data obtained here.

The basis of the calculations of Andreev and Nikitin, which employs a Landau-Zener formalism[44,45] at a pseudocrossing point of vibronic terms, is connected with the excitation of a molecular vibration yielding $N_2(v = 3)$ as follows:

$$I(5^2P_{\frac{1}{2}}) + N_2\,(v = o) \rightarrow I(5^2P_{3/2}) + N_2\,(v = 3),\quad \Delta E = -756\ cm^{-1} \qquad (3.16)$$

The authors have reported an energy barrier of 4.6 - 5.0 kJ $mole^{-1}$, which is in very good agreement with the one determined in the present work. The calculated transition probability leads to a collision cross section , which is less than one order of magnitude smaller than that experimentally determined here. Thus we conclude that although the present data were rough and do not permit any detailed comparison with the calculated results, they provide support for the model proposed by Andreev and Nikitin.

3) Deactivation of $I(5^2P_{\frac{1}{2}})$ by SiH_3I and GeH_3I

The bulk rate constant measured for the deactivation of $I(5^2P_{\frac{1}{2}})$ by SiH_3I and the absence of any other relevant information allows only pure speculation on the removal mechanism. The smaller decay rate observed for SiH_3I than for CH_3I (Table 3.X) may be understood in terms of near resonant energy transfer. From Table 3.XII, we can deduce that at least four vibrational quanta are required to minimize the energy mismatch, as in CD_3I. The quenching rate appears to be larger than for CD_3I, presumably due to more intense vibrational transitions in SiH_3I. However, the contribution of reactive pathways to the relaxation process should not be disregarded. In contrast to CH_3I, where hydrogen atom abstraction and formation of HI was energetically unfavourable, with SiH_3I both iodine and hydrogen atoms may be abstracted on energetic grounds. The effects of this possibility are better illustrated in the deactivation of $I(5^2P_{\frac{1}{2}})$ by GeH_3I.

As shown in Table 3.X, the cross section for GeH_3I is 27 times larger than that for CH_3I and in general larger than cross sections which are normally associated solely with energy transfer collisions of $I(5^2P_{\frac{1}{2}})$. From the vibrational frequencies of GeH_3I given in Table 3.XII, it becomes clear that near resonant energy transfer cannot account for the observed decay efficiency. Thus, this high efficiency is indicative of a favourable reactive pathway.

Experiments employing vacuum ultraviolet kinetic specroscopy [182] have proved that HI is formed following the photolysis of GeH_3I, as a product of a secondary reaction rather than as a primary photolysis product. A series of experimental observations suggested that this reaction involves the abstraction of hydrogen atoms by <u>both</u> $I(5^2P_{\frac{1}{2}})$ and $I(5^2P_{3/2})$. Formation of molecular iodine was not observed and therefore from the reactive channels 3.17 and 3.18 only 3.17 seems to account here for the measured

rate constant.

$$I(5^2P_{\frac{1}{2}}) + GeH_3I \rightarrow GeH_2I + HI \qquad (3.17)$$

$$I(5^2P_{\frac{1}{2}}) + GeH_3I \rightarrow GeH_3 + I_2 \qquad (3.18)$$

The efficient hydrogen atom abstraction from GeH_3I in contrast to CH_3I may be attributed to the steady decrease of the bond strength of single covalent bonds between group IV atoms and hydrogen atoms. Unfortunately, the bond dissociation energies $D(GeH_2I\text{-}H)$ and $D(SiH_2I\text{-}H)$ are not available for a direct comparison with $D(CH_2I\text{-}H)$. However, considering that the dissociation energies for $CH_3\text{-}H$ and $CH_2I\text{-}H$ are comparable with $D(CH_2I\text{-}H)$ slightly smaller, it is reasonable to assume that comparison of the energies $D(MH_3\text{-}H)$, where M denotes the group IV atom, is a very good approximation.* Average bond energies, reflecting the tendencies of the dissociation energies of the iodides are given for the M-H and M-I bonds in Table 3.XIV. From these data, it then becomes clear that the hydrogen atom abstraction from SiH_3I and GeH_3I by $I(5^2P_{\frac{1}{2}})$ is an exothermic reaction, in contrast to CH_3I.

TABLE 3.XIV

Average energies of M-H and M-I bonds in kJ $mole^{-1}$

M	H	I
C	416	213
Si	323	234
Ge	290	213

The increase in the efficiency of the reaction with decreasing bond energy is in agreement with the proposals of Fettis and Knox.[184] These

* Experimental verification of the validity of this assumption was obtained in the kinetic spectroscopy work,[182] where it was found that $D_{298}(GeH_2I\text{-}H) \leq 298$ kJ $mole^{-1}$ compared to $D_{298}(GeH_3\text{-}H) \leq 326$ kJ $mole^{-1}$ obtained by Setser et al.[208]

authors have reported a correlation between the activation energies for a wide range of halogen atom reactions and the exothermicity of the reactions at absolute zero. A schematic representation of the potential surface along the reaction coordinate for the reactions of interest here, is given in Figure 3.8. The relative energy of the products is based on data given in Table 3.XIV and the energy barriers reflect the decrease in the activation energy with increasing exothermicity . Callear and Wilson have obtained experimental evidence for the validity of this correlation by measuring the activation energy for the abstraction of hydrogen atoms from C_3H_8 and C_2H_6 by $I(5^2P_{\frac{1}{2}})$.[185] For C_2H_6 they found an activation energy about 4 kJ mole^{-1} smaller than that expected in terms of the correlation curve given by Fettis and Knox. This disparity was attributed to non-adiabatic transitions between the potential surfaces. In figure 3.8, non-adiabatic or adiabatic transitions leading to quenching of $I(5^2P_{\frac{1}{2}})$ are represented by the arrows. An interesting aspect of the results of Callear and Wilson is the low preexponential Arrhenius factors, which correspond to mean transition probabilities of the order 10^{-3}. These workers have explained this on the basis of a disequilibrium at the transition state due to relaxation to the lower surface. For GeH_3I, quenching processes are expected to be rather inefficient according to the above discussion, resulting in a higher preexponential factor and mean transition probability for the reactive channel.

Although the efficiency of $I(5^2P_{\frac{1}{2}})$ to abstract H atoms changes as the group IV element is altered in the iodide, iodine atom abstraction is an inefficient process for both CH_3I and GeH_3I, while for SiH_3I there are not any available experimental data. The I atom abstraction by $I(5^2P_{\frac{1}{2}})$ atoms is an exothermic process for the three iodides by about the same amount of energy since the M-I bond strengths are almost identical.[183a] The existence of a high energy barrier as well as the fast quenching of $I(5^2P_{\frac{1}{2}})$

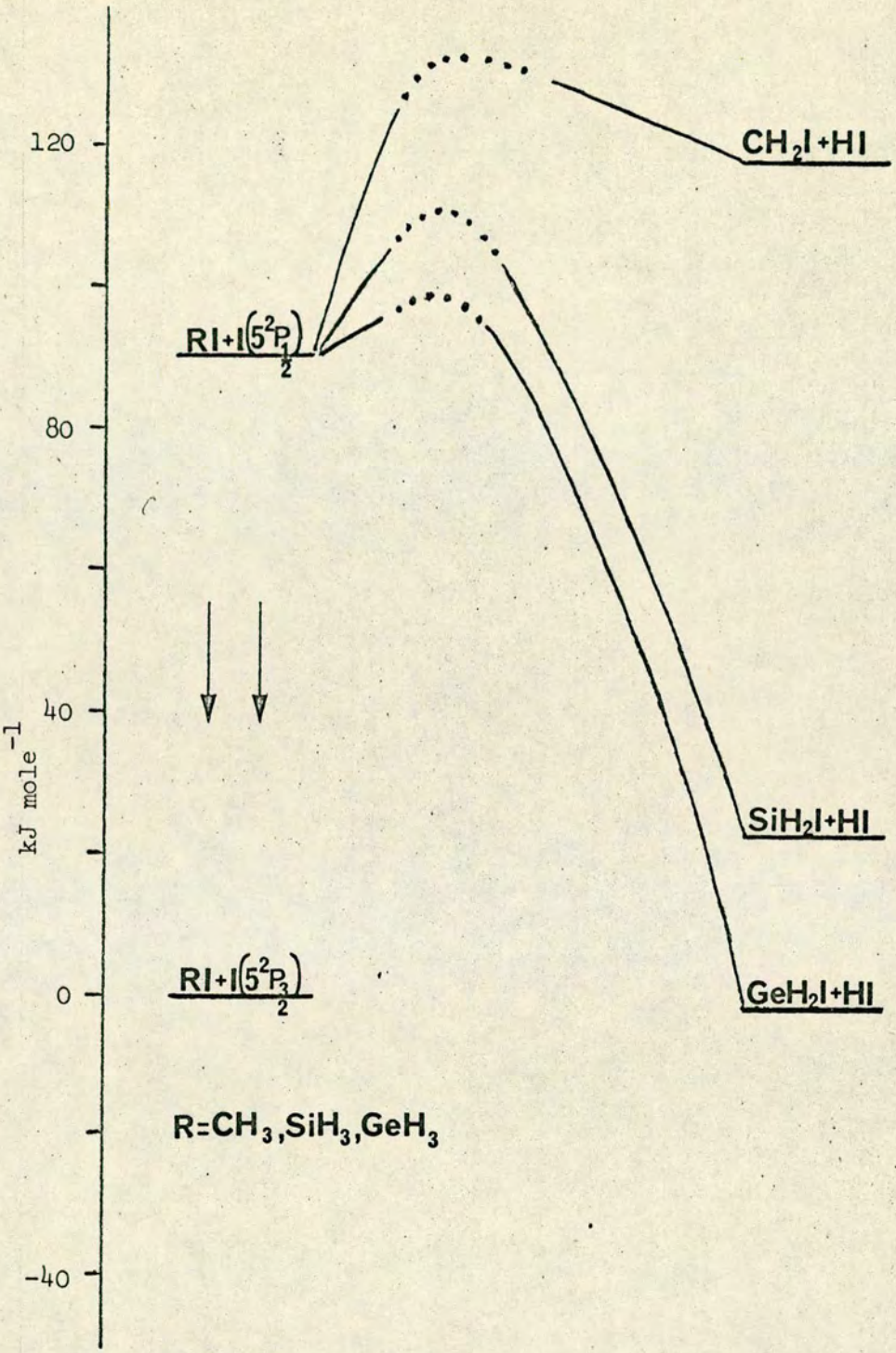

Figure 3.8: Energetics of H atom abstraction from RI by $I(5^2P_{\frac{1}{2}})$. The heights of the energy barriers, (dotted lines), have been drawn arbitrarily but reflect the correlation between the exothermicity of reaction and the activation energy.

by CH_3I may account for the inefficiency of channel 3.1. For GeH_3I however, the quenching channel is expected to be unimportant and an interesting question arises, concerning the relative efficiency of 3.17 and 3.18. The higher efficiency of 3.17 indicates a lower energy barrier for the abstraction of H atom than for I atom from GeH_3I and part of this difference may be due to non-bonding attractive interactions between the attacking $I(5^2P_{\frac{1}{2}})$ and the I or H atoms. Considering the relative sizes of Ge and H atoms, the GeH_3 group can be considered as an atom with a very high polarizability, resulting in a preferential attraction of the $I(5^2P_{\frac{1}{2}})$ atoms by the GeH_3 end of GeH_3I instead of by the bound I atom. As a consequence, higher kinetic energies are required for the formation of an activated complex in the latter case.

To summarize, we can refer to figure 3.8. In the case of CH_3I, where the reactive pathway is closed, non-reactive processes and especially adiabatic transitions leading to near resonant energy transfer determine the decay of $I(5^2P_{\frac{1}{2}})$. For SiH_3I reaction is possible but still an appreciable energy barrier has to be overcome and the measured rate constant presumably consists of contributions from both reactive and non-reactive processes. For GeH_3I the energy barrier for H atom abstraction is very small and the reactive pathway is predominant. Non-reactive processes including near resonant energy transfer are unimportant.

4) Performance of the iodides in the iodine photodissociation laser

The discussion of the relative performance of the examined iodides as laser media may be based on three main items, which effectively determine the laser operation in the present investigation. These are:

(1) The primary photolytic branching ratio in 3.3, determined by the fraction of iodine atoms formed in the $^2P_{\frac{1}{2}}$ state as opposed to the ground $^2P_{3/2}$ state.

(2) The threshold concentration of $^2P_{\frac{1}{2}}$, which is necessary to overcome losses in the optical cavity.

(3) The effective lifetime of the excited state as determined by the deactivation kinetics.

The importance of these items may be realised by considering the following simplified treatment of the conditions necessary for gain in a medium.

Following Mitchelland Zemansky[186] the expression for the absorption coefficient a_o at the centre of a transition which is Doppler broadened and has negligible natural linewidth is given by 3.19.*

$$a_o = \frac{K}{\Delta\nu_D} f_{21} \left(\frac{N_1}{g_1} - \frac{N_2}{g_2}\right) \qquad (3.19)$$

where: K is a constant, $K = \frac{2e^2}{mc} (\pi \ln 2)^{\frac{1}{2}}$, with the symbols having the usual meaning (cf. Reference 187).

f_{21} is the oscillator strength of the transition from state 2 to state 1.

N_1 is the population density in the ground state (state 1).

N_2 is the population density in the excited state (state 2).

g_1, g_2 are the statistical weights for states 1 and 2.respectively.

$\Delta\nu_D$ is the Doppler width of the transition.

When natural broadening is not negligible compared to Doppler broadening, the expression for the absorption coefficient is more complicated than 3.19 but the conclusions derived here are general, being valid for any case.

a_o is usually refered as "gain coefficient" and is a characteristic

* The absorption coefficient at a frequency ν will then be given by:

$$a_\nu = a_o \exp\left(-2\left[\left(\frac{\nu - \nu_o}{\Delta\nu_o}\right)(\ln 2)^{\frac{1}{2}}\right]^2\right) \qquad (3.20a)$$

parameter of the laser. In general a_ν is expressed as,

$$a_\nu = \sigma \Delta N \qquad (3.20)$$

where σ, the stimulated emission cross section,[187] is a function of the Einstein coefficient for stimulated emission, the frequency ν and the linewidth $\Delta\nu$. Thus, for optical gain, a population inversion ΔN resulting in a negative absorption coefficient is necessary, i.e:

$$\Delta N = N_2/g_2 - N_1/g_1 \geq 0 \qquad (3.21)$$

Item (1) is related to 3.21, which, for the atomic iodine states involved here gives $N_2/N_1 \geq 0.5$.

However, for obtaining laser oscillation the fullfillment of 3.21 is insufficient. Enough inversion is necessary so that the optical gain in a single pass through the medium will exceed the single pass losses due to reflection and diffraction. This is expressed by 3.22,

$$\exp(-a_\nu \ell) - 1 > \text{losses} \qquad (3.22)$$

where ℓ is the length of the medium and a_ν is now negative. In the limit of small gain and losses, $a_\nu \ell$ is small and 3.22 can be approximated by 3.23.

$$-a_\nu \ell > \text{losses} \qquad (3.23)$$

Thus on substitution for a_o from 3.19 we obtain for the oscillation condition:

$$\Delta N > \frac{\text{losses}}{\ell} \quad \frac{\Delta\nu_D}{K f_{21}} \qquad (3.24)$$

Expression 3.24 shows the importance of item (2). Finally, N_1 and N_2 are related to the effective lifetimes τ_1 and τ_2 of the corresponding states and under steady state conditions we obtain:

$$N_1 = n_1 \tau_1 \text{ and } N_2 = n_2 \tau_2 \qquad (3.25)$$

where n_1 and n_2 are the pumping rates into states 1 and 2 respectively. Considering 3.25, expression 3.24 can be written as:

$$n_2 \tau_2/g_2 - n_1\tau_1/g_1 > \text{losses } \Delta\nu_D/\ell K f_{21} \qquad (3.26)$$

The effect of an efficient deactivation of $I(5^2P_{\frac{1}{2}})$ on the laser operation,

may be understood in terms of 3.26 (item (3)).

Based on the above analysis, the problem of obtaining laser action from an iodide can be divided into two parts. The first part is connected with the photodissociation mechanism of the iodide and the second with the deactivation processes of $I(5^2P_{\frac{1}{2}})$ atoms.

(i) Photodissociation of CH_3I

In this section we shall discuss some of the factors which determine the yield of $I(5^2P_{\frac{1}{2}})$ following the flash photolysis of the iodides used, by considering the specific example of the photodissociation of CH_3I. Porret and Goodeve[188] have shown that the first absorption band of CH_3I has a maximum at 260 nm and yields both the ground and excited states of the iodine atom, the latter dominating when light of wavelength shorter than about 300 nm is used. The production of both states may be understood in two ways. The first is based on the assumption that the absorption band consists of at least two overlapping transitions to different excited states of CH_3I correlating with the two states of iodine atoms, as in HI. In the second, the absorption is entirely, or almost so, to one state correlating with $I(5^2P_{\frac{1}{2}})$ but deexcitation occurs to some extent via crossing with ground state surfaces, before dissociation.*

The electronic spectrum of CH_3I has been discussed extensively.[190,191] Photolysis in the near U.V. (200-300 nm) involves the promotion of an electron from an essentially non-bonding orbital localised on the I atom to a low lying C-I orbital. This corresponds to the transition from the configuration $(a_1)^2(e)^4$ of the ground state CH_3I to the configuration $(a_1)^2(e)^3(a_1^*)^1$. Considering that in a molecule like CH_3I there is a large spin-orbit coupling due to the I atom, the symmetry species of the

* It has been experimentally verified[189] that the photodissociation of CH_3I is direct, occuring in less than 10^{-13}s.

electronic states will be determined by the symmetry of the total wavefunctions including spin by utilizing extended point groups. The correlation diagram shown in Fig. 3.9 has been constructed following Herzberg.[190] The electronic states of CH_3I in the case of weak spin-orbit coupling have been included in Fig. 3.9. In the C_{3v} point group, the closed-shell ground state configuration results in $^1A_1$ symmetry species, which remain unchanged for strong spin-orbit coupling. From the excited state configuration two symmetry species may arise, namely ^1E and ^3E. For strong spin-orbit coupling, the first changes into E and the latter into $A_1 + A_2 + 2E$. The symmetry species corresponding to the ground state iodine atom are $E_{\frac{1}{2}} + E_{3/2}$ and $E_{\frac{1}{2}}$ for $I(5^2P_{\frac{1}{2}})$ (cf. Table 56 in Reference 190). Considering that the CH_3 radicals are formed in their ground electronic state following the photolysis of CH_3I with wavelengths longer than 200 nm[190] their state will be designated as $E_{\frac{1}{2}}$ in strong spin-orbit coupling and these species must be combined with those of the iodine atom. The resulting states are then correlated with those of the undissociated molecule on the basis of the non-crossing rule. As it is shown in Fig. 3.9, the only transition which leads to formation of $I(5^2P_{\frac{1}{2}})$ in the primary photolysis of CH_3I in the first band is $X\ ^1A_1 \rightarrow\ ^1A_1$. The electric dipole associated with this transition must be parallel to the C-I bond and this has been observed in photofragment spectroscopy experiments.[192] On the contrary, the proposal of Simons[191] that the near U.V. absorption of CH_3I is associated with the transition $X\ ^1A_1 \rightarrow\ ^1E$ does not result in the formation of $I(5^2P_{\frac{1}{2}})$ according to the correlation diagram and predicts an electric dipole moment perpendicular to the C-I bond. It should be therefore disregarded. Transitions in the first band of CH_3I can in general be associated with forbidden singlet-triplet transitions since the excited states arise from a ^3E state. This is

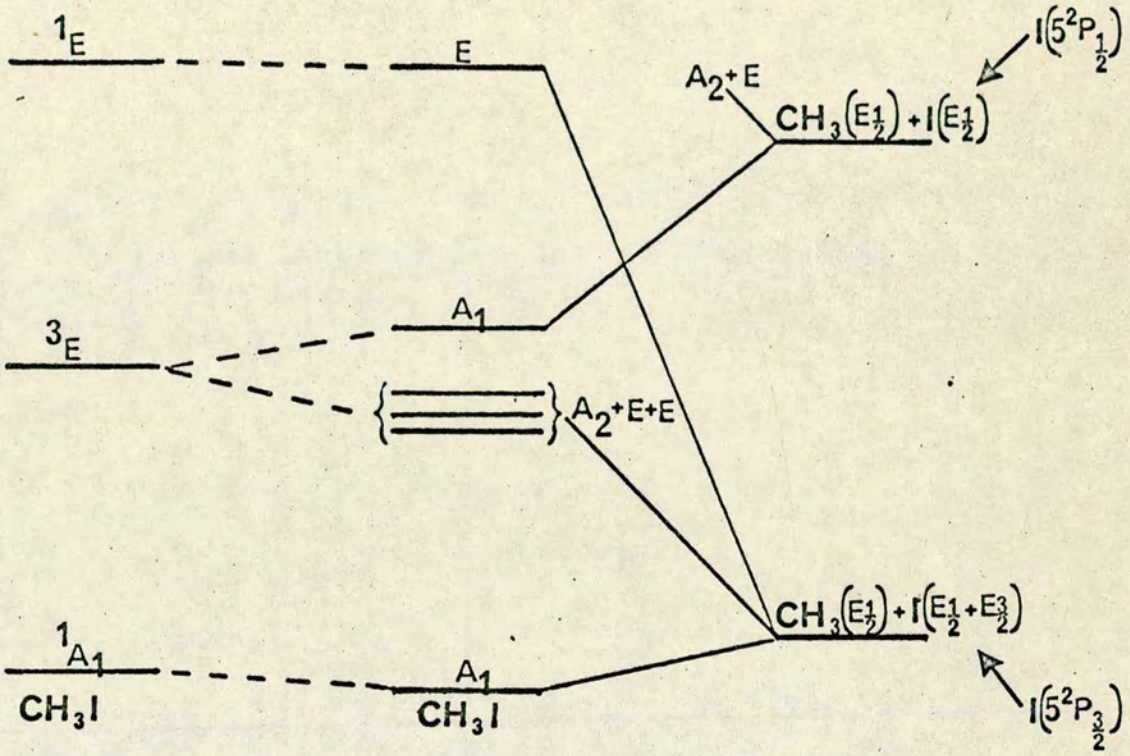

Figure 3.9: Correlation diagram for the photodissociation of CH_3I or in general of iodides with C_{3v} symmetry.

compatible with the observed small intensity of the first band.

In Fig. 3.9, the set of states A_2 + 2E has been drawn below the A_1 state arising from ^3E, accounting for the observed increase of $I(5^2P_{\frac{1}{2}})$ yield with decreasing photolysis wavelength. In general, the proximity of states A_1 and A_2 + 2E is connected with the effective spin-orbit coupling and seems to be of great importance for the branching ratios observed in the photolysis of various iodides. Crossing of the respective surfaces can lead to an internal quenching of $I(5^2P_{\frac{1}{2}})$ before dissociation. The probability of this process decreases as the separation of A_1 and A_2 + 2E increases. Wiesenfeld,[145] based on a similar mechanism, has associated the observed branching ratio with excited states exhibiting zwitterionic character and therefore to the ionization potential of the alkyl group. For many iodides, there is a reasonable correlation. However, the higher branching ratio, Φ, measured[145] for CD_3I (Φ = 80) in comparison to CH_3I (Φ = 11.5), the ionization potential being identical for both CH_3 and CD_3, makes this model questionable.

ii) Effective lifetime of $I(5^2P_{\frac{1}{2}})$

The mean radiative lifetime of $I(5^2P_{\frac{1}{2}})$ is very long (0.13 s) and its effective lifetime is essentially determined by diffusional, collisional or reactive processes in the laser cell. As it is shown in 3.26 the laser output depends strongly on this parameter and therefore the larger output obtained with CD_3I than with CH_3I is attributed to the smaller deactivation efficiency of $I(5^2P_{\frac{1}{2}})$ by the deuterated compound. This explanation can also account for the lack of laser action from CH_3I for pressures larger than 1.1 kNm^{-2} (cf. Table 3.VIII). For the range of small pressures used in this work, CD_3I shows a better performance as a laser medium even than that of CF_3I (cf. Table 3.VIII). This can be rationalised in terms of the much higher branching ratio Φ obtained by CD_3I than by CF_3I

and by the fact that for small pressures, the removal of $I(5^2P_{\frac{1}{2}})$ is unimportant for both molecules.* However, at higher pressures the performance of CF_3I is superior due to its lower removal efficiency. The largest laser output of all the iodides examined here was obtained by $n\text{-}C_3F_7I$. This should be expected, since this molecule exhibits both a small decay cross section and a very high branching ratio Φ.

The number of spikes of the output envelope and the times at which these occur is partly connected with the efficiency of removal of $I(5^2P_{\frac{1}{2}})$ by the parent molecule and partly with the recombination reactions of the radicals produced following the slow flash excitation of the laser medium. Small decay efficiency should be associated with a pattern of many spikes, appearing even when the intensity of the flash is not at its peak. Recombination of iodine atoms to form I_2, instead of recombining with the alkyl radical to regenerate the parent molecule, is a slow termolecular process[2] but can be of importance in eliminating laser action at late times. Accumulation of I_2 also determines the number of times the same sample of iodide can lase when flashed repeatedly. Pyrolysis of the iodide due to the flash can also result in the formation of I_2 restricting the pulsed laser operation.[164] Another reaction causing irreversibility of the photodissociation process is 3.6. Both pyrolysis and the rate of 3.6 are reduced with increasing molecular complexity. This explains the observed superiority of $n\text{-}C_3F_7I$ as a laser medium. On the other hand, CH_3I never lased twice, since the fast alkyl radical recombination[160] and the comparatively large extent of pyrolysis added to the efficient quenching by the parent molecule making

* The branching ratio Φ for CH_3I is somewhat larger than for CF_3I, indicating that differences in Φ cannot account for the large differences in the laser outputs of CH_3I and CD_3I. This was also found in computer simulation of the laser output.[194]

the threshold condition 3.26 inaccessible. It should be noted here that the laser pulse observed for CD_3I after the termination of the flash in the experiments, in which the Zeeman splitting of the $I(5^2P_{\frac{1}{2}})$ sublevels had been eliminated, is analogous to the "late time gain" observed in previous work.[195,196] This phenomenon was initially explained in terms of reaction 3.10 with formation of $I(5^2P_{\frac{1}{2}})$ predominant,[195] which, however, was not confirmed in more recent investigations.[164] The explanation given by Gusinow et al.[196] is based on a physical effect rather than chemical, involving an initial concentration gradient of $I(5^2P_{\frac{1}{2}})$, with higher concentrations off axis, followed by diffusion at late times and consequently an apparent increase of the axial gain. An additional explanation of the late time gain has been given[164] in terms of the decrease of the Doppler frequency $\Delta\nu_D$, as the gas cools, with a subsequent increase of the gain, (c.f. 3.19).

The absence of laser action from GeH_3I, despite the branching ratio of 1.3 which has been observed,[182] can be easily explained in terms of the very fast removal of $I(5^2P_{\frac{1}{2}})$ in the presence of this molecule (c.f. Table 3.X.). Laser action from GeH_3I could possibly be observed if fast flashlamp excitation were used, allowing the threshold condition 3.26 to be reached before significant relaxation of $I(5^2P_{\frac{1}{2}})$ has taken place. Similar considerations for SiH_3I cannot account for the lack of laser action. As it is shown in Table 3.X, the decay rate constant for SiH_3I is smaller than that for CH_3I, which gives laser action. An explanation therefore should be sought within the context of items (1) and (2), i.e. the branching ratio or the absolute yield of $I(5^2P_{\frac{1}{2}})$ resulting from the photodissociation of SiH_3I.

As it is shown in Table 3.IX, the presence of a buffer gas in the laser cell increases the threshold conditions. This may be due to two reasons: a) Appreciable quenching of $I(5^2P_{\frac{1}{2}})$ by the buffer gas, especially at the higher pressures used and b) pressure broadening of the linewidth of the

[illegible] transition (cf. 3.19). In general, an increase of the linewidth is required in high power lasers.[197] This is associated with the decrease of the level of premature laser action due to the decrease of the coefficient a_o (cf. 3.19) and with the subsequent concentration of energy in a single short pulse. Another way of increasing the linewidth is by increasing the temperature of the laser medium. This is particularly interesting in the light of the negative temperature dependence exhibited in the quenching of $I(5^2P_{\frac{1}{2}})$ by certain iodides, like CH_3I.

E) CONCLUSIONS

(1) This work demonstrated how the large isotope effect observed in the deactivation of $I(5^2P_{\frac{1}{2}})$ by CH_3I and CD_3I can be used as a tool to investigate the kinetics of relaxation. On the basis of this large isotope effect, it was proved that the reactive pathway 3.1 is unimportant for the decay of $I(5^2P_{\frac{1}{2}})$ in the presence of CH_3I. The decay occurs via the quenching channel 3.2 predominantly.

(2) The negative temperature coefficient obtained for CH_3I combined with the large isotope effect can be satisfactorily interpreted in terms of near-resonant energy transfer due to long range forces. In contrast, the temperature behaviour observed for CD_3I indicates significant contributions from other decay mechanisms, including reaction.

(3) The result obtained for SiH_3I, although not contradictory with the expectations of inelastic decay via near resonant energy transfer, has been attributed to the reactive channel involving H atom abstraction. The very high removal efficiency of $I(5^2P_{\frac{1}{2}})$ atoms by GeH_3I, combined with observations in kinetic spectroscopy work, provides direct evidence for the importance of this channel. The H atom abstraction can be well understood by assuming a correlation between the activation energy barrier and the exothermicity of the reaction.

(4) The much larger laser outputs obtained with CD_3I as the laser

medium than with CH_3I reflect the difference in the removal efficiency of the two iodides. The reasons no laser action was obtained from SiH_3I are not clear, while the absence of laser action from GeH_3I has been attributed to the high efficiency it exhibits in removing $I(5^2P_{\frac{1}{2}})$.

(5) Finally, the present results indicate that when the reactive pathways are closed, near-resonant inelastic channels can dominate the removal of electronically excited atoms. Whenever isotopic substitution is used, this can result in very large isotope effects, by changing the efficiency of quenching channels. Isotopic substitution can therefore influence the relative importance of other channels, including reactive channels and this should be considered whenever such substitutions are used in determining the mechanisms of reactions involving excited states.

Chapter 4

RELAXATION OF $I(5^2P_{\frac{1}{2}})$ ATOMS BY H_2O-D_2O AND THE HYDROGEN AND DEUTERIUM HALIDES

A INTRODUCTION

Systems of the type $X(^2P_{\frac{1}{2}}) + HY(^1\Sigma)$, where $X(^2P_{\frac{1}{2}})$ is an electronically excited halogen atom and HY a diatomic molecule, have been studied extensively.[120,198-201] Reactive and quenching pathways can in some cases compete in relaxing the excited atom according to 4.1 or 4.2;

$$X(^2P_{\frac{1}{2}}) + HY(v=o,\ J=k) \rightarrow XH(v=m,\ J=l) + Y(^2P_{\frac{1}{2}},\ ^3/_2) + \Delta E \qquad (4.1)$$

$$X(^2P_{\frac{1}{2}}) + HY(v=o,\ J=k) \rightarrow X(^2P_{3/2}) + HY(v=n,\ J=m) + \Delta E \qquad (4.2)$$

where ΔE is the energy which goes into translation. Although clearly of fundamental importance, the factors which control the competition between reaction and quenching in the removal of the excited atoms and the conditions under which one predominates are not yet understood in any detail. One aspect of this problem can be tackled by studying the efficiency of quenching mechanisms in systems in which the reactive channel is closed or its exact contribution is known. Particularly interesting in this respect are quenching processes, in which the electronic energy of the atom is transferred to the internal degrees of freedom of the molecule, as in 4.2. As has been already mentioned (cf. Chapter 1) this type of energy transfer can be used as a pumping technique in developing new I.R. laser systems.[130-132] Furthermore, direct evidence for its importance has been obtained in several studies[120,200] ($Br(4^2P_{\frac{1}{2}})$ + HBr, HCl, HF) employing I.R. chemiluminescence techniques.

A considerable amount of experimental data indicates that near resonant E→V energy transfer can dramatically increase the efficiency of quenching. Thus, the high degree of specificity found[200] in the vibrational excitation of HF in the quenching of $Br(4^2P_{\frac{1}{2}})$ by HF has been attributed[128] to near resonant energy transfer due to long range interactions, as described by 4.3.

$$Br(4^2P_{\frac{1}{2}}) + HF(v=o,\ J=6) \rightarrow Br(4^2P_{3/2}) + HF(v=1,\ J=5) \quad \Delta E=+9cm^{-1} \qquad (4.3)$$

This explanation is analogous to the proposals made earlier (cf. Chapters 1 & 3), in explaining the large isotope effects observed for the quenching of excited atoms by isotopically substituted molecules. However, for the less efficient E→V energy transfer processes, as those observed in the deactivation of $Br(4^2P_{\frac{1}{2}})$ by HCl or HBr, near resonant channels are absent and long range interactions seem to be of limited importance.

Possible interference of reactive pathways, as in 4.1, gives rise to interesting questions concerning the effect of electronic excitation on the rate of the chemical reaction and consequently the nature of the potential surfaces involved in the deactivation process. A characteristic example is provided by the removal of $Br(4^2P_{\frac{1}{2}})$ by HI. As demonstrated by Bergmann et. al.,[198] reaction is slow, accounting for less than 30% of the total decay rate. In sharp contrast, $Br(4^2P_{3/2})$ reacts with HI by more than a factor of ten faster. This illustrates the fact that atomic excitation does not necessarily lead to an increased reaction rate. The theoretical rate constants obtained by Tully[40] for the reaction of $F(2^2P_{\frac{1}{2}})$ and $F(2^2P_{3/2})$ with H_2 provide further evidence in this respect. As mentioned in Chapter 1, the rate of reaction for $F(2^2P_{\frac{1}{2}})$ is predicted to be about one order of magnitude smaller than for $F(2^2P_{3/2})$.

In view of the uncertainty in the mechanisms of removal of excited halogen atoms by hydrogen halides, we determined bulk rate constants for the decay of $I(5^2P_{\frac{1}{2}})$ by molecules of the isotopic pairs HCl-DCl, HBr-DBr and HI-DI. In addition, rate data were obtained for the quenching of $I(5^2P_{\frac{1}{2}})$ by H_2O and D_2O, in an attempt to obtain further information about the mechanisms for quenching by hydrogen-containing molecules when the reactive pathway is closed. To further elucidate the possible relaxation mechanisms we studied the decay of $I(5^2P_{\frac{1}{2}})$ in the presence of HBr and HCl over a wide temperature range.

B) EXPERIMENTAL

The experimental arrangement for time resolved atomic absorption spectrophotometry used in this investigation has been described in Chapter 2. Excited iodine atoms, $I(5^2P_{\frac{1}{2}})$, were produced by flash photolysis of C_3F_7I under isothermal conditions. Mixtures at a total pressure of 2.7 k Nm^{-2} were prepared with N_2 as the diluent gas. Some of the mixtures containing DCl were not diluted with N_2 as the low efficiency for quenching by DCl required a large excess of this gas be added, thus achieving the same purpose as added N_2 in other experiments.

Experiments with HI and DI were carried out in the dark to avoid the photolysis of these compounds. In addition, mixtures containing these reagents were passed through an isopropanol - dry ice bath (195 K) before entering the reaction vessel to eliminate all traces of I_2. Also, to prevent photolysis of these reactants by the atomic emission lamp a shutter, which was only opened a few seconds before the flash, was placed between the reaction vessel and the lamp. The formation of $I(5^2P_{\frac{1}{2}})$ following the photolysis of HI(DI) allowed for the use of these compounds as the source of iodine atoms in some experiments.

Kinetic isotope effects were determined at room temperature (293 ± 2) K by using the parallel reaction vessel flashlamp arrangement. Part of the experiments with HCl were carried out in the coaxial flashlamp-reaction vessel arrangement. Flash energies of about 80 J were employed. With HI(DI), experiments were carried out to determine the effect of flash energy on the measured rate constants (cf. section C). Flash energies never exceeded 20J in the temperature dependence measurements (coaxial system). Particularly in experiments with HI, flash energies were kept as low as possible so as to minimise the extent of photolysis of this molecule.

In the experiments with H_2O and D_2O there was some difficulty due to the high degree of adsorption of these molecules on the walls of the reaction vessel and the vacuum line. Attempts were made to reduce this effect by applying a Tesla coil discharge on the walls of the vessel and the line

during evacuation and allowing for extensive pumping between two successive experimental runs.

Samples of DCl, prepared by the action of D_2O on benzoyl chloride were purified by fractional distillation under vacuum. Byproducts of the reaction were trapped in two baths at acetone-dry ice (195 K) and solid ether (153 K) temperatures. Pure DCl was trapped at liquid N_2 temperature. Reactants were in general thoroughly degassed before use. Their purity was determined as described in Appendix I. Before any experiments with deuterated species the vacuum line and the reaction vessel were deuterated as described in Chapter 2.

C) RESULTS

1) Isotope effects at room temperature (293 ± 2) K

Typical decay traces indicating time resolved resonance absorption by $I(5^2P_{\frac{1}{2}})$ are shown in Figure 4.1. Figure 4.2 includes pseudo first-order plots for the removal of $I(5^2P_{\frac{1}{2}})$ by HBr and DBr, obtained from such decay traces using a Ferranti Freescan Digitiser, as an example of the type of raw data obtained in these experiments. The first-order rate coefficients derived from the slopes of such plots were then plotted against the partial pressure of the deactivating gas and the second order rate coefficients were determined from the slopes of these plots, as was described in Chapter 2.

i) HCl - DCl: The quenching rate constant of $I(5^2P_{\frac{1}{2}})$ in the presence of HCl has been determined by Deakin and Husain,[201] who also employed absorption spectrophotometry. The error limits given by these authors were about 30%, which are rather large in view of the sensitivity of the experimental method used. As the main aim of the present work was a detailed comparison between the efficiency of deactivation of isotopically substituted molecules, we redetermined decay rates for HCl in order to provide a self-consistent and reliable set of data. The results obtained

Figure 4.1: Typical decay traces

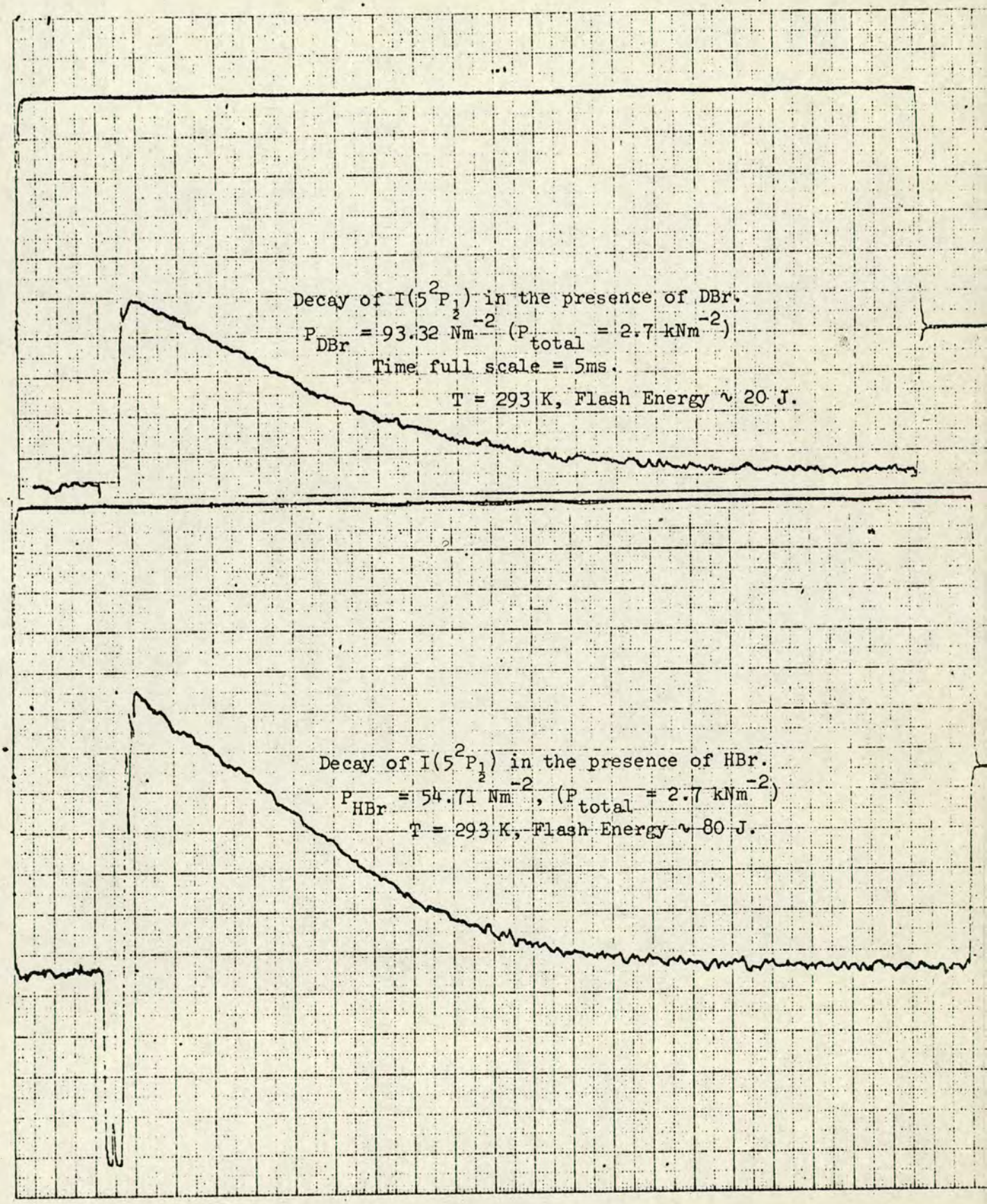

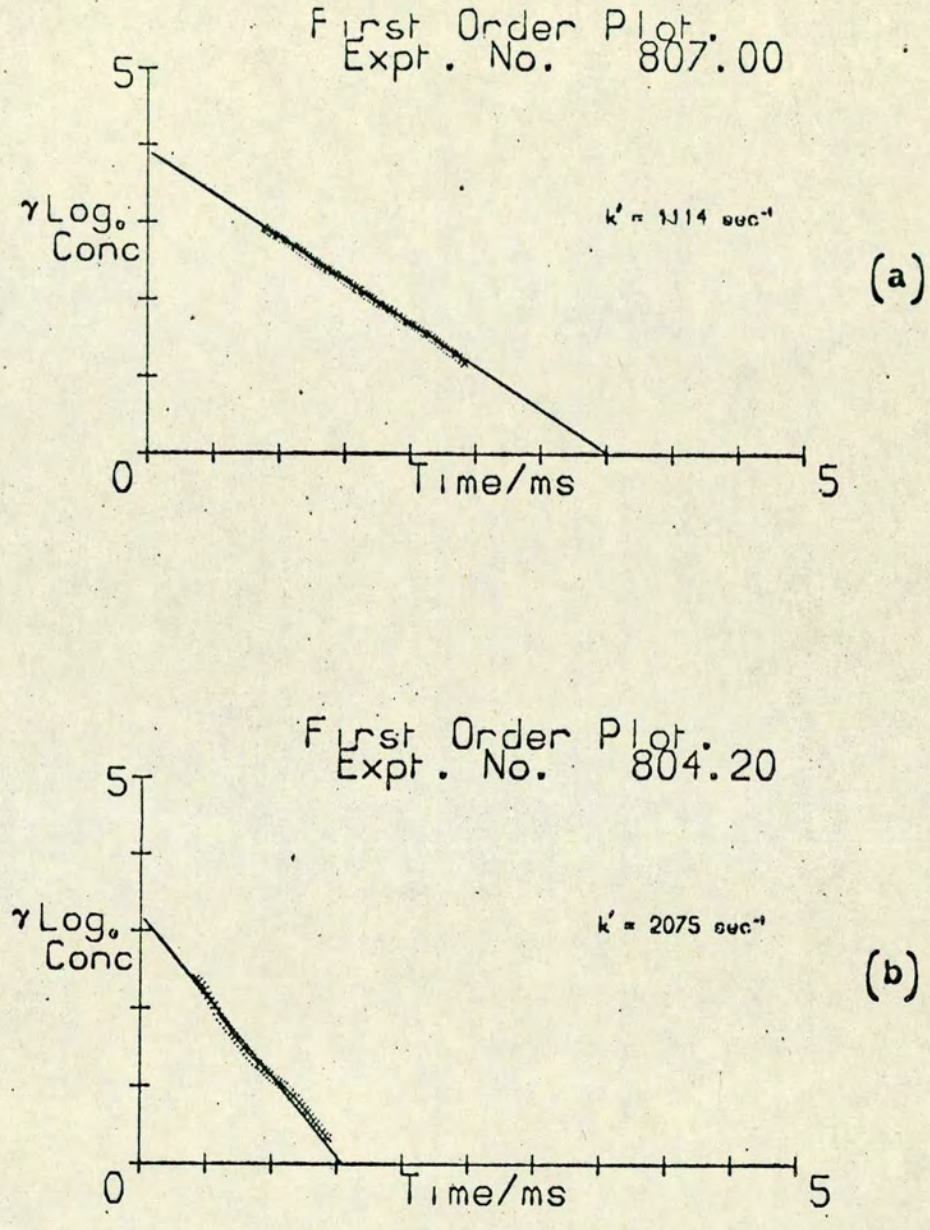

Figure 4.2 Typical first order plots of data for the decay of $I(5^2P_{\frac{1}{2}})$ obtained using a Ferranti Freescan Digitiser; $\gamma \log_e$ conc. $\equiv \log_e \log_e (I_o/I)$; slope, $k' = \gamma(k_q[Q]+k_b)$, where k_b is the first order decay in the absence of added quenching gas.

(a) $P_{DBr} = 93.3$ N m^{-2}, $P_{N_2} = 2.70$ k N m^{-2};
$P_{C_3F_7I} = 33.2$ N m^{-2}, $k_b = 201$ s^{-1}

(b) $P_{HBr} = 69.3$ N m^{-2}, $P_{N_2} = 2.70$ k N m^{-2},
$P_{C_3F_7I} = 32.1$ N m^{-2}, $k_b = 278$ s^{-1}.

are shown in Figure 4.3. The quenching rate constant obtained from this set of experiments is in good agreement with that determined by Deakin and Husain involving, however, smaller error limits.*

The first experiments with DCl were carried out by using mixtures of DCl + C_3F_7I + N_2. The second order rate coefficient obtained on the basis of these experiments (without correcting for the presence of HCl as an impurity) (cf. Figure 4.3) was $k = (4.5 \pm 0.6) \times 10^{-15}$ cm^3 molecule^{-1}s^{-1}. However, since DCl was found to be an inefficient quencher of $I(5^2P_{\frac{1}{2}})$ more accurate kinetic data were obtained by using DCl itself as diluent gas. Table 4.I includes second order rate coefficients, obtained for various mole fractions of DCl, P_{DCl}/P, where P is the total pressure ($P \sim 2.6 - 3.0$ kNm^{-2}). These data, representing averages over five to six experiments for each individual determination resulted in a rate constant: $k_{DCl} = (4.3\ ^{+0.4}_{-1.9}) \times 10^{-15}$ cm^3 molecule^{-1}s^{-1}. The lower error limit given allows for the presence of less than 9% HCl in the sample of DCl used (cf. Appendix I). Rate data for the relaxation of $I(5^2P_{\frac{1}{2}})$ by DCl have not been reported previously.

ii) <u>HBr - DBr</u>: The variation of the first order rate coefficients for the removal of $I(5^2P_{\frac{1}{2}})$ by HBr and DBr as a function of the partial pressure of these molecules is presented in Figure 4.4. From the slopes of these plots and for $\gamma = 0.82$ (cf. Chapter 2) the following rate constants were obtained:

$$k_{HBr} = (1.3 \pm 0.1) \times 10^{-13} \text{ cm}^3 \text{ molecule}^{-1}\text{s}^{-1}$$

and $$k_{DBr} \leqslant (4.9 \pm 0.3) \times 10^{-14} \text{ cm}^3 \text{ molecule}^{-1}\text{s}^{-1}$$

* In a recent work, Pritt and Coombe[202] measured the rate constant for HCl by monitoring the emission of $I(5^2P_{\frac{1}{2}})$ at 1.315 μm. The result was a factor of two smaller than that determined by Deakin and Husain and in this work. The reasons for this discrepancy are not clear yet.

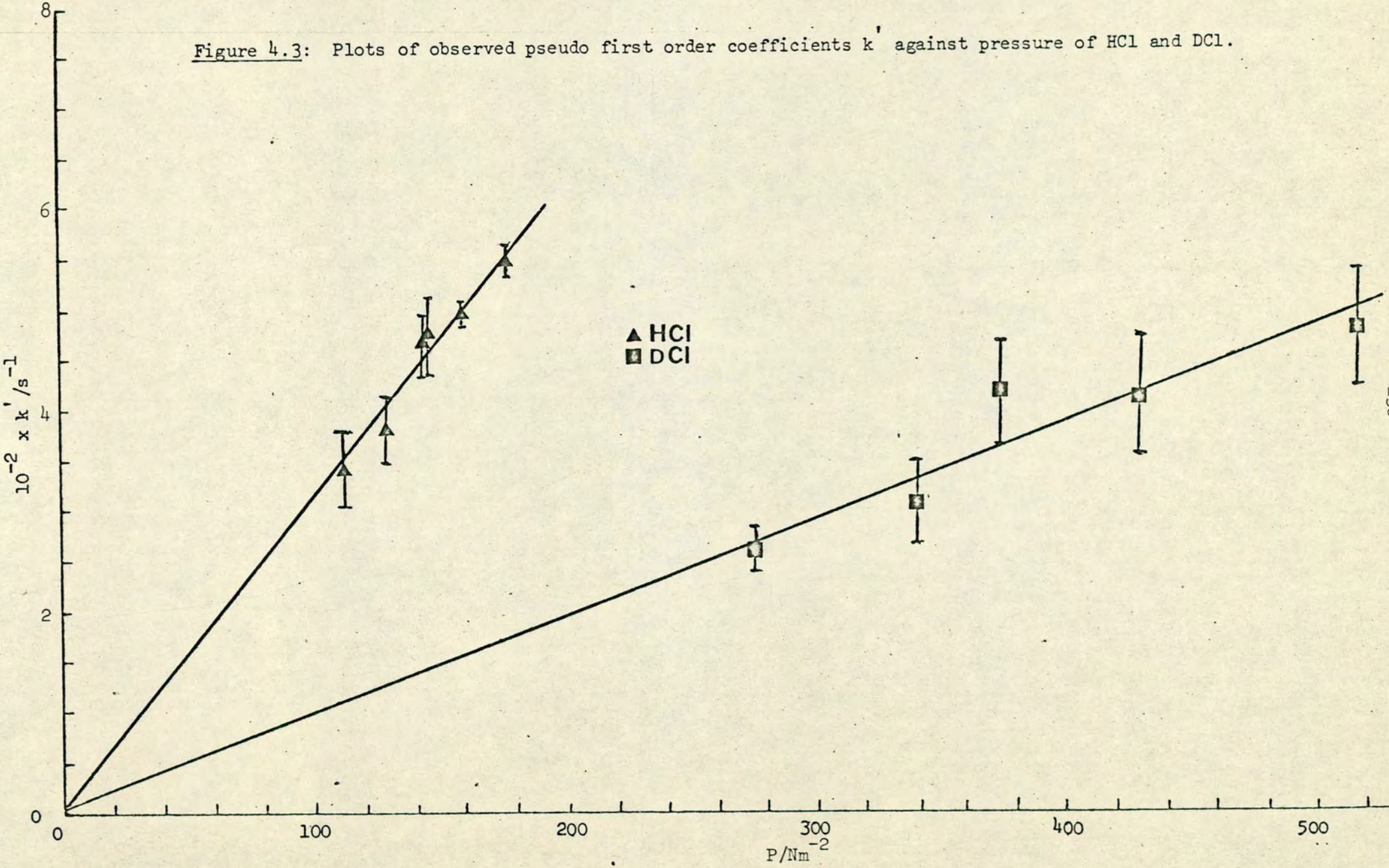

Figure 4.3: Plots of observed pseudo first order coefficients k' against pressure of HCl and DCl.

TABLE 4.I

Data for the decay of $I(5^2P_{\frac{1}{2}})$ in the presence of DCl (293 ± 2)K

P_{DCl}/P	$k \times 10^{15}$ $cm^3\ molecule^{-1}s^{-1}$
0.97	4.1 ± 0.3
0.97	3.7 ± 0.3
0.98	4.7 ± 0.5
0.99	4.7 ± 0.6
0.99	4.1 ± 0.2

$^*k_{DCl} = (4.3^{+0.4}_{-1.9}) \times 10^{-15} cm^3 molecule^{-1}s^{-1}$

$P \sim 2.6 - 3.0\ kNm^{-2}$

* the lower error limit allows for the presence of ≤ 9% HCl.

Figure 4.4. Plots of/first order rate coefficients, observed k', against pressure (Nm^{-2}) of HBr(O) and DBr(●).

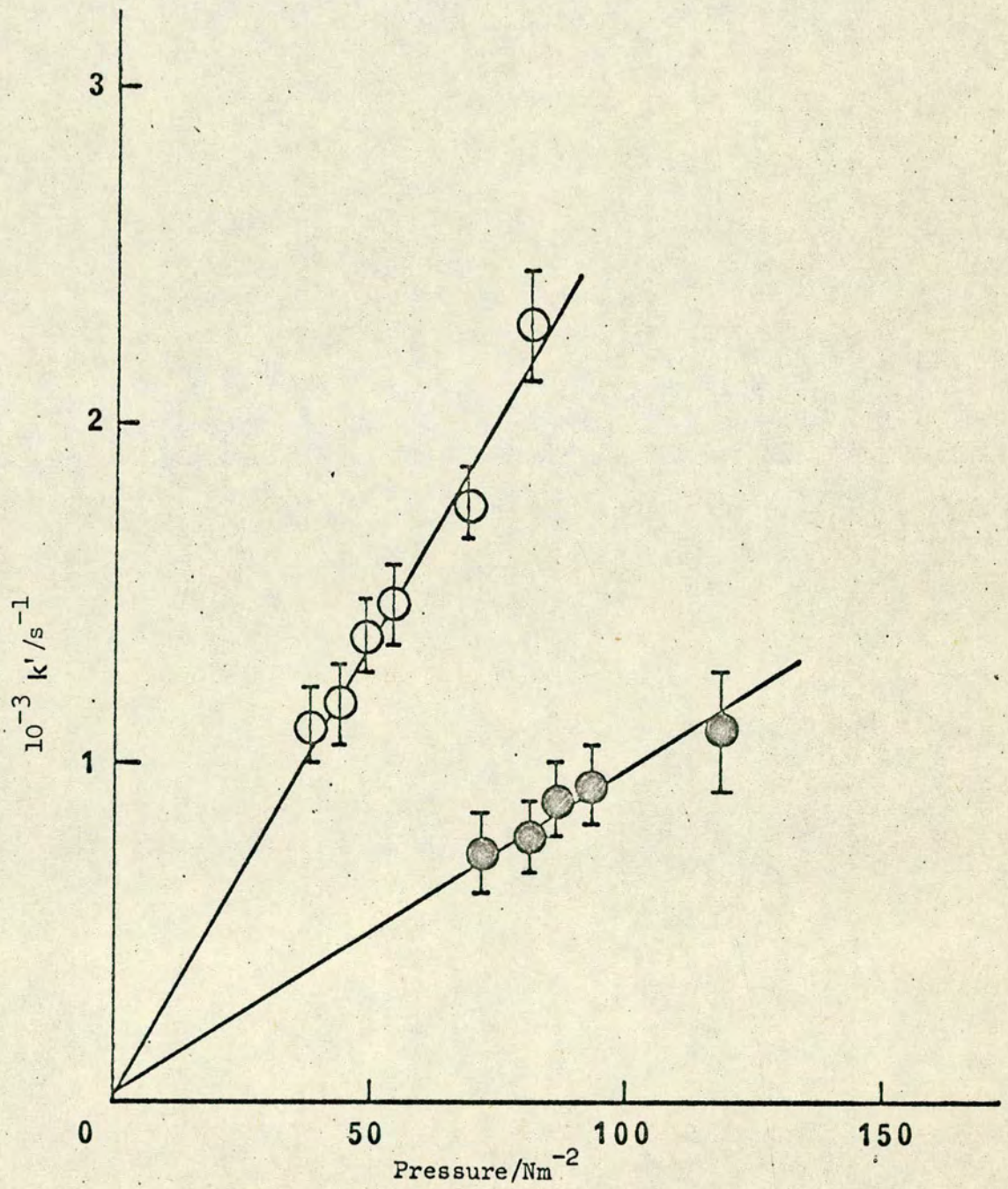

The rate constant for DBr is presented as an upper limit because of the presence of some HBr ($\lesssim$ 36%, cf. Appendix I). We have not attempted to correct k_{DBr} for the presence of HBr as this would reduce its value substantially. The upper limit presented provides a reliable basis for discussion. To our knowledge, decay rates of $I(5^2P_{\frac{1}{2}})$ in the presence of HBr and DBr have not been reported previously.*

Samples of HBr and DBr in the reaction vessel can be photolysed by the flash. A test of possible interference from atom-radical effects, following the photolysis of these molecules, was carried out by photolysing different samples of the same mixture with flashes of different energy. In all experiments at the same total pressure, the decay traces were found to coincide with one another which indicates absence of any atom-radical effects. However, when a given sample was flashed for a second time, a large increase of the decay rate was observed. The degree of this increase was dependent upon the energy or the first flash and increased correspondingly with it. Thus in a typical kinetic run with DBr (P_{DBr} = 72 Nm^{-2}) the measured decay rate was increased from 732 s^{-1} following the first flash ($\sim$ 80 J) to 1939 s^{-1} following the second flash. This is attributed to the formation of molecular bromine, which removes $I(5^2P_{\frac{1}{2}})$ with a very high efficiency. Considering the most recently reported value[207] for the decay rate constant of $I(5^2P_{\frac{1}{2}})$ by Br_2, we evaluated that about 0.2% of the DBr in the reaction vessel was photolysed. Similarly, it was found that a flash energy of 145 J resulted in $\sim$0.6% of photolysis.

iii) HI-DI: Kinetic data obtained for the removal of $I(5^2P_{\frac{1}{2}})$ by HI and DI are included in Figure 4.5. The rate constants obtained on the basis of these data are a factor of three smaller than those determined by plate photometry.[204] As previously mentioned (cf. Chapters 1 & 2),

* Kinetic data reported recently by Pritt and Coombe[202] for HBr and Wiesenfeld and Wolk[203] for HBr and DBr are in good agreement with those obtained in this work.

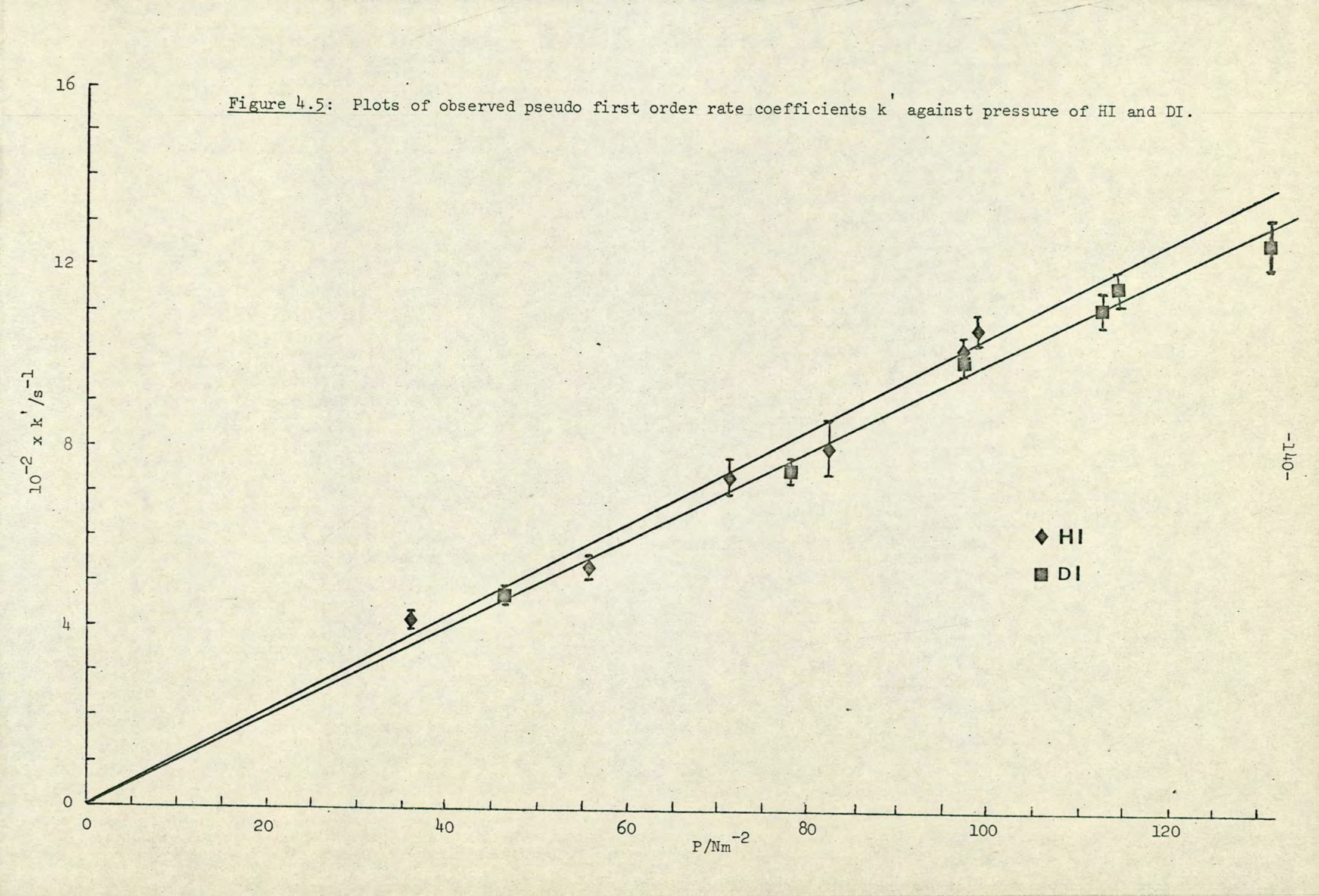

Figure 4.5: Plots of observed pseudo first order rate coefficients k' against pressure of HI and DI.

the latter experimental method is less precise than atomic spectrophotometry. Furthermore, in some cases it has been proved unreliable[2] primarily due to the relatively large atomic and radical concentrations used. Thus the present results are to be preferred. In the present experiments we have shown directly that atom-radical effects are unimportant by measuring quenching rates over a range of flash energies (45-180 J). Results for HI at the highest and lowest flash energies are shown in Table 4.II. As with HBr and DBr however, we noted a large increase in the $I(5^2P_{\frac{1}{2}})$ decay coefficient when a mixture of HI or DI in N_2 was flashed for a second time. This must be due to efficient quenching by a photolysis product, H_2 or I_2 formed as described by 4.4 - 4.6.

$$HI + h\nu \rightarrow H + I \qquad (4.4)$$

$$H + HI \rightarrow H_2 + I \qquad (4.5)$$

$$I + I + M \rightarrow I_2 + M \qquad (4.6)$$

and could be ascribed to I_2, whose quenching rate constant,[137] 3.6×10^{-11} cm^3 $molecule^{-1}s^{-1}$, is about 280 times that for H_2. However, as the formation of I_2 in 4.6 is slow, there is no measurable effect from this species during the decay of $I(5^2P_{\frac{1}{2}})$ for the first flash of a given mixture. From the increase in the first order rate coefficient following a second flash we estimated that the partial pressure of I_2 produced by the first flash was $\sim$0.1% of that of HI, and thus the percentage photolysis was $\sim$0.2%.

We should note here that in view of the rate constant obtained in this work for HI ($k_{HI} = 5.2\pm0.4) \times 10^{-14}$ $cm^3 molecule^{-1}s^{-1}$), formation of H_2 from two HI molecules as in 4.1 and 4.2 should not affect the measured rates, since[64] $k_{H_2} = (1.1\pm0.2) \times 10^{-13} cm^3$ $molecule^{-1}s^{-1}$. Similar considerations applied to the removal of $I(5^2P_{\frac{1}{2}})$ by HBr and DBr.

TABLE 4.II

Data illustrating the absence of atom radical effects in the determination of k_{HI}

Partial Pressure of HI/Nm^{-2}	Flash Energy/J	First-order Rate Coefficients/s^{-1}
78	45	1090±19
78	180	1113±28
82	45	1162±17
82	180	1152±13

iv) H_2O-D_2O: Kinetic data obtained for the removal of $I(5^2P_{\frac{1}{2}})$ by H_2O and D_2O are included in Figure 4.6. The result for H_2O lies within the experimental error limits of the rate constant obtained by Deakin and Husain,[201] who also employed atomic spectrophotometry. In contrast, the decay efficiency for D_2O is a factor of three smaller than that determined by plate photometry.[205] As discussed earlier, the present results are considered more accurate due to possible interference of atom-radical effects in the plate photometry work. It is also interesting to note that in a recent experimental investigation by Burde and McFarlane,[206] in which $I(5^2P_{\frac{1}{2}})$ were produced by photolysis of C_3F_7I by an N_2 laser, the quenching efficiencies of H_2O & D_2O werefound to be larger than that obtained by Deakin and Husain and in this work. Despite this discrepancy however, the measured isotope effects are in good agreement.

The values of the measured rate constants k for all isotopically substituted species studied in this work are listed in Table 4.III. The corresponding quenching cross sections were calculated by dividing k by the mean relative velocity of the colliding species at 293 K.

2) Temperature dependence measurements

i) Removal of $I(5^2P_{\frac{1}{2}})$ by HBr

Pseudo first-order rate coefficients for the removal of $I(5^2P_{\frac{1}{2}})$ by HBr at different temperatures in the range 253-427 K are given in Table 4.IV. As discussed earlier, when these coefficients were plotted against the partial pressure of HBr, the slopes of the latter plots yielded the products γk at each temperature, where k was the decay rate constant at this temperature.

As in Chapter 2, the effect of temperature variation on the value of the correction factor γ in the Beer-Lambert law was examined by determining this empirical coefficient at different temperatures, covering the whole temperature range in which decay rates were measured. The results are shown in Table 4.V. As indicated by these data, no significant

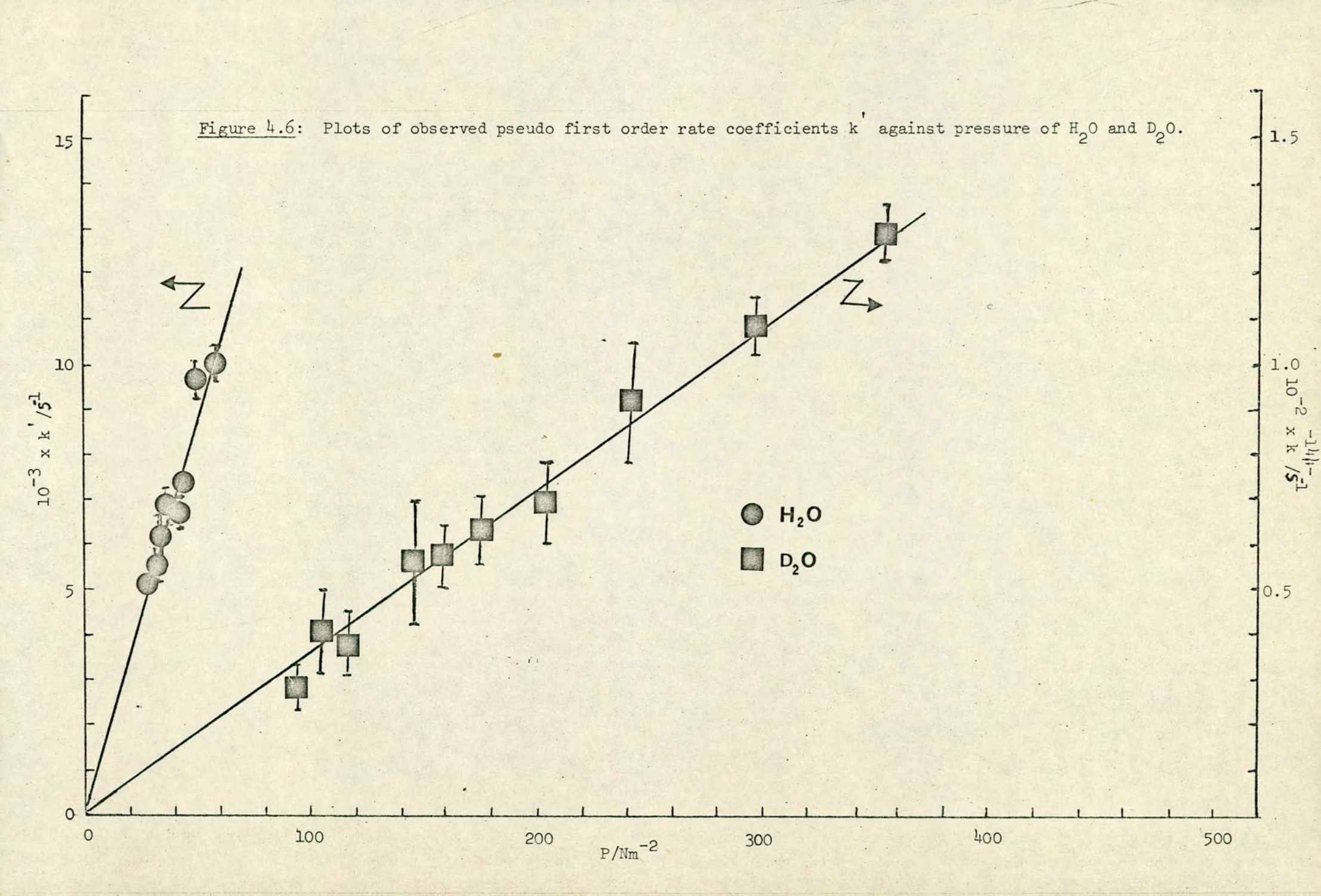

Figure 4.6: Plots of observed pseudo first order rate coefficients k$'$ against pressure of H_2O and D_2O.

TABLE 4.III

Second order rate constants for quenching (k) of $I(5^2P_{\frac{1}{2}})$ by H_2O, D_2O, HCl, DCl, HBr, DBr, HI and DI (T= 293 K).

Quenching Gas	k/cm^3 molecule^{-1} s^{-1} (293±2 K)	σ/cm^2	Ratio of Cross-sections	Previous work (k_q/cm^3 molecule^{-1} s^{-1})	Reference
H_2O	$(8.4\pm1.1)\times10^{-13}$	1.3×10^{-17}	42	$(7.2\pm1.6)\times10^{-13}$	201
D_2O	$(1.8\pm0.4)\times10^{-14}$	3.1×10^{-19}		$(6.2\pm0.8)\times10^{-14}$	205
HCl	$(1.52\pm0.12)\times10^{-14}$	3.2×10^{-19}		$(1.5\pm0.5)\times10^{-14}$	201
DCl	$(4.3^{+0.4}_{-1.9})\times10^{-15}$	9.3×10^{-20}	3.4		
HBr	$(1.3\pm0.1)\times10^{-13}$	3.7×10^{-18}	≥2.6		
DBr	$(\leq4.9\pm0.3)\times10^{-14}$	$\leq1.4\times10^{-18}$			
HI	$(5.2\pm0.4)\times10^{-14}$	1.7×10^{-18}	1	$(1.3\pm0.2)\times10^{-13}$	204
DI	$(5.0\pm0.2)\times10^{-14}$	1.6×10^{-18}		$(1.2\pm0.2)\times10^{-13}$	204

TABLE 4.IV

Rate data for the removal of $I(5^2P_{\frac{1}{2}})$ by HBr at different temperatures.

Temperature (K)	Pressure HBr (Nm^{-2})	Rate (s^{-1})	$k \times 10^{13}$ (cm^3 $molecule^{-1}s^{-1}$)
253 ± 8	69.19	2162 ± 187	
	79.06	2822 ± 147	
	86.79	2989 ± 251	
	87.32	3099 ± 122	1.48 ± 0.12
286 ± 4	65.80	1630 ± 176	
	69.19	1816 ± 48	
	79.06	1990 ± 73	
	86.79	2316 ± 151	
	87.32	2491 ± 156	1.24 ± 0.10
295 ± 2	65.80	1518 ± 49	
	69.19	1634 ± 85	
	79.06	1846 ± 184	
	86.79	2394 ± 97	
	87.32	2170 ± 95	1.23 ± 0.12
354 ± 8	65.80	975 ± 70	
	69.19	1091 ± 71	
	79.06	1376 ± 55	
	86.79	1749 ± 84	
	87.32	1557 ± 100	1.05 ± 0.18
404 ± 10	65.80	712 ± 72	
	69.19	760 ± 78	
	79.06	943 ± 101	
	86.79	1208 ± 46	
	87.32	1053 ± 77	0.89 ± 0.09
427 ± 12	65.80	924 ± 44	
	69.19	1017 ± 86	
	79.06	1201 ± 76	
	86.79	1478 ± 95	
	87.32	1586 ± 32	1.20 ± 0.18

TABLE 4.V

γ coefficient at different temperatures

T (K)	γ
200	0.83 ± 0.07
253	0.86 ± 0.05
286	0.79 ± 0.09
293	0.82 ± 0.03
354	0.84 ± 0.08
427	0.80 ± 0.04
440	0.81 ± 0.08

systematic variation of γ was observed. We have therefore employed the average value $\gamma=0.82$ over the whole temperature range. We note that this value of γ has been determined at room temperature, as an average over a large number of experimental data (cf. Chapter 2). The variation of k_{HBr} as a function of temperature is shown in Figure 4.7. When the kinetic data obtained in the temperature range 253-427 K are fitted to an Arrhenius plot (cf. Figure 4.8), a negative activation energy, $E_a = -(1.7\pm0.7)$kJ mole^{-1} is obtained. The intercept of this plot yields an Arrhenius pre-exponential factor, $A=(6.2\pm1.5) \times 10^{-14}$ cm^{3}molecule^{-1}s^{-1}. We should note, however, that as the data in Figure 4.8 indicates, an Arrhenius plot based on the decay rates obtained in the temperature range 253-404 K may result in a much better fitting than that determined above for the whole temperature range. The activation energy and A factor obtained by the latter plot involve very small error limits. It is reasonable, therefore, to assume that for this particular temperature range the rate constant may be described by the equation:

$$k_{HBr} = (4.09\pm0.25) \exp \frac{(2.7\pm0.2)}{RT} \times 10^{-14} \text{ cm}^3 \text{ molecule}^{-1}\text{s}^{-1}$$

ii) Removal of $I(5^2P_{\frac{1}{2}})$ by HCl

The investigation of the temperature dependence of the decay efficiency of $I(5^2P_{\frac{1}{2}})$ in the presence of HCl was carried out along similar lines as those described for HBr. Kinetic data obtained at different temperatures are shown in Table 4.VI. Decay rate constants determined on the basis of these data are plotted as a function of temperature in Figure 4.9. In contrast to HBr, a slightly positive temperature dependence of the decay efficiency is observed. Thus, the corresponding Arrhenius plot resulted in a positive activation energy, $E_a = (2.4\pm0.6)$ kJ mole^{-1}. The A factor was found to be $A = (4.4\pm0.9) \times 10^{-14}$cm^{3}molecule^{-1}s^{-1}. Considering the small error limits involved in these parameters, a good approximation of the variation of the rate constant with temperature can be described by the equation:

$$k_{HCl} = (4.42\pm0.87) \exp - \frac{(2.4\pm0.6)}{RT} \times 10^{-14} \text{cm}^3 \text{ molecule}^{-1}\text{s}^{-1}.$$

Figure 4.7 Logarithmic plot of experimental and theoretical rate data for the deactivation of $I(5^2P_{\frac{1}{2}})$ by HBr over the temperature range 250-430 K (upper trace experimental data; lower trace theoretical data).

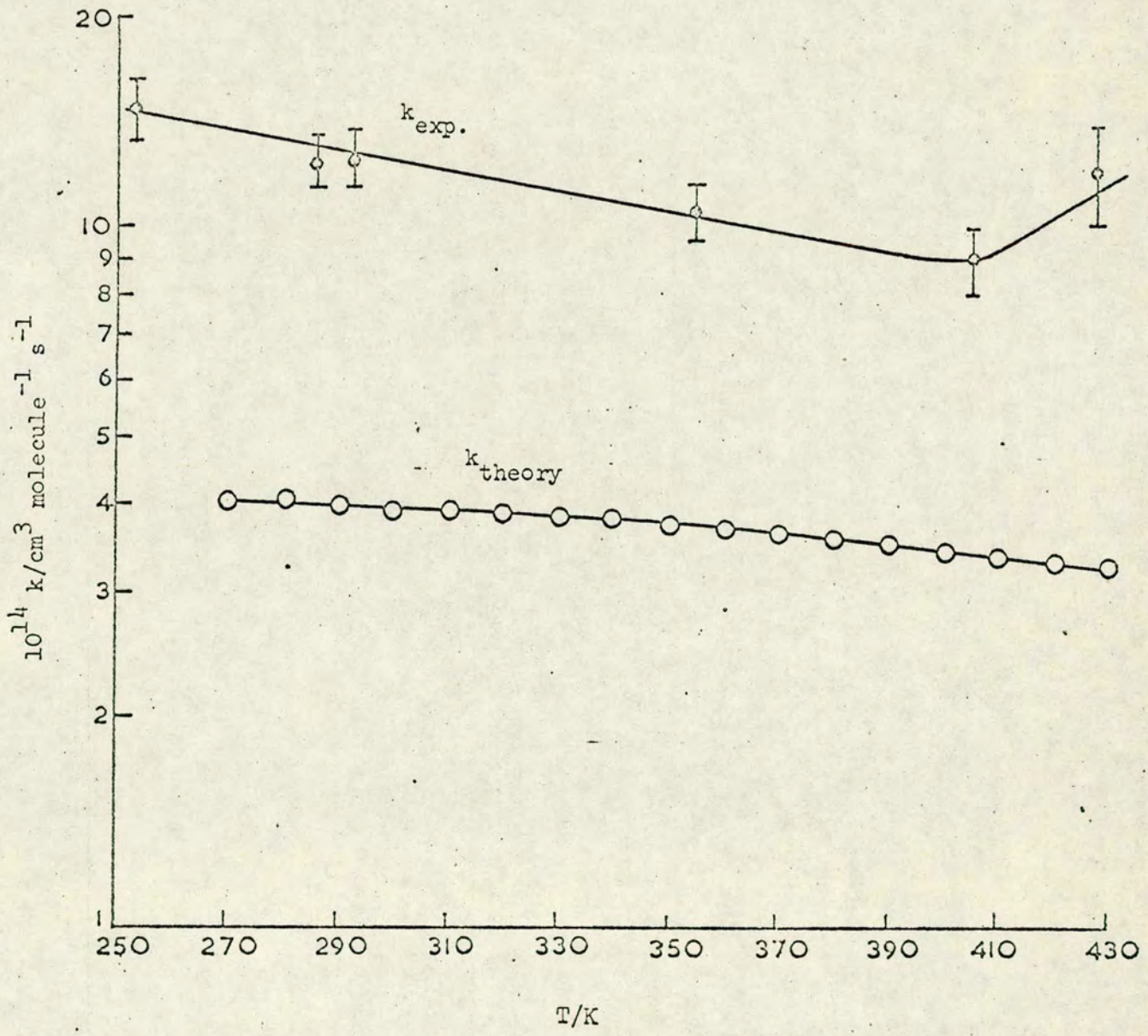

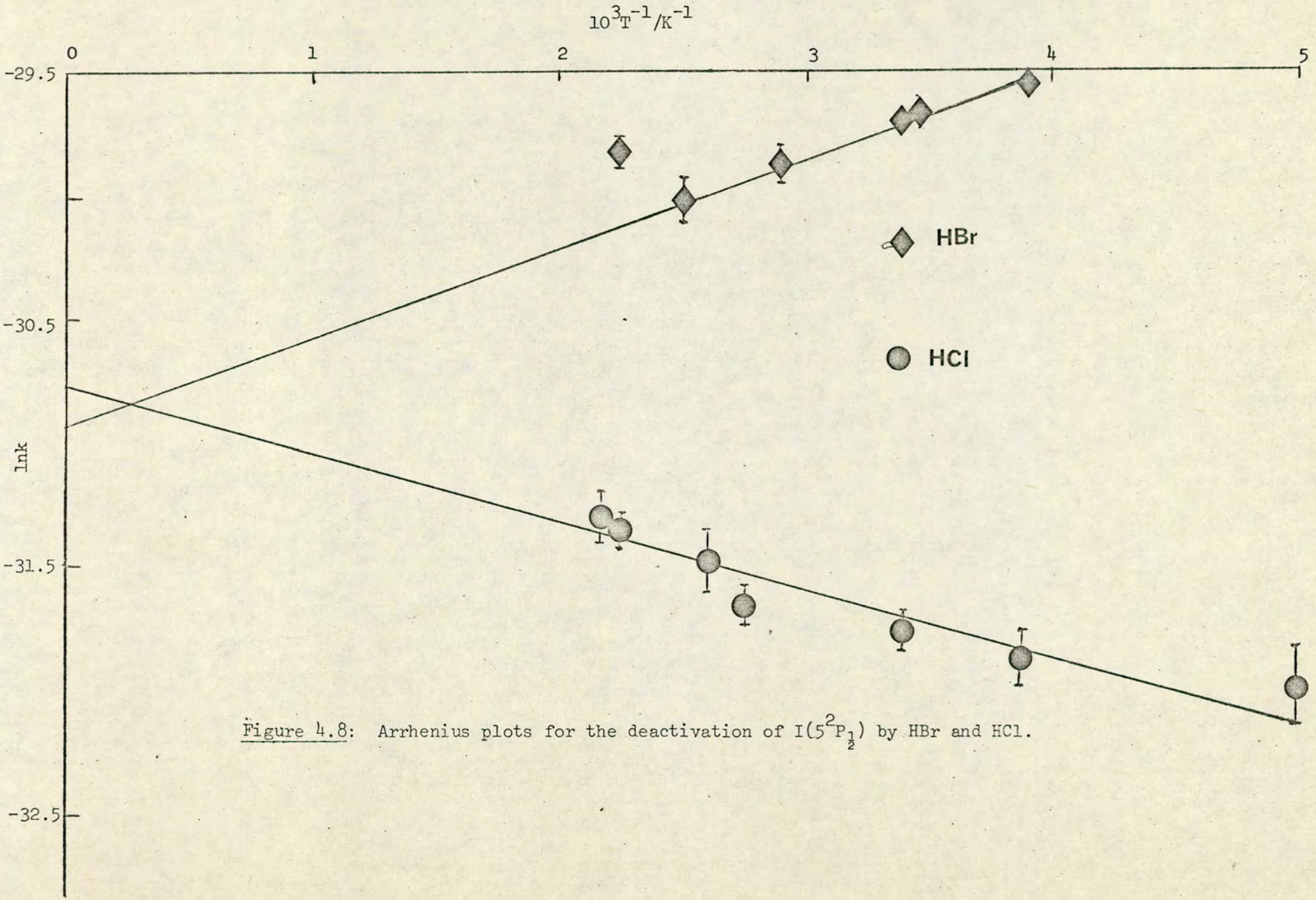

Figure 4.8: Arrhenius plots for the deactivation of $I(5^2P_{\frac{1}{2}})$ by HBr and HCl.

TABLE 4.VI

Rate data for the removal of $I(5^2P_{\frac{1}{2}})$ by HCl at different temperatures

Temperature (K)	Pressure HCl (Nm^{-2})	Rate (s^{-1})	$k \times 10^{14}$ ($cm^3 molecule^{-1} s^{-1}$)
200 ± 16	114.12	497 ± 43	
	116.00	577 ± 68	
	127.45	546 ± 52	
	143.05	672 ± 40	
	176.78	739 ± 103	1.22 ± 0.27
261 ± 8	114.12	378 ± 44	
	127.45	449 ± 36	
	143.05	512 ± 51	
	176.78	592 ± 53	1.48 ± 0.16
297 ± 2	114.12	407 ± 40	
	116.00	472 ± 50	
	127.45	446 ± 71	
	143.05	550 ± 81	
	176.78	606 ± 88	1.56 ± 0.14
361 ± 8	114.12	314 ± 48	
	116.00	321 ± 38	
	127.45	395 ± 50	
	143.05	430 ± 71	
	176.78	492 ± 50	1.67 ± 0.10
385 ± 9	114.12	436 ± 55	
	127.45	545 ± 42	
	143.05	550 ± 23	
	176.78	668.± 58	2.13 ± 0.26
404 ± 10	114.12	406 ± 20	
	116.00	391 ± 25	
	127.45	425 ± 50	
	143.05	508 ± 23	
	176.78	626 ± 47	2.38 ± 0.10

Figure 4.9: Logarithmic plot of experimental data of the quenching of $I(5^2P_{\frac{1}{2}})$ of HCl over the temperature range 200 - 404 K

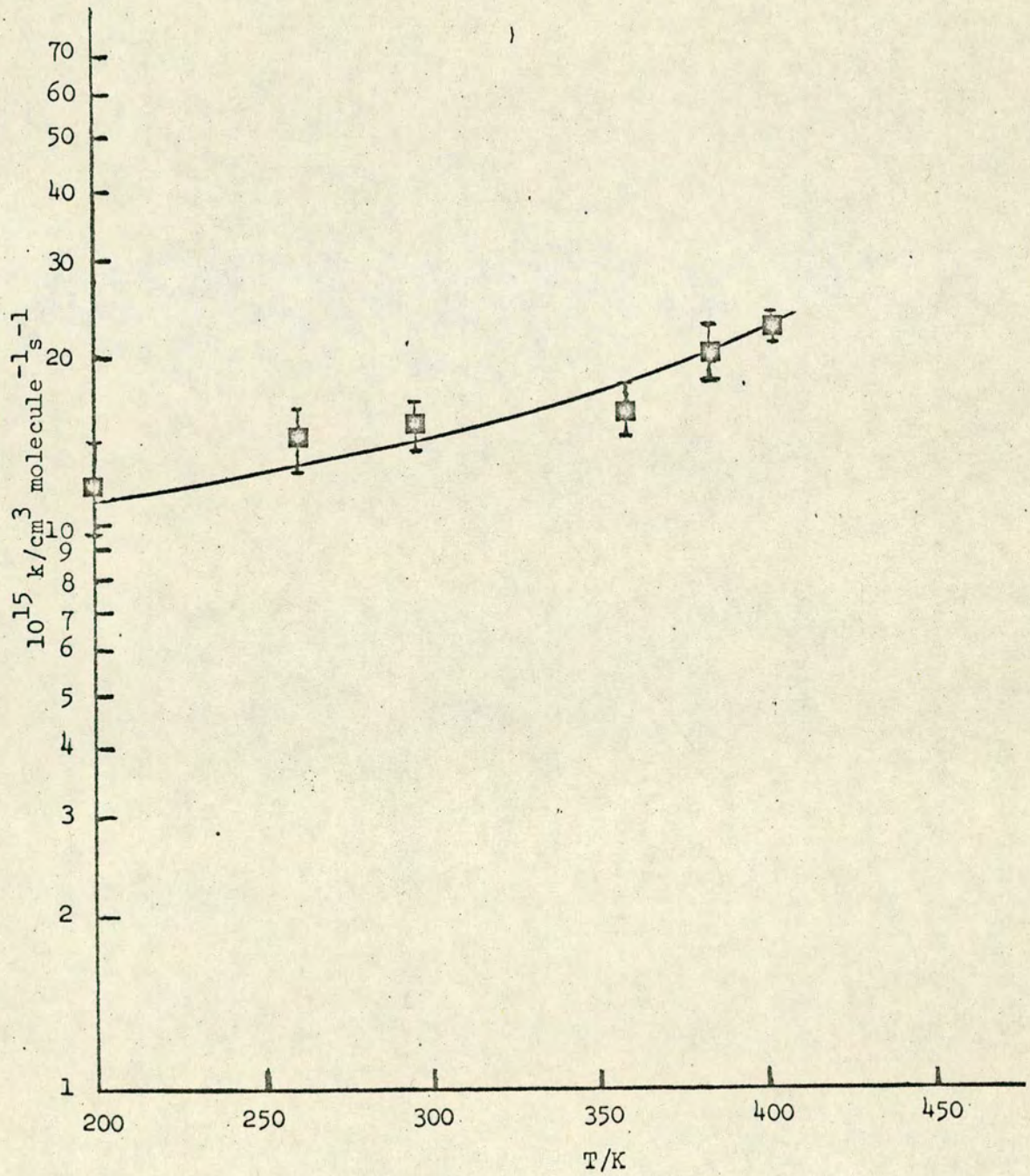

D) DISCUSSION

As the results in Table 4.III indicate, a very large isotope effect, analogous to that observed for the removal of $I(5^2P_{\frac{1}{2}})$ by H_2 and D_2[64] or CH_3I and CD_3I (cf. Chapter 2) is observed only for H_2O and D_2O. In contrast, the isotope effect for the removal of $I(5^2P_{\frac{1}{2}})$ by the HY and DY species is relatively small, never exceeding the value of four. Furthermore, the relative efficiencies of relaxation of $I(5^2P_{\frac{1}{2}})$ atoms in the presence of the latter species exhibit an anomalous trend, as the halogen atom is altered. Thus, while HF is the most efficient quencher, HCl is highly inefficient, and the decay cross section is even smaller than that for HBr and HI. These observations, combined with the different sign of the temperature behavior of the rate constants measured for HCl and HBr, indicate that different decay mechanisms dominate the decay process in each particular case.

In the following section mechanisms which could account for the experimental results will be discussed for each isotopic pair in turn.

1) Relaxation of $I(5^2P_{\frac{1}{2}})$ by H_2O and D_2O

Reactive pathways are generally closed for the relaxation of $I(5^2P_{\frac{1}{2}})$ in the presence of H_2O and D_2O. This can be deduced on the basis of the thermochemical data given in Table 4.VII and the large isotope effect observed. If reactive pathways were important an almost similar decay efficiency would be expected for both H_2O and D_2O. However, on the contrary, the magnitude of the isotope effect observed in the removal of $I(5^2P_{\frac{1}{2}})$ by these molecules implies a highly specific quenching mechanism.

The first low lying vibrational levels of the ground electronic states of H_2O and D_2O are shown in Figure 4.10. These data have been reported on the basis of spectroscopic observations,[174,209,210] and only a few energy levels of D_2O were approximately calculated in the present work by using appropriate formulas* and recent values of molecular vibrational constants.[211]

*cf. Appendix II, section a.

TABLE 4.VII

Thermochemical data for the formation of HI in the reaction of $I(5^2P_{\frac{1}{2}})$ atoms with H_2O and HY molecules

Molecule	σ (cm^2)	D^* (kJ $mole^{-1}$)	ΔH_o^{**} (kJ $mole^{-1}$)
H_2O	1.3×10^{-17}	493.3	+103.7
HF	4.9×10^{-17}	567.0	+226.7
HCl	3.2×10^{-19}	429.7	+40.0
HBr	3.7×10^{-18}	365.3	-24.4
HI	1.7×10^{-17}	298.7	-90.9

* D = Dissociation energy of H-Y or H-OH bonds.

** ΔH_o = Exothermicity of the H atom abstraction

TABLE 4.VIII

Parameters* used in the calculation of the rate constant for the quenching of $I(5^2P_{\frac{1}{2}})$ and $Br(4^2P_{\frac{1}{2}})$ by H_2O

$I(5^2P_{\frac{1}{2}}) + H_2O$	$Br(4^2P_{\frac{1}{2}}) + H_2O$
$Q_I^2 = 4.66 \times 10^{-51} esu^2 cm^4$	$Q_{Br}^2 = 2.63 \times 10^{-51} esu^2 cm^4$
$Q_{H_2O}^2 = 2 \times 10^{-43} esu^2 cm^2$	$Q_{H_2O}^2 = 1.3 \times 10^{-40} esu^2 cm^2$
$n = 4$	$n = 4$
$d = 3.28 \times 10^{-8} cm$	$d^* = 3.08 \times 10^{-8} cm$
$\Delta E = 3\ cm^{-1}$	$\Delta E = 3\ cm^{-1}$
$T = 293\ K$	$T = 300\ K$
$\mu = 2.62 \times 10^{-23}$ gm	$\mu = 2.44 \times 10^{-23}$ gm
$k_{calc} = \sim 2 \times 10^{-13} cm^3 molecule^{-1} s^{-1}$	$k_{calc} = 4.7 \times 10^{-11} cm^3 molecule^{-1} s^{-1}$
$k_{exp} = 8.4 \times 10^{-13} cm^3 molecule^{-1} s^{-1}$	$k_{exp} = 3.2 \times 10^{-11} cm^3 molecule^{-1} s^{-1}$

* The meaning of symbols is given in Chapter 5 (cf. Table 5.II and 5.IV)

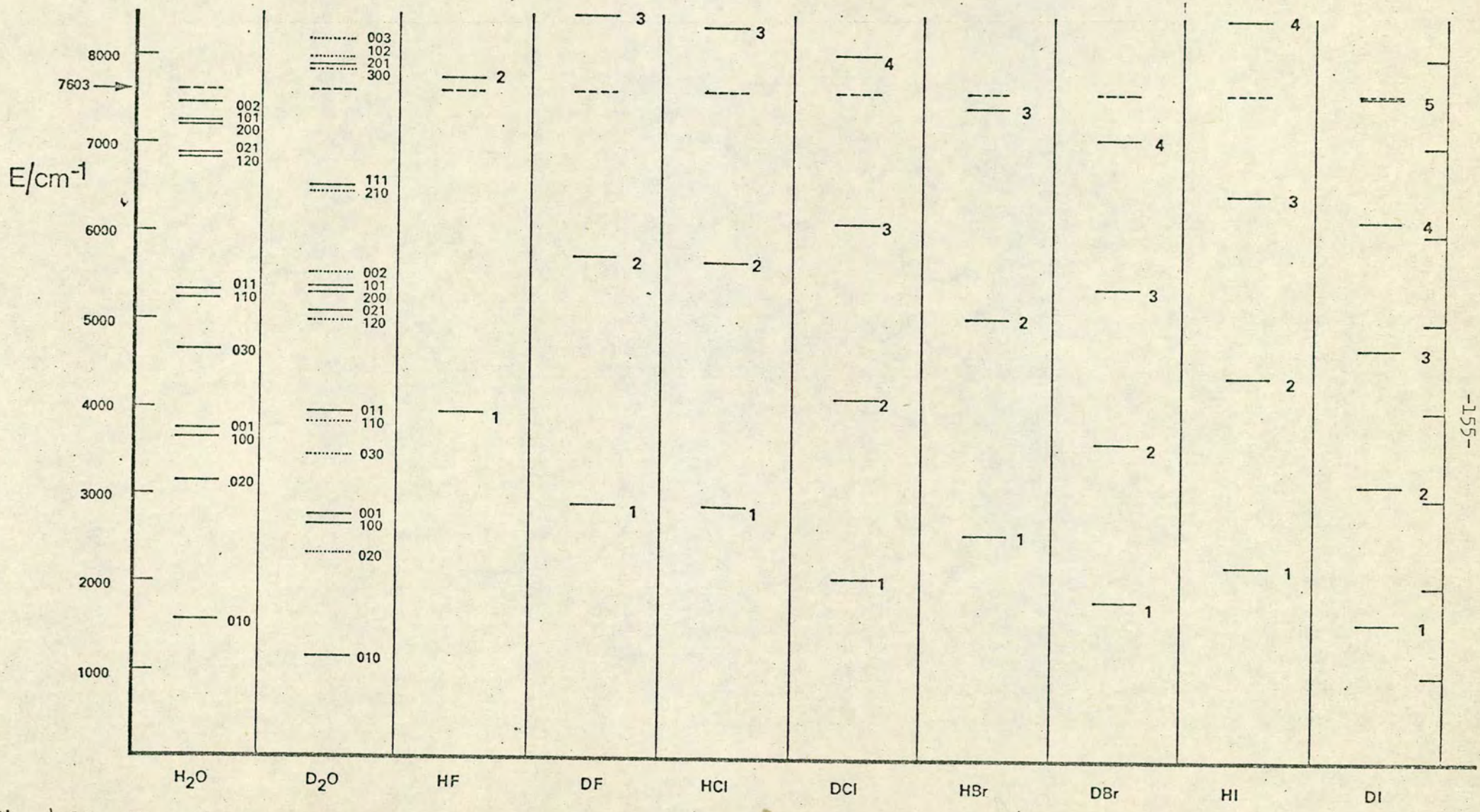

Fig. 4.10 Vibrational energy level diagram for H_2O, D_2O and the H and D halides. For H_2O and D_2O, levels with $v_1 + v_2 + v_3 \geq 4$ have been omitted for clarity.

As can be deduced from this diagram, a quenching mechanism based on near resonant E→V,R energy transfer would involve the favourable (000) → (101), (200), (002) vibrational transitions in H_2O and the (000) → (201) vibrational transition in D_2O. Thus, a large number of channels for E→V, R energy transfer are available for both systems, although the number of near resonant channels (ie. involving energy mismatches less than 200 cm^{-1}) in which large changes in the rotational quantum number J are excluded, is much smaller. Using recent spectroscopic data,[212] it was evaluated that about 80% of the total population of H_2O at 300 K can undergo the above mentioned transitions, with $|\Delta J| \leq 2$; for D_2O near resonant processes are restricted to about 60% of the initial state population.[210] These findings are consistent with a long range E→V,R energy transfer mechanism. As mentioned in Chapter 1, the transition probability for inelastic collisions of this type is proportional to the square of the matrix element for the vibrational transition. It is therefore to be expected that the (000) → (101), (200),(002) transitions in H_2O will be highly favoured over the (000) → (201) transition in D_2O, as two rather than three vibrational quanta are excited in the former case.* We can therefore deduce that this simplified quenching scheme can readily explain the large isotope effect observed. We should also note that these results are in qualitative agreement with those for CH_3I and CD_3I (cf. Chapter 2) and with those obtained for the quenching of $I(5^2P_{\frac{1}{2}})$ by CH_4 and various deuterated methanes.[65,150] However, the large isotope effect provides the key to the quenching mechanism only for H_2O. Considering that long range interactions are expected to be less important in the quenching of $I(5^2P_{\frac{1}{2}})$ by D_2O, contributions from other quenching pathways

* Excitation of two vibrational quanta in D_2O would involve large values of ΔE and/or of ΔJ (ΔK).

including interactions at short range may also play a part in determining the overall small quenching cross section.

An attempt was made to verify the above observations more concretely by calculating the rate constant of quenching of $I(5^2P_{\frac{1}{2}})$ by H_2O, on the basis of a long range multipolar interactions model. A detailed description of the procedure followed is given in Chapter 5. Due to the strong dipole transitions in H_2O, dipole-quadrupole coupling was assumed to predominate the quenching process. The main difficulty encountered in this calculation was the determination of the most important near resonant channels and the corresponding transition matrix elements for H_2O. Detailed spectroscopic data[212] (line frequencies and line strengths) of the relevant absorption bands in H_2O only extended up to $\sim$7500 cm^{-1} and data in the range of 7600 cm^{-1}, which corresponds to the electronic energy released in the relaxation of $I(5^2P_{\frac{1}{2}})$, are insufficient. Consequently, a very approximate calculation was carried out, employing the parameters included in Table 4.VIII. The "effective" matrix element reported for H_2O is the outcome of an indirect estimation, based on the comparison of the intergrated absorption coefficients[214] at the centre of the near resonant water band (7250 cm^{-1}) and at 7600 cm^{-1}. Data for the I.R. transmittance of H_2O at 300 K, averaged over 100 cm^{-1} intervals and having these two frequencies at the centre, have been reported by Wyat et.al.[213] Integrated absorption coefficients for the frequency range (7250 ± 50) cm^{-1} have been measured by Ferriso et.al.[214] "Effective" matrix elements were calculated from these coefficients as described by Herzberg.[174]

The calculated rate constant ($k_{calc} = \sim 2 \times 10^{-13} cm^3 molecule^{-1} s^{-1}$) was found to be smaller than the experimental result by a factor of four. Thus, despite the fact that the theoretical result should be considered only as a rough estimate, it provides some quantitative support for the importance of long range forces in the quenching of $I(5^2P_{\frac{1}{2}})$ by H_2O. Additional

evidence in this respect can be obtained from the calculated rate constant for the analogous system, $Br(4^2P_{\frac{1}{2}}) + H_2O$. Near resonant E↔V energy transfer may occur in this system, as shown in 4.7:

$$Br(4^2P_{\frac{1}{2}}) + H_2O((000), 2_{02}) \rightarrow Br(4^2P_{3/2}) + H_2O((001), 1_{11}) \quad \Delta E=+3cm^{-1} \quad (4.7)$$

Near resonant channels and matrix elements for H_2O were determined on the basis of detailed spectroscopic data[215] for the vibrational band of H_2O at 2.7 μm. However, channel 4.7 was found to dominate the decay process. The calculated rate constant (k_{calc}) accords well with the experimental result[1] (k_{exp}):*

$$k_{calc}=5.7\times10^{-11}cm^3molecule^{-1}s^{-1} \quad \text{vs.} \quad k_{exp}=3.2\times10^{-11}cm^3molecule^{-1}s^{-1}$$

These findings are particularly interesting in the light of the recent development of a pulsed I.R. H_2O laser,[130] in which the pumping mechanism is E↔V energy transfer from $Br(4^2P_{\frac{1}{2}})$. The theoretical result for $Br(4^2P_{\frac{1}{2}}) + H_2O$ indicates that near resonant energy transfer due to multipolar interactions can be of primary importance for the operation of this type of laser system, in which very efficient E↔V energy transfer is required. Similar considerations would seem to apply to the $I(5^2P_{\frac{1}{2}}) + H_2O$ system.

2) Relaxation of $I(5^2P_{\frac{1}{2}})$ by the hydrogen and deuterium halides

i) HCl-DCl

Due to the high endothermicity of the reactive pathway (cf. Table 4.VII) collisional quenching should dominate the removal of $I(5^2P_{\frac{1}{2}})$ by HCl and DCl. However, the results obtained for these molecules are less revealing for the importance of near resonant energy transfer. Thus, the quenching efficiencies are relatively low and the isotope effect is also small (cf. Table 4.III). These data are associated with the virtual absence of near resonant quenching channels with $\Delta E \leq 200\ cm^{-1}$ and small

* In a very recent experimental determination Witting[236] obtained:
$k_{exp} = 6.2 \times 10^{-11}cm^3molecule^{-1}s^{-1}$.

values of ΔJ. Energy levels and initial state populations have been computed for all the HY and DY molecules, as described in Appendix II. For HCl, near resonant channels[216] involving the smallest change in $v(\Delta v = 2)$ and the most highly populated levels require $|\Delta J| \geq 9$. Furthermore, the only channels compatible with resonant energy transfer for $\Delta v = 3$ and transitions with $|\Delta J| \leq 2$ (i.e. dipole-quadrupole coupling) involve very high initial rotational levels ($J \geq 12$), which account for only 0.1% of the total HCl population at room temperature. Even allowing for $|\Delta J| = 4$, the lowest initial J state for near resonant energy transfer involves only 1% of the HCl molecules at 293K. These findings indicate that if multipolar interactions are of some importance for the quenching of $I(5^2P_{\frac{1}{2}})$ by HCl, these should be of high order and consequently shorter range. These types of interactions would be consistent with the large values of ΔJ required for the well-populated initial states of HCl (cf. Chapter 5).

The data for DCl are in many respects similar to those for HCl.[217] Near resonant energy transfer for $\Delta v=3$ requires $|\Delta J| \geq 11$ for the highly populated rotational levels, while transitions with $\Delta J \leq 2$ require $\Delta v = 4$ and are restricted to initial rotational levels with $J \geq 10$ which are occupied by $\sim$8% of the DCl molecules at 293 K. A small initial state population is therefore a common characteristic for both HCl and DCl, and if such states constituted a dominant contribution to the decay of $I(5^2P_{\frac{1}{2}})$, a large positive temperature dependence would be expected for the bulk rate constant and the isotope effect would reflect the larger number of vibrational quanta required for the DCl near resonant channels. However, the very small positive dependence observed for the quenching efficiency of HCl (cf. Figure 4.9) appears to be incompatible with this expectation. In addition, calculations carried out by employing a multipolar interaction model (cf. Chapter 5) resulted in a serious underestimation of the rate

constant for $I(5^2P_{\frac{1}{2}})$ + HCl. It can therefore be deduced that the very low fractions of the population, which can undergo suitable transitions in HCl and DCl, make it very unlikely that the principal mechanism here is near resonant energy transfer from $I(5^2P_{\frac{1}{2}})$ involving long range interactions. At this point it should be noted that the quenching of $Br(4^2P_{\frac{1}{2}})$ by HCl (∿100% E↦V energy transfer) and HBr (∿50% E↦V energy transfer) are also non-resonant processes.[120]

As mentioned in Chapter 1, inelastic processes occuring in electronically non-adiabatic transitions are weakly dependent on the energy discrepancy involved in the process. In Figure 4.11 it is shown how the general potential hypersurfaces for $X(^2P_{\frac{1}{2}})$ + $HY(^1\Sigma)$ and $X(^2P_{3/2})$ + $HY(^1\Sigma)$ can be coupled non-adiabatically. For weak spin-orbit coupling the interaction of a halogen atom (^2P state atom) with $^1\Sigma$ molecules such as the hydrogen halides in their ground electronic states can give rise to Σ and Π states in linear ($C_{\infty v}$) configuration, which become $^2A'$ and $^2A' + {}^2A''$ correspondingly in C_s geometries. For strong spin-orbit coupling all three hypersurfaces are characterised by $E_{\frac{1}{2}}$ symmetry species. Non-adiabatic transitions can then occur between the $^2A'$ hypersurface emanating from the excited atomic state and the $^2A''$ (or $^2A'$) hypersurface correlating with the ground atomic state. Following the transition, the products may separate to yield $X(^2P_{3/2})$ + HY or $Y(^2P_{3/2,\frac{1}{2}})$ + HX (cf. 4.1 and 4.2), the latter channel being important only if there is no large energy barrier.

A detailed discussion of this type of process at short range is hindered by the lack of information concerning excited potential hypersurfaces in the X + HY systems. However, this type of mechanism has been invoked to account for efficient quenching of $Br(4^2P_{\frac{1}{2}})$ by HCl and HI. Bergmann et. al.[198] have discussed the approach of a halogen atom (X) to the hydrogen halide molecule (HY) in terms of a naive model,

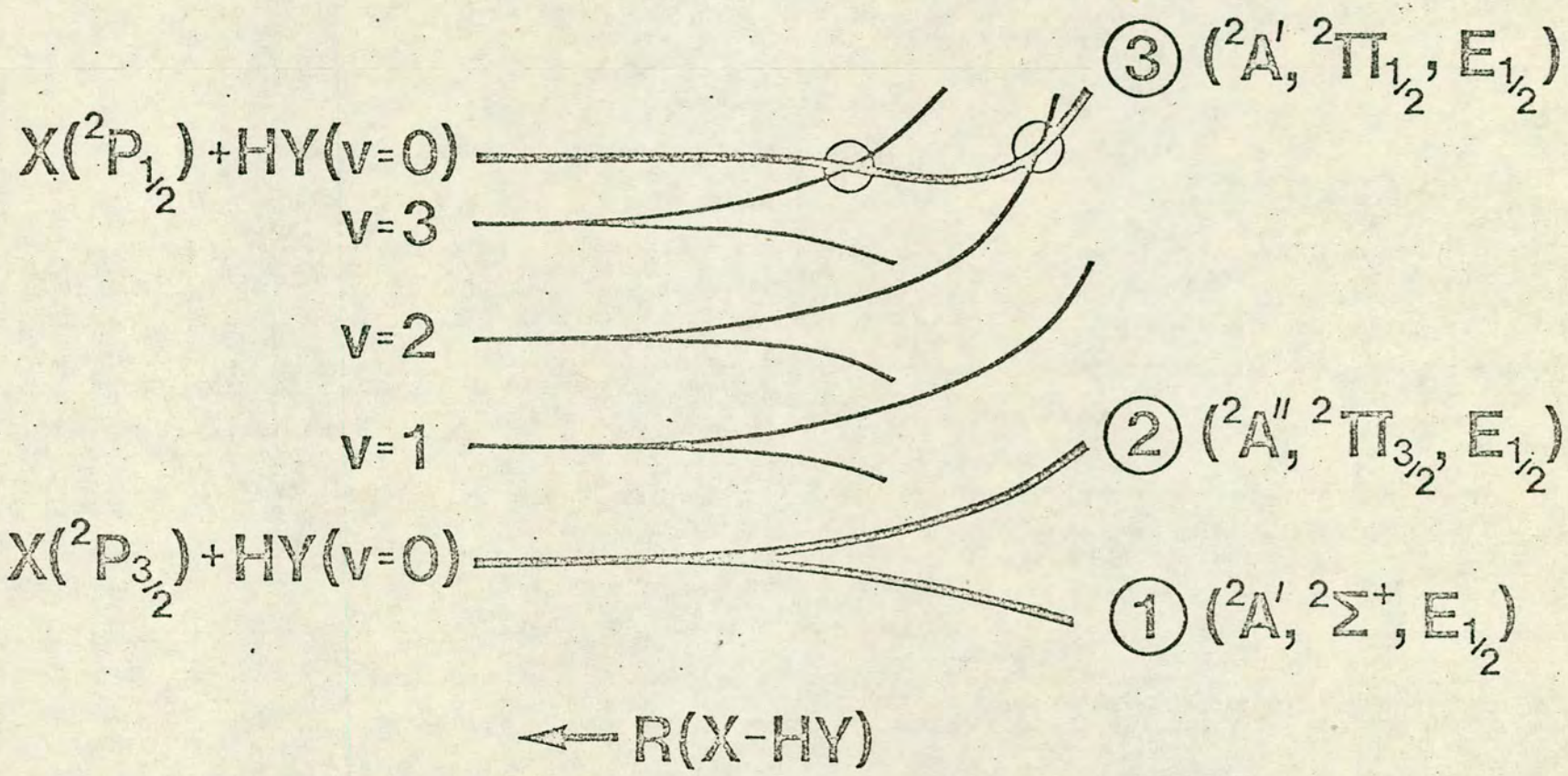

Figure 4.11: Diagramatic representation of a section through the potential energy surfaces for the X + HY system.

based on simple valence bond theory, whereby the ^2P atomic states are characterised by an unfilled p orbitals lying along and perpendicular to the molecular axis. On the basis of this model strongly repulsive $^2A' + {}^2A''$ ($^2\Pi$) hypersurfaces are predicted. Thus, although the model is consistent with the observed low reactive efficiency of $Br(4^2P_{\frac{1}{2}})$ and HI, it also precludes crossing of the hypersurface correlating with $X(^2P_{\frac{1}{2}})$ + HY by any other hypersurface at low energy. The assumptions made in this model have been criticised by Donovan et.al.[223] and its applicability has been further challenged by Houston, in a recent experimental study of the rapid $I(5^2P_{\frac{1}{2}}) + Br_2$ reaction.[207]

In contrast to the suggestions of Bergmann et.al.[198] the small activation energy obtained for $I(5^2P_{\frac{1}{2}})$ + HCl in this work indicates that non-adiabatic surface-crossing processes in the quenching of $I(5^2P_{\frac{1}{2}})$ by HCl and similar $X(^2P_{\frac{1}{2}})$ + HY systems can be important at large X-HY separations. The shape of the potential hypersurfaces at such separations is effectively determined by long range interactions, due to the permanent multipole moments of the colliding species. The interactions between the $^2P_{3/2}$ state atoms and HY can give rise to non-degenerate electronic states with the energy separation between them increasing as the species approach one another (cf. Figure 4.11). It is worth noting that since the quadrupole moment of the $^2P_{\frac{1}{2}}$ state is zero,* the upper $^2A'$ surface will be effectively flat at large separations.

Detailed calculations revealing the effect of quadrupole-quadrupole interaction on the potential hypersurfaces for the $H_2 + F(^2P)$ system have been carried out by Rebentrost and Lester.[41] For the purposes of this work rough estimates of the dipole-quadrupole interaction between

* As can be shown,[218] the matrix element for the expectation value of the 2^n-pole moment vanish unless $J \geq \frac{1}{2}n$, where J is the quantum number of the total angular momentum and n = 2,3,4 for quadrupole, octupole and hexadecapole moments respectively.

HY and $I(5^2P_{3/2})$ molecules were obtained on the basis of the Boltzmann weighted mean interaction potential for non-overlapping charge distributions, as described by Margenau.[219,220] The dipole-quadrupole interaction energy is the leading term of the first order Coulombic interaction and is expected to make the highest contributions at large I-HY separations . The parameters used in these calculations along with interaction energies for some values of R are given in Table 4.IX. The same table includes interaction energies obtained for various atom-molecule orientations by using an angle dependent potential.[220]

We now recall Nikitin's model[47] (cf. Chapter 1), whereby E→V energy transfer can occur if the $X(^2P_{\frac{1}{2}})$ + HY hypersurface is crossed by one or more vibronic hypersurfaces correlating with $X(^2P_{3/2})$ + HY ($v \geq o$) (cf. Figure 4.11). This requires the former hypersurface 3 to be less repulsive than hypersurface 2 or less attractive than hypersurface 1. As can be deduced from the data given in Table 4.IX, these conditions are satisfied at intermediate separations, i.e. at separations in which the spin-orbit splitting is of the same order of magnitude compared to the sum of the coulombic interaction energy and the vibrational excitation. It should be noted that convergence of hypersurfaces 2 and 3 would also be expected on the grounds that, for strong spin-orbit coupling, all three surfaces have the same species $E_{\frac{1}{2}}$ and thus at large X-HY separations hypersurfaces 1 and 2 will strongly repel one another. Conversely, at smaller separations, hypersurfaces 2 and 3 start to repel each other.

In general, crossings between hypersurfaces 2 and 3, the former correlating with $X(^2P_{3/2})$ + HY (v = 0, 1, ...), can lead to a range of transition probabilities for E→V energy transfer into the various vibrational levels of HY. According to the expectations of Nikitin's model, the transition probability should be dependent on the number of vibrational quanta excited in HY. Thus isotope effects such as those

TABLE 4.IX

Dipole-Quadrupole interactions in $I(5^2P_{3/2})$ + HY systems

a) Parameters used in the calculation

Dipole moments (μ) of the hydrogen halides[a]

	$\mu \times 10^{18}$ HY (esu cm)
HF	1.91
HCl	1.07
HBr	0.80
HI	0.42

Quadrupole moment[b] of $I(5^2P_{3/2})$

$Q_I(3/2,3/2) = 4.3\times10^{-26}$ esu cm^2

Estimated error: ±9%

b) Weighted I - HY interaction energies $E(^2A'')$, in cm^{-1}

HY	R = 6×10^{-8} cm	R = 5×10^{-8} cm	R = 4×10^{-8} cm
HF	-5.1	-21.8	-129.7
HCl	-1.6	-6.8	-40.7
HBr	-0.7	-3.8	-22.8
HI	-0.2	-1.0	-6.3

c) Interaction energies (in cm^{-1}) at R = 5×10^{-8} cm for various angles of orientation ϑ (in degrees).

HY	$\vartheta = 0^\circ$	$\vartheta = 30^\circ$	$\vartheta = 45^\circ$	$\vartheta = 60^\circ$	$\vartheta = 90^\circ$
HCl	-56.4	-49.0	-39.8	-28.2	0.0

[a] Ref. 234.

[b] The quadrupole moment was evaluated for atoms with $m_J = 3/2$, on the basis of the expression[218,234] of the quadrupole moment for a given charge distribution.

$$Q_I(3/2,3/2) = e\langle r^2\rangle \frac{\int_0^\pi P_2(\cos\vartheta)\sin^2\vartheta\sin\vartheta\,d\vartheta}{\int_0^\pi \sin^2\vartheta\sin\vartheta\,d\vartheta}$$

where, e is the charge of a "positive hole" equivalent to the electron charge,

$\langle r^2\rangle$ is the mean square radius for the outer p orbitals of $I(5^2P)$, given by Mann[253]

$P_2(\cos\vartheta)$ is a Legendre polynomial

and $\sin^2\vartheta$ represents the charge distribution in the p orbitals considered.

seen for $I(5^2P_{\frac{1}{2}})$ + HCl and DCl, are possible due to the different vibrational frequencies in HY and DY.* Furthermore, this model is compatible with the very small positive activation energy observed for $I(5^2P_{\frac{1}{2}})$ + HCl, which indicates that efficient non-adiabatic transitions possibly occur at smaller separations R, in which hypersurface 3 starts becoming slightly repulsive.

ii) HBr - DBr

Of the hydrogen halides examined in this work, HBr shows a surprisingly high efficiency in removing $I(5^2P_{\frac{1}{2}})$ atoms (cf. Table 4.III). This may be understood either in terms of a highly specific quenching mechanism, such as near resonant E↔V energy transfer due to long range forces, or in terms of a reactive pathway which is exoergic for this system (cf. Table 4.XIII).

The first type of mechanism could be important on the basis of the following data: a large number of channels[221] exist for

*

It should be noted that this model can also account for the proposals[232] according to which the reaction between H atoms and ICI leads in part to $I(5^2P_{\frac{1}{2}})$, viz.

$$H + ICl \rightarrow HCl(v \leq 4) + I(5^2P_{\frac{1}{2}}) \qquad \Delta H_o = -310.5 \text{ kJ mole}^{-1}$$

$\Delta v = 3$ and $\Delta J = 1$ and 2, the initial states involved accounting for over 90% of the HBr population at 293K. For transitions involving $|\Delta J| = 2$ there are five channels, with $\Delta E < 50$ cm^{-1} and with $\Delta E \sim 4$cm^{-1}, viz:

$$I(5^2P_{\frac{1}{2}}) + HBr\ (v = 0,\ J = 6) \rightarrow I(5^2P_{3/2}) + HBr\ (v = 3,\ J = 8) \quad (4.8)$$

These findings indicate that near resonant E↔V energy transfer could play an important role in the decay of $I(5^2P_{\frac{1}{2}})$ by HBr, although they do not provide any firm indication as to whether dipole-quadrupole or quadrupole-quadrupole terms are involved. To obtain further information in this respect, decay rates were calculated at different temperatures for the most favourable near resonant channels. Details concerning these calculations are included in Chapter 5. We note here that according to the theoretical results, the channel described by 4.8 should dominate the quenching process. As shown in Figure 4.7, the calculated rate constants underestimate the experimental data by a factor of four. However, the fact that the temperature dependences of the theoretical and the experimental decay rates exhibit similar functions is noteworthy. In view of the approximations inherent in the theoretical model and the uncertainty in some of the molecular parameters used in the calculations (cf. Chapter 5), we may consider that the theoretical predictions are in accord with the experimental observations. The lower decay efficiency observed for DBr compared with HBr (cf. Table 4.III) is consistent with the virtual absence of any near resonant channels[222] with $\Delta v = 3$ for the $I(5^2P_{\frac{1}{2}})$ + DBr system. However, we should note that although the kinetic data obtained provide only a lower limit for the magnitude of the isotope effect (cf. Table 4.III), a large isotope effect, as that observed for $I(5^2P_{\frac{1}{2}})$ + H_2O and D_2O, is highly unlikely.

However, in contrast to the above considerations Wiesenfeld and Wolk, in a very recent work,[203] obtained experimental evidence which illustrates that reaction (4.1) and not quenching (4.2) is the dominant route for

collisional deactivation of $I(5^2P_{\frac{1}{2}})$ by HBr.* The interpretation of their results was based on an extension of the curve-crossing model proposed earlier by Donovan et.al.[223] According to Wiesenfeld and Wolk, the observed efficiency of the reactive pathway can be attributed to non-adiabatic transitions between the $^2A'$ hypersurface emanating from $I(5^2P_{\frac{1}{2}})$ + HBr (v = o) and the $^2A'$ hypersurface correlating with $I(5^2P_{3/2})$ + HBr (v = 4). As has already been mentioned, this model can account for a relatively small isotope effect such as that observed for HBr and DBr. Multiquantum vibrational transitions are generally unfavourable (cf. Chapter 1) and reaction of $I(5^2P_{\frac{1}{2}})$ with DBr requires the excitation of at least 5 vibrational quanta instead of 4 as for HBr. However, considering the features of the $^2A'$ hypersurfaces (cf. Fig 7 in Ref. 203), an energy barrier should be expected on the basis of the proposed model. Clearly, this is inconsistent with thenegative activation energy observed for $I(5^2P_{\frac{1}{2}})$ + HBr in the present work. The inadequacy of this simple model, originally invoked[223] for collisions at large X-HY separations, is not surprising at the shorter separations which are possibly required for reaction.

Reaction occuring via the formation of a long-lived intermediate complex would be compatible with the small negative activation energy observed for $I(5^2P_{\frac{1}{2}})$ + HBr. It is interesting to note that the reactions of $I(5^2P_{\frac{1}{2}})$ with ICl and IBr, which can also be attributed to long-lived intermediates, have a zero activation energy[225] which may be compared with the data obtained in this work. Direct evidence for bound ionic species of the type YHX^- has been obtained[224] only in matrix isolation investigations.

* Nevertheless, we note that the theoretical predictions for near resonant energy transfer are in accord with the lower limit of the fraction of the overall decay rate constant determined for quenching (~20%).

In gas phase (crossed molecular beam experiments), the trihalogens FIF and ClIF and the pseudotrihalogen HIF have been directly identified.[170] The stability of these compounds is mainly due to the uneven charge distribution of the π orbitals in the Y-X bond, when the electronegativity of Y and X differ substantially. Thus, as mentioned in Chapter 2, the favourable geometries in these compounds are those having the least electronegative atom, i.e. I, in the middle of the molecule.[31] Given these preconditions we can deduce that the formation of an BrHI (or even HBrI) intermediate, as required for the reaction of $I(5^2P_{\frac{1}{2}})$ with HBr, is unlikely.

Considering the large differences in the masses of H and Br or I atoms, an approach based on the spectator stripping model of chemical reactions appears to be realistic for the $I(5^2P_{\frac{1}{2}})$ + HBr system. At short I-HBr separations, the distance between I and Br atoms can be considered constant during the time required for the light H atom to be transferred from Br to I atom. The analogy between this type of process and photochemical reactions has been pointed out by Herschbach.[226] Consequently, a principal model for many of these chemical processes is provided by the Franck-Condon assumption. Eu[227] has shown that the Born scattering amplitude and thus also the reaction cross section, can be regarded as a product of two Franck-Condon factors, one of which corresponds to the decomposition of the reacting molecule (HBr here), and the other to the formation of the molecular product (HI here), through their excited repulsive electronic states. These "free-bound" transitions give rise to Franck-Condon factors, which involve products of translational and vibrational wavefunctions and are collision energy dependent. This has been demonstrated by the recent calculations of Kimura,[228] for the thermoneutral reaction

$$I'(5^2P_{3/2}) + HI\ (v = o) \rightarrow I'H\ (v = o, 1, 2) + I(5^2P_{3/2}) \qquad (4.9)$$

The cross section was found to decrease slightly with increasing translational energy, exhibiting behavior similar to that observed for $I(5^2P_{\frac{1}{2}})$ + HBr. Thus, despite the fact that further investigations are necessary to clarify various subtle aspects of this model, we feel that it can satisfactorily account for the kinetic data obtained for the removal of $I(5^2P_{\frac{1}{2}})$ by HBr. An interesting comparison in this respect is provided by the negative temperature dependences obtained for the rate constants of the exothermic exchange reactions involving Cl + HI and HBr. The highly anisotropic angular distribution observed[34] in molecular beams studies of Cl + HI precludes the formation of a long-lived intermediate and the Franck-Condon factors arising from an impulsive model may be invoked in explaining the observed temperature behavior.

iii) HI - DI

The absence of any detectable isotope effect for the removal of $I(5^2P_{\frac{1}{2}})$ by HI and DI (cf. Table 4.III) is rather intriguing in light of the previous discussion. Near resonant quenching channels[221,229] are virtually absent for $I(5^2P_{\frac{1}{2}})$ + HI, except for $\Delta v = 4$ and $J > 16$. In contrast, all rotational states of DI can undergo near resonant transitions[230] with $|\Delta J| \leq 2$ and $\Delta v = 5$. It could therefore be argued that if long range forces dominate the quenching of $I(5^2P_{\frac{1}{2}})$ by HI and DI, these effects cancel each other, resulting in the observed virtual absence of an isotope effect. Furthermore, if such is the case, HI and DI are expected to show completely different temperature dependences, strongly positive for HI and weakly negative for DI. However, for both these molecules the vibrational transitions are too weak[211,235] to justify the measured rate constant on the basis of near resonant energy transfer. The large discrepancy between calculated and experimental results (cf. Chapter 5) clearly rules out a significant contribution to the quenching mechanism by long range forces. A non-resonant energy transfer mechanism, such as that invoked earlier for HCl and DCl, is also incompatible with the relatively high decay efficiency of HI and DI compared to that of HCl and DCl.

However, taking into account that for these systems reactive pathways are energetically possible (cf. Table 4.VII), chemical interactions between $I(5^2P_{\frac{1}{2}})$ atoms and HI or DI may lead to an increased decay efficiency of $I(5^2P_{\frac{1}{2}})$ in the presence of these molecules.

In general, atom exchange (cf. 4.11) is expected to be more favourable than abstraction of iodine atoms and formation of I_2 (cf. 4.10) due to the endoergicity of the latter reaction.

$$I(5^2P_{\frac{1}{2}}) + HI \rightarrow I_2 + H(1^1S_{\frac{1}{2}}) \qquad \Delta H_o = +55.4 \text{ kJ mole}^{-1} \qquad (4.10)$$

$$I'(5^2P_{\frac{1}{2}}) + HI \rightarrow HI' + I(5^2P_{3/2}) \qquad \Delta H_o = -90.9 \text{ kJ mole}^{-1} \qquad (4.11)$$

This has been verified in previous work in the vacuum U.V., in which it was proved that abstraction does not occur.[204] We therefore suggest that relaxation of $I(5^2P_{\frac{1}{2}})$ by HI and DI involves the atom exchange reaction (4.11).

Although the above suggestion is compatible with the lack of any significant isotope effect, we note that the observed efficiency is rather low for these types of reactive processes.* For example, the exothermic atom exchange reaction,

$$Cl(3^2P_{3/2}) + HI \rightarrow HCl(v) + I(5^2P_{3/2}) \qquad \Delta H_o = -132.6 \text{ kJ mole}^{-1} \qquad (4.12)$$

proceeds with a total cross section of 33.5×10^{-16} cm^2 yielding highly vibrationally excited HCl.[231] Conversely, atom exchange processes have been proposed to explain the observed high efficiency for the vibrational relaxation of some HY(v) molecules by halogen atoms,[233] (e.g. HCl(v) + Cl). The small efficiency observed for the atom exchange reaction in the $I(5^2P_{\frac{1}{2}})$ + HI and HBr systems is then attributed to the large spin-orbit electronic energy to be transferred in these systems, in comparison with

* A similar observation can be made for the reaction of $I(5^2P_{\frac{1}{2}})$ with HBr.

the energy differences of the other degrees of freedom. We note that this should be expected in terms of a mechanism based on Nikitin's model (cf. Chapter 1).

E) CONCLUSIONS

a) The high decay efficiency measured for the quenching of $I(5^2P_{\frac{1}{2}})$ by H_2O and the large isotope effect observed for H_2O and D_2O are consistent with a mechanism based on near resonant E→V energy transfer due to long range forces. These data, analogous to those obtained for the relaxation of $I(5^2P_{\frac{1}{2}})$ atoms by CH_3I and CD_3I (cf. Chapter 3), support the conclusion according to which, where favourable channels are available involving vibrational transitions with appreciable matrix elements, the quenching cross section is a sensitive function of Δv. Channels with Δv differing by unity have associated cross section differing by more than one order of magnitude. This conclusion is further substantiated by the data for the quenching of $Br(4^2P_{\frac{1}{2}})$ by H_2O, where only one vibrational quantum should be excited and the results of calculations are consistent with the long range interaction model. The cross section is found to be forty times that for $I(5^2P_{\frac{1}{2}})$ and H_2O, and is close to the gas dynamic collision cross section.

b) The data for the deactivation of $I(5^2P_{\frac{1}{2}})$ atoms by HY and DY molecules, along with those available for $Br(4^2P_{\frac{1}{2}})$ and HY, illustrate the relative importance of quenching and reactive mechanisms as the Y atom is altered. Thus, the sequence observed for the decay cross sections σ_{HY} at room temperature.

$Br(4^2P_{\frac{1}{2}})$: $\sigma_{HF} > \sigma_{HCl} > \sigma_{HI} > \sigma_{HBr}$

$I(5^2P_{\frac{1}{2}})$: $\sigma_{HF} > \sigma_{HBr} > \sigma_{HI} > \sigma_{HCl}$

may be interpreted on the basis of the following mechanisms:

i) Near resonant E→V energy transfer due to dipole-quadrupole coupling can account for the very efficient quenching of $Br(4^2P_{\frac{1}{2}})$ and $I(5^2P_{\frac{1}{2}})$ by HF.

ii) For non-resonant processes and as long as reactive pathways are energetically unfavourable, E→V energy transfer can occur on the basis of electronically non-adiabatic transitions at intermediate atom-molecule separations. The smaller efficiency of HCl in quenching $Br(4^2P_{\frac{1}{2}})$ or $I(5^2P_{\frac{1}{2}})$ atoms in comparison to that of HF is ascribed to this kind of mechanism. Similarly, the relatively low decay rates determined for E→V energy transfer in $Br(4^2P_{\frac{1}{2}})$ + HBr fall within the expectations of such a model.

iii) The increased interference of reactive pathways is usually accompanied by an increase in the decay rate. Thus, both HBr and HI remove $I(5^2P_{\frac{1}{2}})$ atoms faster than HCl, which reflects the importance of reaction 4.1 in these systems. However, part (~20%) of the decay efficiency of $I(5^2P_{\frac{1}{2}})$ in the presence of HBr may be attributed to E→V near resonant energy transfer due to quadrupole-quadrupole interactions.

A controversy remains for the $Br(4^2P_{\frac{1}{2}})$ + HI system. Recent data challenge the original suggestion that quenching is the most likely path for removal of $Br(4^2P_{\frac{1}{2}})$. Whatever the case, however, a curve crossing mechanism at large atom-molecule separations can account for the observed decay efficiency.

Finally, it is noted that an impulsive model for reaction can account for the kinetic data obtained for $I(5^2P_{\frac{1}{2}})$ + HBr at different temperatures. This indicates the need of incorporating into collision theory the idea of Franck-Condon transitions.

Chapter 5

CALCULATIONS OF E→V ENERGY TRANSFER DUE TO MULTIPOLAR INTERACTIONS

A) INTRODUCTION

In the previous chapters, it was suggested that energy transfer processes of the type,

$$A^* + Q(v'' = n, J'' = k) \rightarrow A + Q^* (v' = m, J' = l) + \Delta E \qquad (5.1)$$

where, A is an atom, Q and Q^* is respectively a molecule in its ground and excited state and ΔE is the energy to be transfered in translation, can be important in the relaxation of electronically excited atoms, denoted by A^*. In general, we can distinguish three categories of mechanisms which could explain process 5.1.

(a) Mechanisms based on adiabatic transitions between "parallel" parts of the potential surfaces correlating with the ground and excited vibronic surfaces. Transitions due to long range forces are included in this type of mechanism. Minimization of the energy mismatch ΔE, i.e. near-resonance, is of great importance for efficient quenching. The deactivation of $I(5^2P_{\frac{1}{2}})$ by CH_3I was explained on the basis of this mechanism (c.f. Chapter 3).

(b) Mechanisms based on non-adiabatic transitions i.e. involving "crossing" of the potential surfaces. Nikitin's theory[48] of vibrational relaxation via electronically non-adiabatic collisions, i.e. the inverse process of that described by 5.1, belongs here. The quenching of $I(5^2P_{\frac{1}{2}})$ by N_2 was interpreted in Chapter 3 in terms of this type of mechanism. Under this category we can also ascribe theories involving coupling of the entrance and exit channels via crossing by coulombic surfaces, as in the quenching of alkali atoms by diatomic molecules.[51] Near resonance is in general of limited importance.

(c) Mechanisms in which A^* and Q exchange energy in a "compound" collision. The passage from the entrance to the exit channel takes place

through a bound potential, which may result in a long-lived intermediate complex. Gait's approach[61] to orbiting collisions is a theory belonging to this category. Near resonance can be of some importance but not as in theories of the first type (a).

The calculations presented in this chapter are based on theories falling into the first category, namely theories which attribute energy transfer to multipolar interactions. Motivation for this work were the large isotope effects observed in the quenching of electronically excited atoms, like $I(5^2P_{\frac{1}{2}})$, by small isotopically substituted molecules and the observed temperature behaviour of the decay efficiency of some efficient quenchers (c.f. Chapter 1, 3 and 4). The observed differences[62,64] in the removal efficiency of excited atomic species by H_2, HD and D_2 are particularly striking in this respect. It has been suggested[64] that $E \rightarrow V$ near resonant energy transfer, due to long range interactions, can explain these results. It has also been proposed[64] that "selection rules" determine the efficiency of electronic energy transfer and arise from the interacting multipoles.

Our purpose in this work is to examine further these suggestions by carrying out calculations based on the proposed model and comparing the results with experimental data for various systems.

B) SOME THEORETICAL CONSIDERATIONS

The fundamental assumption of the present calculations is that the relaxation of electronically excited atoms by small molecules is entirely due to long range forces. The salient feature of this assumption is the interaction potential derived from the multipole expansion of non overlapping charge distributions, as it has been described by Margenau.[220] This expanded potential is the perturbation V(t), which causes the relaxation of the excited atomic state. The problem, therefore, is to calculate the transition

probability P_{if} from an initial state of the system $|i\rangle$, to a final state $\langle f|$, where $|i\rangle$ and $\langle f|$ are in general products of the electronic eigenfunction describing the atom, at its excited state in the former case and at its ground state in the latter, and the rovibrational eigenfunction of the ground and excited state quenching molecule correspondingly.

To calculate this transition probability two methods are usually applied. The first method is a semiclassical approach using time dependent perturbation theory. The internal degrees of freedom, treated quantum mechanically, are perturbed by the time dependent potential acting over the classical trajectory. The second method uses the Born approximation, which treats the problem fully quantum mechanically. The two methods give equivalent results for most cases,[87] but they bring out different aspects of the problem. In this work we have followed the first treatment.

A generalized approach to the time dependent perturbation theory is included in reference 12a. Here, we quote the expressions of P_{if} for the first and second order approximations, in order to discuss some basic features of this theory. First order approximation:

$$P_{if} = [\,(-ih)^{-1} \int_{-\infty}^{\infty} V_{if}(t)\, \exp(i\omega_{fi}t)\, dt\,]^2 \qquad (5.2)$$

where $V_{if} = \langle i|\mathbf{V}(t)|f\rangle$ are the matrix elements for $V(t)$

$\omega_{fi} = \Delta E/h = E_f - E_i/h$, E_f and E_i being the initial and final translational energy of the system.

Second order approximation:

$$P_{if} = [\,(ih)^{-1} \int_{-\infty}^{\infty} V_{if}(t)\exp(i\omega_{fi}t)dt +$$

$$+ (-ih)^{-2} \sum_{v} \int_{t}^{\infty} V_{vf}(t)\, \exp(i\omega_{fv}t)\, x$$

$$x \int_{-\infty}^{t} V_{vi}(t)\, \exp(i\omega_{vi}t')\, dt'dt\,]^2 \qquad (5.3)$$

The summation in the second term of 5.3 is over all the virtual states v, as these appear in the general expression XVII.24 of reference 12a. The first term in 5.3 describes the first order contribution. The second term, or more concisely the second set of terms is the second order contribution. Some of these contributions can interfere with the first order terms constructively and others destructively, depending on the sign of the interacting multipoles. Thus, inclusion of higher order approximations can have as an effect either an increase or a decrease of the overall transition probability. The formulation for higher order approximations is similar to that for second order, since they are derived from identical general expressions. Such calculations however, are extremely difficult and have been carried out only in few cases.[89,90]

The magnitude of P_{if} in 5.2 and 5.3 depends strongly on ω and consequently on the energy mismatch. If the factor $\exp(i\omega t)$ oscillates, while the perturbing potential is significant, the probability decreases rapidly with increasing ω. We can therefore conclude, that shorter range potentials, i.e. potentials involving higher multipolar interactions, allow for larger energy mismatches. Thus, contributions of higher multipoles should not be indiscretely excluded, especially in systems involving large energy discrepancies.

In cases of E → V energy transfer, large energy defects are usually involved. Near resonant conditions, however, may be achieved by including the effect of rotational transitions. In first order approximation, these transitions obey the selection rules corresponding to the multipoles arising from the expansion of the interaction potential. Thus, although the magnitude of the interaction falls off with increasing order of multipole, possible minimization of ω for higher multipoles can lead to a significant contribution to the transition probability. The proposed existence of "selection rules", which determine the efficiency of process 5.1, arises from the consideration

of rotational selection rules.

However, if higher order approximations are considered, the form of such "selection rules" is not straightforward. Higher order approximations can allow for multiquantum rotational transitions via the virtual states which they involve (c.f. v states in 5.3). Such transitions would be effectively forbidden in first order approximation for a given multipolar interaction. Considering that such multiquantum transitions can decrease even further the energy discrepancy, inclusion of higher order perturbations can be of importance in E → V energy transfer. Dillon and Stephenson have shown [89,90] their significance in V - V energy transfer. However, the importance of the relative parameters taken separately can not be assessed from their numerical calculations.

Other authors [238] have also considered the effect of multiquantum rotational transition in V - V energy transfer, although to our knowledge there are no direct studies of this effect in a generalized form.

To sum up, we note that multiquantum rotational transitions can play a very important role in energy transfer processes due to long range forces, by minimizing the energy defect. Such transitions may come about either by considering higher multipolar interactions or by introducing higher order approximations.

C) FORMULATION

The basis of the calculations in this work is the formalism, which has been described by Sharma and Brau [85,86] and modified by Tam, [240] Lev-on et.al. [239] and Gait [61] in a series of papers refering to V - V energy transfer. In all these treatments first order time dependent perturbation theory is used and classical trajectories are assumed for the colliding species. These trajectories are straight lines for impact parameters b larger than d, where d is the hard sphere collision diameter. For b<d,

Sharma and Brau[85] have used parabolic trajectories assuming that the trajectory is determined by the repulsive part of the potential. Lev-on et.al.[239] make a different assumption for b<d. They consider that the collision event occurs on two straight lines. The colliding species come in straight line, undergo a hard sphere collision and rebound on straight line. This is approximated by setting

$$P_{if}(0 \leq b \leq d) = P_{if}(d) \qquad (5.4)$$

In this work we have adopted the latter assumption for small impact parameters.

For simplicity, in these first approximate calculations, the angle averaged rms interaction potential for non-overlapping charge distributions has been used, instead of the axially symmetric potential given by Sharma and Brau. Following Margenau,[220] a simple expression of the matrix elements, which appear in the expression (c.f. 5.2 and 5.3) of the transition probability, may be derived. As it is shown in 5.5, the matrix elements can be expressed in terms of the transition moments of the colliding species and the internuclear separation R(t):

$$V_{if}(t) = \frac{a\, Q_1\, Q_2}{R(t)^n} \qquad (5.5)$$

where: Q_1 and Q_2 are transition moments for the atom and the molecule,

a is a numerical coefficient determined by the multipole coupling involved and

n is an integer, which also depends on the multipole coupling used.

Values of n for the very first terms on the expansion of the potential are given in Table 5.I.

According to 5.5, the type of coupling, which should be expected to contribute most in the quenching process, depends on the magnitude of the transition moments. In general, the first few terms of the expanded potential give a good approximation to the long range interaction, provided the following criterion is satisfied for the final two terms:[82]

$$[\langle i \mid Q_{n-1} \mid f \rangle]\, d \gg [\langle i \mid Q_n \mid f \rangle] \qquad (5.6)$$

Table 5.I

Dependence of n on the type of coupling

Type of coupling		n
dipole-dipole	(d-d)	3
dipole-quadrupole	(d-q)	4
quadrupole-quadrupole	(q-q)	5
dipole-octupole	(d-o)	5
dipole-hexadecapole	(d-h)	6
quadrupole-octupole	(q-o)	6
quadrupole-hexadecapole	(q-h)	7

For some of the systems studied here, this criterion is not fulfilled for the first non-vanishing matrix elements, and consequently higher multipolar interactions must be considered. In such cases, a difficulty may arise in determining the matrix elements i.e. the transition moments of the higher multipoles, for some of the species studied.

The intermolecular separation R(t) can be expressed in terms of the impact parameter b and the initial relative velocity v as:

$$R(t) = [b^2 + (vt)^2]^{\frac{1}{2}} \qquad (5.7)$$

By substituting the expression 5.7 and 5.5 into 5.2 we obtain the following expression for P_{if}.

$$P_{if} = [(ih)^{-1} aQ_1 Q_2 \int_{-\infty}^{\infty} [b^2 + (vt)^2]^{-n/2} \exp(i\omega_{fi} t)dt]^2 \qquad (5.8)$$

Since R(t) is an even function of t, the Fourier cosine inversion theorem may be applied in the integral of 5.8 and the expression for P_{if} is modified as follows:

$$P_{if} = [\frac{-2}{ih} \cdot a Q_1 Q_2 \int_{o}^{\infty} [b^2 + (vt)^2]^{-n/2} \cos\omega t dt]^2 \qquad (5.9)$$

As it can be shown,[241,242] the integral in 5.9 can be evaluated in terms of modified Bessel functions. Further integration over the impact parameters of the expression relating the transition probability to the cross section σ (5.10), can be carried out in closed form as it has been described by Gait.[61]

$$\sigma = 2\pi \int_{o}^{\infty} P_{if}\, bdb \simeq 2\pi [\int_{o}^{d} P_{if} bdb + \int_{d}^{\infty} P_{if}\, bdb] \qquad (5.10)$$

The final expression for the total cross section then becomes:

$$\sigma_{if}(\omega,v) = \frac{\pi^2}{n-2} (2\frac{Q_1 Q_2}{h})^2 (\frac{\omega}{2})^{n-1} \frac{v^{-n-1} d^{3-n}}{\Gamma^2(n/2)} [2K^2_{\frac{n-1}{2}}(\frac{\omega d}{v}) - K^2_{\frac{n-3}{2}}(\frac{\omega d}{v})] \qquad (5.11)$$

where v is the relative velocity, and $K_{\frac{n-1}{2}}$, $K_{\frac{n-3}{2}}$ modified Bessel functions with argument $\frac{wd}{v}$.

The contribution of the first term of 5.10, corresponding to small impact parameters, has been calculated on the basis of 5.4 and included in 5.11. It is given explicitly by 5.12:

$$\sigma\ (o \leqslant b \leqslant d\ ) = (\frac{2Q_1 Q_2}{h})^2 (\frac{\omega}{2})^{n-1} \frac{v^{-n-1} d^{3-n}}{\Gamma^2(n/2)} K^2_{\frac{n-1}{2}}(\frac{\omega d}{v}) \qquad (5.12)$$

To obtain the thermally averaged cross section, expression 5.11 must be averaged over the Maxwell-Boltzmann velocity distribution as in 5.13

$$\sigma_{if}(\omega,T) = \frac{\int_0^\infty \sigma(\omega,v)f(v)vdv}{\int_0^\infty f(v)vdv} =$$

$$2\left(\frac{\mu}{kT}\right)^2 \int_0^\infty \sigma_{if}(\omega,v)v^3 \exp\left(\frac{-\mu}{2kT}\right)^2 dv \qquad (5.13)$$

where μ is the reduced mass of the system. To achieve this, the asymptotic expansion of the modified Bessel functions, given by 5.14, is introduced.[241]

$$K_y(Z) = \left(\frac{\pi}{2Z}\right)^{\frac{1}{2}} \exp(-Z) \sum_{s=0}^{\infty} \frac{(\nu,s)}{(2Z)^s} \qquad (5.14)$$

where $Z = \frac{\omega d}{v}$

(ν,s) is the Hankel's symbol defined by $(\nu,o) = 1$ and if $s = 1,2,3..$

$$(\nu,s) = \frac{\Gamma(\nu + \frac{1}{2} + s)}{s!\,\Gamma(\nu + \frac{1}{2} - s)} = \frac{2^{-2s}}{s!}\left[(4\nu^2-1)(4\nu^2-3^2)\ldots\{4\nu^2-(2^s-1)^2\}\right]$$

This expansion is valid[243] for arguments $|Z| >> \nu$ and $|Z| >> 1$, a condition fulfilled in all the systems studied in this work. The integration over the Maxwell-Boltzmann velocity distribution was carried out numerically as it is described in Appendix III.

The cross section given by 5.13 is a sensible parameter to use in obtaining the magnitude of the isotope effect, especially for light isotopomers like H_2 and D_2. However, since the experimentally determined parameter of the deactivation efficiency is a rate constant, expression 5.13 is not very useful for direct comparisons with the experimental data. Furthermore, when the latter describe the temperature behaviour of the quenching process, comparison of $\sigma(\omega,T)$ with the cross section obtained by the approximation $\sigma = \frac{k}{\bar{v}}$, where k is the experimental rate constant and $\bar{v}$ the average relative velocity at each temperature, is erroneous,

since this approximation is based on the assumption that σ is temperature independent. Theoretical rate constants $k_{if}(T)$ have been obtained by using 5.13 and 5.15:

$$k_{if}(T) = 4\pi\left(\frac{\mu}{2\pi kT}\right)^{3/2} \int_0^\infty \sigma_{if}(\omega,v)v^3 \exp(\frac{-\mu}{2\pi kT})\, dv \qquad (5.15)$$

Finally, expressions for the total cross section or rate constant, which may be compared with the experimental data, are obtained by summation of 5.13 and 5.15 over the initial states i and weighting by the corresponding population $n_i(T)$ as in 5.16 and 5.17.

$$\sigma = \sum_i \sigma_{if}\, n_i\,(T) \qquad (5.16)$$

$$k = \sum_i k_{if}\, n_i\,(T) \qquad (5.17)$$

It should be noted here that implicit with the semiclassical formulation used in this work are the following assumptions:

(i) The deBroglie wavelength $\lambda = h/\mu v$ is small in comparison with d. Considering that typical values for the systems studied here are $\mu \sim 10^{-23}$ gm, $v \sim 10^5$ cm s^{-1} and $d \sim 3\times10^{-8}$ cm, the wavelength is typically $\sim 6\times10^{-9}$ cm and this condition is fulfilled.

(ii) The energy mismatch ΔE, (cf. 5.1), is small compared with the relative kinetic energy of the system at infinite separation. In the present work, the energy discrepancies are in most cases smaller than 130 cm^{-1} and this assumption holds especially at room or higher temperatures.

(iii) The transition probability is small compared with unity. Typical transition probabilities found here are 10^{-3} - 10^{-4}.

(iv) The interaction energy is small compared with the translational kinetic energy at infinite separations. This condition ensures the validity of straight line trajectories and may impose severe limitations at small R(t), in systems where atoms with relatively high quadrupole moments, and molecules with appreciable dipole or quadrupole moments, are

involved.

D) PARAMETERS USED IN THE COMPUTATION

As expressions 5.13 and 5.14 reveal, the following non-adjustable parameters must be determined for the present calculations, characterizing each particular system:

(1) The energy mismatch ΔE, which determines the frequency factor ω.

(2) The matrix elements Q_1 and Q_2 for the atomic and molecular transitions respectively.

(3) The hard sphere collision diameter d.

(4) The value of n depending on the type of coupling used (cf. Table 5.I)

(5) The temperature T, at which process 5.1 occurs.

(6) The reduced mass μ of the system.

(7) The initial state population.

In this section, we make some general remarks concerning some of the above parameters.

(1) Energy mismatch

The energy mismatch ΔE, which determines the possible channels of quenching, is evaluated on the basis of 5.1 by comparing the energy corresponding to the atomic transition with the rovibrational transitions of the quenching molecule.* Energy mismatches up to 150 cm^{-1} have been considered. The relative contribution of a large ΔE to the rate constant depends mainly on n, i.e. the multipolar coupling used. As explained in section B, higher terms allow for larger ΔE. For similar reasons, increase in temperature allows also for larger ΔE by shortening the duration of the collision. As it can be deduced from 5.13, there is a range of ω, which may result in larger cross sections than the most resonant channels. This is due to the factor $(\omega/2)^{n-1}$ appearing in 5.12.

* The rovibrational energy differences for the hydrogen halides were computed as described in Appendix II. For the hydrogen isotopes energy differences has been computed by French.[266]

The characteristics of the dependence of the cross section on the energy mismatch are shown in Figure 5.1 for a hypothetical process having ΔE as an independent variable. The decrease of σ by more than two orders of magnitude for $\Delta E > 150$ cm^{-1} justifies the choice of this limiting value in determining the quenching channels.

In determining the possible quenching channels, the selection rules for electric multipoles were considered. Thus, a check was provided for the possible existence of "selection rules" in the quenching process.

(2) Matrix elements

The matrix elements for the atomic transitions have been obtained by using tabulated values of the Einstein coefficient Aq in 5.18,

$$|Q_1|^2 = \frac{5(2J+1)h\lambda^5 Aq}{32\pi^6} = (2J+1)\lambda^5 Aq \times 1.0769 \times 10^{-30} \text{esu}^2\text{cm}^4 \quad (5.18)$$

where λ is the wavelength of the atomic transition in cm, and $2J + 1$ the degeneracy of the initial excited state. Matrix elements for the atomic transitions relevant to this work are contained in Table 5.II. If not otherwise indicated, the values of Aq are those given by Garstang.[244]

The matrix elements for the molecular transitions have either been used directly from existing data in the literature or estimated, leading to very approximate results. Table 5.III contains matrix elements for molecular transitions involved in the present calculations. Information about the estimated matrix elements will be given together with the discussion of each specific system. Here, we note that the only accurate data which exist in the literature[245,246] for each particular rovibrational transition is those for H_2, HD and D_2. For molecules like H_2O, for which tabulated line strengths exist,[210] matrix elements were calculated by using the formula which relates them to the corresponding integrated intensity, resulting in an "effective" matrix element.[174] For some molecules like HF, the existing matrix elements refer to vibrational transitions only, without

Fig.5.1: Cross section, (σ), as a function of energy mismatch, (ΔE), for a hypothetical process involving q-q (solid lines) and d-q (dashed line) coupling.

Data

	q-q	d-q
Q_1	5×10^{-26} esu cm^2	5×10^{-26} esu cm^2
Q_2	1×10^{-27} esu cm^2	2.5×10^{-20} esu cm
n	5	4
d	4×10^{-8} cm	4×10^{-8} cm
T	300, 400 K	300 K
μ	3×10^{-24} gm	3×10^{-24} gm

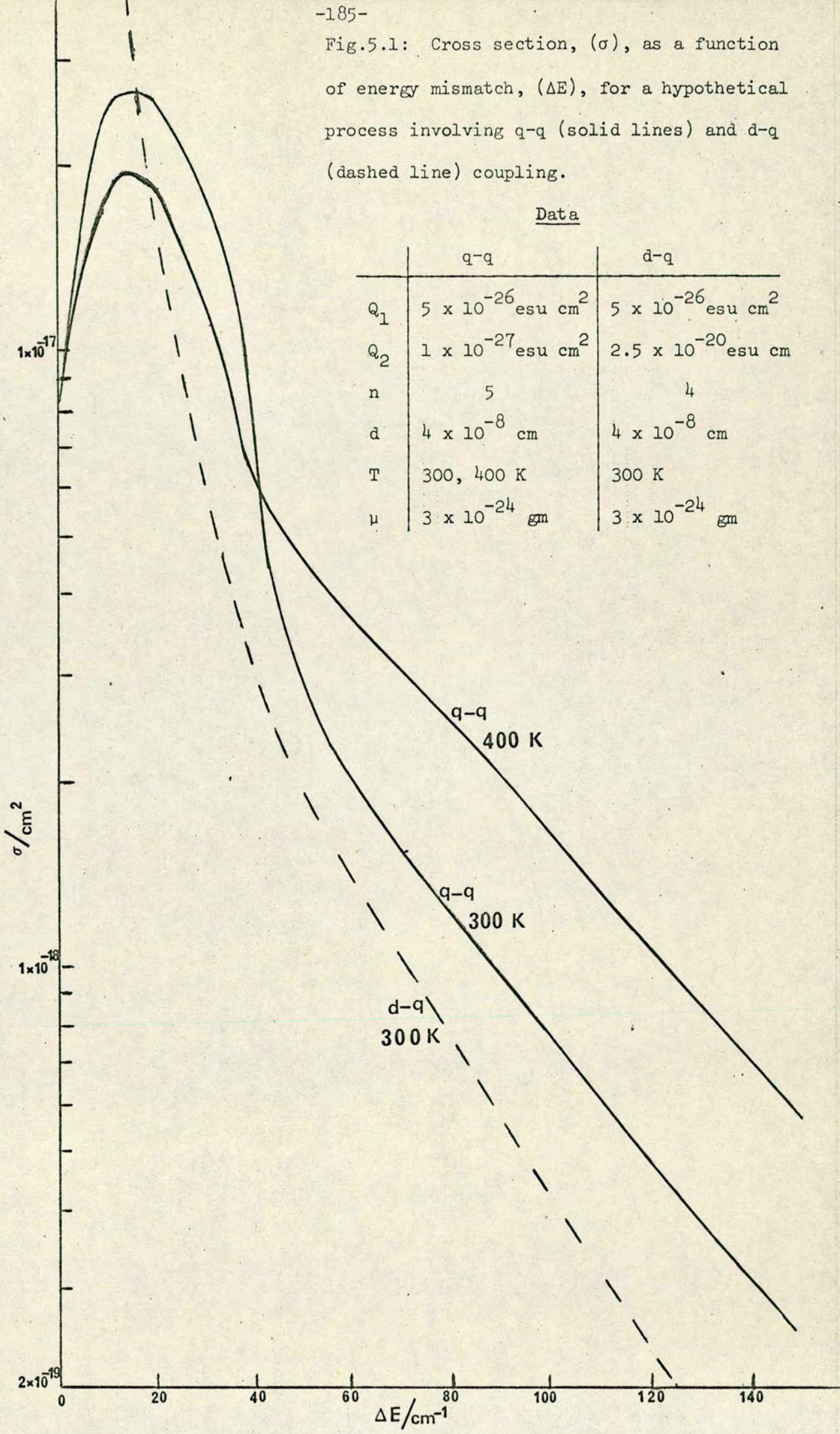

TABLE 5.II

Quadrupole matrix elements $(Q_1)^2$ for atomic transitions

Atom	Transition	Energy (cm^{-1})	$(Q_1)^2 \times 10^{51}$ ($esu^2\ cm^4$)
Br	$4(^2P_{\frac{1}{2}} \rightarrow {}^2P_{3/2})$	3685	2.63
I	$5(^2P_{\frac{1}{2}} \rightarrow {}^2P_{3/2})$	7603	4.66
Sb	$5(^2D_{3/2} \rightarrow {}^4S_{3/2})$	8512	0.72
Sb	$5(^2D_{5/2} \rightarrow {}^4S_{3/2})$	9854	1.53
Sb	$5(^2D_{5/2} \rightarrow {}^2D_{3/2})$	1342	4.75
Te	$5(^3P_o \rightarrow {}^3P_2)$	4707	3.40
Te	$5(^3P_o \rightarrow {}^3P_1)$	44	0.00
Te	$5(^3P_1 \rightarrow {}^3P_2)$	4751	5.87
Sn	$5(^3P_2 \rightarrow {}^3P_o)$	3428	6.71
Sn	$5(^3P_2 \rightarrow {}^3P_1)$	1743	12.41
Sn	$5(^3P_1 \rightarrow {}^3P_o)$	1694	0.00
Bi	$6(^2D_{3/2} \rightarrow {}^4D_{3/2})$	11419	4.66
Bi	$6(^2D_{5/2} \rightarrow {}^4D_{3/2})$	4019	2.46
Bi	$6(^2D_{5/2} \rightarrow {}^4S_{3/2})$	15438	11.80
Pb[a]	$6(^3P_2 \rightarrow {}^3P_1)$	2831	1.85
Pb	$6(^3P_2 \rightarrow {}^3P_o)$	10650	8.25
Pb	$6(^3P_1 \rightarrow {}^3P_o)$	7819	0.00
Tl	$6(^2P_{3/2} \rightarrow {}^2P_{\frac{1}{2}})$	7793	6.51

a) E. Gerjuoy, Phys.Rev. 60, 233, (1941).

TABLE 5.III

Molecular matrix elements

a) Vibrational matrix elements for hydrogen halides.

	$(Q_2)^2 \times 10^{40}$ dipole ($esu^2\ cm^2$)	$(Q_2)^2 \times 10^{57}$ quadrupole ($esu^2\ cm^4$)	$(Q_2)^2 \times 10^{91}$ hexadecapole ($esu^2\ cm^2$)	Ref.
HF (0 → 1)	97.02			247,248
HF (0 → 2)	1.57			247,248
HCl(0 → 3)	0.00265	∿2.0	∿6.5 [a]	249,250
HBr(0 → 3)		∿2.3		250
HI (0 → 2)			∿270 [a]	
HI (0 → 4)			∿0.2 [a]	

a Estimated.

TABLE 5.III

Molecular matrix elements

b) Quadrupole matrix elements for H_2, HD, D_2 (Ref. 245,246).

		H_2 $(Q_2)^2 \times 10^{56}$ ($esu^2\ cm^4$)			HD $(Q_2)^2 \times 10^{56}$ ($esu^2 \times cm^4$)			D_2 $(Q_2)^2 \times 10^{56}$ ($esu^2\ cm^4$)		
v'' → v'	J	O(J)	Q(J)	S(J)	O(J)	Q(J)	S(J)	O(J)	Q(J)	S(J)
0 → 0	6			4531						
	9						4765			
0 → 1	0		139.7	110.3		121.0				
	1		140.0	94.0		121.2	86.5			75.5
	2	172.6	140.7	78.5	145.2	121.5	74.4	124.5		67.3
	3	196.8	141.3	64.7		121.9		125.8		59.6
	4	222.9	142.0	52.2						52.3
	5									
	6	∿252								
	8									∿31
	9						∿26			
0 → 2	0			2.46						
	1			2.53			1.79			
	2	2.03					1.84			
	3	2.00								
	6		∿3.2							
	7		∿3.4							
	9								∿0.8	
0 → 3	2	0.026						0.010		
	5	∿0.009							∿0.034	
	7							∿0.005		
0 → 4	0									0.0008

including rotation. The rovibrational matrix elements have been calculated using appropriate formulas [247] for each initial state, characterised by a quantum number J, and type of transition.

(3) Hard sphere collision diameter

The long range interactions, which are usually considered in first order approximation, act over a longer range than those believed responsible for drastically altering the trajectory in a molecular collision, thus justifying the use of straight line trajectories for large impact parameters. The hard sphere collision diameter d, obtained usually from viscocity and diffusion measurements, is the minimum value of impact parameter for which the straight line trajectory approximation is assumed to be valid;* for smaller impact parameters one makes the assumption discussed in section C. As Sharma and Kern have pointed out,[82] this procedure is justifiable only when a substantial fraction of the cross section arises from trajectories for which the impact parameter is larger than d. This fraction can be as small as $\sim$ 30% for first order approximation. In the present work, results were obtained for both $b > d$ and $b \leq d$, so that it was possible to evaluate this fraction in general. In all cases, impact parameters larger than d were found to contribute more than 30% to the calculated cross section.

The error introduced due to the uncertainty in the value of d depends on the magnitude of ω. As shown in 5.11, d figures in the argument of the

* In such a case and for small ΔE, the transition probability for $b > d$ can be approximated[82] by 5.19, which specifies how P_{if} depends on the impact parameter.

$$P_{if}(b > d) = (d/b)^n P_{if}(d) \qquad (5.19)$$

Bessel functions $K_n(^{\omega d}/_v)$ and thus, apart from the absolute value of the rate constants, it can also affect their temperature dependence. However, the error introduced was found to be weakly temperature dependent. Discrepancies in the value of d arise mainly from the various estimations of the atomic radii. These can be considerable, as a comparison of Van der Waals atomic radii with root mean square radii calculated for the outer electron configurations shows (Table 5.IV). In general the uncertainty in d is difficult to estimate. In this work results have been obtained for different values of d for the sake of comparison. However, those based on Van der Waals radii are considered more reliable, since they represent the physical model better. Support for this is provided by a recent work of Chow Chiu,[252] in which the interaction potential is integrated over the entire range of internuclear separations and d is treated as an adjustable parameter. The d values thus determined are, within ~15%, equal to those obtained on the basis of Van der Waals data.

E) RESULTS AND DISCUSSION

Conclusions concerning the importance of the present model in the electronic relaxation of atoms by small molecules may be drawn in the following ways:

(i) By comparing the calculated cross sections or rate constants at a certain temperature to those determined experimentally at the same temperature. Conclusions drawn in this way are only tentative because of the approximations used in the theoretical treatment and the uncertainty in the parameters used for some of the studied systems. In general, a

TABLE 5.IV

Data for atomic and molecular radii*

a) Atomic radii, $\frac{d_1}{2}$

Atom	Van der Waals $\frac{d_1}{2}$ Ref. 254	Root mean square $\frac{d_1}{2}$		
		Ref. 176	Ref. 253	Ref. 254
	(cm x 10^8)	(cmx10^8)	(cmx10^8)	(cmx10^8)
I	2.15	1.35	1.41	
Br	1.95	1.13	1.21	
Tl		1.71	1.99	
Sn		1.58	1.82	
Pb		1.75	1.77	1.95
Sb	2.2	1.61	1.65	
Te	2.2	1.45	1.52	1.53
Bi		1.82	1.70	

b) Molecular radii, $\frac{d_2}{2}$

Molecule	$\frac{d_2}{2}$ cm x 10^8	References
H_2, HD, D_2	1.48, 1.51, 1.46	234, 255, 256
HF	1.30	234
HCl	1.65_5	234
HBr	1.70_5	234
H_2O	1.36, 1.44, 1.13	234,257

* The hard sphere collision diameter is: $d = \frac{d_1 + d_2}{2}$

discrepancy, between the experimental and theoretical results, of less than a factor of ten should be considered as indicative of the importance of the multipolar interactions.

(ii) Comparison of the calculated temperature behavior of the rate constants to experimental data. Conclusions drawn in this way are more reliable concerning the importance of the present model than those based on (i). The calculations should predict the temperature dependence of the rate constants even if they do not reproduce their actual magnitude. As expression 5.17 shows, the overall temperature behavior will be determined by two factors: First the temperature dependence of k_{if} for each particular channel $i \rightarrow f$ and second, the change of the initial state i population as a function of temperature.

(iii) Since the primary motivation for this work was the interpretation of the large isotope effects, the results of the present calculations should be consistent with the observed isotope effect.

In general, assuming that the long range interactions model is applicable in the studied systems,, the present calculations reveal basic trends of the efficiency of $E \rightarrow V$ energy transfer, as a function of energy discrepancy, multipolar interaction and rovibrational transition involved. In this context, they can be helpful in clarifying proposals made for the deactivation of excited atoms by small molecules.

Results will be presented in two parts. In the first part the results refering to the quenching of $Br(4^2P_{\frac{1}{2}})$ and $I(5^2P_{\frac{1}{2}})$ by several small molecules will be discussed. Some of these results are directly related to experimental data obtained in this work (cf. Chapters 4,6). In the second part, the quenching of $Te(5^3P_{1,0})$, $Pb(6^3P_2)$, $Tl(6^2P_{3/2})$, $Sb(5^2D_{3/2})$, $Sn(5^3D_2)$ and $Bi(6^2D_{5/2})$ by hydrogen isotopomers will be examined.

1) Quenching of excited halogen atoms :

i) $Br(4^2P_{\frac{1}{2}})$, $I(5^2P_{\frac{1}{2}})$ + Hydrogen Halides.

In Chapter 4, $E \rightarrow V$ energy transfer in systems involving excited

halogen atoms and hydrogen halides was explained in terms of non-adiabatic transitions between the vibronic surfaces correlating with the ground and excited atomic states. However, the importance of near resonant adiabatic transitions due to long range forces was not ruled out, at least for some of the systems. The present calculations provide one further test for the importance of this mechanism.

Calculated rate constants, k_{calc}, for the quenching $Br(4^2P_{\frac{1}{2}})$ and $I(5^2P_{\frac{1}{2}})$ by hydrogen halides are given in Table 5.V. These rate constants have been calculated on the basis of 5.14 and therefore represent a summation over the rate constants k_i for each particular near resonant channel $(v''=n, J''=k) \rightarrow (v'=m, J'=l)$, denoted in Table 5.V by $(n,k) \rightarrow (m,l)$. Values of k_i for each of the most important channels, along with the percentage of the initial state population determined effectively by the population of the rotational states involved, are also included in Table 5.V.

As a comparison of k_{calc} to experimentally obtained rate constants, k_{exp}, indicates, for systems involving HF there is an excellent agreement between the experimental results and the theoretical predictions. It has already been mentioned, (c.f. Chapters 1 and 4), that there is ample direct experimental evidence[200,128] for the importance of process 5.20 in the deactivation of $Br(4^2P_{\frac{1}{2}})$ by HF.

$$Br(4^2P_{\frac{1}{2}}) + HF(v''=o, J''=6) \rightarrow Br(4^2P_{3/2}) + HF(v'=1, J'=5) \quad \Delta E = 9cm^{-1} \qquad (5.20)$$

E → V energy transfer from $I(5^2P_{\frac{1}{2}})$ atoms to the v = 2 vibrational state of HF has also been reported.[200] The present calculations, therefore, provide a convincing explanation of the experimental observations. The higher efficiency observed for the quenching of $Br(4^2P_{\frac{1}{2}})$ and $I(5^2P_{\frac{1}{2}})$ by HF than by the rest of hydrogen halides may be rationalised on the basis of the following factors:

(i) For the removal of both $Br(4^2P_{\frac{1}{2}})$ and $I(5^2P_{\frac{1}{2}})$ by HF, there are near resonant channels involving $\Delta J = 1$, in contrast to the other hydrogen

TABLE 5.V

Near resonant quenching of $Br(4^2P_{\frac{1}{2}})$ and $I(5^2P_{\frac{1}{2}})$ by hydrogen halides

System	Channel	ΔE (cm^{-1})	Population (%)	k_i (cm^3 molecules$^{-1}s^{-1}$)	k_{calc} (cm^3molecule$^{-1}s^{-1}$)	k_{exp} (cm^3 molecule$^{-1}s^{-1}$)	Ref.
$Br(4^2P_{\frac{1}{2}})$ +HF	(0,6)→(1,5)	+9	2	3.5×10^{-11}	3.5×10^{-11}	$(3.4 \pm 0.6) \times 10^{-11}$	200
$Br(4^2P_{\frac{1}{2}})$ +HCl	none					$(5.2 \pm 0.4) \times 10^{-12}$	120
$Br(4^2P_{\frac{1}{2}})$ + HBr	none					$(8.4 \pm 0.11) \times 10^{-13}$	120
$Br(4^2P_{\frac{1}{2}})$ + HI	(0,14)→(2,10)	+16	0.15	$\sim 2 \times 10^{-20}$			
	(0,15)→(2,11)	-42	0.06	$\sim 1 \times 10^{-21}$	$\sim 2 \times 10^{-20}$	$(2.5 \pm 1.0) \times 10^{-12}$	198
$I(5^2P_{\frac{1}{2}})$ + HF	(0,2)→(2,1)	+64	23	6.5×10^{-15}			
	(0,3)→(2,2)	+17	20	3.1×10^{-12}			
	(0,4)→(2,3)	-33	12	4.3×10^{-13}	3.5×10^{-12}	$(3 \pm 1) \times 10^{-12}$	199
$I(5^2P_{\frac{1}{2}})$ + HCl	(0,10)→(3,6)	+2	0.5	$\sim 6 \times 10^{-19}$			
	(0,14)→(3,12)	+50	0.005	$\sim 3 \times 10^{-20}$			
	(0,15)→(3,13)	-13	0.001	$\sim 2 \times 10^{-19}$	$\sim 8 \times 10^{-19}$	$(1.5 \pm 0.1) \times 10^{-14}$	this work
$I(5^2P_{\frac{1}{2}})$ + HBr	(0,5)→(3,7)	+18	13	1.8×10^{-16}			
	(0,6)→(3,8)	-4	10	4.1×10^{-14}	4.1×10^{-14}	$(1.3 \pm 0.1) \times 10^{-13}$	this work
$I(5^2P_{\frac{1}{2}})$ + HI	(0,16)→(4,12)	-11	0.03	$\sim 8 \times 10^{-22}$	$\sim 8 \times 10^{-22}$	$(5.2 \pm 0.4) \times 10^{-14}$	this work

halides (cf. Table 5.V). As a consequence, electric dipole vibrational transitions are allowed and d-q coupling is involved. This type of coupling leads to larger transition probabilities for the range of energy mismatches involved than coupling due to shorther range interactions, like q-q or h-q, which are the only possible couplings for hydrogen halides other than HF. The sensitive dependence of rate constants on ΔE in the case of d-q coupling is shown, characteristically, by the k_i values for $I(5^2P_{\frac{1}{2}})$ and HF (cf. Table 5.V Neither the small differences in the rovibrational matrix elements of HF, (cf. Table 5.III), nor the differences in the population of the initial states can account for the calculated k_i values, which are determined solely by the degree of energy mismatch. However, as these results indicate and as can be shown in general by treating ΔE as a variable, contributions from d-q coupling drop by about 2 orders of magnitude for energy discrepancies larger than 50 cm^{-1}. In such a case, higher multipolar interactions may become important.

ii) A second factor, which leads to efficient quenching of $Br(4^2P_{\frac{1}{2}})$ and $I(5^2P_{\frac{1}{2}})$ by HF is the relatively high population of the initial states. On the contrary, for the systems of $I(5^2P_{\frac{1}{2}})$ or $Br(4^2P_{\frac{1}{2}})$ and HCl, HBr and HI, near-resonant channels involving $\Delta J = 1$ and d-q coupling are possibly existent but for rotational states with $J'' > 16$. At room temperature, the populations of these states are negligible and therefore have not been considered. Furthermore, even for channels with $\Delta J = 0$, 2 or 4, due to q-q or h-q coupling, the population of the initial state is very small, (less than 0.5%), with the exception of $I(5^2P_{\frac{1}{2}})$ + HBr.

It should be noted here, that the rate constants calculated for systems in which hexadecapole transitions occur in the hydrogen halide, are very approximate and simply indicate the order of magnitude of the expected contribution of transitions with $\Delta J = \pm 4$ in first order approximation. A rough estimation of the vibrational matrix elements for such transitions has been made on the basis of the hexadecapole transition matrix elements

given[82] for H_2 and the assumption;

$$\frac{(Q_d)_{o \to 1}}{(Q_d)_{o \to v}} \simeq \frac{(Q_n)_{o \to 1}}{(Q_n)_{o \to v}} \qquad (5.21)$$

where $(Q_d)_{o \to 1}$ and $(Q_d)_{o \to v}$ are the dipole matrix elements for the fundamental and overtone $o \to v$ transition, with $v = 2$, 3 or 4. Values of these ratios for the hydrogen halides are given by Penner.[258]

Despite these crude approximations, the very poor agreement obtained between the theoretical and experimental results for $Br(4^2P_{\frac{1}{2}})$ + HI and $I(5^2P_{\frac{1}{2}})$ + HCl or HI clearly indicates a breakdown of the present long range model for these systems. Similarly, near resonant quenching of $Br(4^2P_{\frac{1}{2}})$ by HCl or HBr for $J'' < 16$ would involve $\Delta J > 4$, for which no contribution to the rate constant is expected from long range interactions in first order approximation.

The temperature dependence measurements of the rate constant for the removal of $I(5^2P_{\frac{1}{2}})$ by HBr provides a further test for the importance of long range interactions. As was mentioned in Chapter 4, quenching of $I(5^2P_{\frac{1}{2}})$ by HBr may proceed via channels involving electric dipole or quadrupole transitions in HBr. The present calculations show that processes with $\Delta J = 1$, in which d-q coupling occurs, do not contribute to the quenching rate constant whatsoever. The main reason for this is that they involve energy discrepancies larger than 105 cm^{-1} and therefore the effect of d-q coupling is dramatically decreased. From the nine near resonant channels, which are available for q-q coupling, there is only one channel described by 4, in Chapter 4, which is found to dominate the quenching rate constant (cf. Table 5.V). This is attributed to the very small energy mismatch and the relatively high population this channel involves.

The calculated rate constant at room temperature is found ~ 4 times smaller than the experimental result. This indicates reasonable agreement between

theory and experiment, particularly if one takes into account the uncertainty in the quadrupole matrix element for the o → 3 vibrational transition in HBr. Direct estimations for the fundamental and first overtone quadrupole transition matrix elements of HCl and HBr have been reported by Sharma et. al.[250] Matrix elements for the o → 3 overtone were evaluated by using 5.21 for quadrupole transitions.

Another factor, which possibly affects the discrepancy between k_{calc} and k_{exp} for $I(5^2P_{\frac{1}{2}})$ + HBr is the uncertainty in the value of d. To illustrate this we carried out calculations by using a d value based on data of the atomic radius for the outer electron configuration (cf. Table IV). For $d = 3.0 \times 10^{-8}$ cm instead of $d = 3.85 \times 10^{-8}$ cm, corresponding to the Van der Waals atomic radius, k_{calc} was found within the experimental error of k_{exp}.

The predicted temperature dependence of k_{calc} for $I(5^2P_{\frac{1}{2}})$ + HBr has been included in Chapter 4. As Figure 4.7 shows, the temperature behavior of k_{calc} is comparable to that of k_{exp} for a wide range of temperatures This indicates that quenching of $I(5^2P_{\frac{1}{2}})$ atoms by HBr, as a result of long range interactions, should be examined as a possible removal process. These findings have been discussed in Chapter 4.

ii) $Br(4^2P_{\frac{1}{2}})$, $I(5^2P_{\frac{1}{2}})$ + Hydrogen Isotopes

As shown in Table 5.VI, the calculated rate constants for the quenching of $Br(4^2P_{\frac{1}{2}})$ and $I(5^2P_{\frac{1}{2}})$ atoms by H_2 notably differ from the experimental results. Use of a smaller value of d, based on the radius of iodine atoms for outer electron configuration (cf. Table 5.IV), decreases this discrepancy to about one order of magnitude. Thus for $I(5^2P_{\frac{1}{2}})$ + H_2 and for $d = 2.89 \times 10^{-8}$cm instead of $d = 3.61 \times 10^{-8}$ cm used for the result given in Table 5.VI, we obtain: $k_{calc} = 1.3 \times 10^{-14}$ cm^3 $molecule^{-1}s^{-1}$.

However, data obtained for the interaction potential of ground state

TABLE 5.VI

Collisional deactivation of $Br(4^2P_{\frac{1}{2}})$ and $I(5^2P_{\frac{1}{2}})$ by Hydrogen Isotopes

System	Channel	ΔE (cm^{-1})	Population (%)	k_i (cm^3 molecule$^{-1}s^{-1}$)	k_{calc} (cm^3 molecule$^{-1}s^{-1}$)	k_{exp} (cm^3 molecule$^{-1}s^{-1}$)	Ref.
$Br(4^2P_{\frac{1}{2}}) + H_2$	(0,2)→(1,0)	±122	12	1.1×10^{-13}			
	(0,3)→(1,1)	-117	9	1.0×10^{-13}	2.1×10^{-13}	4.7×10^{-12}	1
$Br(4^2P_{\frac{1}{2}})$+HD	(0,0)→(1,0)	-53	20	2.0×10^{-12}			
	(0,1)→(1,1)	-57	39	3.3×10^{-12}			
	(0,2)→(1,2)	-64	28	1.8×10^{-12}			
	(0,3)→(1,3)	-76	11	6.1×10^{-14}			
	(0,0)→(1,1)	+32	20	2.3×10^{-17}			
	(0,2)→(1,3)	+89	28	3.1×10^{-19}	7.1×10^{-12}	$(3.6 \pm 0.5) \times 10^{-11}$	259
$Br(4^2P_{\frac{1}{2}}) + D_2$	(0,4)→(1,6)	-78	9	4.0×10^{-12}			
	(0,5)→(1,7)	+27	2	1.3×10^{-13}	1.3×10^{-12}	5.7×10^{-12}	1
$I(5^2P_{\frac{1}{2}})+H_2$	(0,2)→(2,0)	+129	12	1.2×10^{-15}			
	(0,3)→(2,1)	-115	9	1.2×10^{-15}	2.4×10^{-15}	$(1.1 \pm 0.1) \times 10^{-13}$	64
$I(5^2P_{\frac{1}{2}})$ + HD	(0,1)→(2,3)	-119	39	2.2×10^{-16}			
	(0,2)→(2,4)	+24	28	1.7×10^{-13}			
	(0,8)→(2,9)	-111	0.02	2.6×10^{-21}	1.7×10^{-13}	$(3.2 \pm 0.3) \times 10^{-13}$	64
$I(5^2P_{\frac{1}{2}})$ +D_2	(0,5)→(2,9)	-129	1.4	$\sim 4 \times 10^{-20}$	$\sim 4 \times 10^{-20}$	$(1.0 \pm 0.1) \times 10^{-15}$	64

iodine atoms and H_2 in molecular beam experiments[256] suggest that the Van der Waals atomic radius, i.e the latter value of d, must be used.

Experiments have shown[62] a strongly positive temperature dependence of k_{exp} in the range 180-410K. The Arrhenius parameters were found: $E_a = (+7.2 \pm 0.8)$ kJ mole^{-1} and $A = (2.2 \pm 0.6) \times 10^{-12}$ cm^3 molecule^{-1}s^{-1}. Calculation of k_{calc} at different temperatures, in the same temperature range also resulted in a positive temperature dependence, although much stronger. The theoretical Arrhenius parameters were determined as:

$$E_a = (+14.9 \pm 0.2) \text{ kJ mole}^{-1} \text{ and } A = (8.8 \pm 0.7) \times 10^{-13} \text{ cm}^3 \text{ molecule}^{-1}\text{s}^{-1}$$

The only near resonant channel for quenching of $I(5^2P_{\frac{1}{2}})$ by D_2 involves hexadecapole transitions in the latter and, therefore, a rough value was obtained for k_{calc}. However, since k_{calc} was found to be smaller than k_{exp} by about five orders of magnitude, the present calculations strongly indicate that a mechanism based on long range forces is not important for the quenching process. In sharp contrast, quenching of $Br(4^2P_{\frac{1}{2}})$ by D_2 is very efficient, (c.f. Table 5.VI) and the calculated result is in relatively good agreement with the experimental data.*

Quenching of both $I(5^2P_{\frac{1}{2}})$ and $Br(4^2P_{\frac{1}{2}})$ atoms by HD is found to take place more efficiently than for H_2 or D_2. The calculations reproduce these experimental results for both atoms. Table 5.VI shows that quenching of

* In a recent experimental work[259] the decay rate constants for $Br(4^2P_{\frac{1}{2}})$ + H_2 and D_2 were: $k_{H_2} = (1.8 \pm 0.2) \times 10^{-11}$ cm^3 molecule^{-1}s^{-1} and $k_{D_2} = (1.8 \pm 0.2) \times 10^{-12}$ cm^3 molecule^{-1}s^{-1}. The reasons for the great discrepancy between the results quoted in Table 5.VI have not as yet been satisfactorily explained. If these recent data will be adopted, k_{calc} for D_2 is in excellent agreement with k_{exp}, but the calculations do not reproduce the observed isotope effect.

$I(5^2P_{\frac{1}{2}})$ by HD occurs via one of the proposed[64] channels predominately;

$$I(5^2P_{\frac{1}{2}}) + HD(v''=o,\ J''=2) \rightarrow I(5^2P_{2/3}) + HD(v'=2,\ J'=4) \quad \Delta E = +24\ cm^{-1} \qquad (5.22)$$

This is attributed to the small energy discrepancy of process 5.22. For $Br(4^2P_{\frac{1}{2}})$ + HD there are three main channels which determine the rate constant. In both systems, q-q are more important than d-q interactions, even for small energy mismatches. This may be understood in terms of the weak dipole transitions in HD.

The present calculations indicate that long range interactions can account for the removal of $I(5^2P_{\frac{1}{2}})$ and $Br(4^2P_{\frac{1}{2}})$ by HD. However, temperature dependence data for the rate constants are necessary, to obtain more conclusive evidence. The temperature dependence of k_{calc} for $I(5^2P_{\frac{1}{2}})$ + HD is shown in Figure 5.2.

Calculated cross sections, σ_{calc}, and the corresponding experimental thermal cross sections σ_{exp} at room temperature are included in Table 5.VII. These data show that the calculations reproduce the observed trends of the isotope effects satisfactorily:

$$\sigma_{HD} > \sigma_{H_2} \gg \sigma_{D_2} \text{ for } I(5^2P_{\frac{1}{2}})$$

and $$\sigma_{HD} > \sigma_{D_2} > \sigma_{H_2} \text{ for } Br(5^2P_{\frac{1}{2}})^*$$

However, the isotopic ratios are in error particularly when they involve the less efficient isotopomer. In such a case, the net effect of the calculations is to overestimate seriously the isotope effect. This strongly suggests the interference of another quenching mechanism than the one described here, for the less efficient isotope.

The efficiency of quenching of excited halogen atoms by hydrogen isotopes has been examined by several authors[40,41,102] (cf. Chapter 1). Calculations in systems relevant to the present work have been carried out by Zimmerman and George. In a series of papers[100-103] they determined the probabilities of non-adiabatic transitions leading to the quenching of

*We should note that if the experimental data of reference 259 are valid this trend is incorrect for H_2 and D_2.

Fig. 5.2: $I(5^2P_{\frac{1}{2}})$ + HD: Calculated rate constant, k_{24}, without considering the effect of the initial state (J = 2) population and k_{calc} as a function of temperature.

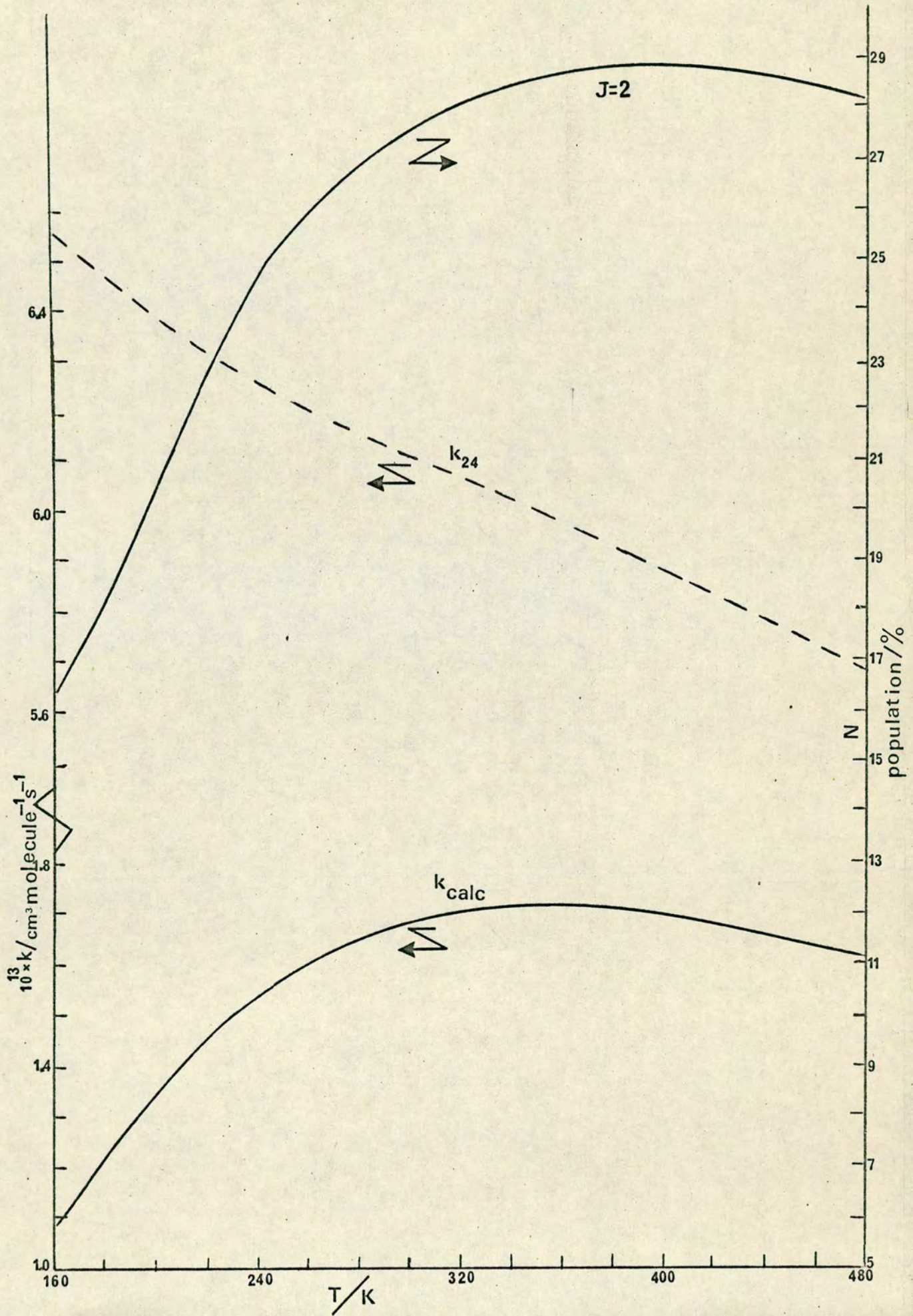

TABLE 5.VII

Calculated, σ_{calc}, and experimental average, σ_{exp}, cross sections at room temperature, for the quenching of excited atoms by hydrogen isotopes.

System	σ^{*}_{calc} (cm^2)	σ^{**}_{exp} (cm^2)
$I(5^2P_{\frac{1}{2}}) + H_2$	6.4×10^{-21}	7.4×10^{-19}
" + HD	5.8×10^{-19}	2.1×10^{-18}
" + D_2	$\sim 3 \times 10^{-25}$	8.0×10^{-21}
$Br(4^2P_{\frac{1}{2}}) + H_2$	6.0×10^{-19}	2.6×10^{-17}
" + HD	4.7×10^{-17}	2.4×10^{-16}
" + D_2	2.8×10^{-17}	4.4×10^{-17}
$Te(5^3P_{0,1}) + H_2$	8.7×10^{-17}	5.8×10^{-17}
" + D_2	$\sim 1 \times 10^{-20}$	6.9×10^{-20}
$Bi(6^2D_{5/2}) + H_2$	1.5×10^{-18}	3.1×10^{-17}
" D_2	1.3×10^{-20}	1.9×10^{-18}
$Sb(5^2D_{3/2}) + H_2$	7.4×10^{-21}	3.7×10^{-17}
" + D_2	3.5×10^{-22}	1.3×10^{-16}
$Sn(5^3P_2) + H_2$	$\sim 7 \times 10^{-20}$	6.4×10^{-18}
" + HD	2.6×10^{-17}	3.7×10^{-17}
" + D_2	4.4×10^{-17}	1.3×10^{-16}
$Pb(6^3P_2) + H_2$	1.2×10^{-20}	9.0×10^{-18}
" + D_2	8.8×10^{-17}	6.8×10^{-17}
$Tl(6^2P_{3/2}) + H_2$	8.2×10^{-20}	2.8×10^{-18}
" + D_2	1.5×10^{-23}	3.9×10^{-19}

* From 5.16

** $\sigma_{exp} = \frac{k_{exp}}{v}$, where v is the average velocity.

$Br(4^2P_{\frac{1}{2}})$ or $I(5^2P_{\frac{1}{2}})$ atoms by hydrogen isotopes by utilizing the quantum mechanical coupled channel technique[100-101] for collinear collisions. The potential surfaces used were obtained in the diatomics-in-molecules (DIM) formulation.[102] In a more recent work they modified their model to include molecular rotation. The corresponding three-dimensional cross sections as well as one-dimensional quenching probabilities for $Br(4^2P_{\frac{1}{2}}) + H_2$, HD and D_2 were integrated over the distribution of collision energies by Wiesenfeld. The results are included in Table 5.VIII.

The above theoretical approach argues in favour of a resonant exchange of energy between electronic and vibrational degrees of freedom, when one vibrational quantum is excited, although the characteristics of the potential causing this effect have not been conclusively identified. Thus, a large isotope effect is predicted for $Br(4^2P_{\frac{1}{2}}) + H_2$, HD and D_2. For multivibrational transitions, however, resonance effects are found weak. It is not clear therefore how the large isotope effect observed for $I(5^2P_{\frac{1}{2}})$ + H_2, HD and D_2 can be justified on the basis of this model. Furthermore, the calculations underestimate the cross sections seriously, especially when carried out in three dimensions (cf. Table 5.VIII). We therefore believe, that the approach used in the present work, although very approximate, provides a better understanding of the decay of $Br(4^2P_{\frac{1}{2}})$ and $I(5^2P_{\frac{1}{2}})$ in the presence of hydrogen isotopes.

In a recent theoretical study,[96] French and Lawley obtained rate constants for transitions induced in some heavy atoms by hydrogen isotopes. As Table 5.VIII shows, their results are in a very good agreement with those obtained here, although different formulations were used for the long range

TABLE 5.VIII

Comparison of the rate constants calculated in this and other works

System	k_{calc} (This work) ($cm^3 molecule^{-1} s^{-1}$)	k_{calc} (Ref. 96) ($cm^3 molecule^{-1} s^{-1}$)	k_{calc} ($cm^3 molecule^{-1} s^{-1}$)	k_{exp} ($cm^3 molecule^{-1} s^{-1}$)
$I(5^2P_{\frac{1}{2}}) + H_2$	2.4×10^{-15}	4.2×10^{-15}		1.1×10^{-13}
$I(5^2P_{\frac{1}{2}}) + HD$	1.7×10^{-13}	1.5×10^{-13}		3.2×10^{-13}
$I(5^2P_{\frac{1}{2}}) + D_2$	$\sim 4 \times 10^{-20}$	2.1×10^{-20}		1.0×10^{-15}
$Te(5^2P_{0,1}) + H_2$	1.7×10^{-11}	1.8×10^{-11}	5×10^{-9} (a)	1.04×10^{-11}
$Te(5^2P_{0,1}) + D_2$	$\sim 2 \times 10^{-16}$	2×10^{-16}		8.8×10^{-15}
$Pb(6^3P_2) + H_2$	2.2×10^{-15}	3.4×10^{-16}		1.5×10^{-12}
$Pb(6^3P_2) + D_2$	1.0×10^{-11}	3×10^{-12}	1×10^{-10} (a)	7.7×10^{-12}
$Tl(6^2P_{3/2}) + H_2$	4.3×10^{-14}	1.2×10^{-15}		4.9×10^{-13}
$Tl(6^2P_{3/2}) + D_2$	1.9×10^{-18}	1.6×10^{-20}		4.3×10^{-14}
$Br(4^2P_{\frac{1}{2}}) + H_2$	2.1×10^{-13}		3×10^{-15} (b)	4.7×10^{-12}
$Br(4^2P_{\frac{1}{2}}) + HD$	7.1×10^{-12}		2.5×10^{-13} (b)	3.6×10^{-11}
$Br(4^2P_{\frac{1}{2}}) + D_2$	1.3×10^{-12}		4×10^{-16} (b)	5.7×10^{-12}

(a) Ref. 95 (b) Ref. 259

interaction model. In the same work it is shown that when long range interactions are found unimportant, the most likely effect accounting for efficient quenching is a short range coupling. This is particularly interesting in explaining the decay efficiency in systems like $I(5^2P_{\frac{1}{2}})$ + H_2, where k_{calc} is appreciably smaller than k_{exp}.

2) Quenching of excited heavy atoms of groups III-VI by Hydrogen Isotopes

i) $Te(5^3P_{o,1}) + H_2, D_2$

The energy separation of the two first excited states of tellurium atoms, $Te(5^3P_o)$ and $Te(5^3P_1)$, is only 44 cm^{-1} and as has been observed, a rapid equilibrium is established between these two states.[66] In consequence, quenching rate constants refer to the quenching of both states, which are denoted as $Te(5^3P_{1,o})$. Assuming therefore that the relative population of the excited atomic states is determined by a Boltzmann distribution, the k_{calc} value shown in Table 5.IX is a weighted average of rate constants calculated for each atomic state. Due to the Boltzmann factor, quenching of $Te(5^3P_1)$ is predicted to be more efficient than that of $Te(5^3P_o)$. Thus, for quenching by H_2, $k_{calc}(^3P_1) = 9.8 \times 10^{-12}$ cm^3 $molecule^{-1}s^{-1}$ vs. $k_{calc}(^3P_o) = 6.8 \times 10^{-12} cm^3$ $molecule^{-1}s^{-1}$, although the $^3P_1$ state involves a larger energy discrepancy, ($\Delta E = +38$ cm^{-1} vs. $\Delta E = -6$ cm^{-1} for ^3P_o).

As shown in Tables 5.VIII and 5.IX, the results obtained in this work are in excellent agreement with those obtained by French and Lawley.[96] In addition the result for $Te(5^3P_{1,o}) + H_2$ accords well with the experimental data[66], in contrast to the calculations carried out for the latter system by Ewing,[95] which overestimated the quenching rate constant appreciably.

There are several factors, which can account for the observed discrepancy in the latter case: First, the approximations used in the formulation described by Ewing lead to a reduced sensitivity of the calculated cross

TABLE 5.IX

Quenching of $Te(5^3P_{0,1})$ by H_2 and D_2

System	Channel	ΔE (cm^{-1})	Population %	k_i ($cm^3 molecule^{-1} s^{-1}$)	k_{calc} ($cm^3 molecule^{-1} s^{-1}$)	k_{exp} ($cm^3 molecule^{-1} s^{-1}$)	Ref.
$Te(5^3P_1) + H_2$	(0,1) → (1,3)	-38	66	9.8×10^{-12}			
$Te(5^3P_0) + H_2$	(0,1) → (1,3)	+6	66	6.8×10^{-12}	1.7×10^{-11}	$(1.04 \pm 0.15) \times 10^{-11}$	66
$Te(5^3P_{0,1}) + D_2$	(0,9) → (2,7)	+17,-27	0.0006	6.4×10^{-18}			
	(0,5) → (1,9)	-58,-14	1.4	$\sim 2 \times 10^{-16}$	$\sim 2 \times 10^{-16}$	$(8.8 \pm 6.5) \times 10^{-15}$	66

section as a function of ΔE. Secondly, the matrix elements used for the quadrupole transition in H_2 correspond to an average over the whole S band. Thirdly, and most important, the hard sphere collision diameter used by Ewing has not been derived on the basis of the Van der Waals atomic radius, as in this work, but from data for the outer electron atomic configuration. As a result a small and non-realistic value for d has been used, resulting in an overestimation of the cross section. We should note, however, that the trends found for the temperature dependence of the rate constant here and in Ewing's work were in very good agreement. A slightly negative temperature dependence is predicted for temperatures higher than $\sim$180 K and an experimental verification of this would provide conclusive evidence of the importance of q-q coupling in the quenching of $Te(5\ P_{1,0})$ by H_2.

In contrast to $Te(5\ P_{1,0}) + H_2$, removal of $Te(5\ P_{1,0})$ by D_2 via q-q coupling is negligible, due to the small initial state population involved in the latter system, (cf. Table 5.IX). This has, in effect, a dominating contribution from h-q interactions although, as the discrepancy between the theoretical and experimental results indicates, mechanisms other than the one based on multipolar interactions must interfere. This is in accord with the more general observation, that the quenching mechanism for the most efficient isotopomer is not necessarily the same as that causing relaxation by the less efficient isotopomer. Thus, although the present calculations predict the observed isotope effect correctly, they overestimate it by about one order of magnitude. This is particularly interesting in connection with the fact that this is the largest quantifiable isotope effect ever reported and that other proposed mechanisms[66] are rather unlikely to produce it.

ii) $Bi(6^2D_{3/2,5/2})$ & $Sb(5^2D_{3/2,5/2}) + H_2, D_2$

The deactivation of the heavier excited atoms of group V has been

discussed [260,261] within the framework of non-adiabatic transitions between surfaces with symmetries determined by strong spin-orbit coupling (J,Ω). Although, for both $Sb(5^2D_{3/2},{}^5/_2)$ and $Bi(6^2D_{3/2},{}^5/_2)$ this coupling scheme provides a satisfactory basis for interpreting the removal behaviour for most collisional partners, whether this involves quenching or reaction, it can not give a clear explanation of the isotope effect observed for the hydrogen isotopes.[260] It has therefore been suggested that long range interactions leading to near resonant energy transfer may play an important role, especially in the quenching of the $^2D_{5/2}$ upper excited state by H_2 or D_2.

As Table 5.II shows, the $^2D_{5/2}$ may be relaxed to the lower excited state $^2D_{3/2}$, with the release of 1342 cm^{-1} for Sb and 4019 cm^{-1} for Bi.[2] Consequently, near resonant conditions could be fulfilled by electronic energy transfer from $Sb(5^2D_{5/2})$ to the rotational degrees of freedom of the ground vibrational level of H_2 or D_2 and from $Bi(6^2D_{5/2})$ to the first rovibrational state of the two isotopes. This scheme provides a basis for understanding the observed high decay efficiency of the upper excited atomic state. Furthermore, it accounts for the more efficient relaxation of $Bi(6^2D_{5/2})$ in comparison to $Bi(6^2D_{3/2})$, although possible contributions from reactive pathways should not be excluded. Deexcitation of the $^2D_{5/2}$ atomic state to the ground $^4S_{3/2}$ state would involve the excitation of three or more vibrational quanta to match up with the amount of electronic energy and therefore are not expected to be important.

To further clarify these points, calculations were carried out for the systems $Sb(5^2D_{3/2})$ + H_2, D_2 and $Bi(5^2D_{3/2},{}^5/_2)$ + H_2, D_2 and the results are shown in Table 5.X. The discrepancy observed between the calculated and the experimental rate constants for $Sb(5^2D_{3/2})$ + H_2, D_2 when combined with the failure of the present model to predict correctly the order of the isotope effect, (cf. Table 5.X), clearly indicates that long range forces can only be of limited importance for the deactivation process. Similar considerations apply for $Bi(6^2D_{3/2})$ + H_2,D_2. The theoretical

TABLE 5.X

Collisional Deactivation of $Sb(5^2D_{3/2})$, $Bi(6^2D_{5/2})$ and $Bi(6^2D_{3/2})$ by hydrogen isotopes

System	Channel	ΔE (cm^{-1})	Population (%)	k_i ($cm^3 molecule^{-1} s^{-1}$)	k_{calc} ($cm^3 molecule^{-1} s^{-1}$)	k_{exp} ($cm^3 molecule^{-1} s^{-1}$)	Ref.
$Sb(5^2D_{3/2})+H_2$	(0,0)→(2,2)	-106	13	3.5×10^{-16}			
	(0,1)→(2,3)	+92	66	2.3×10^{-15}	2.7×10^{-15}	$(6.6 \pm 0.2) \times 10^{-12}$	261
$Sb(5^2D_{3/2})+D_2$	(0,2)→(3,0)	-51	38	3.8×10^{-17}			
	(0,5)→(3,5)	+33	1.4	5.9×10^{-18}	4.5×10^{-17}	$(1.7 \pm 0.1) \times 10^{-11}$	261
$Bi(6^2D_{5/2})+H_2$	(0,0)→(1,0)	+142	13	5.6×10^{-14}			
	(0,1)→(1,1)	+136	66	3.3×10^{-13}			
	(0,2)→(1,2)	+124	12	7.6×10^{-14}			
	(0,3)→(1,3)	+107	9	7.8×10^{-14}	5.4×10^{-13}	$(5.6 \pm 0.5) \times 10^{-12}$	260
$Bi(6^2D_{5/2})+D_2$	(0,2)→(1,6)	+6	38	$\sim 1 \times 10^{-15}$			
	(0,8)→(1,10)	-5	0.01	2.2×10^{-15}	$\sim 3 \times 10^{-15}$	$(2.4 \pm 0.2) \times 10^{-13}$	260
$Bi(6^2D_{3/2})+H_2$	(0,2)→(3,0)	+9	12	2.4×10^{-15}	2.4×10^{-15}	$(7.9 \pm 0.8) \times 10^{-14}$	260
$Bi(6^2D_{3/2})+D_2$	(0,0)→(4,2)	+41	18	2.9×10^{-17}	2.9×10^{-17}	$(1.1 \pm 0.3) \times 10^{-14}$	260

and experimental results* differ by more than one order of magnitude. The hard sphere collision diameter for these systems was evaluated from Hartree-Fock calculations for the atomic radius (cf. Table 5.IV), since the Van der Waals radius, which would have resulted in a larger d, was not available for Bi. Use of the latter d in the calculations would have, as an effect, a further increase in the discrepancy between the theoretical and experimental results. The isotope effect, however, is predicted in the correct order. Quenching by H_2 is more efficient than by D_2.

In the calculations for $Bi(6^2D_{5/2})$ + H_2 the four most resonant channels (cf. Table 5.X) involve $\Delta E > 100 cm^{-1}$, with the first four rotational states of H_2 accounting for more than 99% of the total population. For three of these channels the initial state population decreases as the energy mismatch increases. However, the calculated decay rate is in poor agreement with the experimental data. A similar conclusion can be reached for $Bi(6^2D_{5/2})$ + D_2, although for different reasons. For this system, there is only one channel involving q-q coupling and a very small energy mismatch ($\Delta E = -5\ cm^{-1}$). However, due to the small population of the initial state with J = 8, the contribution of this channel decreases dramatically. Thus, the calculated rate constant is effectively determined by a channel involving h-q coupling which, despite the small energy discrepancy ($\Delta E = +6\ m^{-1}$) and the appreciable initial population, does not account for the observed decay efficiency.

Summarizing, we note that quenching of $Sb(5^2D_{3/2})$ and $Bi(6^2D_{3/2,5/2})$ by H_2 and D_2 can not be explained in terms of the model used. For $Bi(6^2D_{5/2})$, reaction is energetically feasible but should be excluded, if

* We should note here that experimentally, the data showed anomalous behaviour[260] for H_2, leading possibly to smaller k_{H_2}. Indeed in very recent work[262] Trainor measured rate constants for H_2 and D_2, which were more than one order of magnitude smaller than those obtained by Bevan and Husain, and close to the calculated results in this work.

the observed isotope effect ($\sigma_{H_2}/\sigma_{D_2} \simeq 16$) will be taken into consideration. Quenching via non-adiabatic transitions, as it has been proposed by Husain and Bevan,[260] provides a possible mechanism for deactivation, although the emergence of the isotope effect is not clear. By analogy with the proposals of French and Lawley[96] deactivation via the formation of an intermediate complex due to orbiting collisions should be considered as another possible mechanism. The role orbiting collisions can play in V-V energy transfer has been examined by Gait.[61] According to the formulation given by this author, the existence of an isotope effect of the order of magnitude observed here is possible. Within the context of the same proposals short range coupling should be also considered especially in systems involving $\Delta E \simeq 100 - 200\ cm^{-1}$ as in $Bi(6^2D_{5/2}) + H_2$.

iii) $Sn(5^3P_2) + H_2$, HD, D_2 and $Pb(6^3P_2) + H_2$, D_2

The excitation energy of the two low lying states of Sn and Pb is included in Table 5.II. Based on these data, we deduce that quenching of $Sn(5^3P_2)$ by H_2, HD or D_2 may take place either to the $^3P_1$ state with E → R energy transfer or to the ground ^3P_o state by E → V,R energy transfer. The latter also applies to the deactivation of $Pb(6^3P_2)$ by H_2 and D_2 to both the $^3P_1$ and ^3P_o states. We also note that electric multipole transitions from the $^3P_1$ to the ^3P_o state are forbidden and therefore the present model cannot be applied.

Deactivation of $Sn(5^3P_2)$ by the hydrogen isotopes is interesting in that the heavier isotope shows the highest quenching efficiency, in contrast to the trend observed for most systems. The results of the calculations for D_2 and HD are in relatively good agreement with the experimental data[263] (cf. Table 5.XI) and predict the isotope effect satisfactorily (cf. Table 5.VII):

Experiment: $\sigma_{D_2}/\sigma_{HD} \simeq 3$, Theory: $\sigma_{D_2}/\sigma_{HD} \simeq 2$

The model used underestimates the rate constnat for $Sn(5^3P_2) + H_2$ by

about three times (cf. Table 5.XI). For this system, the most resonant channel for E → V energy transfer corresponds to energy mismatches of 99 cm^{-1} and involves a small initial state population at 300 K. This results in a minor contribution of E → V energy transfer to k_{calc}. In contrast, E → R energy transfer due to long range interactions, although it also involves an extremely small initial state population, determines the calculated decay rate effectively. This is understood in terms of the smaller energy mismatch and the larger atomic and rotational matrix elements involved. As the results in Table 5.XI indicate, E → R energy transfer is unimportant for the removal of $Sn(5^3P_2)$ by D_2 or HD. These findings suggest that long range electric interactions leading to E → V or E → R energy transfer may contribute significantly to the removal of $Sn(5^3P_2)$ by hydrogen isotopes. A comparison of the quenching efficiency of the $^3P_2$ and $^3P_1$ states is particularly interesting in this respect. Deactivation of $Sn(5^3P_2)$ is faster compared to that of $Sn(5^3P_1)$ with a possible exception for H_2, for which only an upper limit of k_{exp} has been reported.[263] This phenomenon is more striking for Pb atoms. The rates of removal for the two states differ by about three orders of magnitude[68,69] with $Pb(6^3P_2)$ atoms being removed faster. Following Ewing,[95] these differences may be understood in terms of the absence of electric multipolar interactions in processes involving the $^3P_1$ state.

The results recorded in Table 5.XI for $Pb(6^3P_2) + D_2$ suggest that in accordance with the proposal of Ewing,[95] 5.23 may adequately describe the quenching process.

$$Pb(6^3P_2) + D_2(v=o, J=2) \rightarrow Pb(6^3P_1) + D_2(v=1, J=o), \Delta E = +18\ cm^{-1} \quad (5.23)$$

Reference to Table 5.VIII shows that k_{calc} is in close agreement with that determined by French and Lawley[96] and smaller than the rate constant evaluated from the data given by Ewing.[95] The reasons, which lead to overestimation of k_{calc} in Ewing's work, are similar to those described for $Te(5^3P_{o,1}) + H_2$.

TABLE 5.XI

Quenching of $Sn(5^3P_2)$ and $Pb(6^3P_2)$ by hydrogen isotopes

System	Channel	ΔE (cm^{-1})	Population (%)	k_i ($cm^3 molecule^{-1} s^{-1}$)	k_{calc} ($cm^3 molecule^{-1} s^{-1}$)	k_{exp} ($cm^3 molecule^{-1} s^{-1}$)	Ref.
$Sn(5^3P_2) + H_2$	(0,1) → (0,5)	-31	66	3.4×10^{-14}			
	(0,6) → (0,8)	-54	0.002	3.8×10^{-13}			
	(0,4) → (1,2)	-99	0.4	2.4×10^{-14}	4.4×10^{-13}	$(1.15 \pm 0.3) \times 10^{-12}$	263
$Sn(5^3P_2) + HD$	(0,9) → (0,11)	+59	4×10^{-6}	7.6×10^{-23}			
	(0,2) → (1,1)	+22	12	5.3×10^{-16}			
	(0,2) → (1,0)	-63	12	3.4×10^{-12}	3.4×10^{-12}	$(5.4 \pm 0.8) \times 10^{-12}$	263
$Sn(5^3P_2) + D_2$	(0,5) → (0,9)	-18	1.4	4.1×10^{-15}			
	(0,1) → (1,3)	-156	20	1.6×10^{-14}			
	(0,2) → (1.4)	-41	38	1.0×10^{-11}			
	(0,3) → (1,5)	+64	11	1.1×10^{-13}	1.1×10^{-11}	$(1.6 \pm 0.5) \times 10^{-11}$	263
$Pb(6^3P_2) + H_2$	(0,6) → (1,4)	+26	0.02	2.2×10^{-15}	2.2×10^{-15}	$(2.2 \pm 0.6) \times 10^{-12}$	68
	(0,5) → (3,3)	-3	0.10	4.2×10^{-18}	4.2×10^{-18}	$(1.6 \pm 0.2) \times 10^{-12}$	69
$Pb(6^3P_2) + D_2$	(0,2) → (1,0)	+18	38	1.0×10^{-11}			
	(0,3) → (1,1)	-133	11	1.6×10^{-15}	1.0×10^{-11}	$(7.7 \pm 0.5) \times 10^{-12}$	69

Figure 5.3 illustrates the temperature behavior of k_{calc}. A positive temperature dependence is observed up to ∿ 250 K, followed by a decrease of k_{calc} with increasing temperature. Experimental rate constants found by Trainor and Ewing at three temperatures[264] are also included in Figure 5.3, indicating a slightly positive temperature dependence in the range 298-560 K. However, the small number of experimental data does not allow for a concrete conclusion about the importance of the present model. Further it is highly probable that the importance of long range interactions is minimized in the range of high temperatures covered experimentally (500-560 K). Determination of k_{D_2} within the range of 298-500 K and most important at temperatures below 298 K is expected to provide conclusive evidence about the role of near-resonant energy transfer due to long range forces in the quenching of $Pb(6^3P_2)$ by D_2.

The k_i values shown in Table 5.XI for $Pb(6^3P_2) + H_2$ are characteristic of the dramatic effect a small initial state population or a multivibrational transition, as the one with $\Delta v = 3$, can have on the efficiency of quenching. The poor agreement between theory and experiment, being in accord with the results obtained by French and Lawley,[96] excludes any significant contribution of long range interactions to the decay of $Pb(6^3P_2)$ in the presence of H_2.

iv) $Tl(6^2P_{3/2}) + H_2, D_2$

Table 5.XII illustrates an obvious agreement between the relative efficiencies of deactivation of $Tl(6^2P_{3/2})$ and $I(5^2P_{\frac{1}{2}})$ atoms by H_2 molecules. Considering that for these atoms the spin-orbit coupling splitting (cf. Table 5.II) and, consequently, the energy transferred during the quenching process are almost identical, it is reasonable to assume that the mechanism of deactivation is the same for the two species.

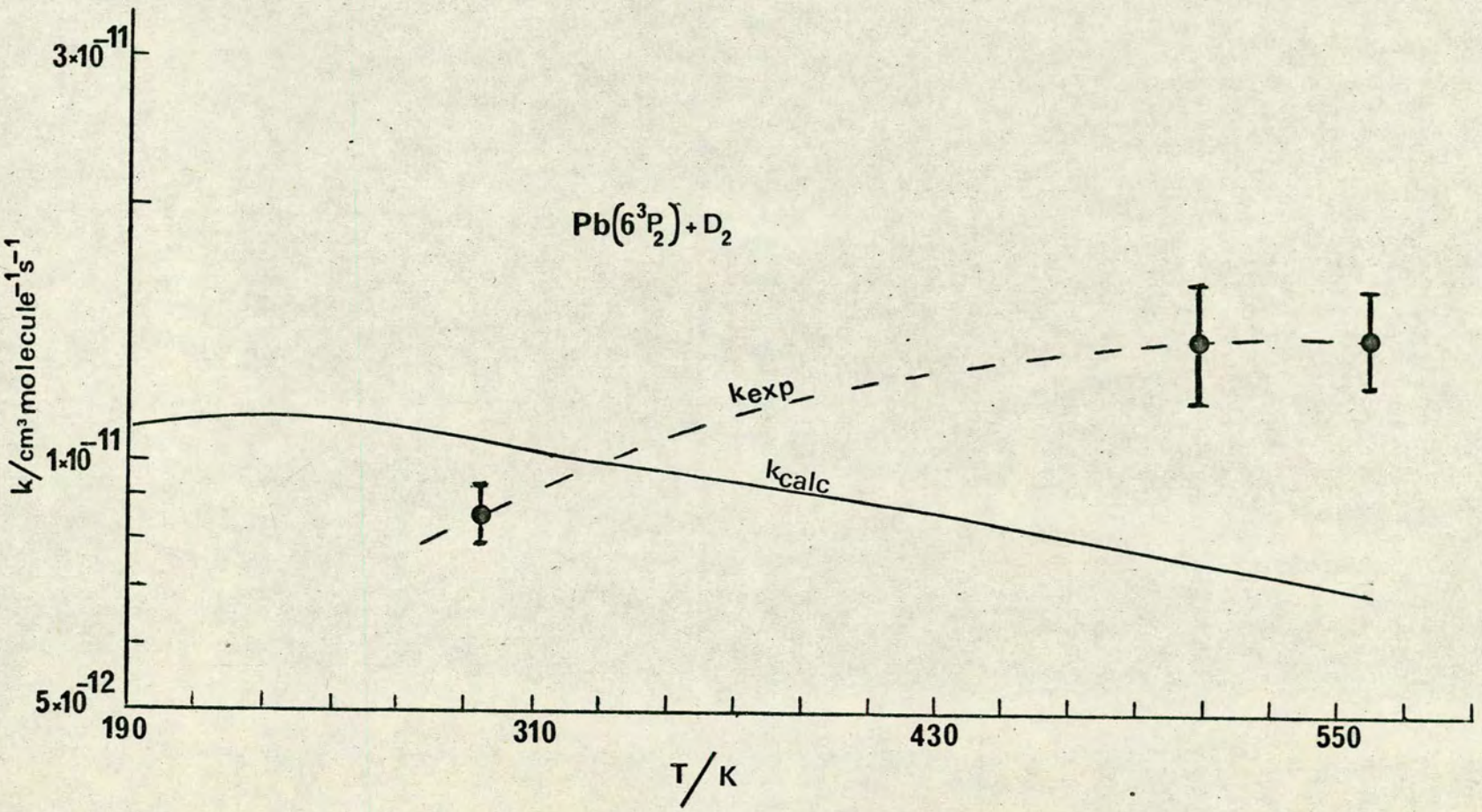

Fig. 5.3: Experimental and theoretical rate constants for the quenching of $Pb(6^3P_2)$ atoms by D_2.

Table 5.XII

Data for the quenching of $I(5^2P_{\frac{1}{2}})$ and $Tl(6^2P_{3/2})$ by H_2

	$A \times 10^{12}$ (cm^3 $molecule^{-1}s^{-1}$)	E_a (kJ $mole^{-1}$)	$k_{298} \times 10^{13}$ (cm^3 $molecule^{-1}s^{-1}$)
$I(5^2P_{\frac{1}{2}})$	2.24	7.11	1.1 ± 0.1
$Tl(6^2P_{3/2})$	1.86	3.35	4.9 ± 0.1

Although the results of the present calculations are consistent with the observed temperature dependence (cf. Table 5.XIII) of the rate constants,[67] they underestimate the experimental data as in the case of $I(5^2P_{3/2}) + H_2$. Thus, they provide support for the above tentative conclusion, which is also in accord with the proposals of French and Lawley[96] for a dominating role of short range coupling in these systems.

In contrast to the comparable quenching efficiency observed for $I(5^2P_{\frac{1}{2}}) + H_2$ and $Tl(6^2P'_{3/2}) + H_2$, quenching of $Tl(6^2P_{3/2})$ by D_2 is about fifty times more efficient than that for $I(5^2P_{\frac{1}{2}})$, indicating the interference of different decay mechanisms for the latter systems. The theoretical result obtained for $Tl(6^2P_{3/2}) + D_2$ (cf. Table 5.XIII) underestimating the measured rate constants by about four orders of magnitude, rules out any significant contribution from long range forces. However, this result is interesting in that it shows the importance of multivibrational transitions, if these lead to a minimization of ΔE in comparison to transitions involving the excitation of a smaller number of vibrational quanta. Thus, the discrepancy between the k_{calc} calculated here and that reported by French and Lawley (cf. Table 5.VIII) is attributed to the neglectance of near resonant channels with $\Delta v = 3$ by the latter authors.

TABLE 5.XIII

Quenching of $Tl(6^2P_{3/2})$ by H_2 and D_2

System	Channel	ΔE (cm^{-1})	Population (%)	k_i ($cm^3 molecule^{-1} s^{-1}$)	k_{calc} ($cm^3 molecule^{-1} s^{-1}$)	k_{exp} ($cm^3 molecule^{-1} s^{-1}$)	Ref.
$Tl(6^2P_{3/2}) + H_2$	(0,2)→(2,0)	-60	12	3.1×10^{-14}			
(300 K)	(0,6)→(2,6)	+53	0.002	9.0×10^{-18}			
	(0,7)→(2,7)	-26	0.0001	3.2×10^{-18}	3.1×10^{-14}	$(4.9 \pm 0.1) \times 10^{-13}$	67
$Tl(6^2P_{3/2}) + H_2$	(0,2)→(2,0)	-60	12	9.2×10^{-14}			
(573 K)	(0,6)→(2,6)	+53	0.8	8.8×10^{-15}			
	(0,7)→(2,7)	-26	0.6	1.7×10^{-14}	1.2×10^{-13}	9.1×10^{-13}	
$Tl(6^2P_{3/2}) + D_2$	(0,7)→(3,5)	-1	0.05	1.9×10^{-18}	1.9×10^{-18}	$(4.9 \pm 0.1) \times 10^{-14}$	67

F) CONCLUSIONS

The approach to the problem of near resonant energy transfer due to long range interactions used in the present work, although approximate, allows for some general conclusions concerning the importance of these interactions in the quenching of low lying excited states of heavy atoms.

1) In most cases experimental data and theoretical predictions accord fairly well in systems involving atomic transitions between the ground state multiplets, in which the quenching process is very efficient, leading to quenching cross sections of the order $\sim 10^{-16} - 10^{-17}$ cm^2. In particular, in systems like Br($4^2P_{\frac{1}{2}}$), I($5^2P_{\frac{1}{2}}$) + HF, for which there is direct experimental evidence for the importance of near resonant energy transfer, the present calculations provide strong evidence for the dominating role of long range interactions.

The calculated results for systems with large energy discrepancies ΔE indicate that long range forces cannot account effectively for the observed efficiency. Indeed, the calculations underestimate the measured rate constants seriously in most cases. This may be understood by considering the increased interference of other less efficient deactivation mechanisms when the present model breaks down. However, there are systems with $\sigma \sim 10^{-18} - 10^{-19}$ cm^2, (cf. I($5^2P_{\frac{1}{2}}$) + HD, HBr), for which the theoretical predictions are consistent with the experimental data.

2) The results for systems involving atomic transitions between different atomic terms, (cf. Sb($5^2D_{3/2}$), Bi($6^2D_{3/2}, 5/2$) + H_2,D_2) are generally in poor agreement with the experimental data even when the quenching is very efficient.* This is attributed to significant contributions from other decay mechanisms along the lines discussed elsewhere.

3) We should note that the theoretical results obtained in this work justify the assumptions made in previous chapters, (cf. Chapters 1,3,4) that long range forces can give rise to large isotope effects. The trend

*Note, however, the footnote on page 211.

of the isotope effect has been correctly predicted for all the systems studied here, with the exception of Sb($5^2D_{3/2}$) + H_2, D_2.

4) The detailed results obtained in this work provide some basic criteria for efficient quenching due to long range forces, depending on the physical parameters which characterise each system:

a) The importance of the magnitude of the energy mismatch, ΔE, depends mainly on the type of coupling involved. Couplings of higher order, (i.e. larger values of n) favour larger ΔE. Thus, contributions from d-q and q-q coupling are dramatically decreased for ΔE values larger than about 30 cm^{-1} and 70 cm^{-1} correspondingly. Processes involving h-q coupling, in the absence of significant contributions from longer range interactions, may be important even for $\Delta E \simeq 120$ cm^{-1}. We can therefore deduce that the larger the energy discrepancy in 5.1, the greater the relative importance of shorter range interactions, which effectively can lead to quenching cross sections of the order of $10^{-18} - 10^{-20}$ cm^2, i.e. about two to four orders of magnitude smaller than those obtained for d-q and q-q coupling under near resonant conditions, ($\Delta E < 30$ and 70 cm^{-1} correspondingly).

b) The question of the existence of "propensity" rules controling the efficiency of process 5.1 can be answered following the above discussion. Considering the great importance of the rotational transitions in the quencher in determining the energy defect and consequently the relative importance of long range interactions, we deduce that the possible "propensity rules", arising from the selection rules for electric multipole transitions in the molecule, are determined by the magnitude of ΔE. Thus, assuming that dipole rovibrational transitions are allowed and that the corresponding ΔE is less than about 30 cm^{-1}, the "propensity rule" is: $\Delta J = \pm 1$. For larger energy defects, contributions due to quadrupole transitions may become important leading to the additional conditions $\Delta J = 0, \pm 2$, which eventually may become the dominating "propensity rules" for a certain range of ΔE.

Similarly, further increase of ΔE may result in the additional "propensity rule" of $\Delta J = \pm 4$, corresponding to hexadecapole transitions.

As the energy mismatch increases even further, apart from higher contributions of shorter range interactions, higher order approximations may also become important. However, as ΔE becomes larger, even allowing for these higher terms in the multipole coupling, the total cross section falls rapidly in magnitude.

c) The minimum number of vibrational quanta excited, so that near resonance be achieved, is another factor determining the efficiency of quenching. The results of the present calculations justify the remark made in previous chapters, (cf. Chapters 3 and 4), that processes involving Δv changes differing by unity should be associated with rate constants differing by more than one order of magnitude (cf. $Br(4^2P_{\frac{1}{2}})$, $I(5^2P_{\frac{1}{2}})$ + HF). We should note however, that this is true only if all the other parameters, (e.g. type of coupling, ΔE, initial state population), do not differ substantially for the two processes.

d) The temperature dependence of the decay rates of processes described by 5.1 can be either negative or positive depending on the range of temperatures covered. Usually for temperatures larger than 300 K, a negative temperature dependence is calculated. However, for light isotopomers like H_2, a positive temperature dependence has been predicted for many systems (e.g. $I(5^2P_{\frac{1}{2}}) + H_2$, $Tl(6^2P_{3/2} + H_2)$, even at very high temperatures ($\sim$ 500 K). Finally, we should note the important effect of changes in the initial state population with temperature on the overall temperature dependence, as this is clearly illustrated in Figure 5.2.

Chapter 6

CONCLUDING REMARKS

CONCLUDING REMARKS

The central theme of this work was the discussion of the conditions which may lead to efficient quenching of electronically excited atoms by small molecules. Energy transfer processes of the type 1.1 received particular attention. The experimental data which included temperature dependence measurements and determinations of isotope effects, indicated that E↔V energy transfer due to long range forces may account for a large number of processes exhibiting a high quenching efficiency. Furthermore, the large isotope effects observed for some of the studied systems, in which both reaction and quenching is possible, proved the dominant role of quenching for the most efficient isotopomer and verified the importance of near resonance in determining the relaxation pathway. In contrast, for the less efficient isotopomer a unique assignment of the relaxation mechanism is less certain.

A practical application of the large isotope effect observed in the removal of $I(5^2P_{\frac{1}{2}})$ by CH_3I and CD_3I was demonstrated in the iodine photodissociation laser. The efficient energy transfer from $I(5^2P_{\frac{1}{2}})$ to CH_3I resulted in a decrease of the extent of stimulated emission observed when CH_3I was employed as the parent molecule instead of CD_3I. Conversely, the high efficiency of near resonant E↔V energy transfer in several systems (e.g. $I(5^2P_{\frac{1}{2}}) + H_2O$) indicates that such systems can be used in obtaining laser action at various molecular transitions.

In systems in which non-resonant energy transfer takes place (e.g. $I(5^2P_{\frac{1}{2}})$ or $Br(4^2P_{\frac{1}{2}}) + HCl$), quenching via electronically non-adiabatic transitions at intermediate separations appears to be consistent with the experimental data. In this type of mechanism, interactions due to the permanent multipole moments of the colliding species appear to be of primary importance for efficient energy transfer.

The calculations carried out for the efficiency of quenching in a large number of systems on the basis of a simplified multipolar interactions model provided further evidence for the importance of near resonant energy transfer. In the vast majority of cases in which efficient quenching occurs ($\sigma \sim 10^{-16} - 10^{-17} cm^2$), the calculated results were in good agreement with the experimental data. In contrast, for less efficient quenching the theoretical predictions usually underestimated the experimental results, thus indicating the increased interference of other types of quenching mechanisms.

The calculations also revealed the relative importance of various parameters for efficient near resonant energy transfer. Thus, the range of energy mismatches which can be assigned as near resonant is largely determined by the type of coupling involved and increases with interactions of decreasing range. Multiquantum vibrational transitions are found to be important in cases in which they lead to a minimization of the energy mismatch and the initial states population is appreciable. In general it can be stated that for systems in which near resonant channels arising from highly populated initial states exist, and the corresponding rovibrational transitions obey the optical selection rules, E→V energy transfer is expected to exhibit an extremely high efficiency.

Despite the fact that the results obtained in this work specify some conditions for efficient energy transfer in processes involving low lying atomic states (cf. 1.1), further direct experimental evidence in the form of state-to-state information is clearly necessary for conclusive support of the above proposals.

APPENDIX I

Reagents

N_2 (B.O.C. 'white spot', O_2 < 10ppm, CO_2 < 1ppm, H_2 < 1ppm) and He (B.O.C., O_2 < 1ppm, H_2 < 10ppm, CO_2 < 1ppm) were used directly.

Kr "Grade X" (B.O.C. Ltd.) was used directly from glass breakseal containers. Purity given as Kr 99.99%.

He (B.O.C., stated purity < 1ppm. O_2) was used directly from the cylinder. Purity given as He 99.995%.

$n\text{-}C_3F_7I$ supplied by the Pierce Chemical Company, was thoroughly degassed and fractionally distilled under vacuum to remove residual traces of I_2.

CH_3I (Fisons Ltd.), CD_3I (Koch-Light Laboratories Ltd.), and CF_3I (Pierce Chemical Co.) were thoroughly degassed and fractionally distilled under vacuum to remove residual traces of I_2. Their purity was checked via U.V. and I.R. spectroscopy.

H_2O and D_2O (B.O.C., stated purity 99.5%) were thoroughly degassed before use.

DCl was prepared by the action of D_2O on benzoyl chloride and purified by fractional distillation under vacuum. The purity determined by infrared analysis showed that the sample contained $\leq 9\%$ HCl. No other impurities were detected.

HI and DI were kindly supplied by colleagues of this Department and the purity was checked by infrared spectroscopy. The purity of DI was further checked using an A.E.I. MS902 mass spectrometer and shown to contain <6% HI.

HCl and HBr (Matheson Co.) were degassed under vacuum and their purity checked via infrared and mass spectroscopy.

DBr (Merck, Sharp & Dohme, stated minimum isotopic purity, 99 atom % D) was degassed under vacuum and its purity checked via infrared and mass spectroscopy. With the limited amount of sample available, the infrared spectrum did not allow a sensitive estimate of HBr and the inlet system to our A.E.I. MS902 mass spectrometer, despite repeated exposure to D_2O, gave only a poor limit to the amount of HBr present (<36% HBr). We believe that the HBr content was in fact much lower than this and probably close to the manufacturers' stated limit, as successive samples admitted to the mass spectrometer showed increases in the DBr/HBr ratio, but we had insufficient sample to obtain a better limit. We are indebted to Professor J.J. Turner for the gift of this DBr sample.

GeH_3I & SiH_3I samples were kindly provided by Dr. J. Savage and Mr. T. Fraser whom I thank. Their purity was checked via I.R. and U.V. spectroscopy.

APPENDIX II

a) A rough calculation of the energy of some of the vibrational levels of H_2O and D_2O was based on the following expression:[174]

$$E(v_1,v_2,v_3) = \sum_i^3 \omega_i(v_i + \tfrac{1}{2}) + \sum_i^3 \sum_{k\geq i}^3 x_{ik}(v_i + \tfrac{1}{2})(v_k + \tfrac{1}{2}) \qquad (II.1)$$

where w_i and x_{ik} are the vibrational constants.

b) The rovibrational energy differences for the hydrogen or deuterium halides were computed by using Dunham's potential[174] to evaluate the rovibrational energy levels of a rotating vibrator. This assumption has been proved satisfactory[217] for the first vibrational levels of these molecules since the corresponding energies are much smaller than the dissociation energy. The computation was carried out on the basis of the following expression:

$$E = \omega + B_v[J(J+1)] - D_v[J(J+1)]^2 + H_v[J(J+1)]^3 \qquad (II.2)$$

where,

$$\omega = \omega_e - \omega_e x_e(v + \tfrac{1}{2}) + \omega_e y_e(v + \tfrac{1}{2})^2 \qquad (II.3)$$

and ω_e, $\omega_e x_e$, $\omega_e y_e$ are the vibrational molecular constants,

$$B_v = B_e - a(v + \tfrac{1}{2}) + b(v + \tfrac{1}{2})^2 \qquad (II.4)$$

and B_e a,b are the rotational molecular constants,

$$D_v = D_e - a_D(v + \tfrac{1}{2}) + b_D(v + \tfrac{1}{2})^2 \qquad (II.5)$$

and D_e, a_D, b_D the centrifugal distortion constants.

$H_v \simeq H_e$, being negligible for most hydrogen or deuterium halides.

For those molecular constants of the deuterated species, for which experimental values were not available the values employed were evaluated on the basis of those for the hydrogen containing species, by using appropriate expressions.[174]

APPENDIX III

Expressions 5.13 and 5.15 were computed numerically in the following way:

The Bessel functions were expressed in powers of v (cf. 5.14) and the integration was carried out by using the Chensaw-Curtis method.* This is efficient if the function to be integrated is well behaved all over the domain of the independent variable v. Thus, computing limitations are imposed for non-well behaved functions. In the present work, such limitations appeared mostly for calculations involving n = 7 and low temperatures. In many cases, a small change at the lower limit of integration removed these difficulties. It should be noted here, that another limitation was imposed by the necessary conditions for the expansion 5.14 to be valid. We may consider that an exaggerated example of the effect of invalidity of 5.14 is provided by the hypothetical process illustrated in Figure 5.1 for very small ΔE. The decrease in the cross section observed for $\Delta E < 20$ cm^{-1} is due entirely to the mathematical invalidity of 5.14. However, as mentioned in Chapter 5, for the systems studied in this work, 5.14 is valid. This can be also verified computationally. The principal routine used in computing rate constants and their temperature dependences was the DØ1AAF of the NAG Library.

The limits of integration were set in the majority of cases between 1 and 10^7 cm s^{-1}.

A typical version of one of the computer programs used is given on pages 228 and 229.

*V.I. Krylov, "Approximate Calculation of Integrals", Macmillan, (1962).

```
C    THIS PROGRAM CALCULATES THE RATE CONSTANT
C     FOR ENERGY TRANSFER DUE TO MULTIPOLAR INTERACTIONS
C     AT A GIVEN TEMPERATURE
C     U(I) AND Q(I) ARE THE MATRIX ELEMENTS FOR THE ATOM AND
C     THE MOLECULE
C     ED IS THE ENERGY MISMATCH
C     L IS THE ORDER OF INTERACTION
C     T IS THE TEMPERATURE
C     XM IS THE REDUCED MASS OF THE SYSTEM
      IMPLICIT REAL *8 (A-H,O-Z)
      DIMENSION U(20),Q(20)
      COMMON/Z/P,X2,X,G,L
      EXTERNAL FUN
      CALL FPRMPT ('J= ',3)
      READ,J
      CALLFPRMPT ('U(I)= ',6)
      READ, (U(I),I=1,J)
      CALL FPRMPT ('Q(I)= ',6)
      READ, (Q(I),I=1,J)
      CALL FPRMPT('L= ',3)
      READ,L
      CALL FPRMPT('ED= ',3)
      READ,ED
      CALL FPRMPT ('D= ',3)
      READ,D
      CALL FPRMPT('T= ',3)
      READ,T
      CALL FPRMPT('XM= ',4)
      READ,XM
      XK=1.38053 E-16
      G=XM/(2*XK*T)
      C=(3.14159*3.14159*3.14159*8)/(1.054*1.054 )
      E=0
      DO 1I=1,J
    1 E=E+U(I)*Q(I)
      W=(ED*1.9610E11)/1.0546
      P=W*D
      X=(L*(L-2))/(W*D*8)
      X2=((L-3)*(L-3)-1)/W*D*8
      WRITE(6,99)X
   99 FORMAT(' X= ',D17.7)
      XH=DGAMMA(DFLOAT(L)/2)
      XL=(XM/T)
      F=(4.9189E23)*XL**1.5
      R=F*E*E*((W/2)**(L-1))*(D**(3-L)*C)
     C/((XH*XH)*2*P*(L-2))
      WRITE(6,33)R
   33 FORMAT(' R= ',D17.8)
      A=1.0
      WRITE (6,11)P
   11 FORMAT(' P= ',D15.8)
      WRITE(6,6)G
    6 FORMAT( ' G= ',D15.8)
      B=10. E6
```

```
      ACC=0.1
      NMAX=32
      N=-1
      IFAIL =1
      CALL D01AAF(A,B,FUN,ACC,NMAX,N,ANS,IFAIL)
      IF (IFAIL.NE.1) GO TO 20
      WRITE (6,100)
  100 FORMAT(' FAULT IN INTEG PROGRAM')
      STOP
   20 WRITE(6,88)ANS
   88 FORMAT(' ANS= ',D17.7)
      XSECT=ANS*R*(1.0E-26)
      WRITE(6,300)XSECT
  300 FORMAT(' RATE CONSTANT= ',D20.7)
      STOP
      END


      DOUBLE PRECISION FUNCTION FUN(V)
      IMPLICIT REAL * 8 (A-H,O-Z)
      COMMON/Z/P,X2,X,G,L
      PDASH=(-2*P/V)
      VDASH=(-G*V*V)
      EXP1=DEXP(PDASH)
      EXP3=DEXP(VDASH)
      EXP2=(V**(3-L))*((1+X*V)*(1+X*V)*2-(1+X2*V)*(1+X2*V))
      FUN=EXP1*EXP2*EXP3
      RETURN
      END
```

BIBLIOGRAPHY

1a) R.J. Donovan and D. Husain, Chem.Rev., 70, 489, (1970).

b) R.J. Donovan and D. Husain in "Adv. in Photochem.", 8, 1, (1971).

2. R.J. Donovan and H.M. Gillespie, Specialist Periodical Reports, "Reaction Kinetics", ed. P.G. Ashmore, 1, 14, (1974).

3. S.C. Barton and J.E. Dove, Can.J.Chem., 52, 1584, (1974).

4. C. Zetsch and F. Stuhl, J.Chem.Phys., 66, 3107, (1977).

5. D.L. King and D.W. Setser, in Ann.Rev.Phys.Chem., 27, 407, (1976).

6. N.G. Basov, A.N. Oraevsky and A.V. Pankratov, "Stimulation of Chemical Reactions with Laser Radiation" in "Chemical and Biological Applications of Lasers", ed. by C.B. Moore, Academic Press (1974).

7. R.B. Bernstein, Isr.J.Chem., 9, 615, (1971).

8. M.J. Berry, in "Molecular Energy Transfer", ed. by J. Jortner and R.D. Levine, p.114, Willey (1976).

9. E.E. Nikitin, in "Physical Chemistry: An Advanced Treatise", ed. by H. Eyring, D. Henderson and W. Jost, Ch.4, Academic Press, (1974).

10. R.S. Berry, in "Molecular Beams and Reaction Kinetics", p.193, Academic Press, (1970).

11. M.F. Golde, Specialist Periodical Reports, "Gas Kinetics and Energy Transfer", 2, 123, (1977).

12a) A. Messiah, "Quantum Mechanics" Vol.1 and 2, North Holland Publ. Co (1965).

b) L.D. Landau and E.M. Lifshitz,"Quantum Mechanics", Pergamon Press, (1959).

13. F.A. Matsen and D.J. Klein, Adv. in Photochemistry, 7, 1, (1969).

14. E. Wigner and E.E. Witmer, Z.Physik 51, 859, (1928).

15. J.O. Hirschfelder and W.J. Meath, Adv.Chem.Phys., 12, 3,(1967).

16. R.F. Heidner, D. Husain and J.R. Wiesenfeld, J.C.S. Faraday II, 69, 927, 1973.

17. E.R. Fisher and E. Bauer, J.Chem.Phys., 57, 1966, (1972).

18. J.B. Delos, J.Chem.Phys., 59, 2365, (1973).

19. J.C. Tully, J.Chem.Phys.,61, 61, (1974).

20. T.G. Slanger and G. Black, J.Chem.Phys. 60, 468, (1974).

21. J.C. Polanyi, Accounts Chem.Res., 5, 161, (1972).

22. G. Wolken Jr. and M. Karplus, J.Chem.Phys., 60, 351, (1974).

23. K.E. Shuler, J.Chem.Phys., 21, 624, (1953).

24. E. Teller, J.Phys.Chem., 41, 109, (1937).

25. K.R. Naqvi and W. Byers Brown, Int.J.Quantum Chem., 6, 271, (1972), and K.R. Naqvi, Chem.Phys.Lett., 15, 634, (1972).

26. G.J. Hoytink, Chem.Phys.Lett., 34, 414, (1975).

27. H.C. Longuet-Higgins, Proc.R.Soc. Lond. A 344, 147, (1975).

28. G.H. Herzberg and H.C. Longuet-Higgins, Disc.Far.Soc., 35, 77, (1963).

29. J.R. Wiesenfeld, Chem.Phys.Lett., 45, 384, (1977).

30. A. Persky, J.Chem.Phys., 59, 5578, (1973) and M.J. Berry, J.Chem. Phys. 59, 6229, (1973).

31. D.A. Dixon, D.D. Parrish and D.R. Herschbach, Far.Disc.Chem.Soc., No.55, 385, (1973).

32. R.D. Levine and R.B. Bernstein "Molecular Reaction Dynamics". Clarendon Press, 1974.

33. J.C. Polanyi and D.C. Tardy, J.Chem.Phys., 51, 5717, 1969.

34. C.A. Parr, J.C. Polanyi and W.H. Wong, J.Chem.Phys., 58, 5, (1973) and references therein.

35. M.J. Berry, J.Chem.Phys., 59, 6229, (1973) and references therein.

36. R.D. Levine and R.B. Bernstein, Accounts Chem.Res., 7, 393, (1974).

37. S.R. Leone, R.G. Macdonald and C.B. Moore, J.Chem.Phys., 63, 4735, (1975).

38. I.W.M. Smith, Chem.Phys.Lett., 47, 219, (1977).

39. I.W.M. Smith, Specialist Periodical Reports, "Reaction Kinetics", ed. P.G. Ashmore and R.J. Donovan, 2, 1, (1977).

40. J.C. Tully, J.Chem.Phys., 60, 3042, (1974).

41. F. Rebentrost and W.A. Lester, Jr., J.Chem.Phys., 63, 3737, (1975).

42. H.F. Krause, S.G. Johnson, G. Dayz, F.K. Schmidt-Bleek, Chem. Phys.Lett., 31, 577, (1975).

43. E.E. Nikitin, "Theory of Elementary Atomic and Molecular Processes", Clarendon Press, (1974).

44. L.D. Landau, Physik Z. Sovjetunion 2, 46, (1932).

45. C. Zener, Proc.Roy.Soc., A137, 696, (1932).

46. E.C.G. Stückelberg, Helv.Phys.Acta, 5, 369, (1932).

47. E.E. Nikitin and S.Ya.Umanski, Far.Disc.Chem.Soc. 53, 1 (1972).

48. V.K. Bykhovskii and E.E. Nikitin, Opt.Sprectrosc. 16, 111, (1964).

49. R.D.H. Brown, G.P. Glass and I.W.M. Smith, Chem.Phys.Lett., 32, 517, (1975).

50. E.E. Nikitin, J.Chem.Phys., 43, 744, 1965.

51. E. Bauer, E.R. Fisher and F.R. Gilmore, J.Chem.Phys., 51, 4173, (1969).

52. J.L. Magee and T.Ri, J.Chem.Phys., 9, 638, (1941).

53. M. Polanyi, "Atomic Reactions" ed. Williams and Norgate, (London), (1932).

54. J.L. Magee, J.Chem.Phys., 8, 687, 1940.

55. E.A. Gislason and J.G. Sachs, J.Chem.Phys., 62, 2678, (1975).

56. J.R. Barker, Chem.Phys., 18, 175, (1976).

57. J.R. Barker and R.E. Weston Jr., Chem.Phys.Lett., 19, 235, (1973).

58. J.R. Barker and R.E. Weston Jr., J.Chem.Phys., 65, 1427, (1976).

59. R.J. Donovan and W.H. Breckenridge, Chem.Phys.Lett., 11, 520, (1971).

60. J.P. Simons, C. Boxall and P.W. Tasker, Faraday Discuss.Chem.Soc., No.53, 182, (1972).

61. P.D. Gait, Chem.Phys.Lett., 35, 72, (1975).

62. J.J. Deakin and D. Husain, J.C.S. Faraday II, 68, 1603, 1972.

63. T.L. Cottrell, "The Strengths of Chemical Bonds", Butterworths, (1958).

64. R.J. Butcher, R.J. Donovan and R.H. Strain, J.C.S. Faraday II, 70, 1837, (1974).

65. R.J. Donovan, R.H. Strain, and J.McLean, Chem.Phys.Lett., 20, 504, (1973).

66. R.J. Donovan and D.J. Little, J.C.S. Faraday II, 69, 952, (1973).

67. J.R. Wiesenfeld, Chem.Phys.Lett. 21, 517, (1973).

68. D. Husain and J.G.F. Littler, J.C.S. Faraday II, 69, 842, (1973).

69. J.J. Ewing, D.W.Trainor, J. Yatsiv, J.Chem.Phys., 61, 4433, (1974).

70. E. Walentynowicz, R.A. Phaneuf and L. Krause, Canad.J.Phys., 52, 539, (1974).

71. E. Walentynowicz, R.A. Phaneuf, W.E. Baylis and L. Krause, Canad. J.Phys., 52, 584, (1974).

72. E.H. Fink, B. Wallach and C.B. Moore, J.Chem.Phys., 56, 3608, (1972).

73. K. Kear and W. Abrahamson, J.Photochem., 3, 409, (1974-75).

74. F. Stuhl and H. Niki, Chem.Phys.Lett., 7, 473, (1970).

75. M. Braithwaite, J.A. Davidson and E.A. Ogryzlo, J.Chem.Phys., 65, 771, (1976).

76. M. Braithwaite, E.A. Ogryzlo, J.A. Davidson and H.I. Schiff, J.C.S. Faraday II, 72, 2075, (1976).

77. R.N. Schwartz, Z.I. Slawsky and K.F. Herzfeld, J.Chem.Phys., 20, 1591, (1952).

78. F.H. Mies, J.Chem.Phys., 42, 2709, (1965).

79. D. Rapp and T. Kassal, Chem.Rev., 69, 61, (1969).

80. P.G. Dickens, J.W. Linnet and O. Sovers, Disc.Faraday Soc., 33, 52, (1962).

81. M. Braithwaite, E.A. Ogryzlo, J.A. Davidson and H.I. Schiff, Chem.Phys.Lett., 42, 158, (1976).

82, R.D. Sharma and C.W. Kern, J.Chem.Phys., 55, 1171, (1971).

83. B.H. Mahan, J.Chem.Phys., 46, 98, (1967).

84. C.B. Moore in "Adv.Chem.Phys.", 23, 41, (1973).

85. R.D. Sharma and C.A. Brau, J.Chem.Phys., 50, 924, (1969).

86. R.D. Sharma, Phys.Rev., A2, 173, (1970).

87. R.J. Cross, Jr. and R.G. Gordon, J.Chem.Phys., 45, 3571, (1966).

88. C.G. Gray and J.van Kranendock, Can.J.Phys., 44, 2411, (1966).

89. T.A. Dillon and J.C. Stephenson, Phys.Rev., A6, 1460, (1972).

90. T.A. Dillon and J.C. Stephenson, J.Chem.Phys., 58, 2056, (1973).

91. R.D. Sharma, R.B. Malt, R.R. Hart and R.H. Picard, Chem.Phys.Lett., 35, 286, (1975).

92. L.A. Melton and W. Klemperer, J.Chem.Phys., 59, 1099, (1973).

93. R.G. Gordon and Y. Chiu, J.Chem.Phys., 55, 1469, (1971).

94. W.H. Breckenridge, R.P. Blickensderfer and J. Fitzpatrick, J.Phys.Chem., 80, 1963, (1976).

95. J.J. Ewing, Chem.Phys.Lett., 29, 50, (1974).

96. N.P.D. French and K.P. Lawley, Chem.Phys., 22, 105, (1977).

97. R.A. Beyer and W.C. Lineberger, J.Chem.Phys., 62, 4024, (1975).

98. Y.N. Chiu, J.Chem.Phys., 55, 5052, (1972).

99. H.A. Rabitz and R.G. Gordon, J.Chem.Phys., 53, 1831, (1970).

100. I.H. Zimmerman and T.F. George, J.Chem.Phys., 61, 2468, (1974).

101. I.H. Zimmerman and T.F. George, J.Chem.Phys., 63, 2109, (1975).

102. I.H. Zimmerman and T.F. George, J.C.S. Faraday II, 71, 2030, (1975).

103. I.H. Zimmerman and T.F. George, Chem.Phys., 7, 323, (1975).

104. Z.H. Top and M. Baer, J.Chem.Phys., 66, 1363, (1977).

105. F. Rebentrost and W.A. Lester, Jr., J.Chem.Phys., 64, 4223, (1976).

106. R.J. Gordon, J.Chem.Phys., 65, 4945, (1976).

107. M.D. Patengill, Chem.Phys.Lett., 36, 25, (1975).

108. J.N.L. Connor, Chem.Soc.Rev., 15, 125, (1976).

109. J.N.L. Connor, Chem.Phys.Lett., 25, 611, (1974).

110. W.R. Gentry and C.F. Giese, J.Chem.Phys., 63, 3144, (1975).

111. M. Baer, Chem.Phys.Lett., 35, 112, (1975).

112. J.P. Toennies, in Ann.Rev.Phys.Chem., 27, 225, (1976).

113. M. Baer, Chem.Phys., 15, 49, (1976).

114. R.G. Gordon, Disc.Far.Soc., 55, 22, (1973).

115. R.G. Gordon, W. Klemperer and J.I. Steinfeld, in Ann.Rev.Phys.Chem., 19, 215, (1968).

116. B. Gelernt, S.V. Filseth, T. Carrington, J.Chem.Phys., 65, 4940, (1976).

117. M.S. Child, "Molecular Collision Theory", Academic Press, London and New York (1970).

118. S.R. Leone and C.B. Moore, in "Chemical and Biological Applications of Lasers" ed. by C.B. Moore, Academic Press, (1973).

119. C.B. Moore, Adv.Chem.Phys., 22, 41, 1973.

120. S.R. Leone and F.J. Wodarczyk, J.Chem.Phys., 60, 314, (1974).

121. M.A. West, in "Photochemistry", 6, 62, (1975).

122. G. Porter and M.A. West, in "Investigation of Rates and Mechanisms of Reactions", 3rd edition part II, Editor G.G. Hammes, Vol.VI,

Wiley Interscience (1973).

123. M.A.A. Clyne, in "Physical Chemistry of Fast Reactions", ed. B.P. Levitt, Plenum Press, N.Y., 1, 253, (1973).

124. M.A.A. Clyne and A.H. Curran, Specialist Periodical Reports, Gas Kinetics and Energy Transfer", eds. P.G. Ashmore and R.J. Donovan, 2, 239, (1977).

125. R.G.W. Norrish and G. Porter, Nature, 164, 658, (1949).

126. H.M. Gillespie, R.J. Donovan and in part R. Strain, (in press).

127. M.C. Lin and R.G. Shortbridge, Chem.Phys.Lett., 29, 42, (1974).

128. G.P. Quigley and G.J. Wolga, J.Chem.Phys., 62, 4560, (1975).

129. T.W. Hänsch, in Topics in Applied Physics "Dye Lasers", ed. F.P. Schäfer, 1, 194, (1973).

130. A.B. Petersen, L.W. Braverman and C. Wittig, J.Appl.Phys., 48, 230, (1977)

131. A.Hariri, A.B. Petersen and C. Wittig, J.Chem.Phys., 65, 1872, (1976).

132. A.B. Petersen, C. Wittig, and S.R. Leone, Appl.Phys.Lett., 27, 305, (1975).

133. D. Secrest, Ann.Rev.Phys.Chem., 24, 379, (1973).

134. M.G. Stock, D.J. Little, R.J. Donovan, J.Chem. Ed., 51, 51, (1974).

135. LWM.Smith and R. Zellner, J.C.S. Faraday II, 69, 1617, (1974).

136. P.P. Bemand and M.A. Clyne, J.C.S. Faraday II, 69, 1643, (1973).

137. D.H. Burde, R.A. McFarlane and J.R. Wiesenfeld, Chem.Phys.Lett., 32, 296, (1975).

138. C.E. Moore, Ed., "Atomic Energy Levels,"NBS Circular 467, Washington D.C., (1958).

139. R.H. Garstang, J.Res.Nat.Bur.Stand A, 68, 61, (1964).

140. R.S. Derwent and B.A. Thrush, Chem.Phys.Lett, 9, 591, (1971).

141. V.S. Zuev, V.A. Katulin, V.Yu.Noscach and O.Yu.Noscach, Sov.Phys., JEPT, 35, 870, (1972).

142. V. Jaccarino, J.G. King, R.A. Satten and H.H. Stroke, Phys.Rev., 94, 1798, (1954).

143. P.P. Bemand and M.A.A. Clyne, J.C.S. Faraday II, 72, 191, 1976.

144. T. Donohue and J.R. Wiesenfeld, Chem.Phys.Lett., 33, 176, (1975).

145. T. Donohue and J.R. Wiesenfeld, J.Chem.Phys., 63, 3130, (1975).

146. J.W. Boag, Photochem and Photobiol., 8, 565, (1968).

147. D.J. Little, Ph.D. Thesis, University of Edinburgh, (1974).

148. "An Introduction to the photomultiplier", EMI photomultiplier tubes brochure.

149. J.W. Hunt and J.K. Thomas, Rad.Res., 32, 149, (1967).

150. R.H. Strain, Ph.D. Thesis, University of Edinburgh, (1977).

151. W. Braun and T. Carrington, J. Quant.Spectr.Rad.Transf., 9, 1133, (1969).

152. F. Kaufman and D.A. Parker, Trans.Far.Soc., 66, 1579, (1970).

153. J.V.V. Kasper, J.H. Parker and G.C. Pimentel, J.Chem.Phys., 43, 1827, (1965).

154. K. Hohla and K.L. Kompa, Appl.Phys.Lett., 22, 77, (1973).

155. K. Hohla, G. Brederlow, W. Fuss, K.L. Kompa, J. Raeder, R. Volk, S. Witkowski and K.J. Witte, J.App.Phys., 46, 808, (1975).

156. S.J. Riley and K.R. Wilson, Disc.Far.Soc., 53, 32, (1972).

157. R.J. Donovan, F.G.M. Hathorn and D. Husain, Trans.Faraday Soc., 64, 3192, (1968).

158. S. Aditya and J.E. Willard, J.Chem.Phys., 44, 418, (1966).

159. D.M. Haaland and R.T. Meyer, Int.J.Chem.Kinet., 6, 297, (1974).

160. F.K. Truby and J.K. Ric, Int.J.Chem.Kinet., 5, 721, (1973).

161. E.W. Abrahamson, L.J. Andrews, D. Husain and J.R. Wiesenfeld, J.C.S. Faraday II, 68, 48, (1972).

162. J.E. Griffiths and A.L. Beach, Can.J.Chem., 44, 1227, (1966).

163. V. Yu.Zalesskii, Sov.Phys. - JETP, 34, 474, (1972).

164. C.C. Davis, R.J. Pirkle, R.A. McFarlane, G.J. Wolga, IEEE J.Quant. Elec., 12, 334, (1976).

165. R.E. Palmer and T.D. Padrick, J.Chem.Phys., 64, 2051, (1976).

166. R.J. Donovan and C. Fotakis, J.Chem.Phys., 61, 2159, (1974).

167. R.T. Meyer, J.Phys.Chem., 72, 1583, (1968).

168. G. Karl, P. Kruus and J.C. Polanyi, J.Chem.Phys., 46, 224, (1967).

169. J.M. Farrar and Y.T. Lee, J.Am.Chem.Soc., 96, 7570, (1974).

170. J.J. Valentini, M.J. Coggiola and Y.T. Lee, Far.Disc.Chem.Soc., 62, 232, (1977).

171. R.L. Strong, and J.A. Kaye, J.Am.Chem.Soc., 98, 5460, (1976).

172. B.J. Cocksey, J.H.D. Eland and C.J. Danby, J.Chem.Soc. B,790, (1971).

172a V.J. Vedeneyev, L.V. Gurvitch, V.N. Kondratev, V.A. Medvedev and Ye.L. Frankevitch, "Bond energies, Ionization Potentials and Electron Affinities , Edwards Arnold publishers, L.T.D.(London), (1966).

173. R.G. Miller and E.K.C. Lee, Chem.Phys.Lett., 41, 52, (1976).

174. G. Herzberg, "I.R. and Raman Spectra of Polyatomic Molecules", D.Van Nostrand Co. Inc., Princeton, New Jersey (1956).

175. E.W. Jones, R.J.L. Popplewell and H.W. Thomson, Proc.Roy.Soc., A288, 39, (1965).

176. "American Institute of Physics Handbook", 3rd Edition, McGraw Hill Co. London (1972).

177. H.R. Rinton and E.R. Nixon, Spectrochim.Acta, 12, 41, (1958).

178. Y.B. Band and K.F. Freed, J.Chem.Phys., 63, 4479, (1975).

179. O. Atabek, J.A. Beswick, and R. Lefebre, J.Chem.Phys., 4035, (1976).

180. R.E. Weston, Jr. and H.A. Schwarz, "Chemical Kinetics", Prentice-Hall, Inc., New Jersey (1972).

181. E.A. Andreev and E.E. Nikitin, Theoret.Chim.Acta, 17, 171, (1970).

182. R.J. Donovan, C. Fotakis and H.M. Gillespie, J.Photochem., 6, 193, (1977).

183a E.A.V. Ebsworth in "Organometallic Compounds of group IV Elements", ed. A.G. MacDiarmid, Vol.1 (1968).

b F.A. Cotton and G. Wilkinson "Advanced Inorganic Chemistry" 3rd edition (1972), Interscience.

184. G.C. Fettis and J.H. Knox, in"Progress in Reaction Kinetics", ed. G. Porter, 2, 1, (1964).

185. A.B. Callear and J.H. Wilson, Trans.Faraday Soc., 63, 1983, (1967).

186. A.C.G. Mitchell and M.W. Zemansky, "Resonance Radiation and Excited Atoms", Cambridge University Press, (1971).

187. C.K.N. Patel, in "Lasers" Vol.2, ed. A.K. Levine, Edward Arnold publishers L.T.D., (1968).

188. D. Porret and C.F. Goodeve, Proc.Roy.Soc. (London), A165, 31, (1938).

189. M. Kawasaki, S.J. Lee, and R. Bersohn, J.Chem.Phys., 63, 809, (1975).

190. G. Hertzberg, "Electronic Spectra and Electronic Structure of Polyatomic Molecules", Van Nostrand Reinhold Co. (1966).

191. J.P. Simons, "Photochemistry and Spectroscopy", Wiley Interscience,(1971).

192. M.J. Dzvonik, S. Yang and R. Bersohn, J.Chem.Phys., 61, 4408, (1974).

193. A.B. Nikolskii, Opt.Spectrosc., 29, 560, (1970).

194. R.J. Butcher, R.J. Donovan, C. Fotakis, D. Fernie and A.G.A. Rae, Chem.Phys.Lett., 30, 398, (1975).

195. K. Hohla and K.L. Kompa, Chem.Phys.Lett., 14, 445, (1972).

196. R.E. Palmer and M.A. Gusinow, J.Appl.Phys., 45, 2174, (1974).

197. F.T. Aldridge, Appl.Phys.Lett., 22, 180, (1973).

198. K. Bergmann, S.R. Leone and C.B. Moore, J.Chem.Phys., 63, 4161, (1975).

199. A.T. Pritt,Jr, and R.D. Coombe, J.Chem.Phys., 65, 2096, (1976).

200. F.J. Wodarczyk and P.B. Sackett,Chem.Phys., 12 65, (1976).

201. J.J. Deakin and D. Husain, J.C.S. Faraday II, 68, 41, (1972).

202. A.T. Pritt, Jr, and R.D. Coombe, J.Chem.Phys., 65, 2096, (1976).

203. J.R.Wiesenfeld, and G.L. Wolk,J.Chem.Phys., 67, 509, (1977).

204. R.J. Donovan and D. Husain, Trans.Far.Soc., 62, 1050, (1966).

205. R.J. Donovan and D. Husain, Trans.Far.Soc., 62, 2023, (1966).

206. D.H. Burde and R.A. McFarlane, J.Chem.Phys., 64, 1850, (1976).

207. P.L. Houston, Chem.Phys.Lett., 47, 137, (1977).

208. K.C. Kim, D.W. Setser and C.M. Bogan, J.Chem.Phys., 61, 2159, (1974).

209. W.S. Benedict, M.A. Pollack and W.J. Thomson, IEEE, J.Quant.Electr., 5, 1681, (1969).

210. W.S. Benedict, N. Gailar and E.K. Plyler, J.Chem.Phys., 24, 1139, (1956).

211. S. Pinchas and I. Laulicht, "I.R. Spectra of Labelled Compounds", Academic Press, (1971).

212. R.A. Toth and J.S. Margolis, J.Mol.Spec., 55, 229, (1975).

213. P.J. Wyatt, V.R. Stull and G.N. Plass, Appl.Opt., 3, 229, (1964).

214. C.C. Ferriso, C.B. Ludwig and A.L. Thomson, J.Quant.Spec.Radial. Transfer, 6, 241, (1966).

215. NBS Monograph 71, "Line parameters and computed spectra for H_2O Vapor Band at 2.7 μm, U.S. Dept. of Commerce.

216a I.M. Mills, H.W. Thomson and R.L. Williams, Proc.Roy.Soc., A218, 29, (1953).

b E.K. Plyler and E.D. Tidwell, Z. Electrochem., 64, 717, (1960).

217. D.H. Rank, D.P. Eastman, B.S. Rao and T.A. Wiggins, J.Opt.Soc.Amer, 52, 1, (1962).

218. M.E. Rose, "Elementary Theory of Angular Momentum", Chapman and Hall Ltd., (1957).

219. H. Margenau and N.R. Kestner, "Theory of Intermolecular Forces", Pergamon (1971).

220. H. Margenau, Rev.Mod.Phys., 1, 1, (1939).

221. S.M. Naudé and H. Verleger, Proc.Phys.Soc.London, A63, 470, (1950).

222. F.L. Keller and A.H. Nielsen, J.Chem.Phys., 22, 294, (1954).

223. R.J. Donovan, C. Fotakis and M.F. Golde, J.C.S. Faraday II, 72, 2055, (1976)

224. J.C. Evans and G.Y-S Lo, J.Phys.Chem., 70, 543, (1966).

225. J.J. Deakin and D. Husain, J.Photochem., 1, 353, (1973).

226. D.R. Herschbach, Faraday Discussions, 55, 233, (1973).

227. B.C. Eu, Mol.Phys., 31 1261, (1976).

228. M. Kimura, Chem.Phys.Lett., 45, 489, (1977).

229. A.H. Nielsen and H.H. Nielsen, Phys.Rev., 47, 585, (1935).

230. C.A. Burrus and W. Gordy, Phys.Rev., 92, 1437, 1953, and E.D. Palik, J.Chem.Phys., 23 217, (1955).

231. K. Bergmann and C.B. Moore, J.Chem.Phys., 63, 643, (1975).

232. V. Dinur and R.D. Levine, Chem.Phys.Lett., 31 410, (1975).

233. I.W.M. Smith, J.C.S. Faraday II, 71, 1970, (1975).

234. J.O. Hirschfelder, C.F. Curtiss and R.B. Bird, "Molecular Theory of Gases and Liquids", John Wiley and Sons, Inc, 1954.

235. W. Benesch, J.Chem.Phys., 39, 1048, (1963).

236. C. Wittig, private communication.

237. S.H. Lin and R. Bersohn, J.Chem.Phys., 48, 2732, (1968).

238. D.H. Richman, M. Lev-on and R.C. Millikan, Int.J.Chem.Kin., 7, 33, (1975).

239. M. Lev-on, W.E. Palke, R.C. Millikan, Int.J.Chem.Kin., 5, 753, (1973).

240. W.G. Tam, Chem.Phys.Lett., 15, 113, (1972).

241. M. Abramowitz and I.A. Stegun, "Handbook of mathematical functions", Dover, (1965).

242. G. Arfken, "Mathematical methods for physicists", 4th pr., Academic press, (1968).

243. C.J. Tranter, "Bessel functions with some physical applications", Appl.Math.Ser., (1968).

244. R.H. Garstang, J.Res.Nat.Bur.Std., 68A, 61, (1964).

245. A. Birnhaum and J.D. Poll, J.Atm.Sci., 26, 943, (1969).

246. A. Dalgarno, A.C. Allison and J.C. Browne, J.Atm.Sci., 26, 946, (1969).

247. R.E. Meredith and F.G. Smith, J.Quant.Spec.Rad.Transfer, 13, 89, (1973).

248. R.N. Sileo and T.A. Cool, J.Chem.Phys., 65, 117, (1976).

249. F.G. Smith, J.Quant.Spec.Rad.Transfer, 13, 717, (1973).

250. R.D. Sharma, M.L. Chen, and A. Szöke, J.Chem.Phys., 58, 3519, (1973), and references therein.

251. A.R.W. McKellar, Can.J.Phys., 52, 1144, (1974).

252. L.Y. Chow Chiu, Chem.Physics, 16, 269, (1976).

253. J.B. Mann, J.Chem.Phys., 46, 1646, (1967).

254. "Handbook of Chemistry and Physics", CRC Press, 55th edition (1974).

255. S.P. Reddy and C.W. Cho, Can.J.Phys., 43, 793, (1965).

256. Y.C. Wong and Y.T. Lee, J.Chem.Phys., 60, 4619, (1974).

257. W.J. Moore, "Physical Chemistry", Longman, 5th edition, (1974).

258. S.S. Penner, "Quantitative molecular spectroscopy and gas emissivities", Pergamon press (1959).

259. J.R. Wiesenfeld and G.L. Wolk, J.Chem.Phys., 65, 1506, (1976).

260. M.J. Bevan and D. Husain, J.Phys.Chem., 80, 217, (1976).

261. M.J. Bevan and D. Husain, J.Photochem., 4, 51, (1975).

262. D.W. Trainor, J.Chem.Phys., 66, 3094, (1977).

263. P.D. Foo, J.R. Wiesenfeld, M.J. Yuen, J.Phys.Chem., 80, 91, (1976).

264. D.W. Trainor and J.J. Ewing, J.Chem.Phys., 64, 222, (1976).

265. J.A. Bellisio and P.Davidovits , J.Chem.Phys., 53, 3474, (1970).

266. N.P.D. French, Ph.D. Thesis, University of Edinburgh, (1977).

LECTURES ATTENDED

In accordance with the regulations of the University of Edinburgh Department of Chemistry, the post-graduate lecture courses e.t.c. attended during the period of study are listed here.

They were: 1) Quantum Theory of Scattering 2) Molecular Energy Transfer 3) Interactive Computing 4) Vibrational Spectroscopy 5) Chemistry of the Atmosphere 6) Quantum Optics.

In addition, many of the regular departmental seminars in the Chemistry Department and the Spectroscopy and Molecular Beam groups joined meetings were attended.

Finally during the course of this study the following **Conferences** were attended: 1) The 7th National Atomic and Molecular Physics Conference (Edinburgh, April 1975), 2) The International School of Quantum Electronics on Molecular Spectroscopy and Photochemistry with Lasers (Erice, Italy, June-July 1975), 3) The 4th International Conference on Gas Kinetics (Edinburgh, August 1975), 4) The Faraday Discussion on Potential Energy Surfaces (Brighton, September 1976), 5) The Gordon Conference on Molecular Energy Transfer (Wolfeboro, USA, July 1977), 6) Many meetings of the Gas Kinetics Discussion Group.

PUBLISHED WORK

The papers published in connection with the present work are bound in the following pages.

They were:

1) "Isotope effects in the quenching of electronically excited atoms: Photolysis of CD_3I", J.Chem.Phys., 61, 2159, (1974).

2) "Photodissociation laser isotope effects", Chem.Phys.Letters, 30, 398, (1975).

3) "Isotope effects in the quenching of electronically excited atoms", J.C.S. Faraday II, 72, 2055, (1976).

4) "Primary and Secondary processes in the photolysis of GeH_3I", J.Photochem., 6, 193, (1977).

The Journal of Chemical Physics, Vol. 61, No. 5, 1 September 1974

Letters to the Editor

Isotope effects in the quenching of electronically excited atoms: Photolysis of CD_3I

R. J. Donovan and C. Fotakis

Department of Chemistry, University of Edinburgh, West Mains Road, Edinburgh, Scotland
(Received 19 June 1974)

There has been renewed interest in the photochemistry of alkyl and perfluoroalkyl iodides owing to their use in high powered photochemical lasers,[1-3] and the potential application of such lasers to the fusion research program.[3] An interesting feature of the output from alkyl iodide lasers is the marked difference in power as a function of iodide pressure, when alkyl and perfluoroalkyl iodides are compared.[4] The output power from the lower alkyl iodides passes through a maximum at relative low pressures (typically ~20 Torr) while the output from perfluoro alkyl iodides continues to rise significantly well beyond this point (≳120 Torr). The reason for this behavior is known to be associated with the higher efficiency for removal of $I(5^2P_{1/2})$ by the alkyl iodides.[5] However a controversy remains regarding the relative efficiencies for the quenching and reactive channels:

$$I(5^2P_{1/2}) + CH_3I \rightarrow CH_3\cdot + I_2 \quad , \tag{1}$$

$$I(5^2P_{1/2}) + CH_3I \rightarrow I(5^2P_{3/2}) + CH_3I \quad . \tag{2}$$

Haaland and Meyer[6] have recently redetermined k_1 using time resolved mass spectroscopy and report a value of $k_1 = (1.0 \pm 0.6)\ 10^{-14}$ cm^3 molecule$^{-1}\cdot$ s^{-1} (over the temperature range 316–447 K). This conflicts with previous work,[7] and with the work of Aditya and Willard[8] when combined with data[9] for $k_1 + k_2$, which yield $k_1 \leqslant 3\times10^{-16}$ cm^3 molecule$^{-1}\cdot$ s^{-1}.

We here report the results of our most recent work which exploits the large isotope effects observed in the quenching of some excited atoms and small molecules,[10-12] and which demonstrates that $k_1 \leqslant 2.7\times10^{-2}\, k_2$.

The total rates for removal ($k_1 + k_2$) of $I(5^2P_{1/2})$ by CH_3I and CD_3I were determined (at 293 K) using time resolved atomic absorption spectrophotometry[9] ($\lambda = 206.2$ nm). The result for CH_3I ($k_1 + k_2 = (2.6 \pm 0.6)\ 10^{-13}$ cm^3 molecule$^{-1}\cdot$ s^{-1}) was found to be in good agreement with previous work.[9] The result for CD_3I, which has not previously been determined,[13] was found to be very significantly less than that for CH_3I [$k_1' + k_2' = (4.6 \pm 0.8)\ 10^{-15}$ cm^3 molecule$^{-1}\cdot$ s^{-1}]. The rate constant for Channel (1) is expected to be almost identical for the isotopomers CH_3I and CD_3I, as the potential surface and C–I bond dissociation energies are essentially the same. We therefore conclude that $k_1 = k_1' \leqslant 5.4\times10^{-15}$ cm^3 molecule$^{-1}\cdot$ s^{-1}. Whilst this is consistent with the lower bound given by Haaland and Meyer,[6] it requires that removal of $I(5^2P_{1/2})$ by CD_3I occurs almost exclusively by Channel (1). It would be interesting therefore if the experiments employing time resolved mass spectroscopy could be repeated using CD_3I.

Finally, we feel that the large isotope effects observed here, and in our previous work,[10,11] are of considerable significance to the field of radiation chemistry and other studies in which electronically excited states are involved. Thus, isotopic substitution is frequently used as a means of determining the mechanism by which reactions occur. Our results show that such substitutions can lead to a marked change in the efficiency for quenching channels and can thus influence the proportional decay by other channels, including reactive channels.

[1] J. V. V. Kasper and G. C. Pimentel, Appl. Phys. Lett. 5, 231 (1964).
[2] J. V. V. Kasper, J. H. Parker and G. C. Pimentel, J. Chem. Phys. 43, 1827 (1965).
[3] K. Hohla and K. L. Kompa, Appl. Phys. Lett. 22, 77 (1973).
[4] M. A. Pollack, Appl. Phys. Lett. 8, 36 (1966).
[5] D. Husain and R. J. Donovan, Adv. Photochem. 8, 1 (1971).
[6] D. M. Haaland and R. T. Meyer, Int. J. Chem. Kinet. 6, 297 (1974).
[7] R. J. Donovan, F. G. M. Hathorn and D. Husain, Trans. Faraday Soc. 64, 3192 (1968).
[8] S. Aditya and J. E. Willard, J. Chem. Phys. 44, 418 (1966).
[9] M. G. Stock, D. J. Little, and R. J. Donovan, J. Chem. Educ. 51, 51 (1974).
[10] R. H. Strain, J. McLean, and R. J. Donovan, Chem. Phys. Lett. 20, 504 (1973).
[11] R. J. Butcher, R. J. Donovan, and R. H. Strain, J. Chem. Soc. Faraday Trans. II (to be published).
[12] P. B. Merkel and D. R. Kearns, J. Am. Chem. Soc. 94, 7244 (1972).
[13] The first experiments indicating that CD_3I is significantly less efficient than CH_3I in removing $I(5^2P_{1/2})$ where carried out using a chemical laser, in this laboratory, and will be reported in the near future.

PHOTODISSOCIATION LASER ISOTOPE EFFECTS

R.J. BUTCHER, R.J. DONOVAN, C. FOTAKIS
Department of Chemistry, University of Edinburgh, Edinburgh, UK

and

D. FERNIE and A.G.A. RAE
Department of Physics, University of Edinburgh, Edinburgh, UK

Received 23 September 1974

Marked differences in the laser action (1.315 μm) observed following the flash photolysis of CD_3I and CH_3I are reported (substantially greater outputs are observed with CD_3I). These differences result from the significantly smaller cross section for quenching of $I(5\,^2P_{1/2})$ by CD_3I, relative to that for CH_3I. Absolute values for the quenching cross sections have been determined using time resolved atomic absorption spectrophotometry. These data were employed in a computer simulated model which satisfactorily reproduced the light output from CH_3I, CD_3I and CF_3I photochemical laser systems. It is concluded that isotopic substitution can markedly influence the cross section for quenching of an excited state and thus influence partitioning between the various available channels.

1. Introduction

There has been renewed interest in the iodine atom photodissociation laser, first reported by Kasper and Pimentel [1], and based on the process

$$I(5\,^2P_{1/2}) \rightarrow I(5\,^2P_{3/2}) + h\nu(1.315\ \mu m),$$

particularly with regard to the generation of high power output [2–4]. Gigawatt pulses have recently been reported [4], suggesting that the iodine atom laser may be suitable for applications in nuclear fusion research.

It is well established that substantially higher laser output can be achieved when perfluoro-alkyl iodides are used in place of the corresponding alkyl iodides [5]. This difference is attributed to the higher cross section for removal of $I(5\,^2P_{1/2})$ by alkyl compared with perfluoro-alkyl iodides [6]. Removal of $I(5\,^2P_{1/2})$ may occur by both reactive and inelastic channels:

$$I(5\,^2P_{1/2}) + CH_3I \xrightarrow{k_1} I(5\,^2P_{3/2}) + CH_3I,$$
$$\Delta H = -0.94\ \text{eV}; \qquad (1)$$

$$I(5\,^2P_{1/2}) + CH_3I \xrightarrow{k_2} I_2 + CH_3,$$
$$\Delta H = -0.15\ \text{eV}. \qquad (2)$$

It is now established that channel (1) is dominant for the removal of $I(5\,^2P_{1/2})$ at 300 K and that $k_1 > 4k_2$; however, there is disagreement over the magnitudes of k_1 and k_2. Haaland and Meyer [7] have employed time resolved mass spectrometry to investigate the photolysis of CH_3I and report $k_2 = (1.0 \pm 0.6) \times 10^{-14}$ cm^3 $molecule^{-1}$ s^{-1} but results obtained using other techniques support a significantly lower value [8]. Furthermore, it is clear [9] that $k_2\,(CF_3I) \leqslant 4.1 \times 10^{-16}$ cm^3 $molecule^{-1}$ s^{-1}, and in view of the weaker [10] C–I bond in CF_3I, compared with CH_3I it would be surprising if the rate constant for reaction were very much greater for the latter.

We have recently reported the observation of large isotope effects in the quenching of electronically excited atoms [11–13] and have discussed them with respect to the availability of resonant energy transfer channels [13]. Thus for example, the cross section for quenching of $I(5\,^2P_{1/2})$ by CH_4 is almost two or-

ders or magnitude greater [12] than for CD_4. We have therefore examined the photolysis of CD_3I to see if similar large isotope effects are observed for the removal of $I(5\,^2P_{1/2})$ and to determine whether such effects can significantly influence the output of photochemical lasers.

2. Experimental

The experimental arrangement employed for the photochemical laser studies was of conventional design. A quartz flash lamp and photolysis cell, both 1 m in length and 15 mm o.d., were placed parallel and optically coupled using aluminium foil. Microscope slides, set at the Brewster angle, were used as end windows for the laser tube. The mirrors forming the optical cavity were gold coated for total reflection in the near infrared, and a small (0.5 mm) hole in one mirror was used to couple out a fraction of the radiation. One of the mirrors used had a radius of curvature of 1.5 m while the other was a plane mirror (having the coupling hole): the mirrors were placed 1.1 m apart thus forming a stable configuration. An indium antimonide detector (Mullard ORP-10) was used at room temperature and the output observed using a Tektronix 549 series storage oscilloscope.

The experimental arrangement employed for time resolved atomic absorption spectrophotometry has been described in detail previously [14]. To obtain the best possible signal to noise ratio the atomic emission lamp, described previously [14], was replaced by a standard microwave powered version. Data were collected via both a Datalab transient recorder (DL905) and a storage oscilloscope.

Gases were handled with a conventional vacuum line constructed with greaseless high vacuum taps (Young Scientific "O" ring taps) capable of holding a vacuum of better than 10^{-4} N m^{-2}. Particular care was taken to degas the iodides before use.

3. Results and discussion

3.1. Photodissociation laser

Three iodides were investigated with the photodissociation laser (CF_3I, CH_3I and CD_3I) and the laser output examined over a wide range of conditions (pressure of iodide and flash energy). As expected CF_3I and CH_3I were found to differ markedly [5] in their characteristics which may be summarised as follows:

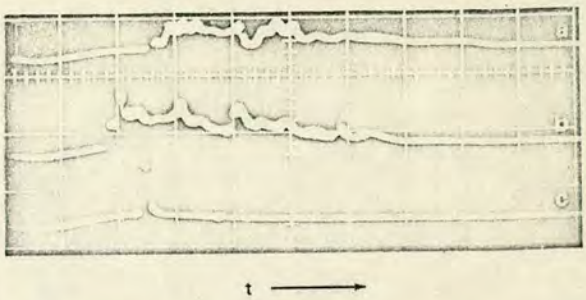

Fig. 1. Laser emission as a function of time, (a) CF_3I (b) CD_3I (c) CH_3I; pressure of iodide = 0.33 kN m^{-2}; flash energy 320 J; horizontal scale 10 μs/div.; vertical scale (a) and (b) 0.1 V/div., (c) 0.05 V/div.

(i) For CF_3I pressures of $\approx 7 \times 10^2$ N m^{-2} and a flash energy of 320 J, a broad envelope of laser emission was observed (from 15–70 μs after the start of the flash), while CH_3I gave only a single spike at ≈ 15 μs under the same conditions.

(ii) As the pressure of CF_3I was reduced the laser action was reduced in duration until at 10^2 N m^{-2} a single spike was observed in the tail of the flash (≈ 60 μs). The threshold pressure for laser action from CH_3I under the same conditions was significantly higher, 3.3×10^2 N m^{-2}, and again only a single spike was observed at ≈ 25 μs.

(iii) Laser action was observed from CF_3I after two or three flashes (i.e., without pumping and refilling the laser tube); however, CH_3I never gave rise to laser action after the first flash under our conditions.

These observations can be accounted for by the large difference in cross section for quenching of $I(5\,^2P_{1/2})$ by CF_3I and CH_3I ($\sigma_{CH_3I} : \sigma_{CF_3I} > 10^3 : 1$). Recent observations reveal similar large differences in quenching cross section when isotopically substituted molecules are compared (e.g., $\sigma_{CH_4} : \sigma_{CD_4} = 50 : 1$ [12]). We therefore examined CD_3I in the photochemical laser. Surprisingly, CD_3I gave a somewhat larger output, even than CF_3I, demonstrating that CD_3I was very much less efficient than CH_3I at quenching $I(5\,^2P_{1/2})$. Fig. 1 illustrates the laser out-

put observed for CF_3I, CH_3I and CD_3I under identical conditions.

3.2. Computer simulation

To obtain a more detailed understanding of the observed differences a computer program was written to simulate the output from the laser as a function of time. A four level model [15] was used (CF_3I, $I(5\,^2P_{1/2})$, $I(5\,^2P_{3/2})$ and I_2). The ratio of $I(5\,^2P_{1/2})$: $I(5\,^2P_{3/2})$ produced by the flash was taken to be 3 : 1, but the computed results were not strongly dependent on this parameter. Simulation was attempted for conditions only a little above threshold so that a comparison could be made with experiments conducted under isothermal (300 K) conditions. Hwang and Kasper [16] have demonstrated the importance of hyperfine splitting in the iodine atom and the mixing between sublevels which occurs in the presence of magnetic fields. In our experiment the parallel flash tube will produce a large time-varying magnetic field and we have therefore used a line-width function which varies with time during the flash. The effect of the time-varying magnetic field will be a minimum in the tail of the flash ($t > 20\ \mu s$) and it is therefore a further advantage to compare experimental and computed results close to threshold as the onset time for laser action then lies outside the main part of the flash. With $k_1 = 4.6 \times 10^{-15}$ cm^3 molecule^{-1} s^{-1} and $k_2 = 10^{-16}$ cm^3 molecule^{-1} s^{-1}, the program reproduced the CD_3I and CF_3I outputs quite well with respect to the gross features and general oscillation of output (the detailed structure observed experimentally varied slightly from flash to flash) and with respect to changes in the flash energy and pressure of iodide. However, the output was not sensitive to the value used for $k_2(k_1)$ in the range $4.6 \times 10^{-15} - 1 \times 10^{-17}$ cm^3 molecule^{-1} s^{-1}, provided that $k_1\,(k_2) = 4.6 \times 10^{-15}$ cm^3 molecule^{-1} s^{-1}. The somewhat higher output observed experimentally for CD_3I may be associated with its higher extinction coefficient, compared with CF_3I, in the ultraviolet.

Results for CH_3I were less satisfactory and the simulation predicted an upper limit to the pressure of CH_3I for which laser action would occur, which was lower than the experimentally observed value. Nevertheless, the simulation for CH_3I did show that the output can be critically dependent on the values chosen for some of the rate constants, and in particular on the value of k_1. Thus as k_1 was varied in the range $10^{-13} - 10^{-14}$ cm^3 molecule^{-1} s^{-1}, marked changes in the simulated output were observed, and while laser action may just occur for $k_1 = 3.3 \times 10^{-13}$ cm^3 molecule^{-1} s^{-1} (just above the upper limit for $k_1 + k_2$ determined here), values greater than this did not result in light amplification. This critical behaviour reflects the restrictive conditions for light amplification observed experimentally with CH_3I.

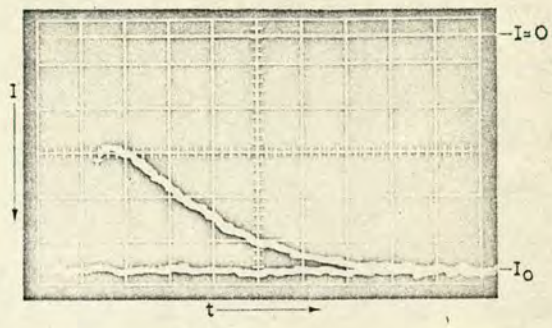

Fig. 2. Decay of $I(5\,^2P_{1/2})$ in the presence of pure CD_3I. (λ = 206.2 nm; horizontal scale = 0.2 ms/division; p_{CD_3I} = 2.7 kN m^{-2}.)

3.3. Time resolved atomic absorption spectrophotometry

To obtain a more precise value for the quenching cross section of CD_3I, the technique of time-resolved atomic absorption spectrophotometry was employed. By observing the attenuation of the atomic resonance line at 206.2 nm ($6s\,^2P_{3/2} \leftarrow 5p^5\,^2P_{1/2}$) as a function of time, following the flash photolysis of a given iodide, the rate constant and hence cross section for quenching of $I(5\,^2P_{1/2})$ can be obtained [14]. The cross sections for quenching by CH_3I and CD_3I were obtained in the present work, using this technique. Experimental conditions were again varied over a wide range (partial pressures of iodide from 13–2.7×10^3 N m^{-2} and flash energies of 20–500 J). The total cross section for removal of $I(5\,^2P_{1/2})$ by CH_3I was found to be in good agreement with recently published data [14]

$$\sigma_{CH_3I} = (8.5 \pm 2.1) \times 10^{-4}\ \text{nm}^2;$$

$$k_1 + k_2 = (2.6 \pm 0.6) \times 10^{-13}\ \text{cm}^3\ \text{molecule}^{-1}\ \text{s}^{-1}.$$

The cross section for CD_3I was found to be about sixty times smaller:

$$\sigma_{CD_3I} = (0.15 \pm 0.03) \times 10^{-4}\ nm^2;$$

$$k_1' + k_2' = (4.6 \pm 0.8) \times 10^{-15}\ cm^3\ molecule^{-1}\ s^{-1}.$$

The decay of $I(5\,^2P_{1/2})$ in pure CD_3I is illustrated in fig. 2. Similar decays were observed for pure CH_3I, but *only* when the partial pressure of CH_3I was 60 times less than that used for the trace shown in fig. 2.

3.4. Isotope effects

We have recently reported large isotope effects for the quenching of electronically excited atoms [11–13]. In all of the cases studied so far, which exhibit large isotope effects, quenching has been the only available channel for removal of the excited atom. When reactive channels are available, e.g., for $Se(4\,^1D_2) + H_2$ and D_2 [17], isotope effects are small, and in the example quoted fall within the experimental error (± 20%). This would suggest that the large difference observed in this work for the isotopomers CH_3I and CD_3I is due to a difference in the cross sections for *quenching*, particularly as the ratio of quenching cross sections is similar to that observed for CH_4 and CD_4. However, the present results do not allow us to rule out the possibility that the observed small cross section for CD_3I is dominated by reactive channels, with the quenching channel representing only a small fraction of the total cross section. The lower limit of Haaland and Meyer's [7] value for k_2 (CH_3I) is just consistent with the upper limit of our data for CD_3I ($< 5.4 \times 10^{-15}$ cm^3 $molecule^{-1}$ s^{-1}). This implies that removal of $I(5\,^2P_{1/2})$ by CD_3I occurs predominantly via the *reactive channel*. Further work to determine the ratio of reactive to quenching cross sections is desirable as the implications are rather interesting. Thus for example, if the reactive channel is dominant for CD_3I, the initial quantum yield for photolysis of CD_3I should be close to two, while that for CH_3I would be unity. Whether or not this actually proves to be the case, following more detailed investigation, the general conclusion remains, namely that isotopic substitution can markedly influence the magnitude of the quenching cross section for an excited state and thus influence the partitioning between the various available channels. This may lead to differences in the yield of a given end product of reaction, or perhaps in some cases even the type of products observed.

The greater efficiency for quenching of $I(5\,^2P_{1/2})$ by CH_3I compared with CD_3I may be understood in terms of resonant energy transfer of electronic to vibration and rotational energy in the iodide. Energy matching by CH_3I requires the excitation of three quanta, while CD_3I requires the excitation of at least four quanta, and the matrix element for the transition in the latter case is expected to be smaller. This point together with data on CH_4, CD_4 and CD_3H will be discussed in more detail elsewhere [18].

Finally we note that the use of perdeutero alkyl iodides (CD_3I is a fairly common NMR solvent) offers an interesting alternative to the use of perfluoro alkyl iodides for the production of high powered laser pulses.

Acknowledgement

We are indebted to Professor C. Kemball for his encouragement and laboratory facilities and to the S.R.C. for an equipment grant. We are also indebted to The Royal Society for the award of a European Science Exchange Fellowship and to the University of Edinburgh for the award of a Research Studentship, to C.F. We thank M.A.D. Fluendy and J. Costello for help in initiating the computer simulation studies.

References

[1] J.V.V. Kasper and G.C. Pimentel, Appl. Phys. Letters 5 (1964) 231.
[2] C.M. Ferrar, Appl. Phys. Letters 12 (1968) 381.
[3] F.T. Aldridge, Appl. Phys. Letters 22 (1973) 180.
[4] K. Hohla and K.L. Kompa, Appl. Phys. Letters 22 (1973) 77.
[5] M.A. Pollack, Appl. Phys. Letters 8 (1966) 36.
[6] D. Husain and R.J. Donovan, Advan. Photochem. 8 (1971) 1.
[7] D.M. Haaland and R.T. Meyer, Intern. J. Chem. Kinetics 6 (1974) 297.
[8] R.J. Donovan and C. Fotakis, J. Chem. Phys. 61 (1974) 2159.
[9] D. Husain and J.R. Wiesenfeld, Trans. Faraday Soc. 63 (1967) 1349.
[10] E.N. Okafo and E. Whittle, J. Chem. Soc. Faraday Trans., to be published.

[11] R.J. Donovan and D.J. Little, J. Chem. Soc. Faraday Trans. II 69 (1973) 952.
[12] R.H. Strain, J. McLean and R.J. Donovan, Chem. Phys. Letters 20 (1973) 504.
[13] R.J. Butcher, R.J. Donovan and R.H. Strain, J. Chem. Soc. Faraday Trans. II 70 (1974) 1837.
[14] M.G. Stock, D.J. Little and R.J. Donovan, J. Chem. Educ. 51 (1974) 51.
[15] D.E. O'Brien and J.R. Bowen, J. Appl. Phys. 40 (1969) 4767.
[16] W.C. Hwang and J.V.V. Kasper, Chem. Phys. Letters 13 (1972) 511.
[17] R.J. Donovan and D.J. Little, to be published.
[18] R.J. Butcher, R.J. Donovan and R.H. Strain, to be published.

Offprinted from the *Journal of The Chemical Society, Faraday Transactions II*, 1976, vol. 72.

Isotope Effects in the Quenching of Electronically Excited Atoms

Part 4.—Quenching of $I(5^2P_{\frac{1}{2}})$ by Hydrogen and Deuterium Halides, H_2O and D_2O

BY ROBERT J. DONOVAN,* CONSTANTINE FOTAKIS AND MICHAEL F. GOLDE

Department of Chemistry, University of Edinburgh,
West Mains Road, Edinburgh EH9 3JJ

Received 6th April, 1976

Spin-orbit relaxation of $I(5^2P_{\frac{1}{2}})$ by the molecules H_2O, D_2O, HCl, DCl, HBr, DBr, HI and DI has been studied using time resolved atomic absorption spectrophotometry ($\lambda = 206$ nm; $T = 293$ K). It is concluded that quenching by the two most efficient molecules, H_2O and HBr, proceeds via resonant energy transfer channels (electronic → vibration + rotation) probably involving quadrupole–dipole coupling. However, the small isotope effects and relatively large cross-sections observed for the other molecules suggest that an efficient curve crossing mechanism dominates for HCl, DCl, DBr, HI and DI. This is consistent with other recent work involving $Br(4^2P_{\frac{1}{2}})$ and the hydrogen halides.

Recent experiments have shown that cross-sections for quenching of electronically excited atoms and small molecules by hydrogen-containing species may change by several orders of magnitude on substituting D for H. Such observations provide a particularly powerful means for examining the molecular dynamics of energy transfer because the potential surfaces are not altered by isotopic substitution within the Born–Oppenheimer approximation.

Large isotope effects have been reported for spin-orbit relaxation of $I(5^2P_{\frac{1}{2}})$,[1-5] $Te(5^3P_{1,0})$[6] and $Tl(6^2P_{\frac{1}{2}})$,[7] and for quenching of $Ar(4s^3P_1, {}^1P_1)$,[8] $O_2(b^1\Sigma_g^+)$[9] and $O_2(a^1\Delta_g)$.[10] The temperature dependences of the relaxation rates for $I(5^2P_{\frac{1}{2}})$[11] and $Tl(6^2P_{\frac{1}{2}})$[7] have also been examined. They show marked differences for isotopically substituted molecules; *e.g.*, with $I(5^2P_{\frac{1}{2}})$, the temperature dependences for quenching by H_2 and D_2 have opposite signs.

Quenching of $Ar(4s^3P_1, {}^1P_1)$ by H_2, HD and D_2 is accompanied by highly specific excitation of rovibrational levels of the $B^1\Sigma_u^+$ excited states of these molecules and the dominant excitation channels have been explained in terms of near resonance energy transfer induced by long range dipole-dipole interaction.[8] The quenching of $O_2(a^1\Delta_g)$[10] and $O_2(b^1\Sigma_g^+)$[12] has also been discussed in terms of near resonant energy transfer, electronic to vibrational (E → V) in these cases.

More recently, Ewing [13] has calculated the rate constants for spin-orbit relaxation of $Te(5^3P_{1,0})$ and $Pb(6^3P_2)$ by hydrogen in terms of E → V + R energy transfer due to long-range quadrupole–quadrupole coupling. This approach is essentially based on the theory given by Sharma *et al.*[14] for near-resonant vibration–vibration energy transfer which, by employing linear trajectories and first order perturbation theory, introduces no adjustable parameters. We have adopted a phenomenological approach within the framework of the theories for long-range multipole interactions and have been successful in accounting for rate data and temperature dependences for spin–orbit relaxation of $Te(^3P_{1,0})$, $Tl(6^2P_{\frac{1}{2}})$ and $I(5^2P_{\frac{1}{2}})$ by H_2 and its isotopes.[1] In these systems, it was concluded that the energy transfer process,

$$M^* + Q(v_i,J_i) \rightarrow M + Q(v_f,J_f) + \Delta E_T, \qquad (1)$$

occurred preferably via specific channels involving definite selection rules for J and very small amounts of energy, $|\Delta E_T| < 200\ cm^{-1}$, transferred into or from translation.

Most quenching studies have been directed towards obtaining total cross-sections and thus provide only indirect evidence for the importance of $E \rightarrow V+R$ energy transfer. However, vibrationally excited products have been detected by absorption and emission spectroscopy in a few studies, and in one case by laser action.[15] The channel

$$Br(4^2P_{\frac{1}{2}})+HX(v = 0) \rightarrow Br(4^2P_{\frac{3}{2}})+HX(v = 1) \quad (2)$$

has been identified [16-19] for X = F, Cl and Br. For X = F, a rapid equilibrium is established in this near-resonant process [17, 18] [ref. (18) also states that the analogous process involving $I(5^2P_{\frac{1}{2}})$ and HF leads to the direct population of $HF(v = 2)$]. For X = Cl and Br also, the $E \rightarrow V$ channel (2) has been confirmed as the major mechanism;[19] however, these processes are non-resonant unless large changes in the rotational quantum number occur and it has been proposed that they proceed by non-adiabatic transitions between crossing potential surfaces.

In view of the uncertainty in the mechanisms for quenching by some hydrogen-containing molecules, we have extended our previous total quenching cross-section measurements to quenching of $I(5^2P_{\frac{1}{2}})$ by HCl, DCl, HBr, DBr, HI, DI, H_2O and D_2O. Long-range interaction models prove satisfactory for explaining the results for H_2O and HBr; for the other hydrogen halides, the effect of crossing potential surfaces is considered.

Rate data for spin–orbit relaxation of $I(5^2P_{\frac{1}{2}})$ by H_2O, D_2O, HCl, HI and DI have been reported previously;[2, 20, 21] however the data for HI, DI and D_2O were obtained using plate photometry [20, 21] which is less precise and in some cases has proved unreliable [22] (due to the relatively large atomic and radical concentrations used). As the aim of the present work was to make a detailed comparison between isotopically substituted species we have redetermined data for all the above mentioned molecules in order to provide a self-consistent and reliable set of data.

EXPERIMENTAL

The experimental arrangement for time resolved atomic absorption spectrophotometry, used in the present work, has been described in detail previously.[23a] Electronically excited iodine atoms, $I(5^2P_{\frac{1}{2}})$, were produced by flash photolysis of C_3F_7I under isothermal conditions (rate data refer to $T = 293 \pm 2$ K). Flash energies of ~ 80 J were employed and mixtures of the iodide and quenching gas were diluted one hundred fold with pure nitrogen, which is a relatively inefficient quencher, yielding a total pressure of $\sim 2.7\ kN\ m^{-2}$ (some mixtures containing DCl were not diluted with N_2 as the low efficiency for quenching by DCl required that a large excess of this gas be added, thus achieving the same purpose as added N_2 in other experiments).

The decay of $I(5^2P_{\frac{1}{2}})$ atoms was monitored using the 206.2 nm line, $I(6s^2P_{\frac{3}{2}}) \leftarrow I(5^2P_{\frac{1}{2}})$, produced by a microwave discharge through molecular iodine in a quartz tube terminating in a flat Spectrosil window. Decay curves were obtained from single flash experiments using a fast analogue-to-digital converter with integral memory (Datalab DL905). Data were inspected on a visual display unit before being recorded in analogue form on an XY-plotter, and were analysed using a Ferranti Freescan Digitiser.

Reagents were handled using a vacuum line constructed with greaseless taps (Young Scientific) capable of holding a vacuum of better than $10^{-4}\ N\ m^{-2}$. For experiments with deuterated molecules (DCl, D_2O, DBr, DI), the vacuum line was deuterated several times with D_2O over a period of two or three days. Experiments with HI and DI were carried out in the dark to avoid the photolysis of these compounds. In some experiments, mixtures containing these reagents were passed through an isopropanol+dry ice bath (198 K) before

entering the reaction vessel to eliminate all traces of I_2. Gas mixtures were made up in 500 cm^3 bulbs and allowed to mix for at least two hours before use.

REAGENTS

(i) N_2 (B.O.C. "white spot", $O_2 < 10$ ppm, $CO_2 < 1$ ppm, $H_2 < 1$ ppm) and He (B.O.C., $O_2 < 1$ ppm, $H_2 < 10$ ppm, $CO_2 < 1$ ppm) were used directly.

(ii) C_3F_7I, supplied by the Pierce Chemical Company, was thoroughly degassed and fractionally distilled under vacuum to remove residual traces of I_2.

(iii) H_2O and D_2O (B.O.C., stated purity 99.5 %) were thoroughly degassed before use.

(iv) DCl was prepared by the action of D_2O on benzoyl chloride and purified by fractional distillation under vacuum. The purity determined by infrared analysis showed that the sample contained $\leqslant 9$ % HCl. No other impurities were detected.

(v) HI and DI were kindly supplied by colleagues and the purity checked by infrared spectroscopy. The purity of DI was further checked using an A.E.I. MS902 mass spectrometer: it was shown to contain < 6 % HI.

(vi) HCl and HBr (Matheson Co.) were degassed under vacuum and their purity checked using infrared and mass spectroscopy.

(vii) DBr (Merck, Sharp and Dohme, stated minimum isotopic purity, 99 atom % D) was degassed under vacuum and its purity checked using infrared and mass spectroscopy. With the limited amount of sample available, the infrared spectrum did not allow a sensitive estimate of HBr, and the inlet system to our A.E.I. MS902 mass spectrometer, despite repeated exposure to D_2O, gave only a poor limit to the amount of HBr present (< 36 % HBr). We believe that the HBr content was much lower than this and probably close to the manufacturers' stated limit, as successive samples admitted to the mass spectrometer showed increases in the DBr/HBr ratio, but we had insufficient sample to obtain a better limit. We are indebted to Prof. J. J. Turner for the gift of this DBr sample.

RESULTS

Typical pseudo first-order plots for the quenching of $I(5^2P_{\frac{1}{2}})$ by HBr and DBr are shown in fig. 1. The first-order rate coefficients derived from the slopes of such plots (k') were then plotted against the partial pressure of quenching gas, as illustrated in fig. 2.

The slopes of these plots yield the products γk_q, where γ is an empirical correction-factor [22] in the Beer–Lambert Law expression (for the 206.2 nm line employed here, $\gamma = 0.82 \pm 0.03$) and k_q is the second order quenching rate constant for a given quenching gas. Values of k_q for the quenching molecules studied here are listed in table 1. The corresponding quenching cross-sections were evaluated by dividing k_q by the mean relative velocity of the quenching molecule at 293 K.

The result for HCl is in good agreement with that of Deakin and Husain,[2] and the result for H_2O lies within the experimental error limits given by these workers. The rate constants for D_2O, HI and DI are a factor of three smaller than those determined by plate photometry.[20, 21] The present results are to be preferred as discussed earlier. In these experiments we have shown directly that atom–radical effects are unimportant by measuring quenching rates over a range of flash energies (45-180 J). Results for HI at the highest and lowest flash energies are shown in table 2. We noted, however, a large increase in the $I(5^2P_{\frac{1}{2}})$ decay coefficient when a mixture of HI or DI in N_2 was flashed for a second time. This must be due to efficient quenching by a photolysis product, H_2 or I_2:

$$HI + h\nu \rightarrow H + I \quad (3)$$

$$H + HI \rightarrow H_2 + I \quad (4)$$

$$I + I + M \rightarrow I_2 + M \quad (5)$$

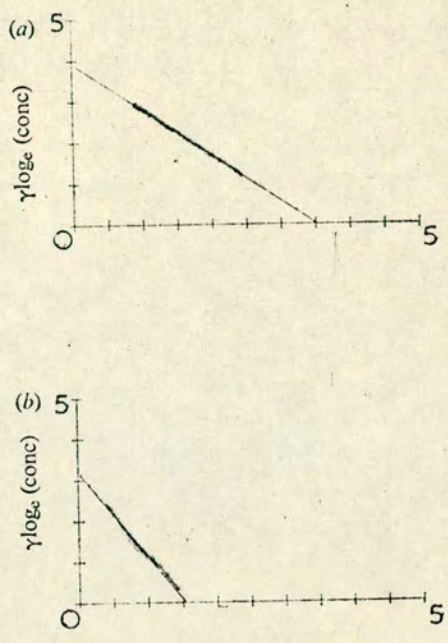

FIG. 1.—Typical first order plots of data for the decay of $I(5^2P_{\frac{1}{2}})$ obtained using a Ferranti Freescan Digitiser ; $\gamma \log_e(\text{conc.}) \equiv \log_e[\log_e(I_0/I)]$; slope, $k' = \gamma(k_q[Q]+k_b)$, where k_b is the first order decay in the absence of added quenching gas.

(*a*) $P_{DBr} = 93.3$ N m^{-2}, $P_{N_2} = 2.70$ k N m^{-2} ; $P_{C_3F_7I} = 33.2$ N m^{-2}, $k_b = 201$ s^{-1}, $k' = 1114$ s^{-1}.
(*b*) $P_{HBr} = 69.3$ N m^{-2}, $P_{N_2} = 2.70$ k N m^{-2}, $P_{C_3F_7I} = 32.1$ N m^{-2}, $k_b = 278$ s^{-1}, $k' = 2075$ s^{-1}.

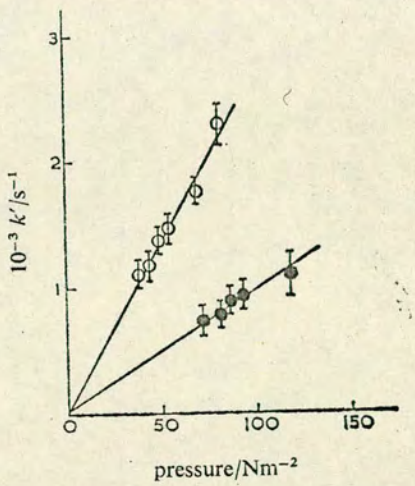

FIG. 2.—Plots of observed first order rate coefficients, k', against pressure (N m^{-2}) of HBr(○) and DBr(●).

and could be ascribed to I_2, whose quenching rate constant,[23b] 3.6×10^{-11} cm^3 molecule^{-1} s^{-1}, is about 280 times that for H_2. However, as the formation of I_2 (5) is slow, there is no measurable effect from this species during the decay of $I(5^2P_{\frac{1}{2}})$ for the first flash of a given mixture. From the increase in the first-order rate coefficient following a second flash we estimate that the partial pressure of I_2 produced by the first flash is ~ 0.1 % of that of HI, and thus the percentage photolysis is ~ 0.2 %.

The rate constant for DBr is presented as an upper limit because of the presence of some HBr in the sample (< 36 %, see section on reagents). We have not attempted to correct k_q(DBr) for the presence of HBr as this would reduce its value substantially. The upper limit presented provides a reliable basis for discussion.

TABLE 1.—SECOND ORDER RATE CONSTANTS FOR QUENCHING (k_q) OF $I(5^2P_{\frac{1}{2}})$ BY H_2O, D_2O, HCl, DCl, HBr, DBr, HI AND DI ($T = 293$ K)

quenching gas	k_q/cm^3 molecule^{-1} s^{-1} (293 ± 2 K)	σ/cm^2	ratio of cross-sections	previous work (k_q/cm^3 molecule^{-1} s^{-1})	reference
H_2O	$(8.4 \pm 1.1) \times 10^{-13}$	1.3×10^{-17}	42	$(7.2 \pm 1.6) \times 10^{-13}$	2
D_2O	$(1.8 \pm 0.4) \times 10^{-14}$	3.1×10^{-19}		$(6.2 \pm 0.8) \times 10^{-14}$	20
HCl	$(1.52 \pm 0.12) \times 10^{-14}$	3.2×10^{-19}	3.4	$(1.5 \pm 0.5) \times 10^{-14}$	2
DCl	$(4.3^{+0.4}_{-1.9}) \times 10^{-15}$ *	9.3×10^{-20}			
HBr	$(1.3 \pm 0.1) \times 10^{-13}$	3.7×10^{-18}	$\geqslant 2.6$		
DBr	$(\leqslant 4.9 \pm 0.3) \times 10^{-14}$	$\leqslant 1.4 \times 10^{-18}$			
HI	$(5.2 \pm 0.4) \times 10^{-14}$	1.7×10^{-18}	1	$(1.3 \pm 0.2) \times 10^{-13}$	21
DI	$(5.0 \pm 0.2) \times 10^{-14}$	1.6×10^{-18}		$(1.2 \pm 0.2) \times 10^{-13}$	21

* the lower limit allows for the presence of < 9 % HCl.

TABLE 2.—DATA ILLUSTRATING THE ABSENCE OF ATOM RADICAL EFFECTS IN THE DETERMINATION OF k_q

partial pressure of HI/N m^{-2}	flash energy/J	first-order rate coefficients/s^{-1}
78	45	1090 ± 19
78	180	1113 ± 28
82	45	1162 ± 17
82	180	1152 ± 13

DISCUSSION

H_2O, D_2O

The very large isotope effect observed in the quenching of $I(5^2P_{\frac{1}{2}})$ by H_2O and D_2O implies a highly specific mechanism. Although a large number of channels for electronic to vibration+rotation energy transfer [eqn (1)] are allowed for both systems, the number of near-resonant channels, in which large changes in J are excluded, is much smaller. According to recent spectroscopic data,[24] about 80 % of the total population of H_2O at 300 K can undergo the favourable (000) → (101), (200), (002) vibrational transitions in process (1) with $|\Delta J| = |J_f - J_i| \leqslant 2$ and $\Delta E_T < 200$ cm^{-1}; for D_2O, near-resonant processes are restricted to about 60 % of the population and the (000) → (201) vibrational transition.[25] These findings are consistent with a long-range resonant E → V+R energy transfer mechanism, in which the transition probability is proportional to the square of the matrix element for the vibrational transition. Although it is not certain whether dipole ($|\Delta J| = 1$ in 1st order perturbation treatment) or quadrupole ($|\Delta J| = 0, 2$) terms contribute more strongly to the transition probability, it is expected, on the basis of the absorption spectrum of H_2O, that the (000) → (101), (200), (002) transitions (for H_2O) will be

highly favoured over the (000) → (201) transition (for D_2O), as 2 rather than 3 vibrational quanta are excited. The large isotope effect thus provides the key to the quenching mechanism for H_2O; for D_2O quenching by the long range interaction mechanism is expected to be less important and interactions at short range may also play a part in determining the overall small quenching cross-section.

We deduce from these results that the quenching cross-section is a sensitive function of Δv and that channels with Δv differing by unity have associated cross-sections differing by more than one order of magnitude. This conclusion is consistent with data [26] for quenching of $Br(4^2P_{\frac{1}{2}})$ by H_2O. In this case, only one vibrational quantum should be excited and a large number of channels are available. The cross-section is found to be forty times greater than that for $I(5^2P_{\frac{1}{2}})$ and H_2O, and is close to the gas dynamic collision cross-section.[26]

(ii) HCl, DCl

The results for HCl and DCl are less readily interpreted in terms of near-resonant energy transfer. The rather low quenching efficiency and the small isotope effect observed (table 1) are associated with the virtual absence of near resonant quenching channels with $\Delta E < 200$ cm^{-1} and small values of ΔJ. For HCl, resonant channels [27] involving the most highly populated rotational levels require $|\Delta J| \geqslant 9$ for $\Delta v = 2$. Transitions with $|\Delta J| \leqslant 2$ (*i.e.*, dipole and quadrupole transitions) occur only with $\Delta v = 3$ and are restricted to very high rotational levels ($J_i \geqslant 12$) which account for only 0.1 % of the total HCl population at room temperature. Even allowing for $|\Delta J| = 4$, the lowest initial J state which can lead to resonant transfer is $J_i = 9$ and this state is occupied by only 1 % of the HCl molecules at 300 K. Clearly the involvement of well-populated rotational levels would require very large values of ΔJ and thus the participation of high order multipolar interaction terms, about which we have little knowledge.

For DCl the availability of channels for resonant transfer shows a similar pattern but requires vibrational changes [28] of $\Delta v = 3$ or 4. Thus for $\Delta v = 3$, $|\Delta J| \geqslant 11$ for the highly populated rotational levels, while transitions with $\Delta J \leqslant 2$ require $\Delta v = 4$ and are restricted to $J_i \geqslant 10$ (occupied by ~ 8 % of the DCl molecules at 300 K). If these levels contributed dominantly to the quenching of $I(5^2P_{\frac{1}{2}})$, then a large positive temperature dependence would be expected and the isotope effect would reflect the larger number of vibrational quanta required for DCl compared with HCl.

The combination of very low fractions of the population, which can undergo suitable transitions, and the weakness of $\Delta v = 3$ and 4 radiative transitions in HCl and DCl make it very unlikely that near-resonant energy transfer from $I(5^2P_{\frac{1}{2}})$, involving long-range interactions, is the principal mechanism here. Extension of similar models for V → V energy transfer beyond the domain of " near-resonance ", has proved generally unsuccessful, calculations seriously underestimating the experimentally observed rates, even when second order perturbation theory or higher terms in the multipole expansion of the interaction potential were involved.[29, 30] It has been pointed out [31] that the use of linear trajectories and the selection rules for ΔJ become increasingly invalid as the energy mismatch ΔE_T increases and it is possible that further refinements of these models will allow further tests of the role of long-range forces in inducing quenching of $I(5^2P_{\frac{1}{2}})$ by HCl and DCl.

(iii) HBr, DBr

Of the hydrogen halides studied here, HBr is the most efficient in quenching $I(5^2P_{\frac{1}{2}})$. A large number of channels [32] exist for $\Delta v = 3$ and $|\Delta J| = 1$ and 2, the

J_i states involved accounting for over 90 % of the population at 300 K. For transitions involving $|\Delta J| = 2$, there are five channels with $\Delta E_T < 50\,cm^{-1}$ and one with $\Delta E_T \simeq 4\,cm^{-1}$, *viz*;

$$I(5^2P_{\frac{1}{2}}) + HBr(v_i = 0, J_i = 6) \rightarrow I(5^2P_{\frac{3}{2}}) + HBr(v_f = 3, J_f = 8).$$

For DBr the only available channels [33] involving $|\Delta J| < 2$ require $\Delta v = 4$ and J_i states having a negligible population at 300 K. This is consistent with the lower efficiency for quenching by DBr compared with HBr and we conclude that quenching of $I(5^2P_{\frac{1}{2}})$ by HBr proceeds at least in part by near-resonant energy transfer. The data do not provide any firm indication as to whether dipole–quadrupole, or quadrupole–quadrupole forces are involved; however, the fact that the cross-section for HBr ($\Delta v = 3$) is five times greater than that for $H_2(\Delta v = 2)$ suggests that dipole–quadrupole forces dominate for HBr.

(iv) HI, DI

The results for HI and DI are perhaps the most intriguing in that the quenching cross-sections are higher than those for HCl and DCl, but virtually no isotope effect is observed. Near-resonant quenching channels [reaction (1)] are again virtually absent for $I(5^2P_{\frac{1}{2}})+HI$. no transition with $|\Delta J| \leqslant 2$ and $\Delta E_T < 200\,cm^{-1}$ being available [32, 34] except for $\Delta v = 4$ and $J > 16$; this probably rules out a significant contribution by long-range forces to the quenching mechanism. In sharp contrast, all rotational levels of DI can undergo resonant transitions [35] with $|\Delta J| \leqslant 2$ and $\Delta E_T < 200\,cm^{-1}$, but these involve the transition $\Delta v = 5$, which is expected to be too weak to account for the large quenching cross-section observed. It can only be stated that, if long-range forces dominate the quenching of $I(5^2P_{\frac{1}{2}})$ by HI and DI, widely different temperature dependences of the cross-section should be observed, strongly positive for HI and weakly negative for DI; the absence of an isotope effect at 300 K would thus be fortuitous.

For $I(5^2P_{\frac{1}{2}})+HI$ and DI, in contrast to $I(5^2P_{\frac{1}{2}})+HCl$ and DCl, a reactive pathway (6) is energetically possible

$$I'(5^2P_{\frac{1}{2}}) + HI \rightarrow HI' + I(5^2P_{\frac{3}{2}}). \qquad (6)$$

This atom exchange process is one channel of a more general mechanism in which a non-adiabatic transition occurs by crossing from the excited potential surface correlating with $I(^2P_{\frac{1}{2}})+HI$ to a lower surface correlating with $I(^2P_{\frac{3}{2}})+HI$ (see general potential surfaces, fig. 3). Following the jump, the products may separate to yield $I'(^2P_{\frac{3}{2}})+HI$ (no reaction) or $I(^2P_{\frac{3}{2}})+HI'$ (reaction), the latter channel being important only if there is no large energy barrier.

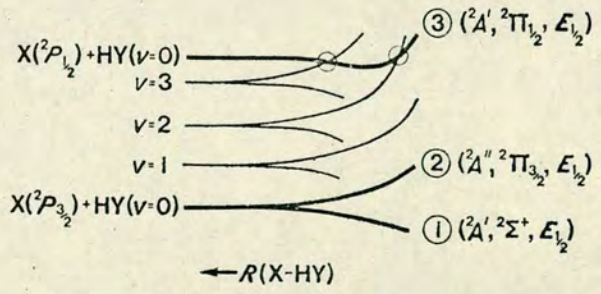

FIG. 3.—Diagramatic representation of a section through the potential energy surfaces for the X+HY system.

A detailed discussion of this short-range mechanism, which has recently been proposed to account [36] for efficient quenching of excited $Br(4^2P_{\frac{1}{2}})$ atoms by HCl and HI, is hindered by the lack of information concerning excited potential surfaces in the X+HY system. Moore and co-workers [36] have discussed the approach of a halogen atom (X) to the hydrogen halide molecule (HY) in terms of simple valence bond theory, whereby the ^2P atomic states are characterised by an unfilled p-orbital lying along or perpendicular to the molecular axis. In this model, the former orbital leads to the ground $^2A'$ state ($^2\Sigma^+$ for linear configuration) of the XHY intermediate and correlates with ground state $HX(^1\Sigma^+)+Y(^2P_{\frac{3}{2}})$ species. The other orbitals, including that arising from the $X(^2P_{\frac{1}{2}})$ atom, are considered to yield strongly repulsive $^2A'+^2A''$ surfaces ($^2\Pi$) of XHY and to correlate with highly excited products, $HX(^1\Pi)+Y(^2P_{\frac{3}{2}})$.

This simple model, although consistent with the observed absence of reactive quenching of $Br(4^2P_{\frac{1}{2}})$ by HI, unfortunately also precludes crossing of the state correlating with $X(^2P_{\frac{1}{2}})+HY$ by any other surface at low energy.

For heavy atoms such as Br and I, the splitting of the $^2P_{\frac{1}{2}}$ and $^2P_{\frac{3}{2}}$ atomic states is so large (7603 cm^{-1} for iodine) that the $M_J = \frac{1}{2}$ components cannot be visualised as simple hydrogen-like p-orbitals and the behaviour of the potential surfaces, particularly at large X–HY separations, is correspondingly less certain. We propose that non-adiabatic surface-crossing processes in the quenching of $I(5^2P_{\frac{1}{2}})$ by HI and DI (and similar X*+HY systems) are most important at large X–HY separations, where the shapes of the surfaces are determined by intermediate range forces. $E \rightarrow V$ transfer can occur if the $X(^2P_{\frac{1}{2}})+HY$ surface is crossed by one or more vibronic surfaces correlating with $X^2P_{\frac{3}{2}}+HY$ ($v \geqslant 0$) (fig. 3). This requires the former surface (surface 3) to be less repulsive than one of the surfaces 1 and 2, which can be satisfied if, as in the case of diatomic potential curves derived from $^2P+^1S$ atoms, surfaces 3 and 2 rapidly converge as X and HY approach, to a separation approximately $\frac{2}{3}$ that of the free $^2P_{\frac{1}{2}}$ and $^2P_{\frac{3}{2}}$ atoms. A convergence of surfaces 2 and 3 would also be expected on the grounds that, for strong spin–orbit coupling, all three surfaces have the species $E_{\frac{1}{2}}$ and thus surfaces 1 and 2 will repel strongly and separate at relatively large internuclear distances (at smaller separations, surfaces 2 and 3 in turn start to repel each other).

In general, several crossing-points of surface 3 with the set of vibronic surfaces 2, correlating with $X^2P_{\frac{3}{2}}+HY$ ($v = 0, 1, ---$), lead to a range of transition probabilities for $E \rightarrow V$ transfer into the various vibrational levels of HY and thus this mechanism can explain the " non-resonant " $E \rightarrow V$ processes observed for $Br(4^2P_{\frac{1}{2}})+HCl$ and HBr. Further, because of the different vibration frequencies in HY and DY, isotope effects, such as seen for $I(5^2P_{\frac{1}{2}})+HCl$ and DCl, are possible; however, as the probability of a non-adiabatic transition at each crossing point does not specifically depend on the value of v, it is also possible that such isotope effects are very small, as for $I(5^2P_{\frac{1}{2}})+HI$ and DI.

While a curve crossing mechanism explains the results for $I(5^2P_{\frac{1}{2}})$ with HCl, DCl, DBr, HI and DI, and for $Br(4^2P_{\frac{1}{2}})$ with HCl and HBr, the efficient quenching of $I(5^2P_{\frac{1}{2}})$ by HF ($k \simeq 10^{-11}$ cm^3 $molecule^{-1}$ s^{-1}), in which the direct population of $HF(v = 2)$ has been observed,[18] provides strong evidence for the involvement of resonant energy transfer in cases where this can effectively compete with a curve crossing mechanism. We conclude that quenching of $I(5^2P_{\frac{1}{2}})$ by H_2O, HBr and HF involves near-resonant energy transfer and, from comparison with the lower quenching cross-section for H_2 ($\sigma = 7.4 \times 10^{-19}$ cm^2; attributed to quadrupole–quadrupole coupled channels), that dipole–quadrupole coupling is involved and leads to large values for the quenching cross-section even for transitions involving $\Delta v = 2$ and 3.

Added note: In a very recent theoretical study of the quenching of excited $^2P_{\frac{1}{2}}$ halogen atoms by hydrogen,[37] Zimmerman and George have considered the importance of non-adiabatic coupling of potential surfaces even in cases where near-resonant energy transfer is possible.

We thank Prof. C. Kemball for his support and encouragement, and the University of Edinburgh for financial support for C. F. We also thank Drs. K. P. Lawley and I. W. M. Smith for helpful discussions.

[1] R. J. Butcher, R. J. Donovan and R. H. Strain, *J.C.S. Faraday II*, 1974, **70**, 1837.
[2] J. J. Deakin and D. Husain, *J.C.S. Faraday II*, 1972, 68, 41.
[3] R. J. Donovan and C. Fotakis, *J. Chem. Phys.*, 1974, **61**, 2159.
[4] R. H. Strain, J. McLean and R. J. Donovan, *Chem. Phys. Letters*, 1973, **20**, 504.
[5] R. J. Butcher, R. J. Donovan, C. Fotakis, D. Fernie and A. G. A. Rae, *Chem. Phys. Letters*, 1975, **30**, 398.
[6] R. J. Donovan and D. J. Little, *J.C.S. Faraday II*, 1973, **69**, 952.
[7] J. R. Wiesenfeld, *Chem. Phys. Letters*, 1973, **21**, 517.
[8] E. H. Fink, D. Wallach and C. B. Moore, *J. Chem. Phys.*, 1972, **56**, 3608.
[9] F. Stuhl and H. Niki, *Chem. Phys. Letters*, 1970, **7**, 473.
[10] P. B. Merkel and D. R. Kearns, *J. Amer. Chem. Soc.*, 1972, **94**, 7244.
[11] J. J. Deakin and D. Husain, *J.C.S. Faraday II*, 1972, 68, 1603.
[12] K. Kear and W. Abrahamson, *J. Photochem.*, 1974-75, **3**, 404.
[13] J. J. Ewing, *Chem. Phys. Letters*, 1974, **29**, 50.
[14] R. D. Sharma, H. L. Chen and A. Szoke, *J. Chem. Phys.*, 1973, **58**, 3519 and references therein.
[15] A. B. Petersen, S. R. Leone and C. Wittig, *Appl. Phys. Letters*, 1975, **27**, 305.
[16] R. J. Donovan, D. Husain and C. D. Stevenson, *Trans. Faraday Soc.*, 1970, **66**, 2148.
[17] G. P. Quigley and G. J. Wolga, *J. Chem. Phys.*, 1975, **62**, 4560.
[18] F. J. Wodarczyk and P. B. Sackett, *Chem. Phys.*, 1976, **12**, 65.
[19] S. R. Leone and F. J. Wodarczyk, *J. Chem. Phys.*, 1974, **60**, 314.
[20] R. J. Donovan and D. Husain, *Trans. Faraday Soc.*, 1966, **62**, 2023.
[21] R. J. Donovan and D. Husain, *Trans. Faraday Soc.*, 1966, **62**, 1050.
[22] R. J. Donovan and H. M. Gillespie, *S.P.R. Reaction Kinetics* (Chemical Society, London 1975), **1**, 14.
[23] (*a*) M. G. Stock, D. J. Little and R. J. Donovan, *J. Chem. Educ.*, 1974, **51**, 51; (*b*) D. H. Burde, R. A. McFarlane and J. R. Wiesenfeld, *Chem. Phys. Letters*, 1975, **32**, 296.
[24] R. A. Toth and J. S. Margolis, *J. Mol. Spectr.*, 1975, **55**, 229.
[25] W. S. Benedict, N. Gailar and E. K. Plyler, *J. Chem. Phys.*, 1956, **24**, 1139.
[26] R. J. Donovan and D. Husain, *Trans. Faraday Soc.*, 1966, **62**, 2987.
[27] I. M. Mills, H. W. Thompson and R. L. Williams, *Proc. Roy. Soc. A*, 1953, **218**, 29; E. K. Plyler and E. D. Tidwell, *Z. Elektrochem.*, 1960, **64**, 717.
[28] D. H. Rank, D. P. Eastman, B. S. Rao and T. A. Wiggins, *J. Opt. Soc. Amer.*, 1962, **52**, 1.
[29] J. C. Stephenson and C. B. Moore, *J. Chem. Phys.*, 1972, **56**, 1295.
[30] R. D. Sharma, *Chem. Phys. Letters*, 1975, **30**, 261.
[31] T. A. Dillon and J. C. Stephenson, *J. Chem. Phys.*, 1973, **58**, 3849.
[32] S. M. Naude and H. Verleger, *Proc. Phys. Soc. (London)*, 1950, **63**, 470.
[33] F. L. Keller and A. H. Nielsen, *J. Chem. Phys.*, 1954, **22**, 294.
[34] A. H. Nielsen and H. H. Nielsen, *Phys. Rev.*, 1935, **47**, 585.
[35] C. A. Burrus and W. Gordy, *Phys. Rev.*, 1953, **92**, 1437; E. D. Palik, *J. Chem. Phys.*, 1955, **23**, 217.
[36] K. Bergmann, S. R. Leone and C. B. Moore, *J. Chem. Phys.*, 1975, **63**, 4161.
[37] I. H. Zimmerman and T. F. George, *J.C.S. Faraday II*, 1975, **71**, 2030.

(PAPER 6/666)

PRINTED IN GREAT BRITAIN AT
THE UNIVERSITY PRESS
ABERDEEN

Journal of Photochemistry, 6 (1976/77) 193 - 198

PRIMARY AND SECONDARY PROCESSES IN THE PHOTOLYSIS OF GeH_3I

R. J. DONOVAN, C. FOTAKIS and H. M. GILLESPIE

Department of Chemistry, University of Edinburgh, West Mains Road, Edinburgh EH9 3JJ (Gt. Britain)

(Received June 10, 1976)

Summary

Time-resolved atomic absorption spectrophotometry and flash spectroscopy in the vacuum ultra-violet have been employed to investigate primary and secondary processes in the photolysis ($\lambda > 200$ nm) of GeH_3I. The initial yield of $I(5^2P_{1/2})$ and $I(5^2P_{3/2})$ atoms has been measured ($[I(5^2P_{1/2}]_0/[I(5^2P_{3/2})]_0 \cong 1.3$) and the subsequent reactions of these two states to yield HI have been investigated. Formation of HI by reaction of $I(5^2P_{3/2})$ atoms with GeH_3I implies a limit to the bond dissociation energy D (H–GeH_2I) $\lesssim 298$ kJ/mol. The rate constant for removal of $I(5^2P_{1/2})$ by GeH_3I has been determined as $k_2 = (6.9 \pm 1.0) \times 10^{-12}$ cm^3 molecule^{-1} s^{-1}: failure to observe laser emission at 1.315 μm, in this work, is ascribed to the large value for k_2.

Introduction

In the past few years considerable effort has been directed towards an understanding of primary and subsequent processes in the photolysis of alkyl and related iodides, inspired partly by interest in the iodine atom photodissociation laser. Progress has been made towards a detailed description of the photofragmentation at various wavelengths, particularly for methyl iodide [1], and initial relative populations of ground state $I(5^2P_{3/2})$ and electronically excited $I(5^2P_{1/2})$ atoms, produced in broad-band photolysis of a number of iodides have been measured [2]. Electronic to vibration–rotation energy transfer from $I(5^2P_{1/2})$ atoms to a range of molecules has also been investigated [3].

The photolyses of other Group IV iodides have not previously been studied and may provide interesting comparisons with CH_3I both in the manner in which the absorption spectrum and photofragmentation change as the central atom is altered, and in the possibilities which may appear of competition between inelastic and chemically reactive channels in collisions of $I(5^2P_{1/2})$ atoms with the parent molecule. We describe here an investigation of some aspects of the photochemistry of GeH_3I employing three complemen-

tary techniques: kinetic absorption spectrophotometry to monitor the decay of excited iodine atoms, time-resolved spectroscopy in the vacuum ultraviolet and a photodissociation laser apparatus, all employing flash photolysis at $\lambda > 200$ nm.

Experimental

Kinetic absorption spectrophotometry

This apparatus has previously been described in detail [4]. $I(5^2P_{1/2})$ atoms were monitored by attenuation of the resonance line at 206.2 nm, produced by a microwave discharge in molecular iodine. Decay curves were stored in a fast analogue to digital converter (DL 905) and recorded with an $X-Y$ plotter for subsequent analysis. GeH_3I was photolyzed under isothermal conditions at a flash energy of 45 J. The pressure of iodide employed was between 3 and 6 N/m^2, diluted with pure N_2, which is a relatively inefficient quencher of excited I atoms, to a total pressure of 2.8 kN/m^2. Mixtures were prepared in blackened bulbs and experiments conducted in the dark to minimize decomposition of GeH_3I prior to photolysis.

Vacuum ultra-violet kinetic spectroscopy

A Vitreosil quartz reaction vessel, length 20 cm, with LiF or MgF_2 end windows, was mounted at the entrance slit of a Hilger E766 1 m vacuum spectrograph. Parallel to this within an aluminium reflector was a flashlamp filled with Kr (1.33 kN/m^2) typically dissipating ~845 J (10 μF capacitor charged to 13 kV, giving a flash of ~4 μs FWHM). The spectroscopic source was a quartz capillary flashlamp filled with Kr (2.67 kN/m^2) dissipating 147 J (1.5 μF capacitor changed to 14 kV, flash duration ~2.5 μs FWHM). Spectra were recorded on Ilford HP4 film sensitized with sodium salicylate (0.5 *M* in methanol). Optical density traces were obtained with a Joyce–Loebl recording microdensitometer.

Chemical laser system

This comprised a quartz reaction vessel, active length 15 cm, with demountable sapphire Brewster angle windows, parallel to two Kr-filled flashlamps in an aluminium reflector. The optical cavity was defined by two totally reflecting gold-coated mirrors. The lamps were fired simultaneously, in parallel, so that the substantial time-varying magnetic fields associated with the two lamps cancel along the axis of the reaction vessel: the effect of the field generated by a single flashlamp is to reduce the gain of the laser in a complex manner by Zeeman splitting of the zero-field hyperfine sublevels and magnetic field induced mixing between states [5]. Chemical laser emission at 1.315 μm reflected from one of the Brewster windows was detected with an InSb detector (Mullard ORP-10) operated at room temperature, the output being displayed on a storage oscilloscope (Tektronix 549).

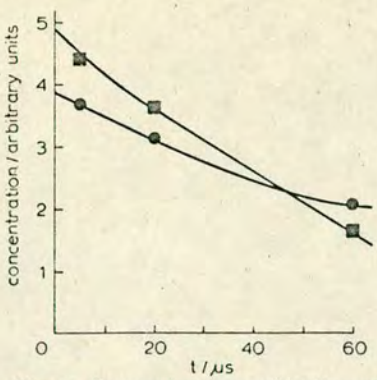

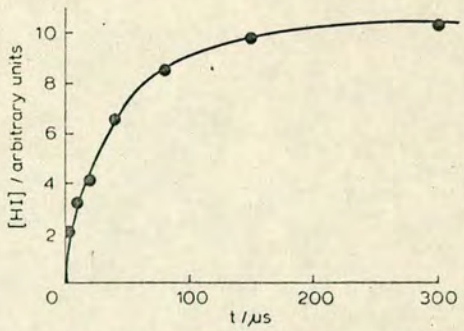

Fig. 1. Concentrations of iodine atoms following photolysis of GeH_3I. P_{GeH_3I} = 8 N/m^2, P_{Ar} = 10.9 kN/m^2; flash energy = 845 J; ▪, $I(5^2P_{1/2})$; •, $I(5^2P_{3/2})$.
Fig. 2. Formation of HI following photolysis of GeH_3I. P_{GeH_3I} = 1.33 N/m^2, P_{Ar} = 667 N/m^2; flash energy = 845 J.

Results and Discussion

Time resolved spectrographic investigation

Photolysis of GeH_3I ($\lambda > 200$ nm) resulted in production of both ground and excited state iodine atoms, $I(5^2P_{3/2})$ and $I(5^2P_{1/2})$, whose initial relative yield was determined by plate photometry using the transitions at 178.3 nm ($5p^4 6s\ ^2P_{3/2} \leftarrow 5p^5\ ^2P_{3/2}$) and 179.9 nm ($5p^4 6s\ ^2P_{1/2} \leftarrow 5p^5\ ^2P_{1/2}$). The continuous absorption by the parent molecule overlies these lines quite strongly under the conditions required to produce sufficient concentrations of atoms for plate photometry, but by using 8 N/m^2 of GeH_3I and recording multiple exposures (12 exposures at each time delay with a fresh sample for each exposure) the points on Fig. 1 were obtained. Line heights have been converted to relative concentrations using the Einstein A coefficients calculated by Lawrence [6] assuming equal pressure broadening for the two lines. Thus the initial relative populations are $[I(5^2P_{1/2})]_0/[I(5^2P_{3/2})]_0 = 1.3 \pm 0.1$, corresponding to population inversion by a factor of 2.6.

HI was formed in these experiments and detected by the intense Rydberg transitions at 160.47 nm and 176.21 nm. By photolyzing identical mixtures of GeH_3I in Ar with varying flash energies, and monitoring [HI] at a fixed delay of 200 μs, it was verified that absorption by HI followed the Beer–Lambert law. The kinetic behaviour (Fig. 2) indicates that HI is the product of a secondary reaction, rather than a primary product of photolysis.

Possible sources of HI are: (i) H abstraction by $I(5^2P_{3/2})$ or $I(5^2P_{1/2})$ atoms, if the GeH_2I–H bond dissociation energy is sufficiently low:

$$I(5^2P_{3/2}) + GeH_3I \rightarrow GeH_2I + HI \quad (1)$$

$$I(5^2P_{1/2}) + GeH_3I \rightarrow GeH_2I + HI \quad (2)$$

(ii) a sequence involving H atoms:

$$GeH_3I + h\nu \rightarrow GeH_2I + H \quad (3)$$

$$H + GeH_3I \rightarrow GeH_3 + HI \quad (4)$$

Behaviour analogous to reactions (3) and (4) has been observed in the short wavelength photolysis (140 nm $< \lambda <$ 170 nm) of CH_3I [7].

While a contribution from reactions (3) and (4) is not necessarily excluded, a number of observations suggest that H abstraction by both $I(5^2P_{1/2})$ and $I(5^2P_{3/2})$ is occurring: (i) as far as the present results allow a comparison to be made, the growth of [HI] appears to mirror the decay of $[I]_{total}$; (ii) disappearance of $I(5^2P_{3/2})$ is very fast and cannot be explained by atomic recombination: if it is assumed that all the I atoms are removed in collisions with GeH_3I, the data in Fig. 1 yield the approximate rate constants $k_I \cong 5 \times 10^{-12}$ cm^3 molecule^{-1} s^{-1}, $k_{I^*} \cong 9 \times 10^{-12}$ cm^3 molecule^{-1} s^{-1}. The figure for ground state atoms may conceal the effect of feeding from the excited state; (iii) further evidence that ground state iodine atoms can abstract H from GeH_3I may be adduced in the observation that in photolysis in the presence of a large excess of H_2 (P_{GeH_3I} = 1.33 N/m^2, P_{H_2} = 13.3 kN/m^2), conditions such that 99.5% of $I(5^2P_{1/2})$ atoms were quenched to $I(5^2P_{3/2})$ before reacting further [8], HI formation was very similar to that observed in the presence of Ar, an inefficient quencher.

Following photolysis of GeH_3I at 200 nm to give $I(5^2P_{3/2}) \sim 400$ kJ/mol excess energy is available. Under the conditions of the present experiments, however, excess translational energy is essentially thermalized in less than 1 μs, so that it may be concluded that the GeH_2I–H bond dissociation energy $D_{298}(GeH_2I\text{–}H) = \Delta H^\circ_{f,298}(GeH_2I) + \Delta H^\circ_{f,298}(H) - \Delta H^\circ_{f,298}(GeH_3I) \lesssim 298$ kJ/mol. No previous determination appears to have been made. This value may be compared with the limit $D(GeH_3\text{–}H) \lesssim 326$ kJ/mol obtained by Setser and coworkers [9] from observation of the highest (v,J) level of HF populated in the reaction of F atoms with GeH_4. A lower value in the iodine-substituted molecule is to be expected. We note that no I_2 was detected in these experiments, indicating that any removal of I atoms by reactions (5) and (6) is negligible:

$$I(5^2P_{3/2}) + GeH_3I \rightarrow I_2 + GeH_3 \quad (5)$$

$$I(5^2P_{1/2}) + GeH_3I \rightarrow I_2 + GeH_3 \quad (6)$$

Kinetic spectrophotometry

The present data do not permit an evaluation of the extent of deactivation of $I(5^2P_{1/2})$ to $I(5^2P_{3/2})$ by GeH_3I and hence a determination of k_2. The *overall* rate constant for removal of $I(5^2P_{1/2})$ atoms by GeH_3I was determined by atomic absorption spectrophotometry (Table 1 and Fig. 3). Rate constants previously determined [10] for CH_3I and CD_3I are included in Table 1 for comparison. Because of polymerization of products of GeH_3I photolysis in the reaction vessel, leading to a reduction in signal, only a limited number of experiments were performed. It was verified that the measured rate for

TABLE 1

Rate constants (k/cm^3 molecule^{-1} s^{-1}, at 298 K) for removal of electronically excited iodine atoms, I($5^2P_{1/2}$), by GeH_3I, CH_3I and CD_3I.

Molecule	k/cm^3 molecule^{-1} s^{-1}
GeH_3I	$(6.9 \pm 1.0) \times 10^{-12}$
CH_3I	$(2.6 \pm 0.6) \times 10^{-13}$
CD_3I	$(4.6 \pm 0.8) \times 10^{-15}$

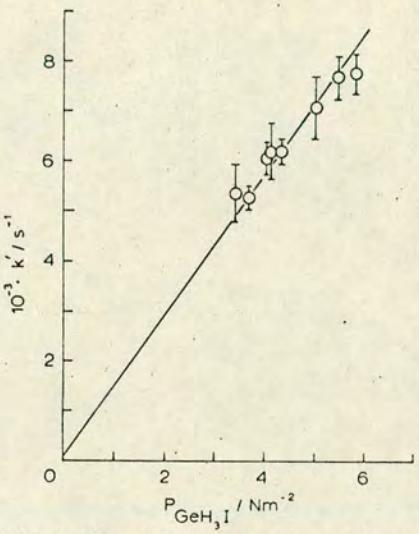

Fig. 3. Plot of first order rate coefficients k' for decay of I($5^2P_{1/2}$) *vs.* pressure of GeH_3I. $P_{total(with\ N_2)}$ = 2.8 kN/m^2, flash energy = 45 J.

identical mixtures remained constant for flash energies in the range 10 - 125 J, indicating that there is no complication by radical–radical processes. Flashing the same mixture repetitively had no effect on the rate of removal of excited atoms, showing that there was no significant build-up of products which have substantially different rate constants for removal of I($5^2P_{1/2}$), such as I_2. As expected in view of the discussion in the previous section, the rate constant is larger than would normally be associated with purely energy-transfer collisions of I($5^2P_{1/2}$) atoms. A determination of the relative contributions of energy transfer and chemical reaction would be of great interest, but experimentally very difficult to obtain.

Photochemical laser investigation

The population inversion observed for the lowest spin-orbit states of the iodine atom, following photolysis of GeH_3I, suggests that under appropriate conditions laser action (1.315 μm) should occur. We have previously

investigated CH_3I and CD_3I photochemical laser systems [11] and could therefore optimize conditions for laser action with our experimental arrangement. However, no laser emission could be observed from GeH_3I even under conditions where CH_3I gave a large output of stimulated emission. Thus although a sizeable population inversion occurs for GeH_3I, rapid removal of the excited atoms appears to prevent the system reaching threshold. We may compare this with CH_3I, where rather restrictive conditions for lasing have been observed [11]. The difference in laser output between CH_3I and CD_3I has been ascribed to the difference in quenching rate constants for the two molecules, and in a computer simulation of the CH_3I laser, output was found to be critically dependent on the value of the rate constant for quenching of $I(5^2P_{1/2})$ by the parent molecule. Laser action with GeH_3I might be achieved if the photochemical pumping rate were increased (*i.e.* the flash lamp duration reduced), thus allowing threshold to be reached on a time scale which is short by comparison with the relaxation time for $I(5^2P_{1/2})$.

Acknowledgements

We thank Professor C. Kemball for his support and encouragement, the University of Edinburgh for a studentship to C.F., and the S.R.C. for a Research Fellowship to H. G. and equipment grants. We also thank Dr. J. Savage and Mr. S. Henderson for providing samples of GeH_3I.

References

1 S. J. Riley and K. R. Wilson, J. C. S. Faraday Discuss., 53 (1972) 132; M. Dzvonik, S. Yang and R. Bersohn, J. Chem. Phys., 61 (1974) 4408.
2 T. Donohue and J. R. Wiesenfeld, J. Chem. Phys., 63 (1975) 3130.
3 R. J. Butcher, R. J. Donovan and R. H. Strain, J. C. S. Faraday Trans. II, 70 (1974) 1837; R. J. Donovan, C. Fotakis and M. F. Golde, J. C. S. Faraday Trans. II, 1976 (in press).
4 M. G. Stock, D. J. Little and R. J. Donovan, J. Chem. Educ., 51 (1974) 51.
5 W. C. Hwang and J. V. V. Kasper, Chem. Phys. Lett., 13 (1972) 511.
6 G. M. Lawrence, Astrophys. J., 148 (1967) 261.
7 M. R. Levy and J. P. Simons, J. C. S. Faraday Trans. II, 71 (1975) 561.
8 J. J. Deakin and D. Husain, J. C. S. Faraday Trans. II, 68 (1972) 41.
9 K. C. Kim, D. W. Setser and C. M. Bogan, J. Chem. Phys., 60 (1974) 1837.
10 R. J. Donovan and C. Fotakis, J. Chem. Phys., 61 (1974) 2159.
11 R. J. Butcher, R. J. Donovan, C. Fotakis, D. Fernie and A. G. A. Rae, Chem. Phys. Lett., 30 (1975) 398.